STUDIES ON PHYSICO-CHEMICAL CHARACTERISTICS OF SURFACTANT AGGREGATION AND BEHAVIOUR OF SELECTED ORGANIC MOLECULES IN THE ORGANIZED MEDIA

THESIS SUBMITTED FOR THE DEGREE OF
DOCTOR OF PHILOSOPHY (SCIENCE)
OF THE
UNIVERSITY OF NORTH BENGAL

2008

By

AMITABHA CHAKRABORTY, M. Sc.

DEPARTMENT OF CHEMISTRY
UNIVERSITY OF NORTH BENGAL
RAJA RAMMOHANPUR
DARJEELING 734 013
INDIA

Th 547.7
C 435 s

STOCKTAKING 2011

223041

23 APR 2010

Acknowledgement

I take this opportunity to express my heartfelt gratitude to my supervisor, Professor S. K. Saha, Department of Chemistry, University of North Bengal for his valuable guidance, continued interest and incessant encouragement throughout the entire period of work.

I would like to thank the University Grants Commission, New Delhi, for providing financial support (under Special Assistance Program) and appreciate the authority of the University of North Bengal for extending the required laboratory and other facilities. I am also thankful to Professor James L. Dye, Department of Chemistry, Michigan State University, USA for kindly providing his well known general non-linear curve fitting program, KINFIT.

I extend my sincere thanks to Mr. M. Ali, Mr. B. Debnath, Mr. M. Jha, Mr. S. Chakraborty, Dr. G. Bit, Dr. S. K. Das and Mr. S. Bardhan of this laboratory for their good gesture and generous help. I must appreciate them for their kind cooperation and sharing many happy moments with them during these years. Thanks are also due to Mr. B. Mitra, Department of Zoology, University of North Bengal and many other friends who support me in all occasions to their best during my whole research period.

I am particularly indebted to my younger brother Late Arindam Chakraborty, for his encouragement and enthusiasm which supported me the first two years of my research period.

I express my best regards to my mother and other elders of my family for their blessings and thank the other family members for their inspiration and support.

Department of Chemistry
University of North Bengal
December 08, 2008

Amitabha Chakraborty

Amitabha Chakraborty

Contents

	Page No.
Acknowledgement	**i**
Contents	**ii**
Chapter – 1	**1 – 14**
General Introduction	
1.1 Surfactants and Micelles	1
1.2 Thiazine Dyes	6
1.3 Dye-Surfactant Interactions	8
1.4 Electrochemical Behaviour of Dyes	9
References	11
Chapter – 2	**15 – 20**
Scope and Object	
Chapter – 3	**21 – 66**
Studies on Micellization of Anionic Surfactants in Aqueous Media: Effect of Counterions and Alcohols	
3.1 Introduction and Review of the Previous Work	21
3.2 Effect of Counterions on Temperature Dependant Micellization in Aqueous Media	33
3.2.1 Experimental Section	34
3.2.2 Results and Discussion	35
3.3 Effect of Alcohols on the Aggregation Properties of Micellar systems in Aqueous Medium	52
3.3.1 Experimental Section	55
3.3.2 Results and Discussion	55
References	60
Chapter – 4	**67 – 130**
Studies on Physico-chemical Characteristics of Progressively Alkylated Thiazine Dyes in Micellar and Microemulsion Media	
4.1 Introduction and Review of the Previous Work	67
4.1.1 Dye-Surfactant Interaction in Sub-Micellar Concentrations of Surfactant	72

4.1.2 Dye-Surfactant Interaction in Super Micellar Concentrations of Surfactant 75
4.1.3 Dye-Surfactant Interaction in Microemulsion Media 80
4.1.4 Aggregation of Organic Dyes 82
4.1.5 The Molecular Exciton Model 86
4.1.6 Spectral Properties of Dimer in terms of Exciton Theory 94
4.2 Experimental 96
4.3 Results and Discussion 98
4.3.1 Interaction of thiazine dyes with SDS and AOT in aqueous media 98
4.3.2 Determination of cmc of surfactants and dye-surfactant association constant 100
4.3.3 Studies on monomer-dimer equilibrium of progressively alkylated thiazine dyes in aqueous and microemulsion media 104
4.3.4 Analysis of monomer spectra in aqueous and micro-emulsion media in terms of vibronic Exciton Model 110
4.3.5 Analysis of dimer spectra in terms of Molecular Exciton Model 115
Referenceas 121

Chapter – 5 **131 – 151**

Electrochemical Studies of Thiazine Dyes on the Glassy Carbon Electrode

5.1 Introduction and Review of the Previous Work 131
5.2 Electrochemistry of Dyes 134
5.3 Experimental 136
5.4 Results and Discussion 136
References 150

Chapter – 6

Summary and Conclusions **152 – 159**

List of Publications 160

Chapter 1

General Introduction

General Introduction

1.1 Surfactants and Micelles

The self association process of surfactant molecules into micelles, vesicles or membranes plays an important role in many fields ranging from biological systems to technical applications. This aggregation, as well as protein and nucleic acid folding and their association, is governed by the intricate balance between hydrophobioc interactions and other types of noncovalent solute-solute and solute-solvent interactions [1-3]. This interest continues to grow because of the flexibility of the properties of these surfactants. A surfactant (a contraction of the term "surface active agent") is a substance that shows ability to adsorb at interfaces. The surfaces (interfaces), at which surfactants adsorb, can be between two immiscible liquids, the liquid-gas (air) surface or between a solid and a liquid. The surfactants are also often called amphiphiles, surface-active agents or "soft-matter". Surfactant molecules have two parts: a hydrophilic (polar) part which likes water, and a hydrophobic (non-polar) part which does not. The amphiphilic nature of these molecules results in many unique phenomena when surfactants are dissolved in aqueous or non-aqueous solutions. In the case of a surfactant dissolved in aqueous medium, the lyophobic (hydrophobic) group distorts the structure of the water by breaking hydrogen bonds between the water molecules and results an orientation of the water in the vicinity of the hydrophobic group. As a result of this distortion some of the surfactant molecules are expelled to the interfaces of the system with their hydrophobic groups oriented so as to minimize contact with the water molecules. The concentration above which aggregate (known as micelle) formation becomes appreciable is termed critical micelle concentration (cmc).

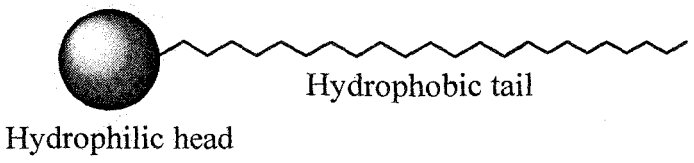

Figure 1.1 Schematic representation of a surfactant molecule

The hydrophobic part of a surfactant is usually a long-chain hydrocarbon residue, and less often halogenated or oxygenated hydrocarbon or siloxane chain. The hydrophilic group on the other hand is an ionic or highly polar group. Depending on the nature of the hydrophilic groups, surfactants are classified as:

(i) *Anionic.* The surface-active portion of the molecule bears a negative charge, e.g. $RCOO^-Na^+$ (soap), $RC_6H_4SO_3^-Na^+$ (alkyl benzene sulfate).

(ii) *Cationic.* The surface-active portion of the molecule bears a posetive charge, e.g. RNH_3^+ (salt of long chain amine), $RN(CH_3)_3^+Br^-$ (quarternary ammonium bromide).

(iii) *Zwitterionic.* Both positive and negative charges may be present in the surface-active portion, e.g. $RN^+(CH_3)_2CH_2CH_2SO_3^-$ (sulfobetaine), $RN^+H_2CH_2COO^-$ (long-chain amino acid).

(iv) *Nonionic.* The surface active portion bears no apparent ionic charge, e.g. $RCOOCH_2CHOHCH_2OH$ (monoglyceride or long chain fatty acid), $RC_6H_4(OC_2H_4)_xOH$ (polyoxyethylenated alkylphenol).

Although surfactants are often present in very small amounts in solution, they do affect the overall properties of the system greatly, such as surface tension, osmotic pressure, solubility, etc., because of their ability to adsorb at surfaces and to form micelles in the solutions. In fact, a large number of experimental observations can be summed up and almost all physicho-chemical properties versus concentration plots for a given surfactant-solvent system will show an abrupt change in slope in a narrow concentration range (the cmc value), that can be illustrated by a classic graph [3], shown in Figure 1.2. The characteristics of surfactants have attracted huge attention from the scientific community. For example, in 1991, de Gennes's Nobel Lecture was on "Soft Matter", i.e. polymers, surfactants and liquid crystals.

The term "micelle" is used for an entity of colloidal dimensions, in dynamic equilibrium with the monomer from which it is formed. As the surfactant concentration increases above the cmc, the addition of fresh monomer results in the formation of new micelles, so the monomer concentration remains essentially constant and approximately equal to the cmc. Water has an open structure because of three dimensional hydrogen bonding, which permits the existence of clusters of

water molecules containing cavities of specific sizes which can accommodate non-polar chains [3-5].

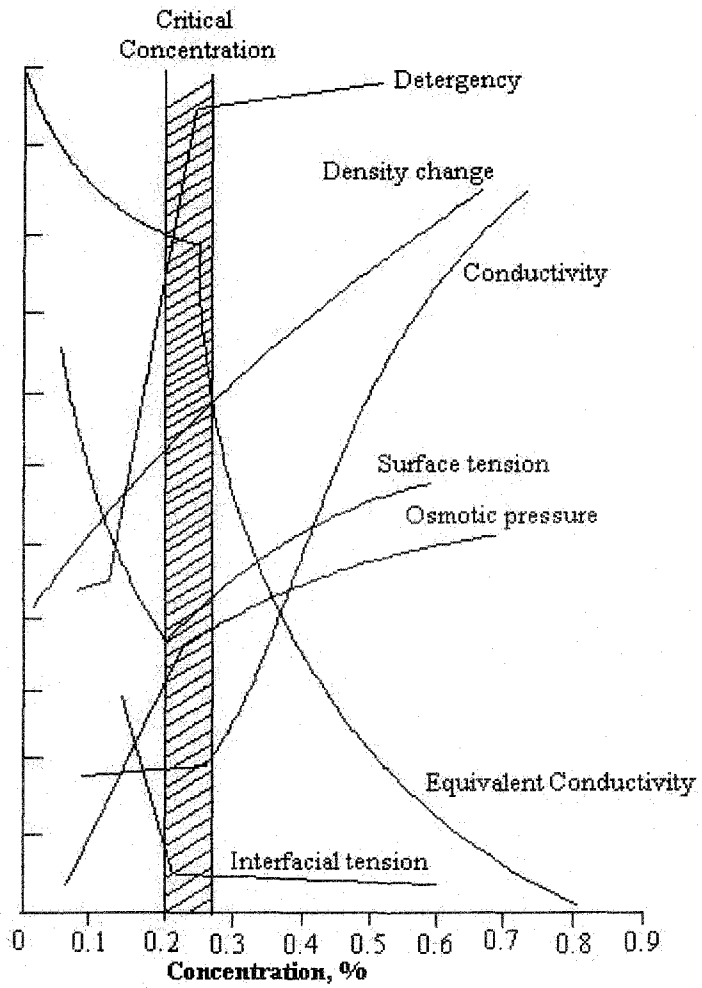

Figure 1.2 Schematic representation of the concentration dependency of some physical properties for solutions of a micelle forming surfactant.

Creation of the cavity restricts the motions of solvent molecules in the hydration shell of a nonpolar solute. This restriction leads to loss of entropy, which is exceptionally large in aqueous solution due to the small size of water molecules [4-9]. For a given surfactant, at a given temperature, only a certain amount of monomer can be accommodated in the cavities and any further addition of surfactant will result in the formation of micelles. In other words, the further addition of surfactant provides a driving force to minimize contact of the monomer hydrocarbon chains with water. Therefore, according to Langmuir's principle of differential solubility,

the hydrocarbon chains clusters to form a core (micellar core) while the polar groups interact with the water [2].

Each micelle consists of a certain number of monomer molecules (aggregation number, n) which determines its general size and shape. The exact size and shape of micelles is still uncertain but it is assumed that an ionic micelle in dilute aqueous solution is roughly spherical, though micellar shape transition under dilute salt-free conditions in presence of different hydrotops are also known [6]. The charged (or polar) hydrophilic groups are directed towards aqueous phase (stern layer), while the hydrocarbon chains are directed away from the water (forming the hydrophobic central core). The region adjacent to the stern layer contains a high density of counter- ions of the polar heads (Gouy Chapman double layer) and separates the hydrophobic interior from the bulk aqueous phase [10].

It is interesting to note that although it is usually assumed that there is a fairly well-defined water layers around the micellar surface, there is no agreement on the composition of the micellar core, i.e. whether it consists of pure hydrocarbon or of hydrocarbon mixed with water. However, water penetration in micellar core is still a matter of controversy.

The idea on controversial "water exposure of micelles" is founded mainly on low angle neutron scattering experiments [11]. This modern concept discusses the main characteristics of the molecular conformation in micelles in terms of the predictions of the "phase separation" or "mass action" model [12-14]. Phase separation model predictions are in agreement with experimental data and are particularly consistent with some principal features of micellar structure.

(i) The micellar core is virtually devoid of water, according to Langmuir's original principle of differential solubility.

(ii) Micellar chains are randomly distributed and steric forces determine the final structure.

(iii) Contact of the hydrophobic sections of the micelle with water results from a disordered structure in which the terminal groups or chain ends are near the micellar surface and thus exposed to bulk water [15]

Although the "water penetration" concept of the hydrophobic sections of micelle is now less acceptable than the "water exposure" concept, this controversial

topic is still under debate [16,17]. However the phase separation model along with the related thermodynamics of micelle formation is discussed in chapter 3.

Another important characteristic of surfactants is there ability to form microemulsion [18,19]. Microemulsions are compartmentalized liquids having huge application in several physico-chemical and technological processes [20,21]. They are optically isotropic, transparent, normally low viscous and thermodynamically stable solutions (dispersions) having a prolonged life-span [22,23] and can be prepared by mixing appropriate proportion of oil, water and surfactant. In many cases the presence of co-surfactants (polar compounds of intermediate chain length, e.g. medium chain alkanols) may stabilize microemulsions by providing the proper balance between hydrophilic properties for the required oil and water phases under the conditions of use. But cosurfactant free microemulsions are also known [19]. Microemulsions are of two types, based on the nature of the dispersed phase: oil-in water (O/W) and water-in-oil (W/O) having average particle size with in the range of 5-100 nm [18]. Pictorial representations of reverse micelles and microemulsions are shown in Figure 1.3. They are polydispersed in nature and the polydispersity decreases with decreasing particle size. In the formation of microemulsions, one of the two immiscible liquids (viz. oil or water) breaks up into particles that are dispersed in the second liquid. They can be formed with expenditure of a very little energy (can be supplemented by the thermal energy of the system) and are thus thermodynamically stable. A mixture of the right proportion of water, amphiphile and oil may spontaneously homogenize itself forming a microemulsion. In case of W/O microemulsion each water droplet is covered by an oriented monolayer of surfactant molecules.

In recent years microemulsion have been extensively applied to many fields, such as chemical reactions [24,25], nanometerials preparation [26] and drug delivery systems [27]. Reactions performed therein may significantly deviate from the normal courses and are often catalyzed in compartmentalized environments. Recently, attempts have also been made to prepare and study nonaqueous microemulsions for ionic liquids [28-30]. These microemulsions have attracted much interest from both theoretical (thermodynamics, particle interactions, etc.) and practical (potential use as a novel reaction media) view point [30].

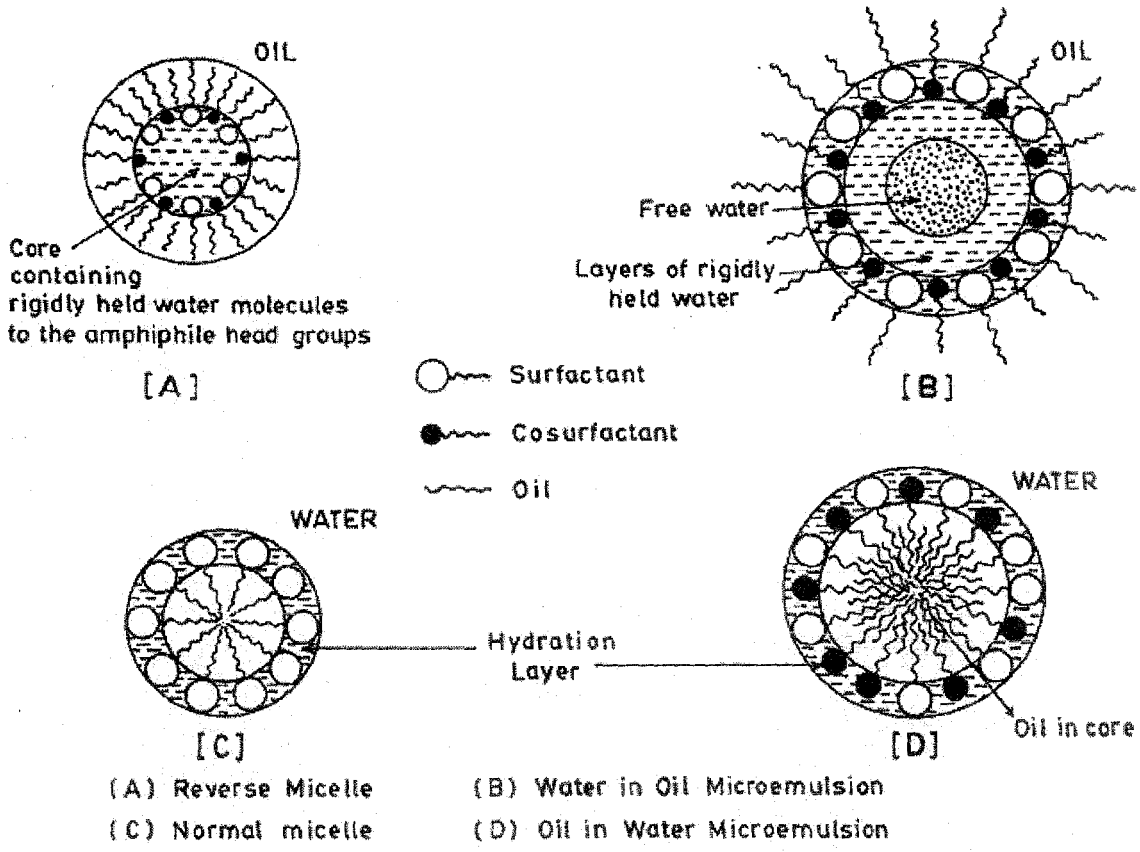

Figure 1.3 Schematic representations of reverse micelles and microemulsions.

1.2 Thiazine Dyes

Continuously tunable lasers can now be produced to cover the entire visible spectrum using organic dyes as lasing medium. The visible absorption spectra of organic dyes exhibit strong dependence on concentration in aqueous solution because of self aggregation [31]. Aggregation affects colour, solubility, photophysical and photo chemical behaviour of dyes. A systematic study of the aggregation characteristics of dyes from spectrophotometric data has become a useful field of research because of its possible application in understanding such phenomena on energy transfer in biological systems, metachromatia, hypochromism and confirmation of polypeptides, and staining properties of dyes for biological specimens etc. The force responsible for holding the component molecules in the dimer or on polymer is not yet well understood. Nevertheless, it is clear that for ionic dyes, aggregation would be possible if there exists some very strong attractive interaction, which first of all overcomes the coulombic repulsion and then brings the

component molecules to a reasonable distance to form dimers and subsequently high polymer. Photochemical systems for photoreduction of water and photoinduced electron transfer reaction in surfactant solutions are of considerable interest as models for understanding of photobiology [32,33] and the conversion of solar energy [34,35]. Compared with inorganic complexes, organic dyes have been investigated only rarely as sensitizers for the photo reduction of water [36-38]. Because of their photophysical properties, thiazine dyes (Figure 1.4) are used as photosensitizer in light-induced reactions. These studies are important particularly from the standpoint of the possibility of their utilization in photodynamic therapy (PDT) [39], photodegradation of environmental contaminants [40-42], molecular recognition and photo sensitized modification of DNA [43]. It has been found that the thiazine dyes designed as azures (Figure 1.4c, 1.4d and 1.4e) are promising photosensitizers for PDT [44]. Structures of different thiazine dyes are shown in Figure 1.4.

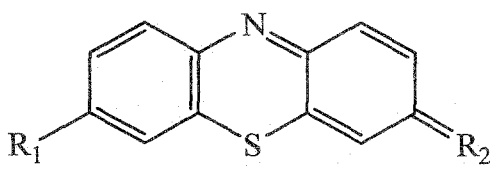

a) **Th**$^+$	R_1 :NH_2	R_2 : $\overset{+}{N}H_2$
b) **MB**$^+$	R_1 : $N(CH_3)_2$	R_2 : $\overset{+}{N}(CH_3)_2$
c) **AzA**$^+$	R_1 : $N(CH_3)_2$	R_2 : $\overset{+}{N}H_2$
d) **AzB**$^+$	R_1 : $N(CH_3)_2$	R_2 : $\overset{+}{N}H(CH_3)$
e) **AzC**$^+$	R_1 : $NH(CH_3)$	R_2 : $\overset{+}{N}H_2$

Figure 1.4 Structures of thiazine dyes: (a) thionine, (b) methylene blue, (c) azure A, (d) azure B and (e) azure C.

The course of the photosensitized reactions can be significantly affected when they occur in organized systems, i.e. thin films, microemulsions, vesicles and micelles [45,46]. These systems can simulate the environment in biological systems and are thus frequently used as relatively simple models [47]. The choice of a suitable micellar system is very important, as the electrostatic interactions between the studied substances and the surface charge of the micelles can have a favourable or unfavourable effect on the properties of interest.

1.3 Dye – Surfactant Interactions

Although from early time the changes in the colour of ionic dyes in the presence of oppositely charged ionic surfactants in aqueous solution have led many workers [48-50] to propose dimer and multimer formation of dye molecules in the surfactant micelle, this area are still important and interesting for the theoretical, ecological and technological point of view. The enhanced energy transfer between dyes in dye-surfactant systems made them good model membrane systems of chloroplast [51,52]. The peculiar behaviour in both absorption [53] and fluorescence [54] spectra of dyes in the presence of surfactants of opposite charge were attributed to the formation of a continuum of dye-surfactant aggregates or mixed micelles depending on the surfactant: dye ratio (S/D). Among other things, the investigations into the behaviour of different dyes in surfactant aqueous solutions, give useful information about the mechanisms according to which surfactants operate as leveling agents and provide information on the influence of dye–surfactant interactions on the thermodynamics and kinetics of dyeing process. This may directly affect the quality of dyeing, which is one of the goals of textile finishing. Surfactants are also used as solubilizers for water insoluble dyes, to break down dye aggregates in order to accelerate adsorption process on fiber, as auxiliaries for improving dye adsorption and as leveling or dispersing agents [55-57]. According to the structures of dye and substrate, surfactants used as levelling agents operate by different mechanisms. Consequently, a great deal of research work focused on dye–surfactant interactions in binary mixtures including the interactions between ionic dyes and ionic surfactants of the opposite and the same charges [58–61], ionic dyes and nonionic surfactants [58,62,63] as well as between nonionic dyes and ionic or nonionic surfactants [64] in the submicellar and micellar concentration ranges of surfactants. It seems probable that once the electrostatic forces have brought together the oppositely charged molecules, hydrophobic interactions take place, dramatically changing the microenvironment experienced by the chromophore. Knowledge of dye surfactant interaction should also be of great value on understanding the chemical equilibria, mechanism and kinetics of surfactant sensitized colour reactions.

The results of spectral studies on phenosafranin, a cationic phenazine dye, in aqueous solution containing three different types of surfactants such as cetyltrimetylammonium bromide (CTAB), sodium lauryl sulfate (SLS) and Triton X-

100 have been reported [65]. The dye forms 1:1 molecular complexes with Triton X-100 and SLS, but there is no interaction of phenosafranin with CTAB. The thermodynamic and spectrophotometric properties of these complexes suggest that phenosafranin forms a strong charge-transfer (CT) or electrondonor-acceptor (EDA) complex with Triton X-100, whereas the interaction with SLS is coulombic in nature. This conclusion is confirmed by photovoltage and photoconductivity measurement of phenosafranin in these surfactants. The same studies confirm the CT interaction of Triton X-100 with other cationic dyes such as crystal violet, fuchsin and rhodamin B [66]. Thiazine dyes are structurally very similar to phenosafranin and we have chosen some thiazine dyes such as thionine, methylene blue, azure A, azure B and azure C for our consideration.

1.4 Electrochemical Behaviour of Dyes

The search for renewable sources of energy has led to an increasing interest in photochemical cells because of their possible role as transducers of solar to electrical energy. It has been observed that photo effects in electrochemical systems are enhanced if the electrodes are coated with dye stuff, wherein their redox chemistry playes an important role [67,68]. There have been reports in the past that use of dyes as sensitizers in photo-electrochemical devices for solar energy conversion suffer from very poor power conversion efficiency [69,70]. This drawback has been variously attributed to slow discharge of photo-produced intermediate dye radicals (viz., semi reduced 'leuco' dyes) at the cell electrode as compared to radical - radical recombination reaction in the bulk of the solution. The reaction with thionine can be stated as follows:

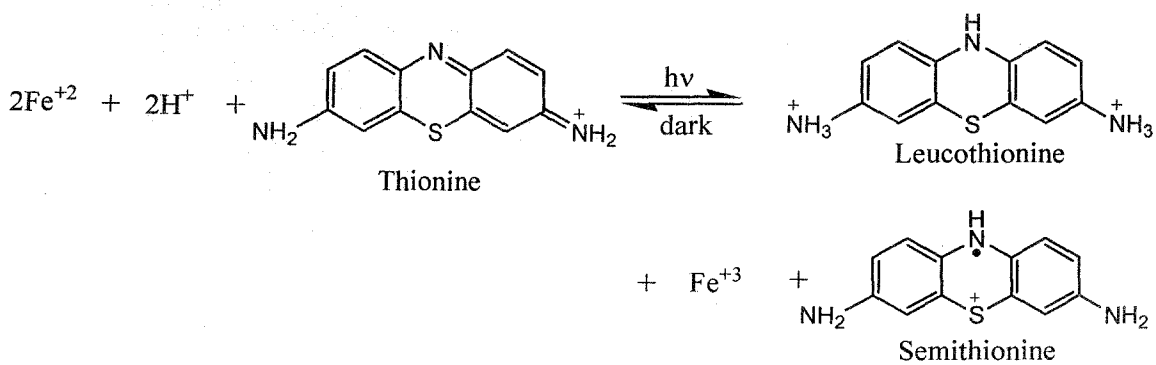

To make the discharge process favorable, it is necessary to arrest the recombination reaction in the bulk homogeneous phase. Attempts have been made in

the past to slow down the bulk reactions in a suitable micellar medium [71]. In this connection some oxazine dyes have been considered sensitizers in photogalvanic devices in the past. The dye surfactant interactions have been the subject of interest also because they mimic many biological processes taking place between the large organic molecules and biomembranes and can act as a model redox system [72,73]. Further such interactions between ionic dyes and charged surfaces are of interest in numerous applications ranging from the design of electronic devices to the characterization of drug-delivery system. It has been reported that pure metal electrodes becomes sensitive to light when coated with a dye or immersed in a dye solution [74]. Phenothiazine and substituted-phenothiazine dyes are thought to be important in the direct conversion of solar energy to electricity [75,76]. For example, the photochemical redox reaction between thionine and Fe^{2+} has been used advantageously to devise and understand the mechanism of the photogalvanic cell. Early workers have extensively examined the photogalvanic activity of various dyes with reversible and irreversible reducing agents [77,78]. In order to understand the mechanism of photogalvanic action it is essential to investigate the electrochemical behaviour of these dyes.

References

1. Schramm L. L., *Surfactants: Fundamentals and Applications in the Petroleum Industry*, Cambridge University Press, 2000.

2. Tanford, C. *The Hydrophobic Effect: Formation of Micelles and Biological Membranes*, 2nd Ed., Wiley - Interscience, New York 1980.

3. Lindman, B.; Wennerström, H. Topics in Current Chemistry, Vol. 87, Springer-Verlag, Berlin, 1980.

4. Lindman, B.; Marie-Claude, P.; Kamenka, N.; Rymdén, R.; Stilbs, P. *J. Phys. Chem.* **1984**, *88*, 5048.

5. Blokzijl, W.; Engberts, J.B.F.N. *Angew. Chem., Int. Ed. Engl.* **1993**, *32*, 1545.

6. Mancera, R.L. *J. Chem. Soc., Faraday Trans.* **1996**, *92*, 2547.

7. Saha, S. K.; Jha, M.; Ali, M.; Chakraborty, A.; Bit, G.; Das, S. K. *J. Phys. Chem. B* **2008**, *112*, 4642.

8. Graziano, G.; Barone, G. *J. Am. Chem. Soc.* **1996**, *118*, 1831

9. Graziano, G. *Phys. Chem. Chem. Phys.* **1999**, *1*, 1877.

10. Fendler, J.H. and Fendler, E.J. *Catalysis in Micellar and Macromolecular Systems*, Academic Press, New York, 1975.

11. Dill, K.A.; Koppel, D.E.; Cantor, R.S.; Dill, J.D.; Bendedouch, D.; Sow. H. *Nature Chem.*, **1984**, *42*, 309.

12. Myers, D., *Surfactant Science And Technology*, VCH: New York, 1992.

13. Suarez, M.J.; Lopez-Fontan, J.L.; Sarmiento, F.; Mosquera, V. *Langmuir* **1999** *15*, 5265.

14. González-Pérez, A.; Czapkiewicz, J.; Del Castillo, J.L.; Rodríguez, J.R. *Colloid Polym. Sci.* **2004**, *282*, 1359.

15. Dill, K.A.; Flory, P.J., *Proc. Natt. Acad. Sci.* USA, 1980, **77**, 3115; **78**, 676, 1981.

16. Menger, F.M. *Nature*, **1985**, *313*, 603.

17. Cabane, B. *Nature*, **1985**, *314*, 385.

18. Moulik, S.P.; Paul, B.K.; *Adv. Colloid Interface Sci.* **1998**, *78*, 99.

19. Holmberg, K.; Osterberg, E. *J. Dispersion Sci. Technol.* **1986**, *7*, 299.

20. Schwuger, M.-J.; Stickdorn, K.; Schomacker, R. *Chem. Rev.* **1995**, *95*, 849.

21. Velazquez, M.M.; Valero, M.; Ortega, F. *J. Phys. Chem. B* **2001**, *105*, 10163.

22. Holt, S.L.; *J. Dispersion Sci. Technol.* **1986**, *1*, 423.

23. Kahlweit, M. *Science* **1988**, *240*, 617.

24. Oh, S.; Kizling, J.; Holmberg, K. *Colloid Surf. A* **1995**, *97*, 169.

25. Spiro, M.; de Jesus, D.M. *Langmuir* **2000**, *16*, 2464.

26. Bonini, M.; Bardi, U.; Berti, D.; Neto, C.; Baglioni, P. *J. Phys. Chem. B* **2002**, *106*, 6178.

27. Lv, F.F.; Zheng, L.Q.; Tung, C. *Int. J. Pharm.* **2005**, *301*, 237.

28. Ray, S.; Moulik, S.P. *Langmuir* **1994**, *10*, 2511.

29. Peng, S.; An, X.; Shen, W. *J. Colloid Interface Sci.* **2005**, *287*, 141.

30. Falcone, R.D.; Correa, N.M.; Biasutti, M.A.; Silber, J.J. *langmuir* **2000**, *16*, 3070.

31. Horng, M ; Quitevis, E.L. *J. Chem. Edu.* **2000**, *77*, 637.

32. Buryak, A.; Severin, K. *Chem. Comm.*, **2007**, 2366.

33. Kwon, J.Y.; Singh, N.J.; Kim, H.N.; Kim, S.K.; Kim, K.S.; Yoon, J. *J. Am. Chem. Soc.* **2004**, *126*, 8892.

34. De Groot, M.S.; Hendriks, P.A.J.M. ; Brokken-Zijp, J.C.M. *Chem. Phys. Lett.* **1983**, *97*, 521.

35. Lal, C. *J. Power Sources*, **2007**, *164*, 926.

36. Kalyanasundaram, K.; Dung, D.; *J. Phys. Chem.* **1980**, *84*, 2551.

37. Chan, M.S.; Bolton, J.R.; *Photochem. Photobiol.* **1981**, *34*, 537.

38. Hashimoto, K.; Kawai, T.; Sakata, T. *Chem. Lett.* **1983**, *5*, 709.

39. Wainwright, M. *Chem. Soc. Rev.* **1996**, *25*, 351.

40. Gak, V.Y.; Nadtochenko, V.A.; Kiwi, J. *J. Photochem. Photobiol. A* **1998**, *116*, 57.

41. Tanielian, C.; Mechin, R.; Sakinullah, M. *J. Photochem. Photobiol. A* **1992**, 64,191.

42. Lang, K.; Luňák, S.; Sedlák, P.; Brodilová, J. *Zeit. Phys. Chem.* **1995**, *190*, 203.

43. Fujimoto, B.S.; Clendenic, J.B.; Delrow, J.J.; Heath, P.J.; Schurr, M. *J. Phys. Chem.* **1994**, *99*, 6633.

44. Jirsa, M.; Jirsaa, Jr. M.; Kubát, P. *J. Photochem. Photobiol. B* **1996**, *36*, 99.

45. Barra, M.; Redmond, R.W.; Allen, M.T.; Colabrese, S.S.; Sinta, R.; Scaina, J.C. *Macromolecules* **1991**, *24*, 4972.

46. El-Torki, F.M.; Schmehl, R.M.; Reed, W.F. *J. Chem. Soc. Faraday Trans. 1* **1989**, *85*, 349.

47. Barbes, J., *Photosynthesis in relation to model systems*, Elsevier, New York, 1979.

48. Mukerjee, P.; Mysels, K.J. **1955** *J. Am. Chem. Soc. 77*, 2937.

49. Hiskey, C.P.; Downery, T.A. **1954** *J. Phys. Chem. 58*, 835.

50. Cockbain, E.G. *Trans. Faraday Soc.* **1954**, *49*, 104.

51. Sato, H.; Kusumoto, Y.; Nakashima, N.; Yoshihara, K. *Chem. Phys. Lett.* **1980**, *71*, 326.

52. Usui, Y.; Saga, K.; *Bull. Chem. Soc. Japan* **1982**, *55*, 3302.

53. Reeves, R.L.; Harkaway, S.A. *Micellization, Solubilization and Microemulsion*, Mittal, K. (Ed.), Vol. 2, Plenum Press, New York, 1979.

54. Vaidyanathan, S.; Patterson, L.K.; Möbius, D.; Gruniger, H.-R. *J. Phys. Chem.* **1985**, *89*, 491.

55. Akbaş, H.; İşcan, M. *Turk. J. Chem.* **1994**, *18*, 80.

56. Sudbeck, E.A.; Dubin, P.L.; Curran, M.E.; Skelton, J. *J. Colloid Interface Sci.* **1991**, *142*, 512.

57. Missclyn-Bavduin, A.M.; Thibaut, A.; Grandjean, J.; Broze, G.; Jerome, R. *Langmuir* **2000**, *16*, 4430.

58. Gou, L.N.; Arnaud, I.; Petit-Ramel, M.; Gauthier, R.; Monnet, C.; Le Perchec, P., Chevalier, Y. *J. Colloid Interface Sci.* **1994**, *163*, 334.

59. Simončič B, Špan J. *Dyes and Pigments* **2000**, *46*, 1.

60. Bračko, S.; Špan, J. *Dyes and Pigments* **2001**, *50*, 77.

61. Moulik, S.P.; Ghosh, S.; Das, A.R.; *Colloid Polym. Sci.* **1979**, *257*, 645.

62. Tanaka, F.; Harada, Y.; Ikeda, N.; Aratono, M.; Motomura, K. *Bull. Chem. Soc. Japan* **1994**, *67*, 2378.

63. Bhattacharya, S.C.; Das, H.; Moulik, S.P. *J. of Photochem. Photobio. A* **1993**, *74*, 239.

64. Ogino, K.; Kasuya, T.; Abe, M. *Colloid Polym. Sci.* **1988**, *266*, 539.

65. Rohatgi-Mukherjee, K.K.; Chaudhuri, R.; Bhowmik, B.B. *J. Colloid Interface Sci.* **1985**,106, 45.

66. Bhowmik, B.B.; Chaudhuri, R.; Rohatgi-Mukherjee, K.K. *Indian J. Chem.* **1987**, 26A, 95.

67. Perkinson, B.A.; Spitler, M.T. *Electrochem. Acta* **1992**, *37*, 943.

68. Das, S.; Thomas, K.G.; Kamat P.V.; George, M.V. *Proc. Ind. Acad. Sci. (Chem. Sci.)* **1993**, *105*, 513.

69. Kamat, P.V.; Karkhanavala, M.D.; Moorthy, P.N. *Ind. J. Chem. A.* **1977**, *15*, 342.

70. Kamat, P.V.; Karkhanavala, M.D.; Moorthy, P.N. *Solar Energy* **1978**, *20*, 171.

71. Kiwi, J.; Kalyan Sunderam, K.; Gratzel, M.; *Struct Bonding* **1982**, *49*, 37.

72. Shah S.S.; Ahmed, R.S.W.H.; Asif, K.M.; Naeem, K. *Colloid Surf. A.* **1998**, *137*, 301.

73. Chibisov, A.K.; Prokhorenko, V.I.; Gomer, H. *Chem. Phys.* **1999**, *250*, 47.

74. Jana, A.K. *J. Photo Chem. Photo Biol. A : Chem.* **2000**, *132*, 1.

75. W. J. Albery, Photovoltaic and Photoelectrochemical Solar Energy Conversion, ed. F. Cardon, W. P. Gomes and W. DeKeyser, NATO Advanced Study Institute Series Plenum Press: New York, 1980

76. Petritsch, Dipl.Ing. K., *Ph.D. Thesis*, Technische Universität Graz, Austria, 2000.

77. Ahmed, S.; Saha, S.K. *Can. J. Chem.* **1996**, *74*, 1896.

78. Murthy, A.S.N.; Reddy, K.S. *Electrochim. Acta*, **1983**, *28*, 473.

Chapter 2

Scope and Object

Scope and Object of the Present Investigation

Considerable interests have been generated recently in studying physico-chemical properties of self assembled surfactant aggregates, especially micelles, reverse micelles and unilamellar vesicles [1-3]. Although many reasons can be cited for the wide spread interest in elucidating the physico-chemical properties of these self organized systems, primarily there are three important reasons. Firstly, one can consistently and easily prepare aqueous micellar and vesicular solutions which have aggregates of colloidal dimensions with, characteristic size, shape and surface properties. Hence micellar and vesicular system have been employed as a model system in investigations concerned with understanding colloidal physico-chemical phenomena. Secondly, the similarities between self-assembled surfactant aggregates, such as micelles and vesicles, and biological lipid membranes prompted researchers to employ micelles and vesicles as model biological systems. Thirdly, it has been found that micelles and vesicles can act as unique reaction media. Therefore, investigation on physico-chemical characteristics of micelles and vesicles forms a considerable volume of literature [4-7]. Some studies conclude that the changing of the nature of surfactant counter ions affect the properties and structure of the surfactant micelles [8-10]. Another important aspect of the amphiphile that draws the attention is the ability to form aggregate in nonaqueous media. These aggregates in nonaqueous media are of nanometer size and being almost spherical can solubilize large amounts of water, forming water-pool, whose properties have been determined with different techniques [11-13]. The surfactant counter ion is responsible for surface electric interactions at the micellar interface. These interactions can have a strong influence both on the equilibrium shape and size of the micellar aggregates [4,5,8].

Alcohols also affect the micellization process to a large extent [14-16]. They play the role of cosurfactant in the aggregation process. From a practical point of view, alcohols have been used in tertiary oil recovery because they bring about a large decrease of the viscosity of micellar systems used in the process [17]. Moreover they strongly accelerate the rate at which these systems reach equilibrium in the polyphasic range and appear to decrease the adsorption of surfactants in the pores of the rock in the oil field, thereby increasing the efficiency and decreasing the cost of the tertiary oil recovery process. From a fundamental point of view, the approach of

microemulsions also led some authors [18] to suggest that the formation and the stability of microemulsions might in part result from their dynamic character enhanced by the presence of alcohol.

Microemulsions differ from micelles by the complex composition and larger sizes of the particles as they contain compartmentalized water (sometimes called water-pool) with surfactants and alcohols having medium hydrocarbon chains (e.g. n-hexanol, n- heptanol, etc.), generally called co-surfactant along with a nonpolar solvent. They are, therefore, characterized by a higher solubilizing capacity of organic molecules and can also be treated as analogical model of biologically functioning systems, which are the basis of living matter. Solubilization of water in microemulsion systems has been found to be dependent on various factors involving the rigidity of the interfacial film, which in turn depends upon the size of the polar head group and the hydrocarbon moiety of surfactant, the type of oils, the presence of electrolyte, the nature and valance of counterion, the temperature, etc. The structure of the interfacial water of microemulsion systems is somehow different from bulk water. In the micro-encapsulated domain, the presence of amphiphilic head groups and the counterion may significantly affect the water mobility. Because of the peculiar chemical and physical properties of the polar interior of reverse micellar aggregates, substantial efforts have been focused on the investigation of the state of water in the pool.

During the last two decades, there has been an increasing awareness of the importance of photochemical and electrochemical effects of dyes due to their interesting role in solar energy conversion and for providing convenient means of probing spectroscopic [19-21] and electrodic process [22-24]. It is commonly believed that the primary process which lead to photo voltage generation in a photogalvanic (PG) cell do not occur at the electrod-electrolyte interfaces, but are results of photochemical reactions in the bulk of the solution; which are followed by diffusion of electrodically active photo products to the electrode surface where electron transfer takes place. Knowledge of the self association properties of the PG solution is important because the aggregates produce grater re-absorption and quenching, decreasing quantum yield and residence time of the first singlet excited state of the dye. The electrochemical rate constant, mass transfer, etc. of PG cell are important because they precisely determine whether the species are likely to react on the

LIBRARY

electrode or lost by diffusion away or reacting in the bulk of the solution. Self association of dyes (J-and H-aggregates) [25,26] has become more popular recently since the discovery of lyotropic liquid crystalline phases, which are known as chromonics and the spontaneous occurrence of chirality of some cyanine and other dye aggregates although made up by non chiral molecules. Oxazine dyes are also finding increasing applications in the field of electrocatalysis of electrochemical redox processes. Oxazine dye modified electrodes have been shown to be useful in electrocatalytic oxidation of coenzyme, Nicotinamide Adenine Dinucleotide (NADH) in the context of enzyme-based biosensors [27].

The most successful photogalvanic cell [28,29] for solar energy conversion is the ferrous/thionine cell, yet this too is far from ideal conversion efficiency. A better efficiency would be obtained from a PG cell in which each electrode is perfectly selective for a different couple, which could not be achieved so far. In homogenous solution, thermal back reaction of electron transfer also takes place. This dissipation of free energy constitutes a considerable problem in the use of the ferrous/ thionine PG cell for any practical purpose. Various alky substitutions in thionine seem to influence not only the solubilities but also certain physico-chemical properties which in turn must influence the phenomena occurring in the cell.

Keeping the above in view, two anionic surfactants viz. sodium dodecyl sulfate (SDS) and aerosol-OT (AOT) have been selected for the physico-chemical characteristics including thermodynamics of micelle formation as a function of nature and concentration of counter ions (e.g., Li^+, Na^+, K^+, NH_4^+ $(CH_3)_4N^+$, $(C_2H_5)_4N^+$, $(C_3H_7)_4N^+$ and $(C_4H_9)_4N^+$) in aqueous medium. All the surfactants with necessary counterions are prepared by ion exchange technique. To examine the effect of alcohols on micellization on SDS and AOT water- alcohols (ethanol, 1-propanol, 2-propanol) systems have been studied within a temperature range 298-313K.

To investigate the self association and spectroscopic behavior of progressively alkylated thiazines dyes viz. thionine, azure C (monomethyl thionine), azure A (dimethyl thionine), azure B (trimethyl thionine) and methylene blue (tetramethyl thionine) have been studied in aqueous media in presence of two important anionic amphiphile, SDS and AOT within a wide range of surfactant concentrations covering premicellar and postmicellar region. Spectrophotometric investigation is carried out on the above five thiazine dyes in water pool of microemulsion because the physico-

22304 L 23 APR 2010

chemical environment of the compartmentalized water in microemulsion is different from that of bulk water. The systematic study of the aggregation characteristics of dyes from spectroscopic data is also useful for other important aspects too, e.g., its possible applications in understanding phenomena such as energy transfer in biological systems, metachromasia, hypochromism, conformation of polypeptides and staining properties of dyes for biological specimens. Excitonic interactions between pairs of identical chromophors in a dimer will be considered from spectroscopic measurements and formulated in connection with studies of the concentration dependent properties of dye solutions. Spatial conformations of the dimmer in solution (both in aqueous and microemulsion media) are determined as a function of progressive alkylation of thionine molecule from the consideration of exciton model.

Energy problem has opened new avenues in physical chemistry research ever since electrochemistry has been proved to be the most promising of all modern energy technologies. This is due to its capability in dealing with highest energy densities of all possible alternatives. Two essential features of research activities in this direction are (i) modification of the conventional technologies via incorporating emerging ideas and knowledge in various electrode and electrolytic processes and (ii) development and upgradation of new energy conversion techniques, especially that of solar energy conversion by incorporating new perception of chemistry of electrodics and ionics (specially metal free) at the interfaces and in the bulk. In view of this plan a preliminary study has been drawn.

The area which covers the present investigation is the electrochemical study which includes redox behaviour of all the thiazine dyes at stationary electrode surface in cyclic voltammetry, mechanism of electrode processes and heterogeneous rate constant of electron transfer at the electrodes. Effect of aqueous-organic and micellar media on the electrochemistry of progressively alkylated thiazine dyes at the stationary electrode surface will also be examined. The information will be helpful in further plan of study in electrodics and ionics as mentioned.

References

1. Nilsson, S.; Thuresson, K.; Hansson, P.; Lindman, B. *J. Phys. Chem. B*, **1998**, *102*, 7099.
2. Clint, J.H. *Surfactant Aggregation*, Blackie Chapman and Hall, New York, 1992.
3. Rosen, M.J. *Surfactants and Interfacial Phenomena*, Wiley-Interscience, USA, 2004.
4. Yin, H.; Lei, S.; Zhu, S.; Huang, J.; Ye, J. *Chem. Eur. J.* **2006**, *12*, 2825.
5. Saha, S. K.; Jha, M.; Ali, M.; Chakraborty, A.; Bit, G.; Das, S. K. *J. Phys. Chem. B* **2008**, *112*, 4642.
6. Lindemuth, P.M.; Bertrand, G.L. *J. Phys. Chem.* **1993**, *97*, 7769.
7. Hedin, N.; Sitnikov, R.; Furo, I.; Henriksson, U.; Regev, O. *J. Phys. Chem. B* **1999**, *103*, 9631.
8. Benrraou, M.; Bales, B.L.; Zana, R. *J. Phys. Chem. B* **2003**, *107*, 13432.
9. Pisárčik, K.; Devínsky, F.; Lacko, I. *Acta Facult. Pherm. Univ. Comenianae* **2003**,*50*, 119.
10. Bales, B.L. *J. Phys. Chem. B* **2001**,*105*, 6798.
11. Mittal, K.L. *Micellization, Solubilization and Microemulsion*, Vol. 2, USA, 1977.
12. Foley, M.S.C.; Beeby, A.; Parker, A.W.; Bishop, S.M., Phillips, D. *J. Photochem. Photobiol. B: Bio.* **1997**, *38*, 18.
13. Tatikolov, A.S.; Costa, M.B. *Photochem. Photobiol. Sci.* **2002**, *1*, 211.
14. Brinchi, L.; Di Profio, P.; Germani, R.; Savelli, G.; Spreti, N. *J. Colloid Interface Sci.* **2002**, *247*, 429.
15. Attwood, D.; Mosquera, V.; Rodriguez, J.; Garcia, M.; Suarez, M.J. *Colloid Polym. Sci.* **1994**, *272*, 584.
16. Rafati, A.A.; Gharibi, H.; Rezaie-Sameti, M. *J. Mol. Liq.* **2004**, *111*, 109.
17. Mittal, K.L. *Micellization, Solubilization and Microemulsion*, Vol. 1, USA, 1977.
18. Moulik, S.P.; Paul, B.K. *Adv. Colloid Interface Sci.* **1998**, *78*, 99.

19. Mackay, R.A.; Lai, W.-C. *Colloid Surf. A* **2005**, *254*, 115.

20. Dakiky, M.; Manassra, A.; Abdul Kareem, M.; Jumean, F.; Khamis, M. *Dyes Pigments* **2004**, *63*, 101.

21. Sarma, S.; Gohain, B.; Datta, R.K. *J. Dispersion Sci. Technol.* **2006**, *27*, 899.

22. Ahmed, S.; Saha, S.K. *Can. J. Chem.* **1996**, *74*, 1896.

23. Liu, D.; Kamat, P.V. *J. Electrochem. Soc.* **1995**, *142*, 835.

24. Chen, C.; Gao, Y. *Materials Letters* **2004**, *58*, 3385.

25. Barazzouk, S.; Lee. H.; Hotchandani, S.; Kamat P.V. *J. Phys. Chem. B.* **2000**, *104*, 3616.

26. Von Wandruszka, H.; Böttcher, C. *J. Phys. Chem. B.* **2002**, *106*, 3146.

27. Malinausks, A.; Ruzgas, T; Gorton, L. *J. Electroanal. Chem.* **2000**, *484*, 55.

28. Chamberlain, G.A. *Solar Cells* **1983**, *8*, 47.

29. Jana, A.K. *J. Photo Chem. Photo Biol. A : Chem.* **2000**, *132*, 1.

Chapter 3

Studies on Micellization of Anionic Surfactants in Aqueous Media: Effect of Counterions and Alcohols

3.1 Introduction and Review of the Previous Work

It is known that the science of surface active agents (Surfactants) is one of the important subtopics of the colloidal science. Surfactants have gained great interest in recent years due to a huge benefit achieved in many industries producing detergent, cosmetics and pharmaceuticals. Surfactants with lower concentration greatly reduce the surface tension between two or more incompatible phases. In some sense, the structural features of surfactants are responsible for the surface activity. The structural features of a surfactant are characterized by the existence of a polar head and a non-polar tail. The polar head of the surfactant may be charged or uncharged (but polar). A charged polar head may carry a positive or a negative charge or both, while the nonpolar (hydrophobic) tail is usually a flexible hydrocarbon chain (C_8-C_{18}) which may contain an aromatic ring. Their composite character is described by a property known as 'hydrophilic lipophilic balance' i.e., HLB. It is the HLB which primarily decides their micellization, dispersion and emulsification activities. The four major types of surfactants are classified as anionic, cationic, amphoteric or zwitterionic and nonionic depending on the head group [1-5].

Surfactant molecules in aqueous media form micelles above their critical micelle concentration (cmc), accompanying striking changes in the various physical properties [6]. With increasing surfactant concentration the micelles undergo a special set of structural transitions, transforming from spherical shape into cylindrical, rodlike or long threadlike, disk-like vesicles and other shapes [7].

(a) Spherical micelles are formed with an interior composed of hydrocarbon chains and a surface of polar head groups (pictured as spheres) facing water. Spherical micelles are characterized by a low aggregation number (critical packing parameter) and the hydrocarbon core has a radius close to the length of the extended alkyl chain.

(b) Cylindrical micelles with an interior composed of the hydrocarbon chains and a surface of the polar head groups facing water. The cross section of the hydrocarbon core is similar to that of spherical micelles. The micellar length is highly variable so these micelles are polydisperse in nature.

(c) Surfactant bilayers which build up lamellar liquid crystals for surfactant-water systems having a hydrocarbon core with a thickness of about 80% of the length of two extended alkyl chains.

(d) Reversed or inverted micelles having a water core surrounded by the surfactant polar head groups. The alkyl chains together with a nonpolar solvent make up the continuous medium.

(e) A bicontinuous structure with the surfactant molecules aggregated into connected films characterized by two curvatures of opposite sign. The mean curvature is small (zero for a minimal surface structure).

(f) Vesicles are built from bilayers similar to those of the lamellar phase and are characterized by two distinct water compartments, with one forming the core and one the external medium. Vesicles may have different shapes and there are also reversed-type vesicles.

The shape of a micelle depends on the concentration of surfactant and the presence of additives or hydrotops for single systems, and is controlled by the spontaneous curvature of the micellar interface [8,9]. Since surfactant solutions can have certain aggregation structures which are responsible for giving the solution its physical properties, they are sometimes defined as complex fluids. However, Gruen [10] has described a realistic model for a micelle. This model involves a rather sharp interface between a dry hydrophobic hydrocarbon core and a region filled with surfactant head groups, part of the counter ions and water, viz. the Stern region.

Micelle formation from surfactant monomers has proved an excellent model process for studying the hydrophobic effect. The formation of an ionic micelle from monomeric ions results in a balance between hydrophobic interactions between the hydrophobic part of the micelle-forming ions, electrostatic interactions between their hydrophilic charged parts, as well as with and between the counterions. Hartley's model [4a] for micelles was that of a spherical aggregate of surfactant molecules whose alkyl groups formed a hydrocarbon core and the polar groups formed a charged surface. The hydrocarbon core is liquid-like and, since there is no void space inside this anhydrous region, the radius is not greater than the stretched-out length

of the surfactant molecule. As a result the aggregate comprises at most 50-100 molecules. The charge density on the micelle surface is less than that expected from the density of packing of charged head groups due to the binding of counter ions to the micelle surface. Counterion binding and diffusion coefficient of a micelle, compared with that of a single surfactant molecule, together explain the sudden decrease in equivalent conductivity of surfactant solutions beyond the cmc; i.e. this description of a micelle of an anionic surfactant has not really been superseded and can be judged from a schematic drawing (Figure 3.1) of sodium dodecyl sulfate [9].

Spherical micelles are formed by anionic surfactants since the electrostatic repulsion between adjacent head groups result in a large value for optimal head group area. Despite this fact, direct visualization has been claimed by Bellare and et al. [2a] in a cryo-TEM image of a 10 mM solution of ditetradecyldimethyl-ammonium acetate. Measurements from the photograph suggest a micelle radius of 3.0 ± 0.3 nm. The dimension of a spherical micelle have been established using several techniques but the most precise has been small angle neutron scattering.

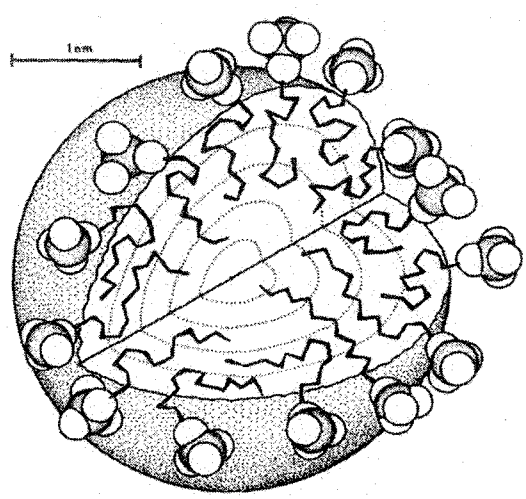

Figure 3.1 Schematic representation of a micelle

In addition, the changes in hydration energies and specific interactions with counterions may also be important [11–15]. The strength and importance of these various interactions depend upon externally controllable factors, such as temperature and ionic strength on the properties of the particular ions involved. Moreover, the structure of the resulting micelle, in particular, its aggregation number, n, its shape, and the compactness of its electrical double layer show some

kind of dependency [14]. Even the molecular conformation of some dimeric surfactants (known as Gemini surfactants) affects the micellization to a large extent [15]. The parameters that illustrates the temperature dependence of hydrophobic effect is the heat capacity of micellization $\left(\Delta_{mic}c_p^0\right)$ which is highly negative and mainly reflects the amount of non-polar solvent accessible area buried on micellization [16]. Since the thermodynamic parameters of micellization are often obtained from the measurements of the critical micelle concentration (cmc), it is important to note that negative values of $\Delta_{mic}c_p^0$ causes a typical U-shaped temperature dependency of cmc. Its minimum occurs at a characteristic temperature (T*) that is often close to room temperature [20]. The shallow minimum around room temperature can be compared with a similar minimum in the solubility of the hydrocarbons in water. Non-ionic surfactants of the polyoxyethylene type deviate from this behaviour and show typically a monotonic, and much more pronounced decrease in cmc with increasing temperature [1,4]. Pressure has little influence on the cmc, even up to high values.

Turning next to the effect of cosolutes, salt addition gives a dramatic lowering of the cmc, though the effect is moderate for short-chain surfactants but is much larger for long-chain ones.

Besides cmc there are many important and intriguing temperature effects in surfactant self-assembly. One, which is of great practical significance, is the dramatic temperature dependant solubility displayed by many ionic surfactants. The solubility may be very low at low temperature and then increases by orders of magnitude in a relatively narrow temperature range. The phenomenon generally denoted as the Krafft phenomenon with the temperature for the onset of the strongly increasing solubility being known as the Krafft temperature [6]. The Krafft phenomenon is best discussed from the interplay between the temperature dependence of the surfactant unimer solubility and the temperature dependence of the cmc.

For surfactants, water does not interact favourably with the hydrophobic groups and there is a driving force for expelling them from the aqueous environment. This may be achieved by a macroscopic phase separation or by 'hiding' the non-polar groups in some other way. For a hydrocarbon in water there is a strong driving force for transfer it to a hydrocarbon phase or some other non-polar

environment. When a polar group is attached to the hydrocarbon an opposing force is created, which counteracts the phase separation. If the opposing force is weak, phase separation will still result. If it is very strong compared to the hydrophobic effect, on the other hand, the amphiphile will occur as single molecules or as small aggregates, like dimmers. It is the common intermediate situation with a balance between hydrophobic and hydrophilic interactions that researchers are concerned within surfactant self-assemblies.

Besides the essential contribution of the hydrophobic effect, the micellization of ionic surfactants in aqueous solution is largely influenced by the electrostatic interactions between the ionized head-groups and their interactions with the surrounding counterions and water molecules. Therefore, the effective charge of the micelle and the nature of counterion have a significant effect on the values of the thermodynamic parameters of micellization. Obviously, the actually existing micelles correspond to the lowest free energy state of the system. Thus, the intense interest in determining the thermodynamic parameters of micelle formation in aqueous solutions, namely, the Gibbs free energy, ΔG^0_m, the enthalpy, ΔH^0_m, and the entropy, ΔS^0_m, because they quantify the relative importance of hydrophobic interactions, surfactant-water contact and (for ionic surfactants) head-group repulsion. These parameters can be derived from the temperature dependence of the critical micelle concentration (cmc), though very highly accurate cmc's are required in order to give satisfactory ΔH^0_m. Among available techniques for studying surfactant aggregation, calorimetry has a distinct advantage, for it is possible to calculate both the cmc and ΔH^0_m directly from the experimental data. Additionally, the calculated enthalpy and entropy characterizes the balance of forces involved in micelle formation. For example, whereas the aggregation is entropy-driven at room temperature, it is enthalpy-driven at higher temperatures [17].

Since the properties of solutions of surface-active agents change markedly when micelle formation commences, many investigations have been concerned with determining values of the cmc in various systems, and a great deal of work has been done on elucidating the various factors that determine the cmc at which micelle formation becomes significant, especially in aqueous media. Among the factors known to affect cmc in aqueous solution are (i) the structure of the surfactant, (ii) the presence of added electrolyte in solution, (iii) the presence of various organic

compounds in solution, (iv) the presence of a second liquid phase and (v) temperature of the solution.

In aqueous medium, the cmc decreases as the number of carbon atoms in the hydrophobic groups increases. For ionic surfactants it was generally found that the cmc became halved by the addition of one methylene group to a straight chain hydrophobic part attached to a single terminal hydrophilic group [4]. Compared to non-ionic surfactants ionic surfactants have much higher cmc values containing equivalent hydrophobic groups. For 12-carbon straight-chain ionics have cmc of ~ 1×10^{-2} M, whereas nonionics with the same hydrophobic group have cmc values of ~1×10^{-4} M. Zwitterionics appear to have slightly smaller cmc value than ionics with the same number of carbon atoms in the hydrophobic groups.

It has also been found [18] that the cmc is higher when the charge on an ionic hydrophilic group is closer to the α-carbon atom of the alkyl hydrophobic group. This is explained as being due to an increase in electrostatic self-potential of the surfactant ion when the ionic head groups moves from the bulk water to the vicinity of the nonpolar micellar core during the process of micellization; work is required to move an electric charge closer to a medium of lower dielectric constant.

In the old literature, the counterion binding of the ionic micelles was not considered; the choice of the standard state was also not consistent [18,19]. In the current literature, the role of the counterion binding has been recognized and the mole fractional scale has been used in the evaluation of the energetics of the process [20,21]. Some cationic surfactants display dramatic effects associated with the nature of the counterion, such as micelle growth, viscoelasticity, shear-thickening, etc. [22,23]. It has been reported that the cetyltrimethylammonium chloride micelles remain nearly spherical over a large range of concentration, even in the presence of NaCl [24]. A substantial amount of work have already been carried out on the binding of monovalent counterions to micelle [13,25,26] for single tail anionic surfactant like dodecyl sulfate. The study of the effect of counterions eliminates some of the complications by leaving the properties of the amphiphilic ion as a constant factor and thus simplifies some of the interpretation of the experimental results. But, it often leads to complications connected with limited stability and preparative difficulties of the surfactant containing different counterions. For cationic surfactants micelle growth is even more pronounced in the presence of lyotropic counterions

such as salicylate, chlorate and nitrate [27,28]. These differences in behaviour reflect differences in the extent of counterion binding to micelles. Thus, the degree of counterion binding to cationic micelles increases in the order Cl^- < Br^- < NO_3^- < salicylate$^-$ [28-30]. However, the critical micellization concentration (cmc) varies only little in going from lithium to cesium dodecyl sulfate [32]. The variations are not dramatic even when replacing the monovalent alkali metal ions by divalent cations such as Mg^{2+}, Co^{2+} and Cd^{2+}. For instance in the case of the dodecyl sulfate surfactants, this substitution results in a decrease of the cmc (expressed in mole of surfactant ion per liter) by a factor of 2 and an increase of the micelle aggregation number from about 65 to 90 [33,34]. However, when compared with Na^+ counterions, polyvalent ions usually markedly reduces the cmc [31] by several order of magnitude and lead the formation of large micelles that may be confirmed from the increase in miceller aggregation number [32,33,41,42]. In aqueous solution the micelles are known to be charged due to a fraction, α, of their counterions dissociates into the aqueous pseudophase. The value of α for a given pure surfactant is important, because both the physical [35,36] and chemical [37] properties of the micelle are influenced by surface charges. The decrease of the surface potential of micelles with decreasing hydrated radius from Li^+ to Cs^+ is in agreement with the modification of the counterion binding [38]. Liu and et al. [39] showed that for a given counterion (Cs^+), the ions are more dissociated in micelles of surfactants with C_{10} chains than with C_{12} chains. From a structural point of view, the effect of counterions has been well documented by Missel et al. [40] for dodecyl sulfates in a salty solution of the same alkali-metal chloride by quasi-elastic light scattering. They proved the tendency of micelles to grow from spherical to long rodlike structures in the order Li^+ < Na^+ < Rb^+ < Cs^+ with a significant change in the aggregation number with temperature.

One of the most interesting aspects of micelles is their ability to accommodate organic molecules [43,44]. An increased flexibility of the micellar membrane and thereby an improved ability to solubilize hydrophobic molecules can be achieved by adding neutral salt and a medium chain alcohol [47-50]. There fore, these elements make the basic components in most microemulsions. However, the intricate behaviour of these mixed micellar aggregates makes it difficult to predict any variation in the system upon variation in the composition of the solution. This

problem is caused by a delicate balance of attractive and repulsive forces among the amphiphilic molecules in the micelles.

The size and shape of micelle aggregates containing commonly used surfactants and co-surfactants have been thoroughly investigated during the past decades [51,52]. The commonly used sodium SDS micelles form spherically aggregates consisting of about 60 monomers in aqueous solutions at cmc [53,54]. Compounds with polar groups such as alcohol molecules can be expected to solubilize in the hydrophilic regions. Addition of alcohol can strongly influence the behaviour of the micelles and changes the micellar size depending on the hydrophilic/hydrophobic character of the alcohol [55,56]. The hydrophilic alcohols (methanol to propanol) mainly solubilize in the aqueous solution and affect the micellization process by modifying the solvent [57], whereas the hydrophobic alcohol molecules (pentanol and higher homologues) take part in the micellization process and become unique components of the micelle aggregates [58]. The degree of solubilization into this shell region depends on the amphiphilic character of the alcohol molecules [57]. The degree of counterion binding also decreses with solubilization of short-chain alcohols (C_2 – C_6) in the palisade layer of the micelle, whereas the solubilization of octane which occurs in the interior of the micelle, does not affect the degree of counterion binding [59]. This is presumably because solubilization in the palisade layer increases the surface area per ionic head group, whereas solubilization in the interior of the micelle does not. It is also decreased by the addition of urea, replacing water from the interface [60].

However, the roles of the amphiphilic alcohol molecules as co-surfactants are still unclear and a matter of discussion. This is especially true for the medium chain length alcohol molecules which are the most commonly used co-surfactants in microemulsions. Even though the influence of *n*-alcohols on the structure of SDS micelles has been extensively investigated, several conflicting results have been reported. Attwood and et al. [61] indicated that SDS micelles decrease progressively in size upon addition of butanol in aqueous salt solutions. Similar result was shown by Boström and et al. [62] in micellar SDS solutions without salt. On the other hand, McGreevy and Schechter [63] observed that the size of the SDS micelles is not influenced upon addition of 1-butanol. Stilbs [64] also reported that SDS micelles grow upon addition of small amounts of butanol and progressively break down

upon addition of butanol in the high concentration range. Førland and et al. [56] on the other hand showed that butanol influences SDS micelles by either increasing or decreasing the size of the micelles depending on the concentration range of the alcohol. However, one can conclude that alcohols affect micellization by extensively regulating the thermodynamics of the process.

Thermodynamics of Micellization: The Mass-action Model

Blandamer et al. [65], Blankschtein et al. [66], Hines, [67] and Zana [68] have reviewed the theories for surfactant solutions. These reviews include many different theories and models for surfactant solutions. However, only few of them have been applied in practice. Different thermodynamic treatments for micelle formation in surfactant solutions are known. Although many efforts have been made towards theoretical understanding of surfactant solutions, capturing the nature of such solutions is still considered rather difficult. In contrast to the rigorous universal thermodynamic treatment of fluid phase equilibrium, many thermodynamic formulations have been proposed for micelle formation. Between those theoretical approaches mass-action model shows its wide acceptance to a number of researchers.

In the mass-action model, the micelle formation is considered as a chemical equilibrium between free surfactant and micelle. At low concentrations, the micelle solution is the formation of aggregates from free surfactant, as shown in equation (3.1).

$$nS \rightleftharpoons S_n \tag{3.1}$$

where n is the number of free surfactant molecules (S), which form a micelle (S_n). Both micelles and free surfactants are treated as solutes in an aqueous solution. In the mass-action model, the thermodynamic formulations are slightly different for nonionic and ionic surfactant solutions. Such thermodynamic formulation may be described as follows (Blandamer and et al.) [65]:

For nonionic (neutral) surfactant solutions, at chemical equilibrium, we have:

$$n_g \mu_{i,mon} = \mu_{i,micelle} \tag{3.2}$$

where $\mu_{i,mon}$ is the chemical potential of monomeric (free) surfactant i, $\mu_{i,micelle}$ is the

chemical potential of surfactant i in the micelle form, n_g is the aggregation number. The chemical potentials of monomeric surfactant and surfactant in micelle are given as:

$$\mu_{i,mon} = \mu^0_{i,mon} + RT \ln x_{i,mon} \gamma_{i,mon} \tag{3.3}$$

$$\mu_{i,micelle} = \mu^0_{i,micelle} + RT \ln x_{i,micelle} \gamma_{i,micelle} \tag{3.4}$$

Now, we have:

$$\Delta G^0_{i,m} = \frac{1}{n_g}\mu^0_{i,micelle} - \mu^0_{i,mon} = RT \ln x_{i,mon} \gamma_{i,mon} - \frac{1}{n_g} RT \ln x_{i,micelle} \gamma_{i,micelle} \tag{3.5}$$

where $x_{i,mon}$ and $x_{i,micelle}$ are the mole fraction of monomeric surfactant and surfactant in micelle, respectively, where $\gamma_{i,mon}$ and $\gamma_{i,micelle}$ are the activity coefficients and $\mu^0_{i,mon}$ and $\mu^0_{i,micelle}$ are the standard state chemical potential of the same, $\Delta G^0_{i,m}$ is the standard Gibbs energy of micellization.

For a dilute solution, the activity coefficients of monomeric surfactant and surfactant in micelle are set equal to 1. Then equation (3.5) becomes

$$\Delta G^0_{i,m} = RT \ln x_{i,mon} - \frac{1}{n_g} RT \ln x_{i,micelle} \tag{3.6}$$

In surfactant solution, the total concentration of surfactant, x_{tot}, which is a sum of free surfactant, $x_{i,mon}$ and surfactants in micelles, $x_{i,micelle}$. Assuming a sufficiently high value for n_g, the second term in the above equation become very small and can be neglected. Then $x_{i,mon}$ can be approximated to CMC.

But for ionic surfactants the micellization equilibrium for ionic surfactant can be expressed as:

$$xS^- + x\beta M^+ \rightleftharpoons (SM_\beta)_x^{-x(1-\beta)} \tag{3.7}$$

where $(SM_\beta)_x$ is the micelle composed of x surfactant monomers and $x\beta$ counterions bearing S^- and M^+ as the monomer and counterion of the surfactant forming micelles. The value of β may corresponds the fraction of bound counterion

in the micelle. But for nonionic surfactants monomers and micelles are obviously uncharged and M^+ does not enter to the equation and the model approaches to a limiting case having $\beta = 0$. However, applying the mass action law to the monomer-micelle equilibrium for the ionic surfactant, and taking into account the charges of counterion along with the other parameters, the Standard Gibbs free energy, ΔG^0_m can be expressed as [21a,68,69]:

$$\Delta G^0_{i,m} = (2-\alpha)RT \ln x_{i,cmc} \qquad (3.8)$$

for an ionic uni-univalent surfactant. Here χ_{cmc} is the cmc expressed in mole fraction scale and $\alpha = 1 - \beta$.

The standard thermodynamic parameters, ΔG^0, ΔH^0 and ΔS^0 indicate what is happening in a process. The standard free energy change upon micellization, ΔG^0_m tells us whether the process is spontaneous ($\Delta G^0_m < 0$) or not and the magnitude of the driving force. The standard enthalpy change upon micellization, ΔH^0_m, on the other hand shows whether bond making ($\Delta H^0_m < 0$) or bond breaking (($\Delta H^0_m > 0$) predominates in the micellization process. The standard entropy change, ΔS^0_m indicates whether the system becomes more structured ($\Delta S^0_m < 0$) or more random ($\Delta S^0_m > 0$).

Because of the characteristic behaviour of surfactants to orient at surfaces and to form micelles, their applicability varies with the phase as foaming agents, emulsifiers, and dispersants. The type of surfactant behaviour, whether acting as an emulsifier or dispersant or otherwise, depends on the structural groups on the molecule. It has been a long-term goal of surfactant chemists to devise a quantitative way of correlating the chemical structure of surfactant molecules with their surface activity to facilitate the choice of material for a particular use.

Sodium lauryl sulfate (SLS) or sodium dodecyl sulfate (SDS), $C_{12}H_{25}SO_4Na$ is an anionic surfactant that is used in industrial products including engine degreasers, floor cleaners and car wash soaps; as well as in household products such as toothpastes, shampoos, shaving foams, some dissolvable aspirins, fiber therapy caplets, and bubble baths for its thickening effect and its ability to create a lather. The molecule has a tail of 12 carbon atoms, attached to a sulfate group, giving the molecule the amphiphilic properties required of a detergent. It is probably the most researched anionic surfactant compound

that attracted researchers from early decades [32,34] to present times [11-13] due to its simple single tail structure and the ability to form stable micelles. Besides micellization interaction with dyes [70], electrophoresis and electrokinetics [72] with SDS has also been reported. It has recently found application as a surfactant in gas hydrate or methane hydrate formation reactions, increasing the rate of formation as much as 700 times [71].

On the other hand Aerosol-OT (AOT, sodium bis-(2-ethyl-1-hexyl) sulfo-succinate), bears great myths in surfactant science [73,74] due to reach phase behaviour and its ability to form microemulsion. It is a nontoxic compound and can be used in pharmaceutical and medicinal preparations. Unlike most amphiphiles and like many phospholipids, it is a double tailed anionic surfactant which can conveniently used in solubilization and emulsification purposes. Its versatile surface chemical performance, wide use and nontoxic nature classify AOT with a distinction, and a comprehensive discussion on its physicochemical and surface chemical properties and uses is, therefore needed. This promoted us to select the above single and double tailed anionic surfactants (viz., SDS and AOT) for the present study. Figure 3.2 shows the molecular structures of SDS and AOT schematically.

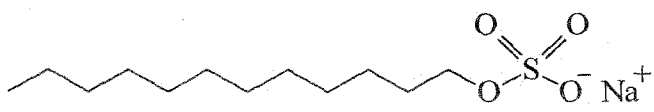

(a)

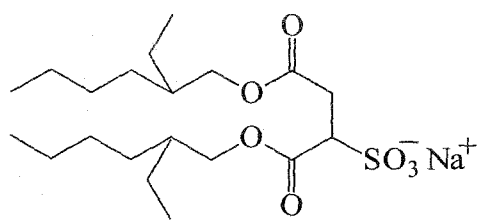

(b)

Figure 3.2 Schematical molecular structures of (a) SDS and (b) AOT surfactants.

3.2 Effect of Counter Ions on Temperature Dependant Micellization in Aqueous Medium

In a number of series of cationic surfactants, Zana [6b] has shown that the degree of binding is related to the surface area per head group in the micelle. It was observed that as the degree of binding increasing, the surface area per head group decreases (i.e., as the surface charge density increases). Counterion binding also increases with increase in the electrolyte content of the solution [21b] and may also increase when surfactant concentration increase produces micellar growth [22b], presumably because both of these are accompanied by a decrease in head group area. The ionic micelles that have more tightly bound counterions are more nonionic in character than those with a greater degree of ionization, have lower water solubility, and are more likely to have nonspherical micelles in aqueous solution.

In connection with micellization it is also evident that the aggregation number of ionic micelles, at a constant temperature, depends only on the concentration of counterions, C_{aq} in the aqueous phase [12]. Ionic micelles grow in response to increase in the value of whether the counterions are provided by the surfactant alone or by the surfactant plus any added electrolyte [12]. Thus C_{aq} can be written as [11]:

$$C_{aq} = F(S_t)[\alpha S_t + (1-\alpha)S_m] \qquad (3.9)$$

where S_m and S_t are the monomeric and the total concentration of the surfactant respectively. The factor $F(S_t) = 1/(1-\theta)$, where θ is related to the volume fraction occupied by the micelles. In this present work some studies with a series of surfactants derived from SDS and AOT (the sodium salt of the diester) by varying the counter ions. Thus a series of alkali metal ions, viz. Li^+, Na^+, K^+ along with the NH_4^+ and tetraalkylammonium ions, viz. $N^+(CH_3)_4$, $N^+(C_2H_5)_4$, $N^+(C_3H_7)_4$, $N^+(C_4H_9)_4$ are investigated. There are some evidences [21,22,32] that the counterions exhibit mainly electrostatic interaction or, no chemical interaction is to be expected on the structural grounds. Therefore, it is the system where the cmc differences are rather small and the effect of ionic size and of physical adsorption can be best investigated. The objective is, therefore, to determine the cmc with high accuracy within a temperature range of 283 - 313K of both SDS and AOT surfactants having different

counter cations in aqueous medium and to calculate different thermodynamic parameters of micellization, viz. changes in standard Gibbs free energy (ΔG_m^0), standard enthalpy (ΔH_m^0), standard entropy (ΔS_m^0), maximum surface excess concentration (Γ_{max}), and the minimum areas per molecule (A_{min}) at the surface in order to examine the effect of ionic sizes on the micellization.

3.2.1 Experimental section

Materials

Surfactants with the desired counterions were prepared by following the technique of Eastoe and et al. [75] and the extended work of Temsamani and et al. [76] and Benrraou and et al. [13]. A high grade purified sample of SDS and AOT from Fluka (Switzerland) were used for the present study. Both of them produced no minima in the surface tension vs concentration plots indicating good purity of the compounds. The samples are converted into the surfactants bearing different counterions by ion exchange technique using a strong ion exchange resin (Amberlite IR-120, 20-50 mesh, Loba Cheme, India). The process is described below:

A 10g sample of SDS or AOT was dissolved in 20mL of a 1:1 (v/v) mixture of water and ethanol. The solution was passed through a column (40cm x 2 sq. cm) of a strong ion exchanger in the H^+ form slowly. The resin was put in the acid form by using a large excess of a 0.20M aqueous hydrochloric acid solution and washed with water until the complete removal of the excess acid takes place. The free acid formed on passing the SDS or AOT through the resin was then immediately neutralized with an aqueous solution of the hydroxides of the desired counter ions (viz. Li^+, K^+, NH_4^+, $N^+(CH_3)_4$, $N^+(C_2H_5)_4$, $N^+(C_3H_7)_4$ and $N^+(C_4H_9)_4$). All the hydroxides of high purity were procured from Across Chem., Belgium. The solvent water was then removed fast by freeze drying and then keeping under vacuum (bath temperature 313K) for several days and the waxy solid was finally dried in vacuum over P_2O_5. These materials contain residual water, which were finally removed by the action of P_2O_5 (from Loba Cheme, India) on a solution of surfactant in isooctane (≥ 99.5% from Merck, India). The extent of Na^+/H^+ ion exchange was optimized by controlling the flow rate of the solution and finally H^+ content of the surfactant solution (acid form) was measured by titrating with standard NaOH. The extent of exchange was found

to be more than 99%. Among all the ion-exchanged surfactants TBADS and tetrabutylammonium-AOT did not crystallize at room temperature even after keeping at low temperature for several months. It appeared as a highly viscous, colourless semi-solid material. Doubly distilled water having conductivity 2 μS cm^{-1} was used throughout the experiment.

Methods

The cmc values were determined [77-80] from the surface tension as well as specific conductance data. It is customary to plot the (i) surface tension γ against the logarithmic value of the surfactant concentration C and the (ii) conductance Λ against the concentration of the surfactant, where the break indicates the cmc of a particular system. The surface tension experiments were done by platinum ring detachment method using a Tensiometer (K9, KRÜSS; Germany), at different temperatures. The accuracy of the measurement was within ±0.1mNm^{-1}. Temperature of the system was maintained by circulating auto-thermostated water through a double-wall glass vessel containing the solution. Similar studies were also done condutometrically by using an electrical conductivity bridge (METTLER TOLEDO, Switzerland). The conductance values were uncertain within the limit of ± 1%. Each measurement was repeated several times at each temperature in the ranges 283 - 313K. Measurements were made at 5K intervals of temperature. In this connection it may be noted that for anionic surfactants of structure $RC(O)N(R^1)CH_2CH_2COO^-Na^+$, it has been found [81-83] that the break in the conductance-surfactant concentration plot may be smaller than expected or absent, yielding binding values (β) much smaller than those of comparable surfactants without the amide group. This may be due to the protonation of the carboxylate group and hydrogen bonded ring formation with the amido group, with simultaneous release of the Na^+, upon micellization.

3.2.2 Results and Discussion

The cmc corresponds to a concentration at which a very small but often clearly detectable concentration of the micelles exists. Typical experimental curves of salt free systems are obtained in both surface tension and conductance measurements. The 'break point' or the point of intersection of the two surface

tension and conductivity lines was taken as the cmc at a particular temperature. The cmc values determined by two methods for both dodecyl sulfate and bis-(2-ethyl-1-hexyl) sulfosuccinate) with each counterion are in close agreement with one another. The cmc of SDS and AOT is also in good agreement with the literature value [13,16,75,76]. Figure 3.3 - 3.31 are the plots obtained in the surface tension and conductivity measurements.

In all instances, the change of cmc with temperature is small. For the present purpose the surfactants having different counterions have been classified into two categories: one containing different alkali metal counterions along with NH_4^+ and the other having various tetraalkylammonium counterions. It is found that at a concentration of 10 times the cmc, potassium dodecyl sulfate and potassium salt of AOT is not completely soluble in water at room temperature. The solution contains hydrated crystals dispersed in a micellar phase. Below 313K K-AOT (bis-(2-ethyl-1-hexyl) sulfosuccinate having K^+ as counter ion) forms clear solution. Thus the micellization of K-AOT has been investigated in the limited range within 283-308K. However, in the case of potassium dodecyl sulfate, which has a Krafft temperature of 307K at the cmc [84] it was impossible to investigate the micellization process since the temperature leading to a clear solution was too high (323K). Mukerjee and et al. [85] and Romsted et al. [86] also reported this solubility gap for potassium alkyl sulfates.

This is well known that hydrophobic property of the tail and the hydrophilic property of the head group of a surfactant molecule are together responsible in forming micelles in water. It is, therefore, not surprising that as the hydrocarbon chain length is increased; micelles are formed at lower concentrations due to increased hydrophobicity of the hydrocarbon tail [92]. Similarly it is quite obvious that as the hydrated ionic size is increased from NH_4^+ to Na^+, cmc value is decreased due to increasing hydrophilicity. The counterionic activity in micellization is not completely similar in dodecyl sulfate and AOT. At a particular temperature (below 303K), cmc depends upon the nature of the counterion following the order $NH_4^+ > Li^+ > Na^+$ in dodecyl sulfate, whereas for AOT cmc decreases in the order $NH_4^+ > Na^+ > Li^+ > K^+$. But at high temperature (above 323K) AOT micelles are rather insensitive to temperature variation. This decrease was explained by considering the binding of counterions to micelles. The determination of partial volumes and

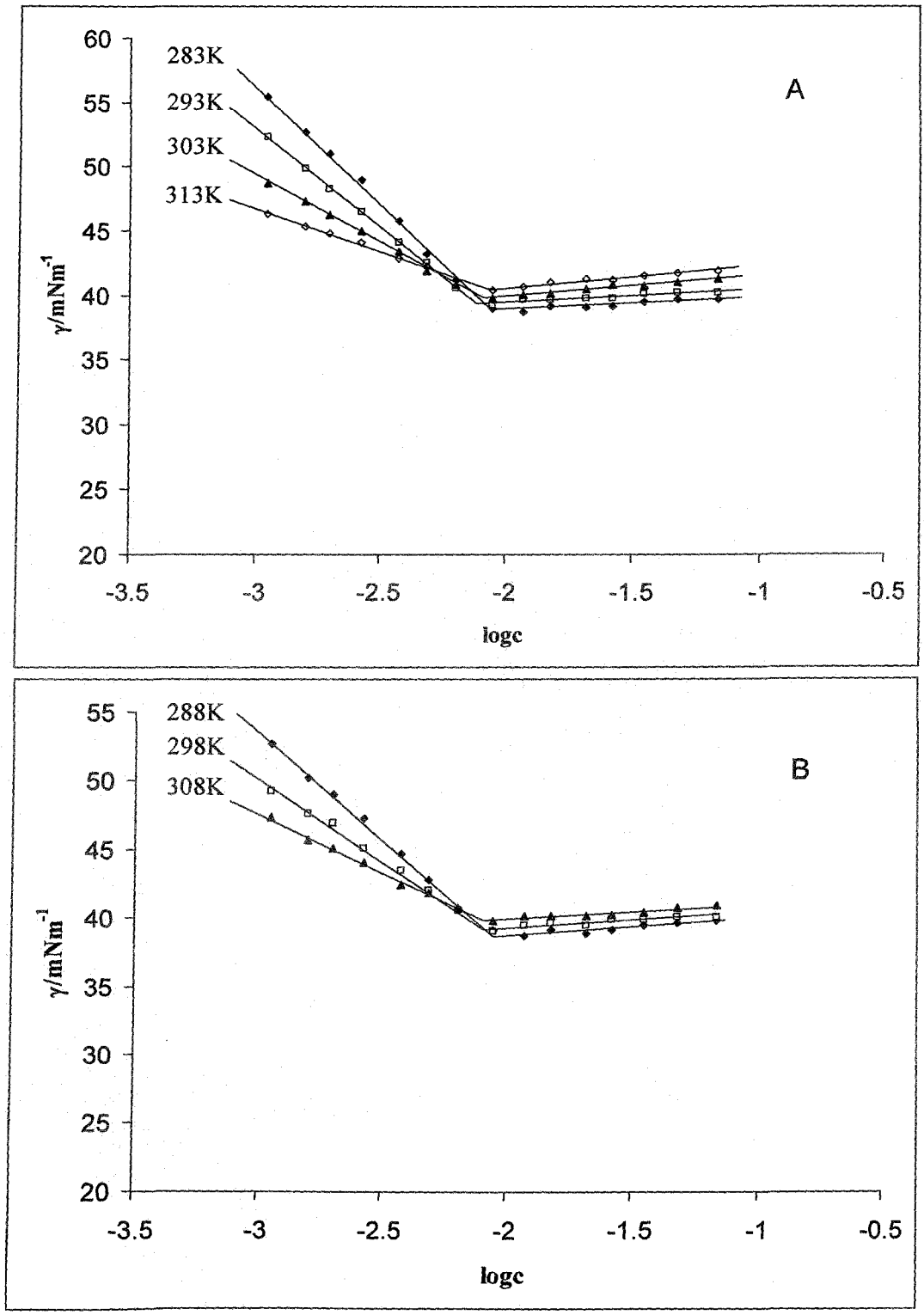

Figure 3.3: Surface tension, γ, of lithium dodecyl sulfate (LDS) in aqueous solution as a function of the logarithm of the surfactant concentration at different temperatures (A: temperature 283K, 293K, 303K, 313K), B: temperature 288K, 298K, 308K).

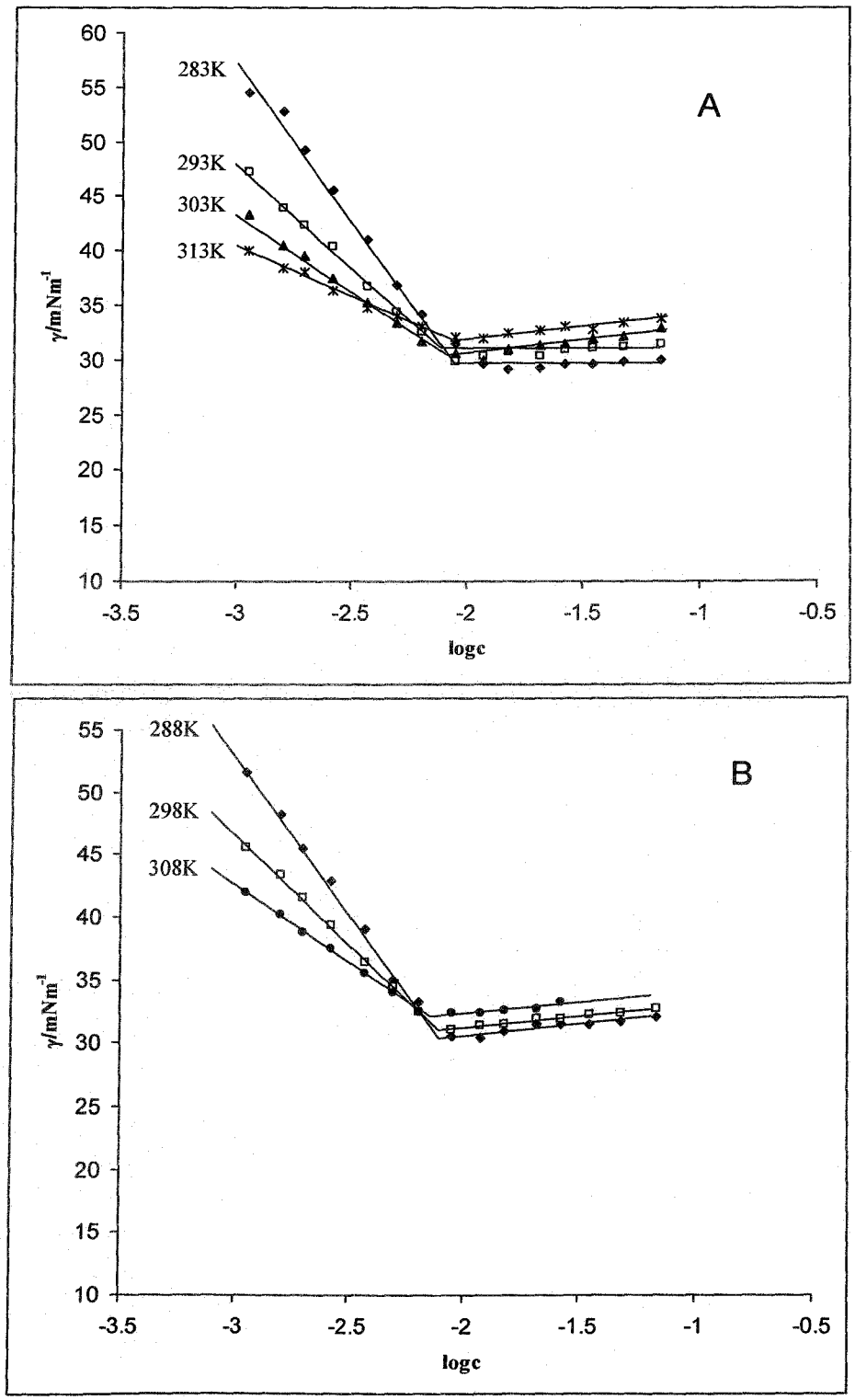

Figure 3.4: Surface tension, γ, of SDS in aqueous solution as a function of the logarithm of the surfactant concentration at different temperatures (A: temperature 283K, 293K, 303K, 313K), B: temperature 288K, 298K, 308K).

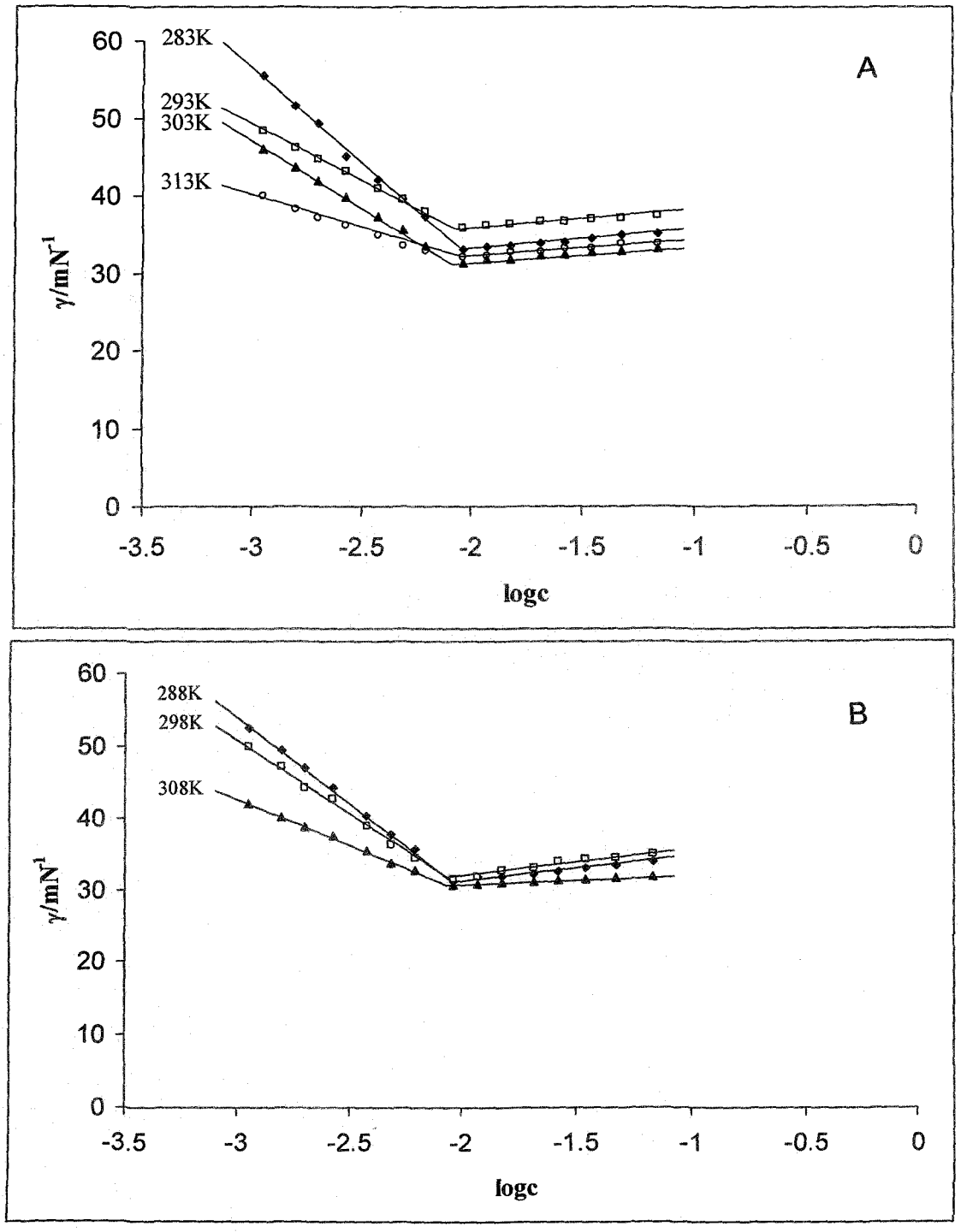

Figure 3.5: Surface tension, γ, of ammonium dodecyl sulfate (ADS) in aqueous solution as a function of the logarithm of the surfactant concentration at different temperatures (A: temperature 283K, 293K, 303K, 313K), B: temperature 288K, 298K, 308K).

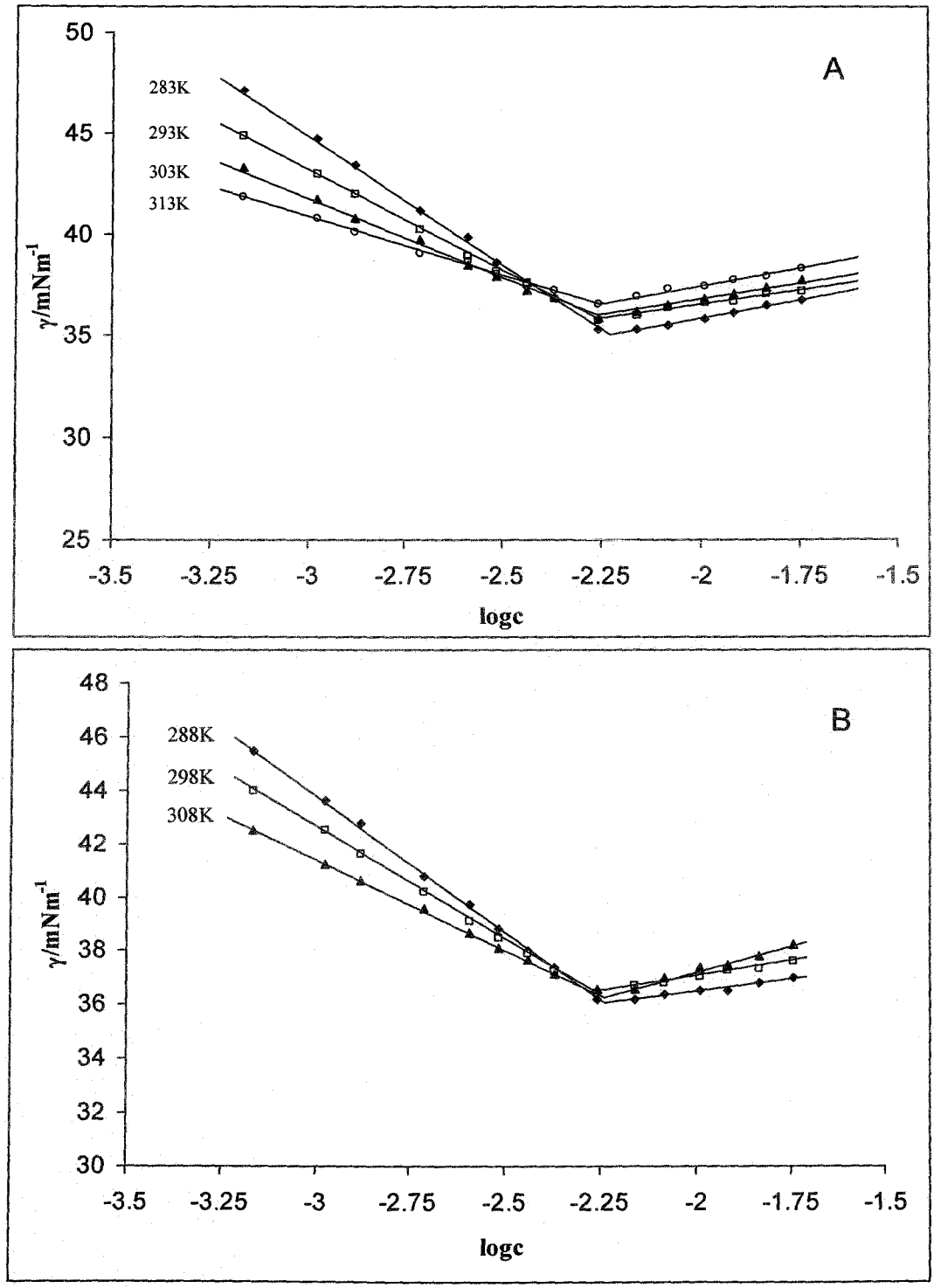

Figure 3.6: Surface tension, γ, of tetramethylammonium dodecyl sulfate (TMADS) in aqueous solution as a function of the logarithm of the surfactant concentration at different temperatures (A: temperature 283K, 293K, 303K, 313K), B: temperature 288K, 298K, 308K).

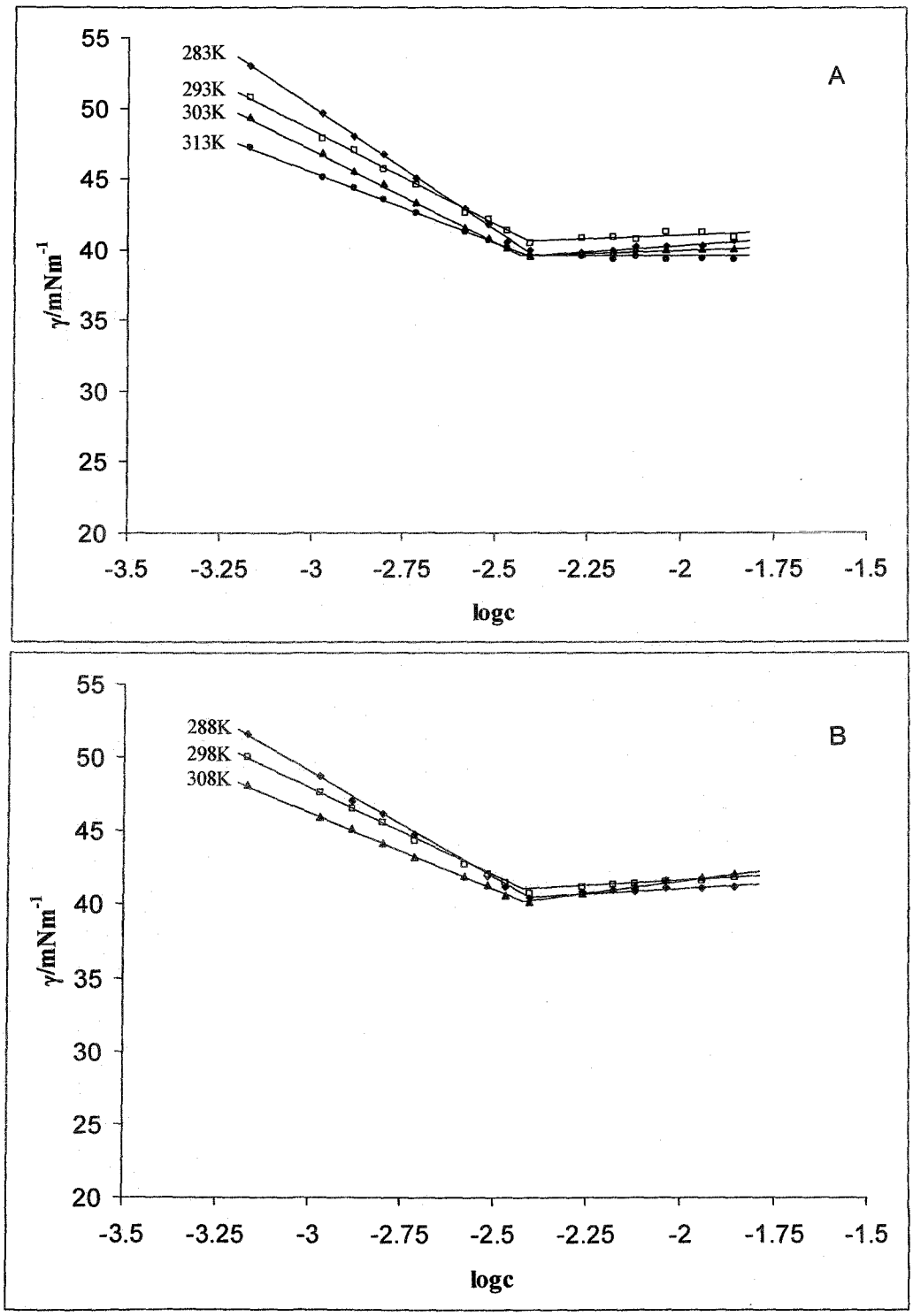

Figure 3.7: Surface tension, γ, of tetraethylammonium dodecyl sulfate (TEADS) in aqueous solution as a function of the logarithm of the surfactant concentration at different temperatures (A: temperature 283K, 293K, 303K, 313K), B: temperature 288K, 298K, 308K).

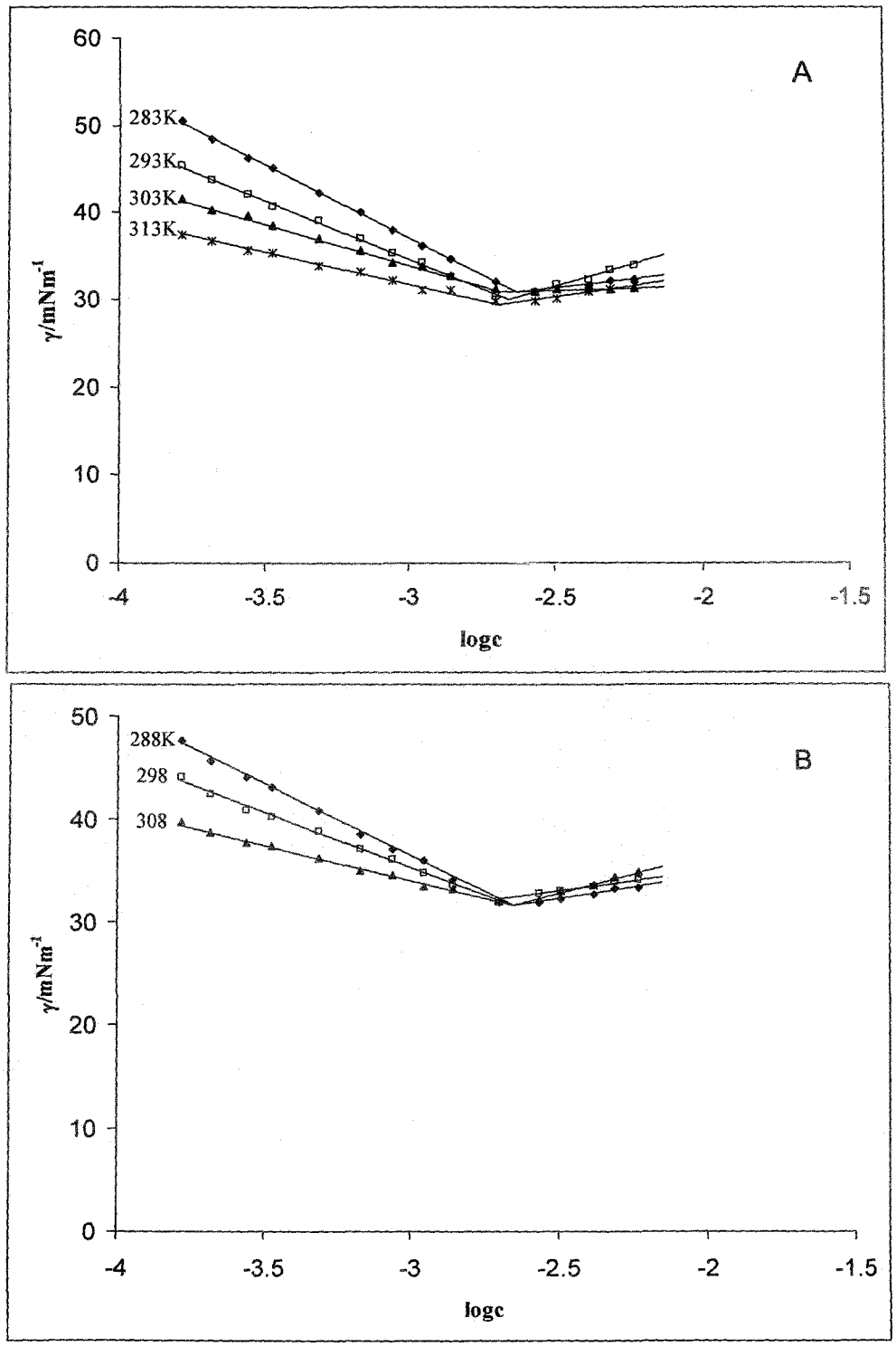

Figure 3.8: Surface tension, γ, of tetrapropylammonium dodecyl sulfate (TPADS) in aqueous solution as a function of the logarithm of the surfactant concentration at different temperatures (A: temperature 283K, 293K, 303K, 313K), B: temperature 288K, 298K, 308K).

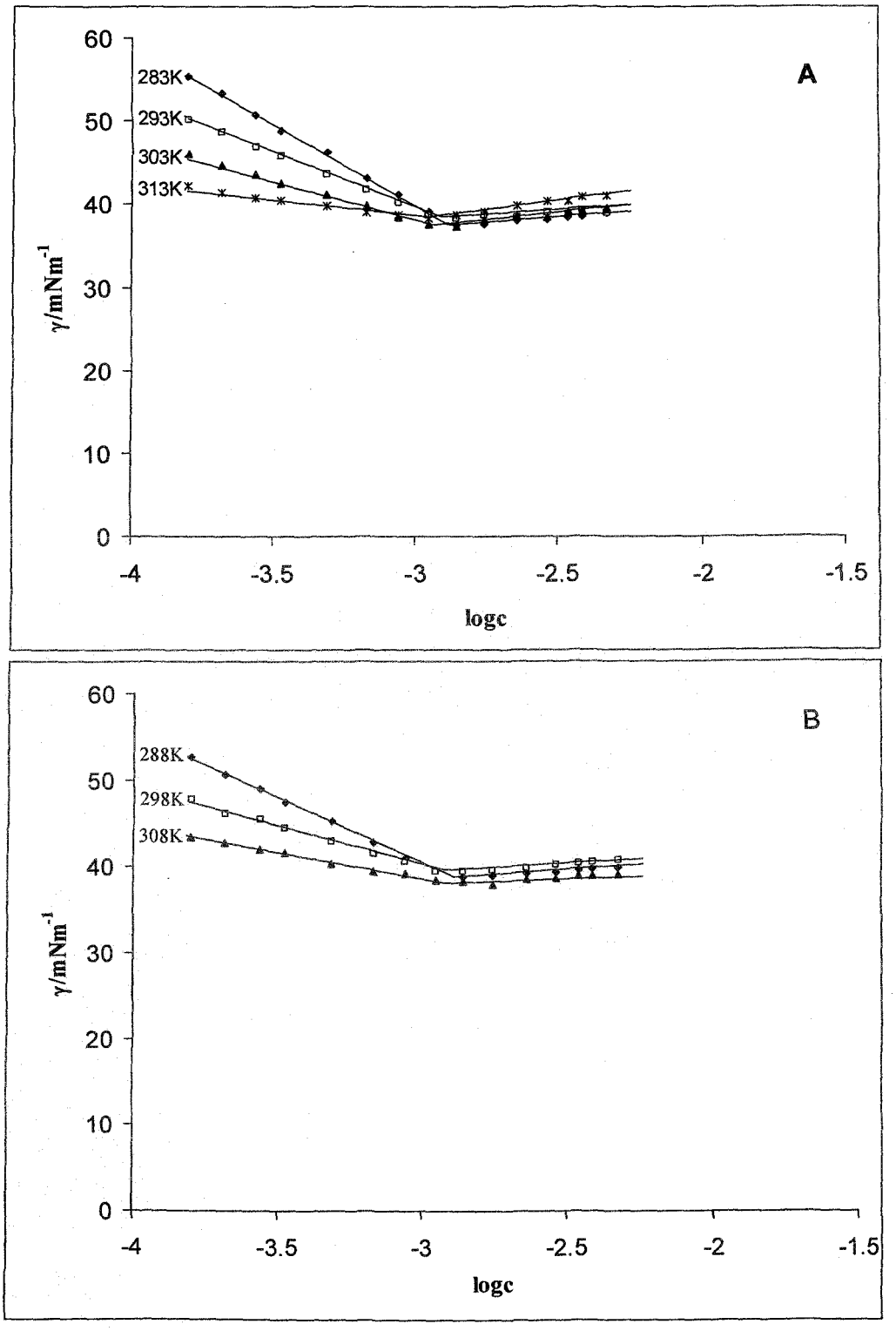

Figure 3.9: Surface tension, γ, of tetrabutylammonium dodecyl sulfate (TBADS) in aqueous solution as a function of the logarithm of the surfactant concentration at different temperatures (A: temperature 283K, 293K, 303K, 313K), B: temperature 288K, 298K, 308K).

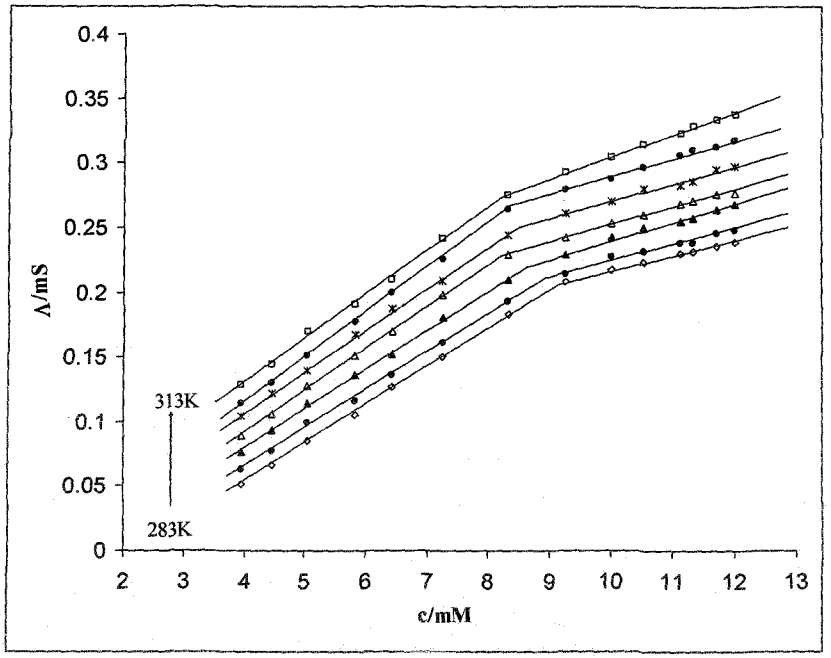

Figure 3.10: Conductance, Λ, of Lithium dodecyl sulfate (LDS) in aqueous solution as a function of the surfactant concentration at temperatures ranging 283K to 313K with 5K interval.

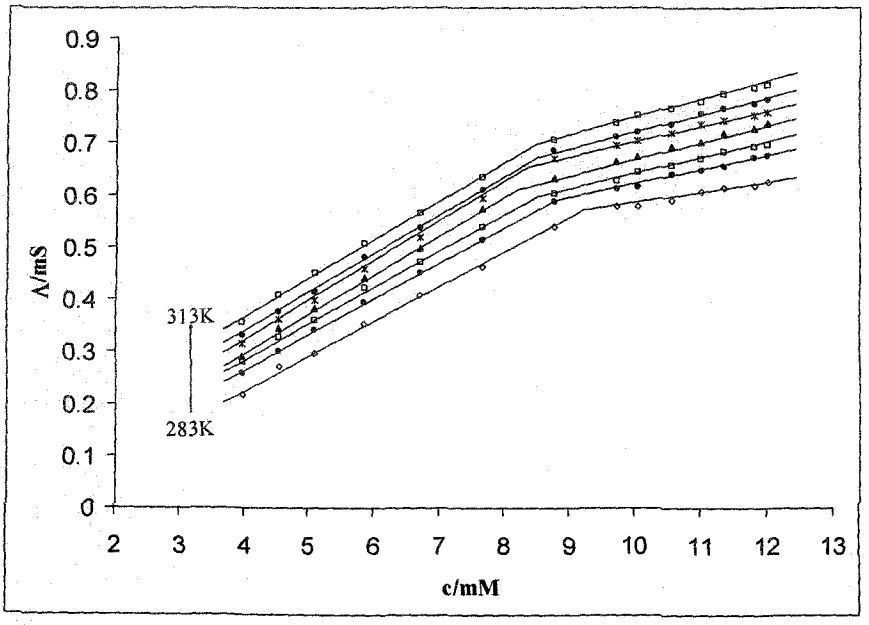

Figure 3.11: Conductance, Λ, of SDS in aqueous solution as a function of the surfactant concentration at different temperatures ranging 283K to 313K with 5K interval.

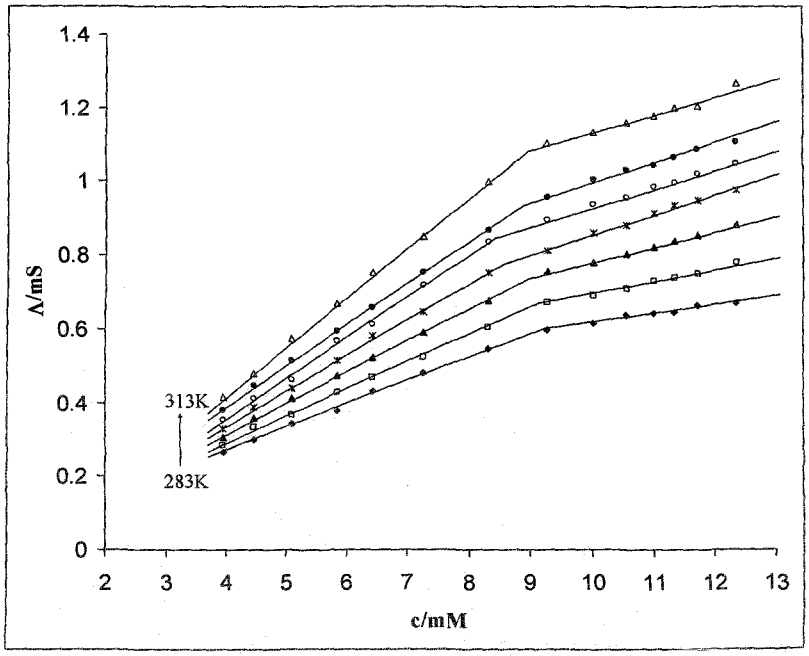

Figure 3.12: Conductance, Λ, of Ammonium dodecyl sulfate (ADS) in aqueous solution as a function of the surfactant concentration at different temperatures ranging 283K to 313K with 5K interval.

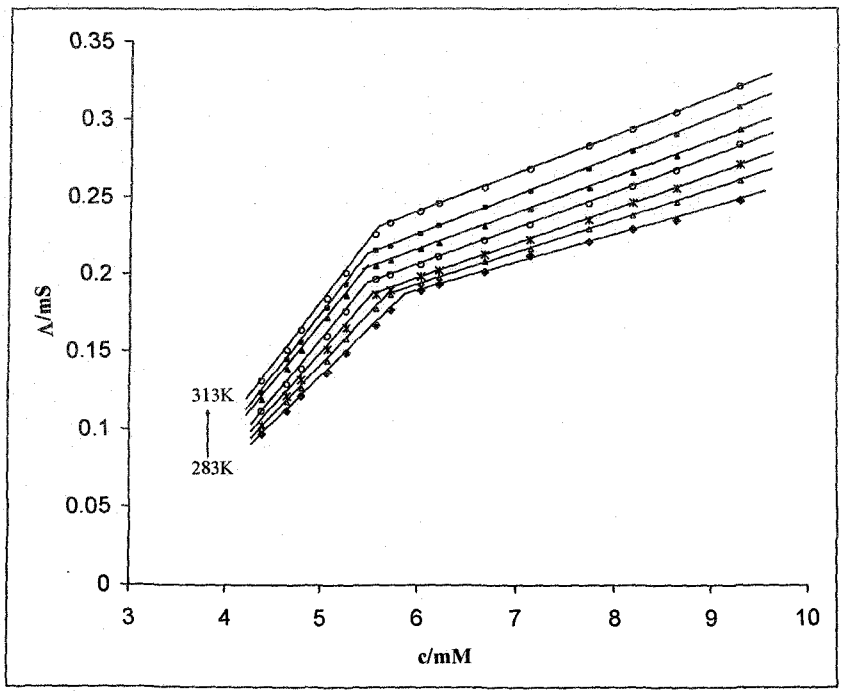

Figure 3.13: Conductance, Λ, of Tetramethylammonium dodecyl sulfate (TMADS) in aqueous solution as a function of the surfactant concentration at different temperatures ranging 283K to 313K with 5K interval.

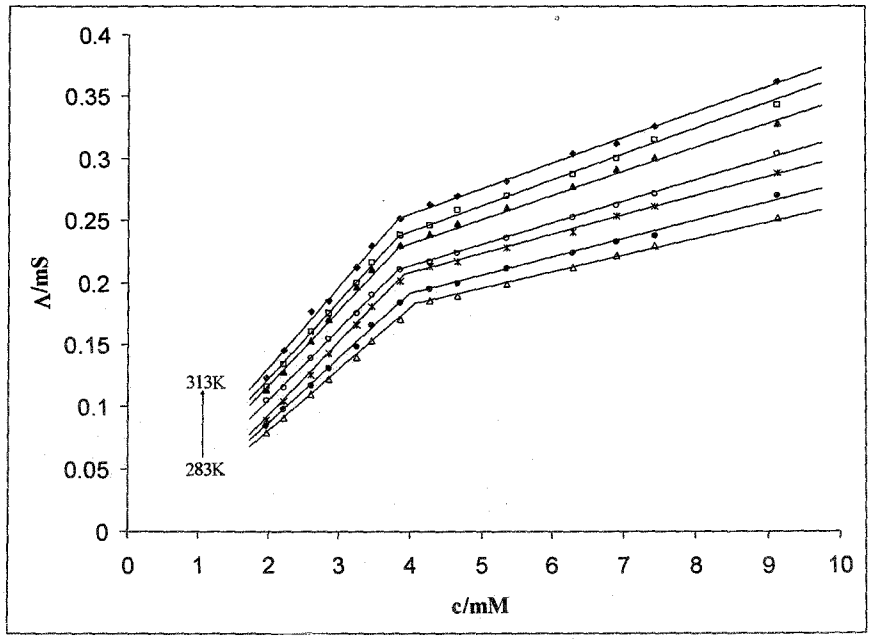

Figure 3.14: Conductance, Λ, of tetraethylammonium dodecyl sulfate (TEADS) in aqueous solution as a function of the surfactant concentration at different temperatures ranging 283K to 313K with 5K interval.

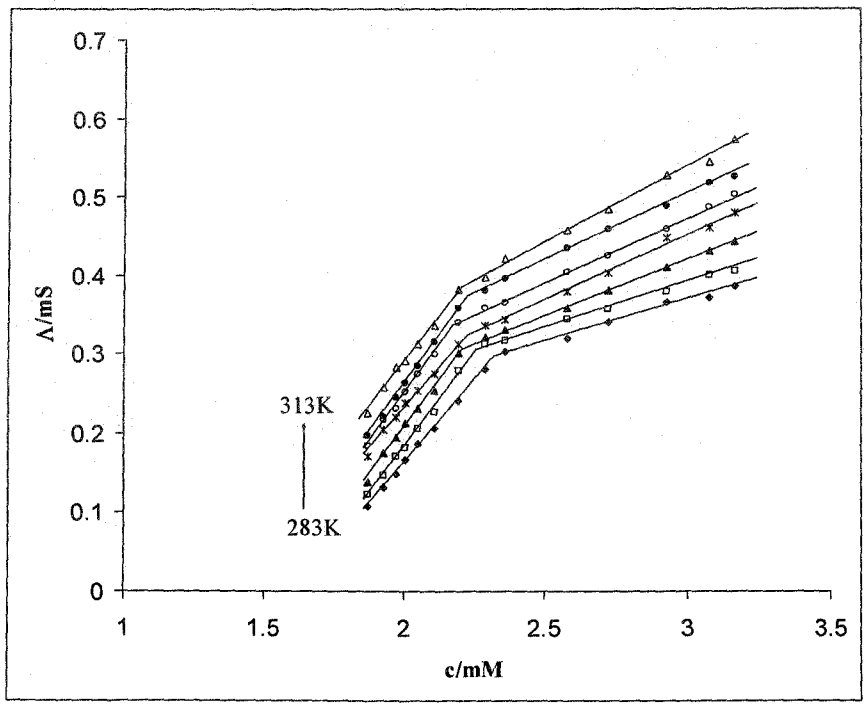

Figure 3.15: Conductance, Λ, of tetrapropylammonium dodecyl sulfate (TPADS) in aqueous solution as a function of the surfactant concentration at different temperatures ranging 283K to 313K with 5K interval.

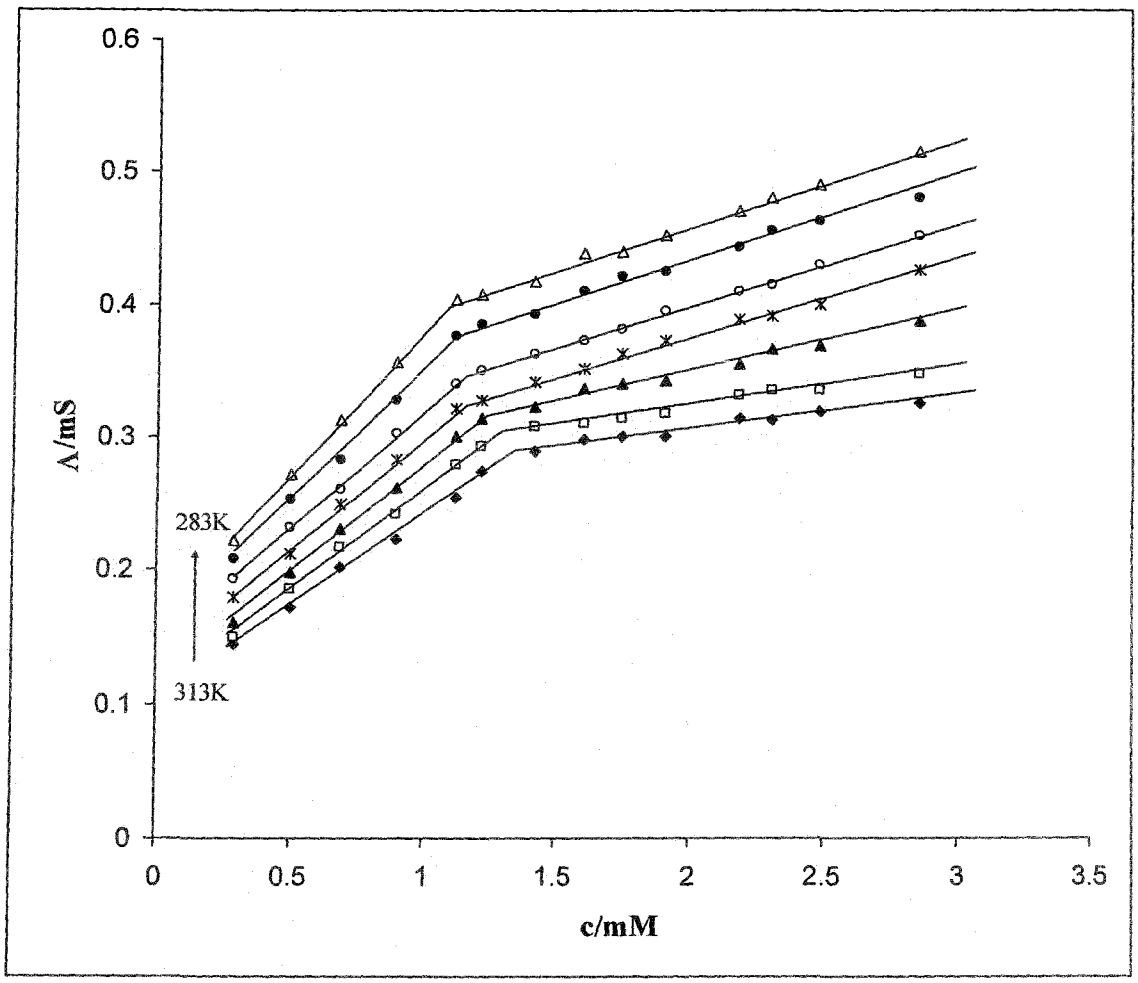

Figure 3.16: Conductance, Λ, of tetrabutylammonium dodecyl sulfate (TBADS) in aqueous solution as a function of the surfactant concentration at different temperatures ranging 283K to 313K with 5K interval.

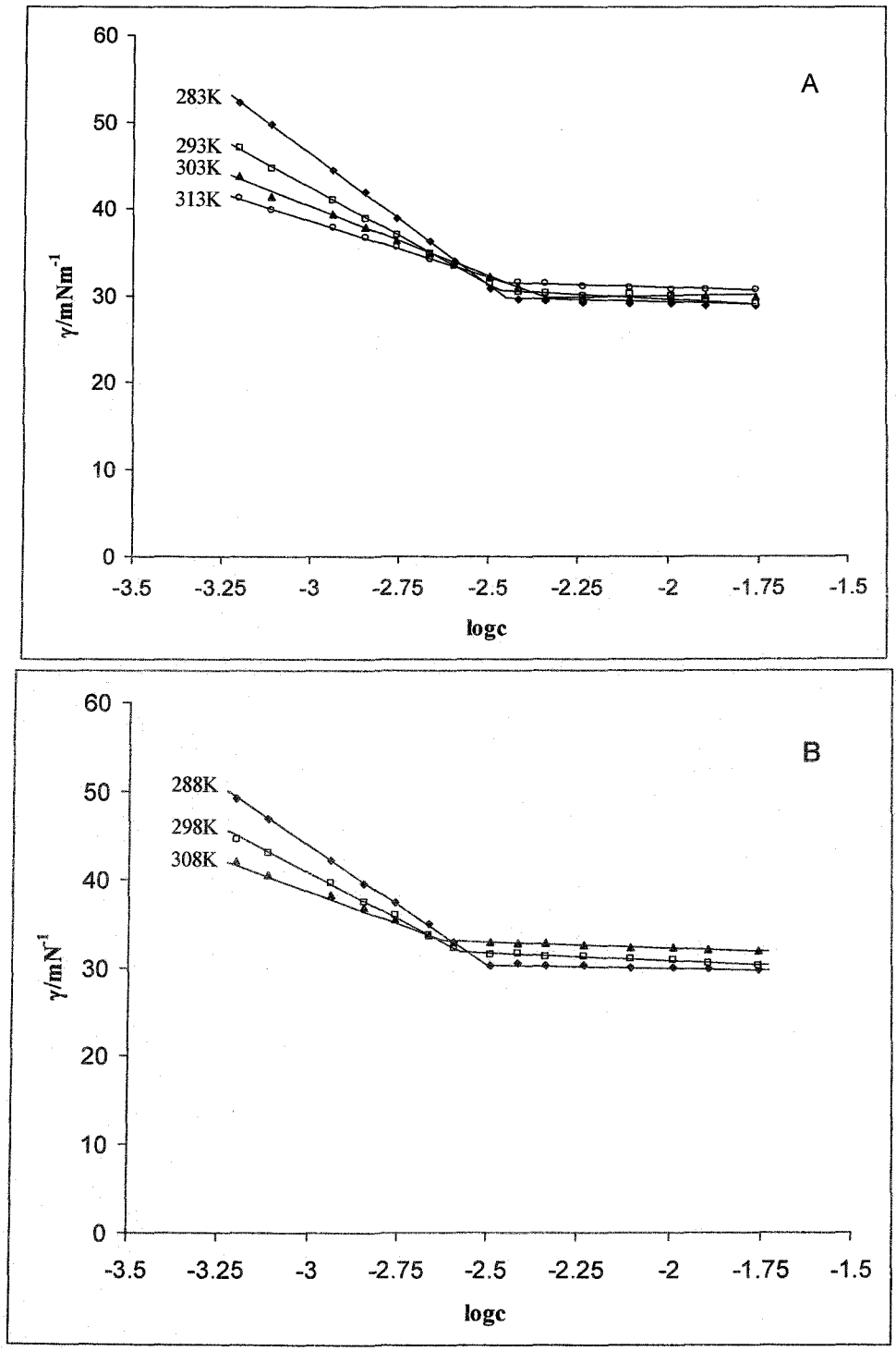

Figure 3.17: Surface tension, γ, of AOT (sodium salt) in aqueous solution as a function of the logarithm of the surfactant concentration at different temperatures (A: temperature 283K, 293K, 303K, 313K), B: temperature 288K, 298K, 308K).

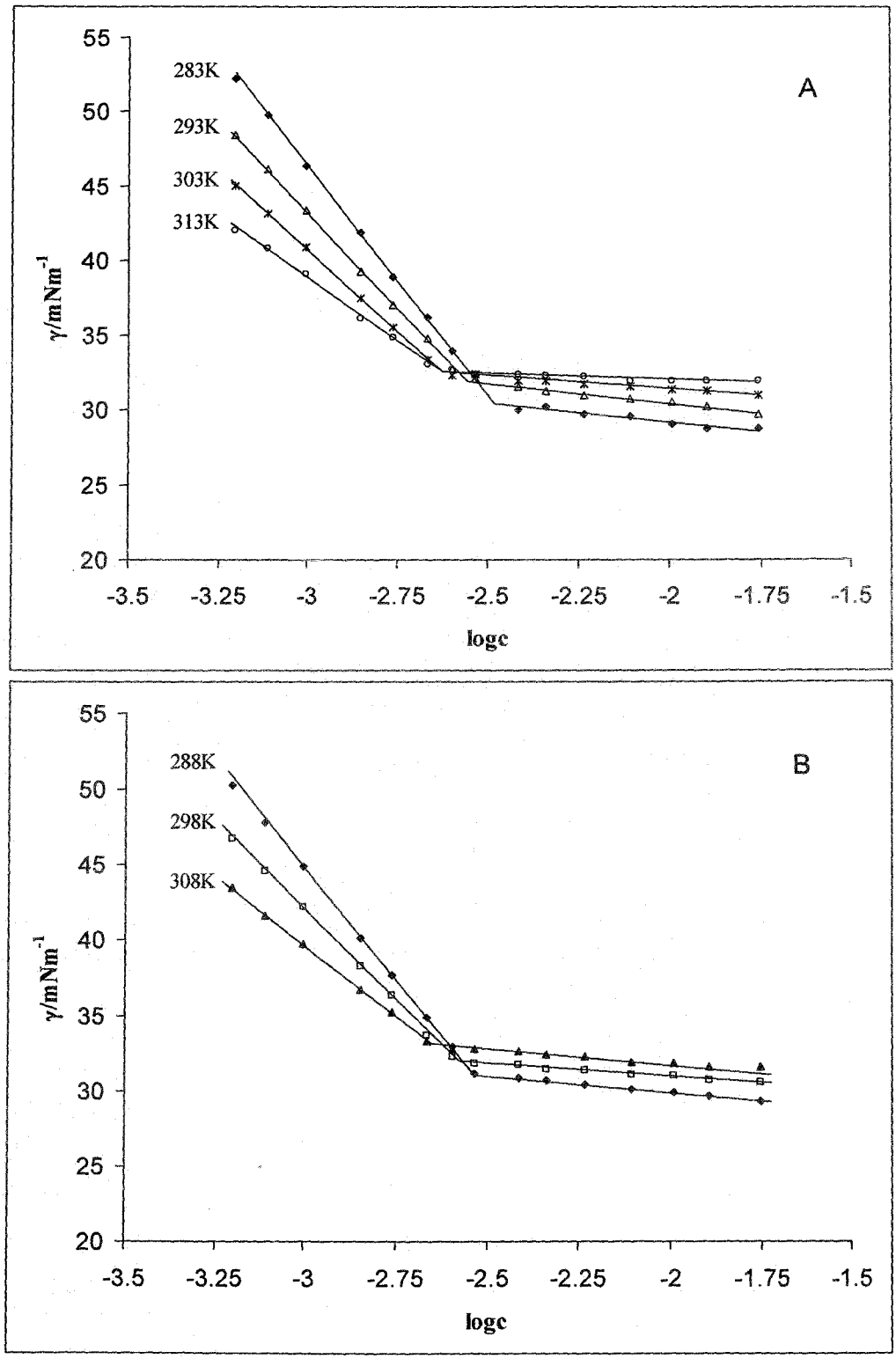

Figure 3.18: Surface tension, γ, of AOT (lithium salt) in aqueous solution as a function of the logarithm of the surfactant concentration at different temperatures (A: temperature 283K, 293K, 303K, 313K), B: temperature 288K, 298K, 308K).

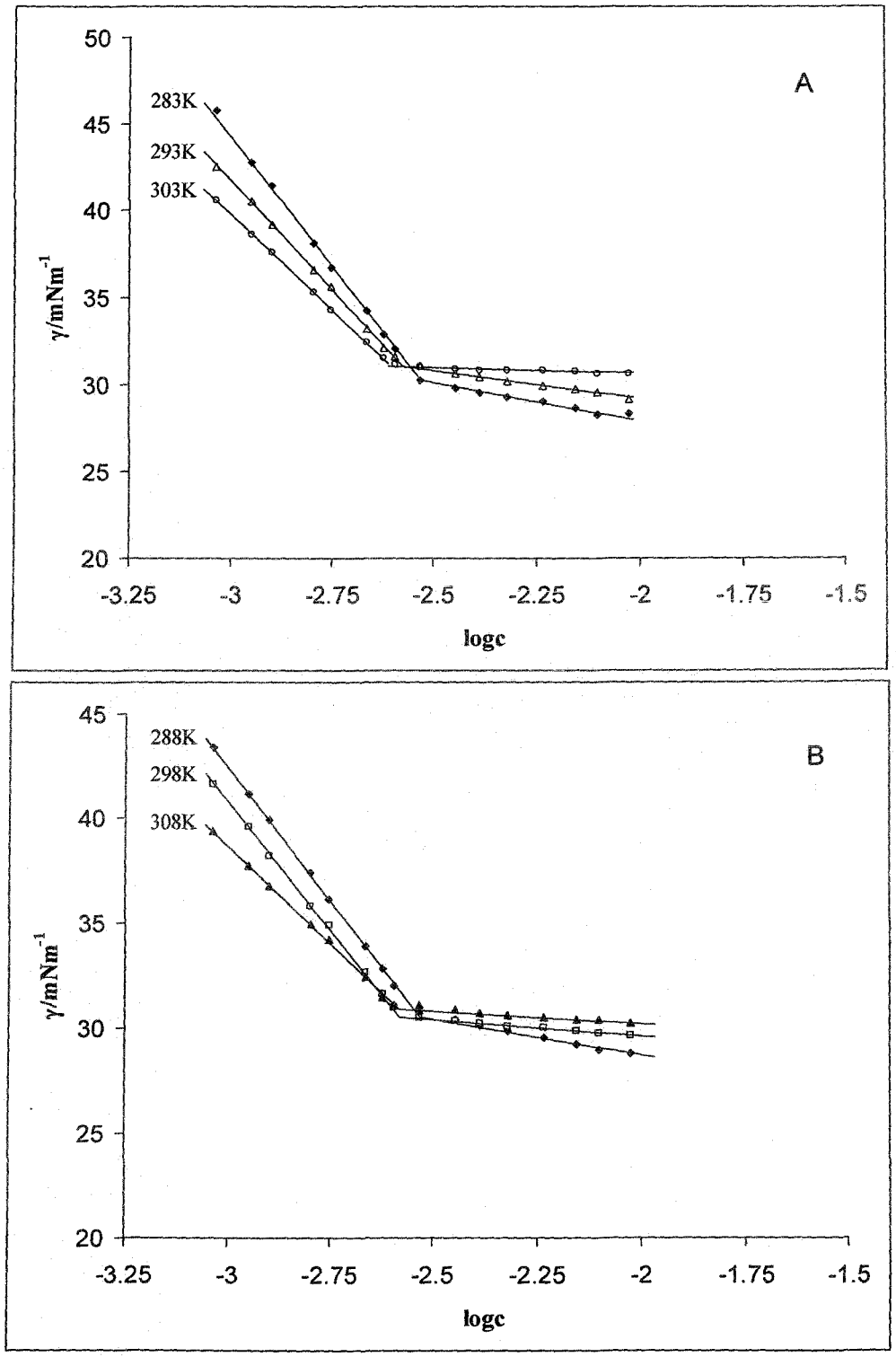

Figure 3.19: Surface tension, γ, of AOT (potassium salt) in aqueous solution as a function of the logarithm of the surfactant concentration at different temperatures (A: temperature 283K, 293K, 303K, 313K), B: temperature 288K, 298K, 308K).

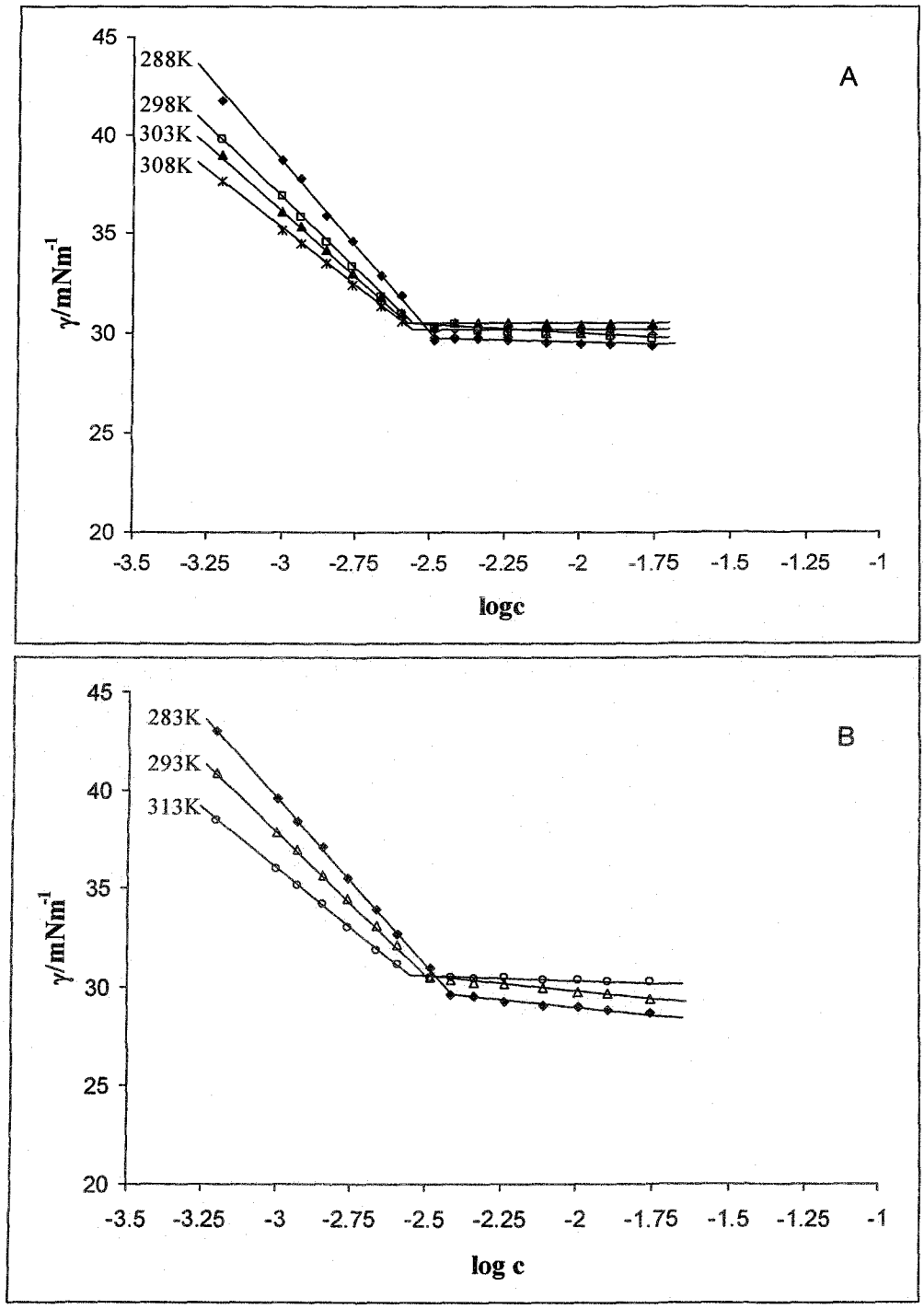

Figure 3.20: Surface tension, γ, of AOT (ammonium salt) in aqueous solution as a function of the logarithm of the surfactant concentration at different temperatures (A: temperature 283K, 293K, 303K, 313K), B: temperature 288K, 298K, 308K).

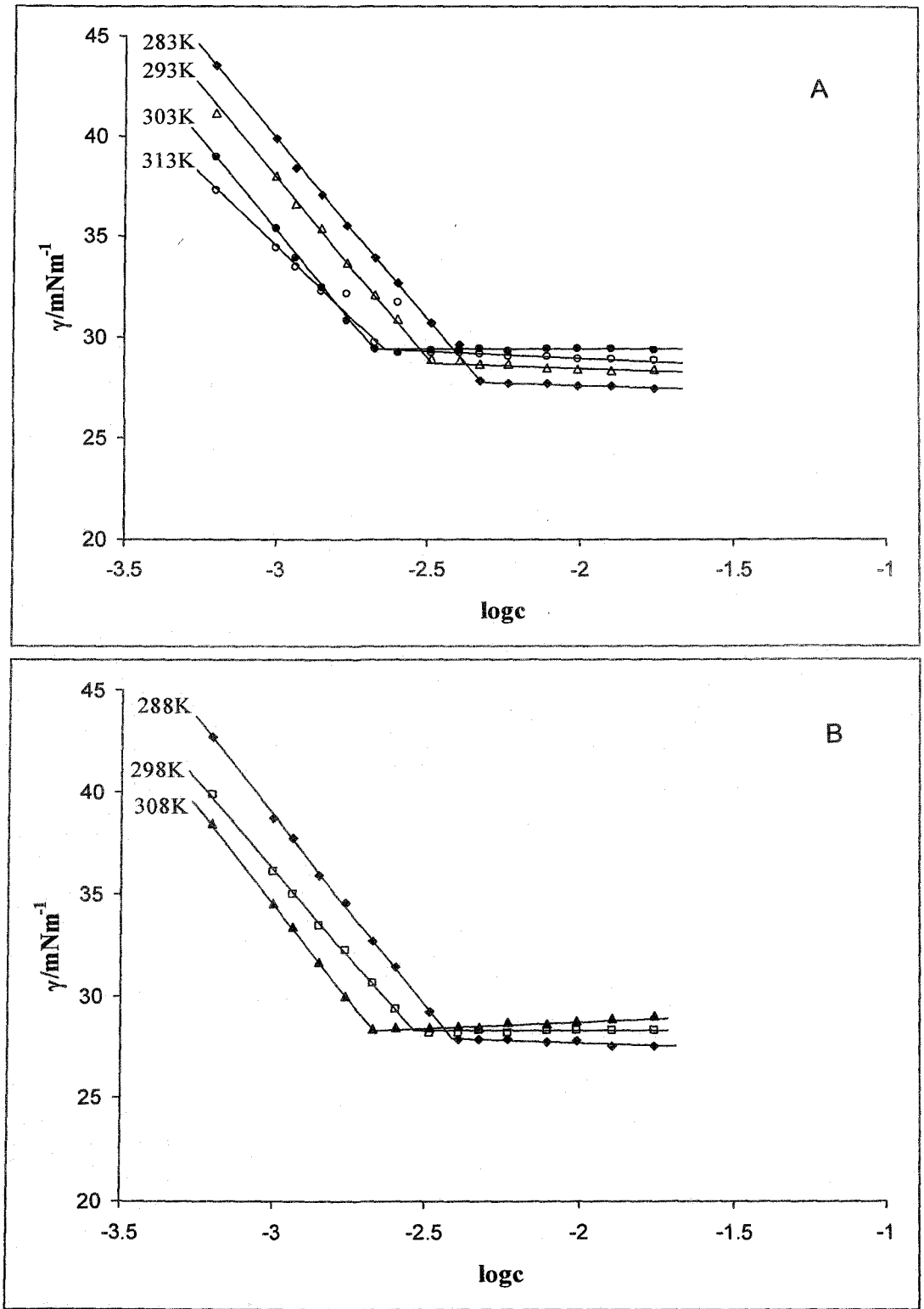

Figure 3.21: Surface tension, γ, of AOT (tetrametylammonium salt) in aqueous solution as a function of the logarithm of the surfactant concentration at different temperatures (A: temperature 283K, 293K, 303K, 313K), B: temperature 288K, 298K, 308K).

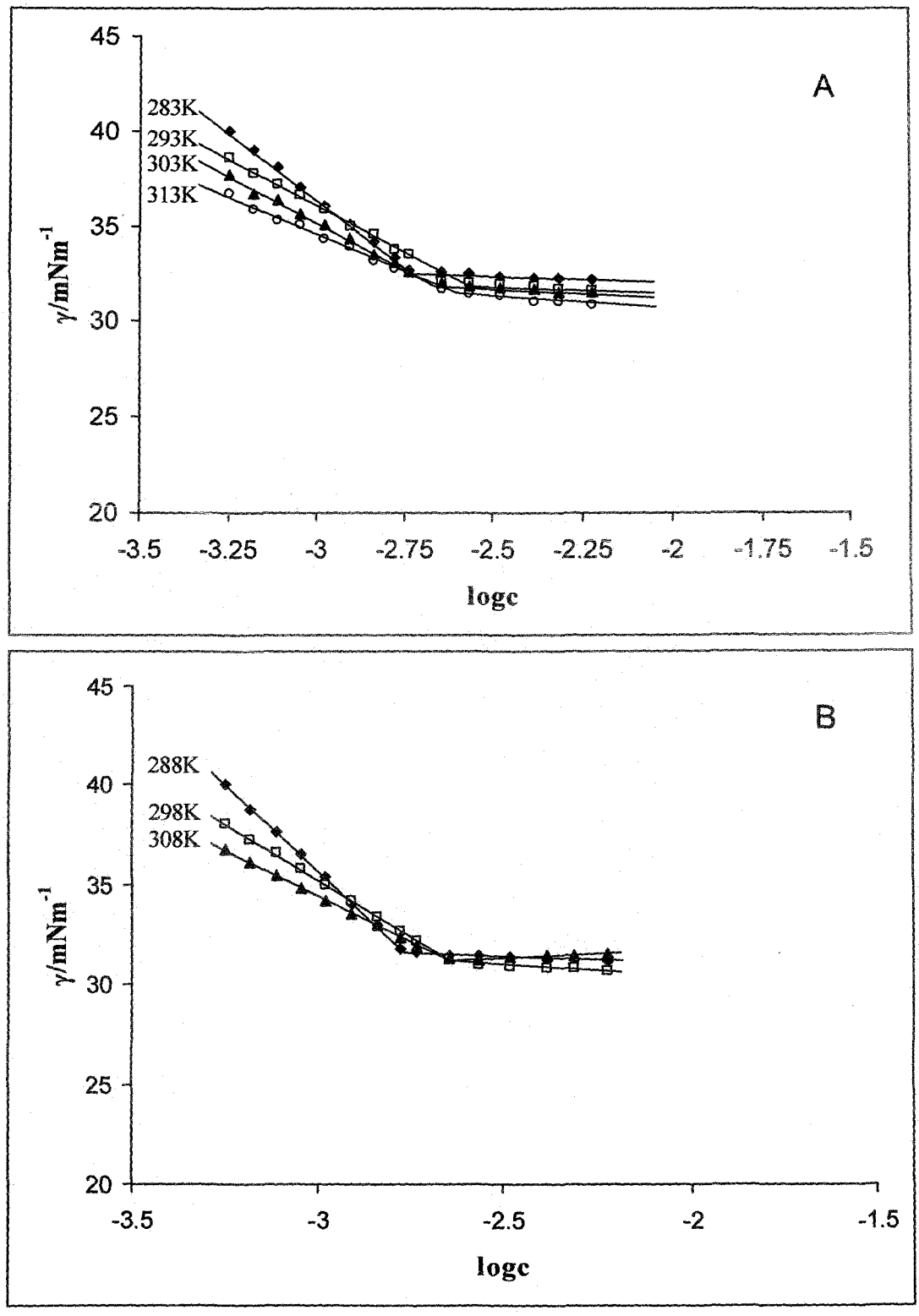

Figure 3.22: Surface tension, γ, of AOT (tetraetylammonium salt) in aqueous solution as a function of the logarithm of the surfactant concentration at different temperatures (A: temperature 283K, 293K, 303K, 313K), B: temperature 288K, 298K, 308K)

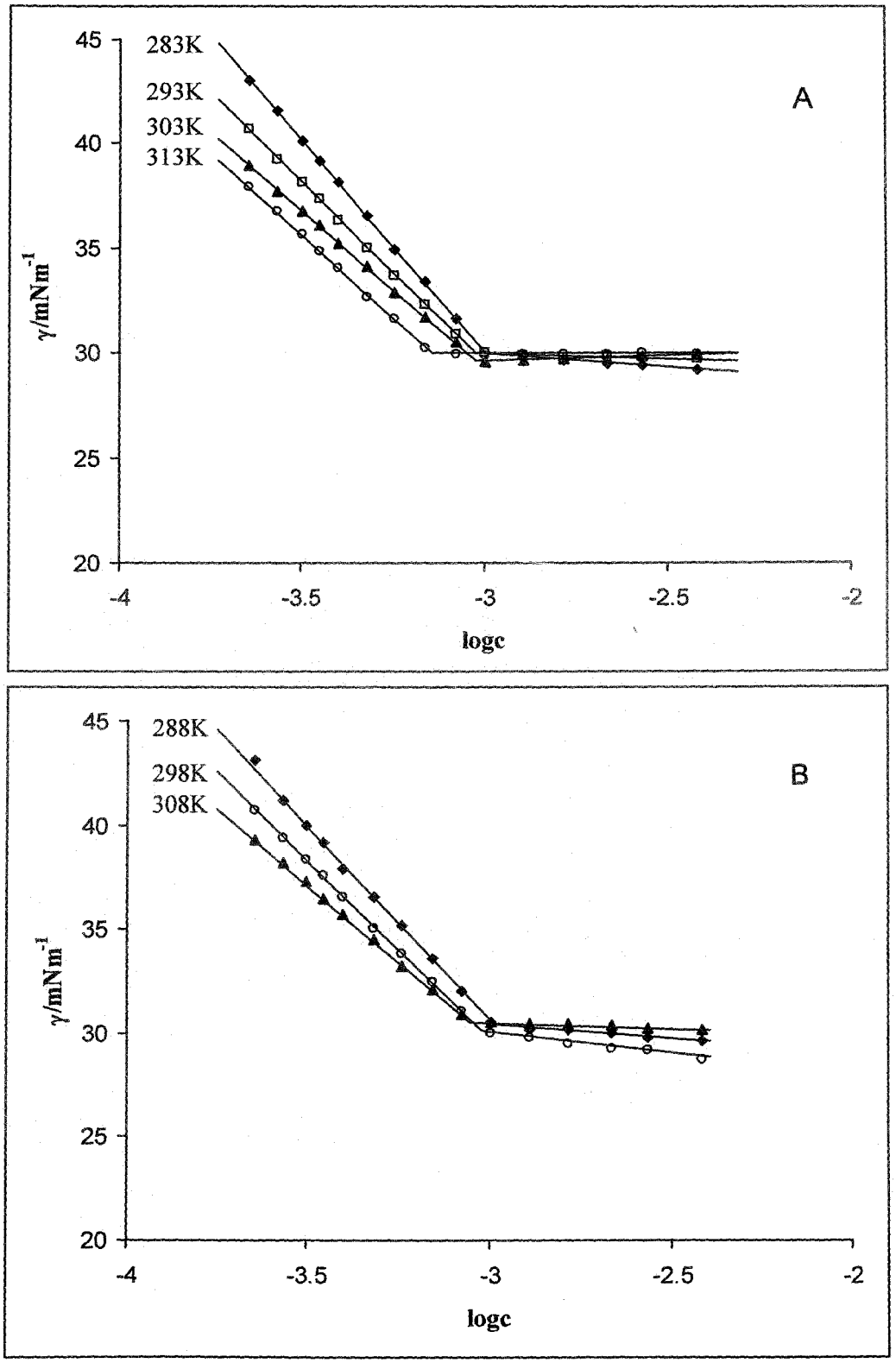

Figure 3.23: Surface tension, γ, of AOT (tetrapropylammonium salt) in aqueous solution as a function of the logarithm of the surfactant concentration at different temperatures (A: temperature 283K, 293K, 303K, 313K), B: temperature 288K, 298K, 308K)

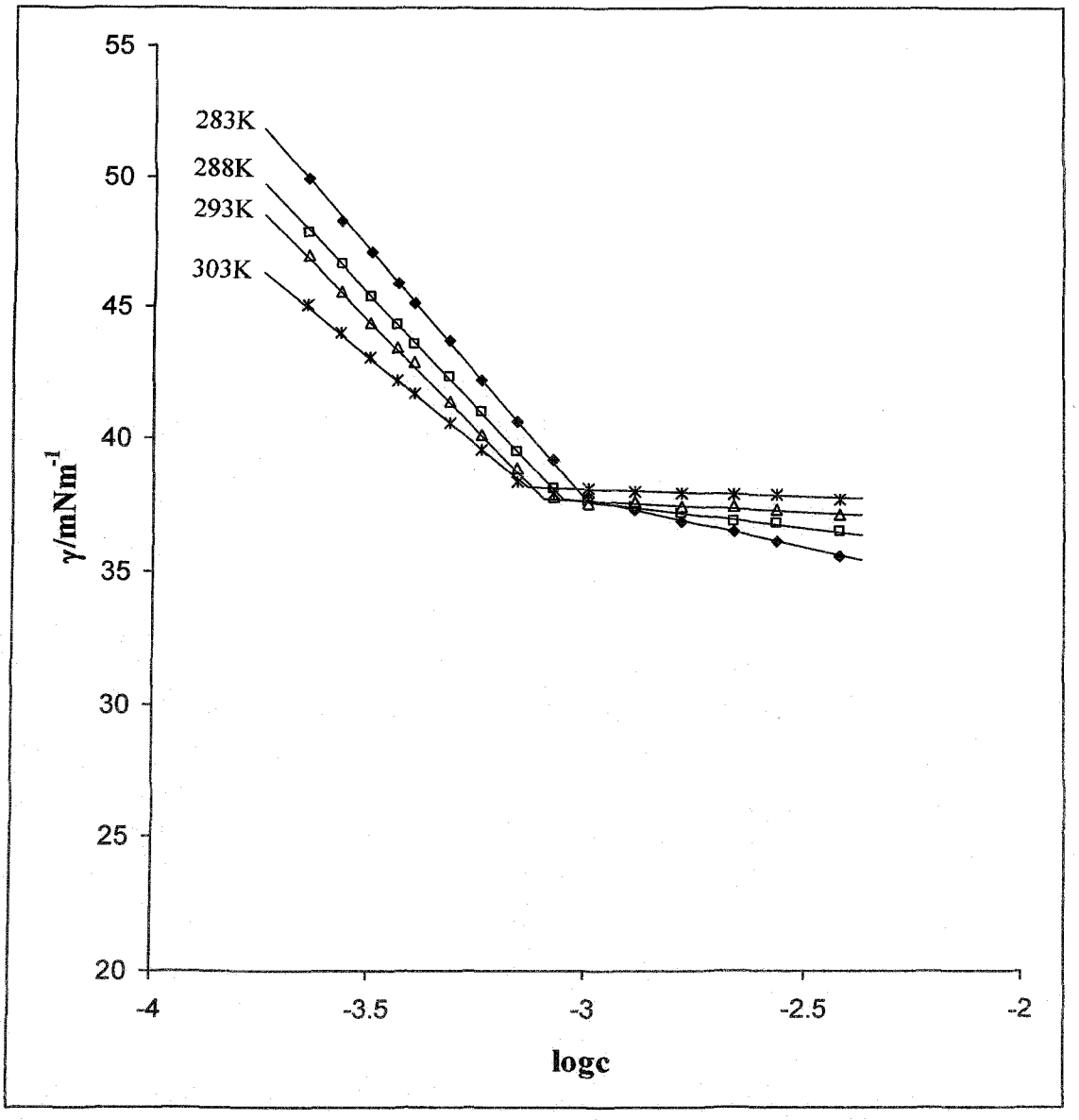

Figure 3.24: Surface tension, γ, of AOT (tetrabutylammonium salt) in aqueous solution as a function of the logarithm of the surfactant concentration at different temperatures

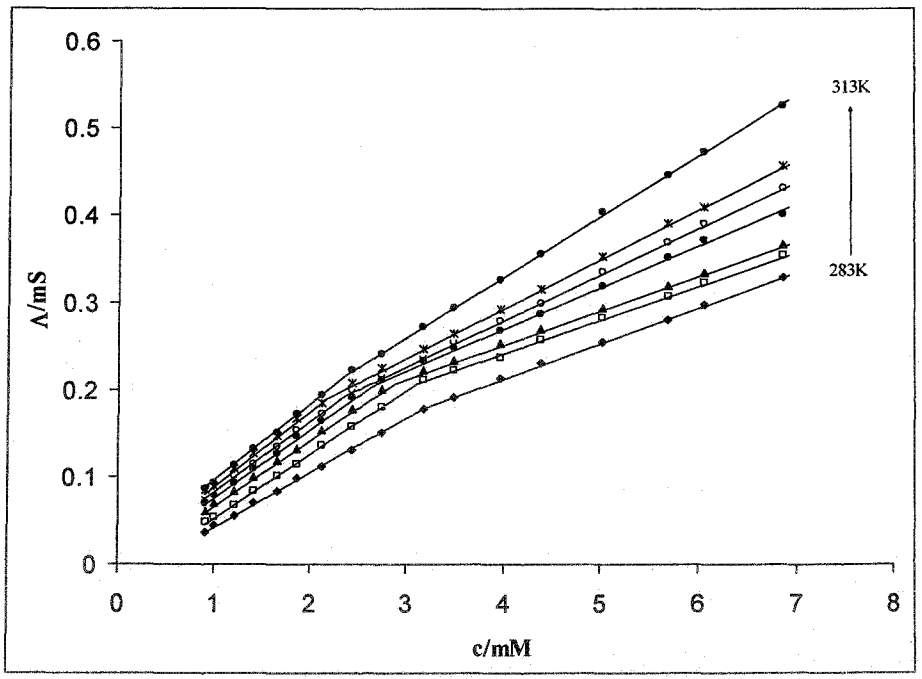

Figure 3.25: Conductance, Λ, of AOT (lithium salt) in aqueous solution as a function of the surfactant concentration at different temperatures ranging 283K to 313K with 5K interval.

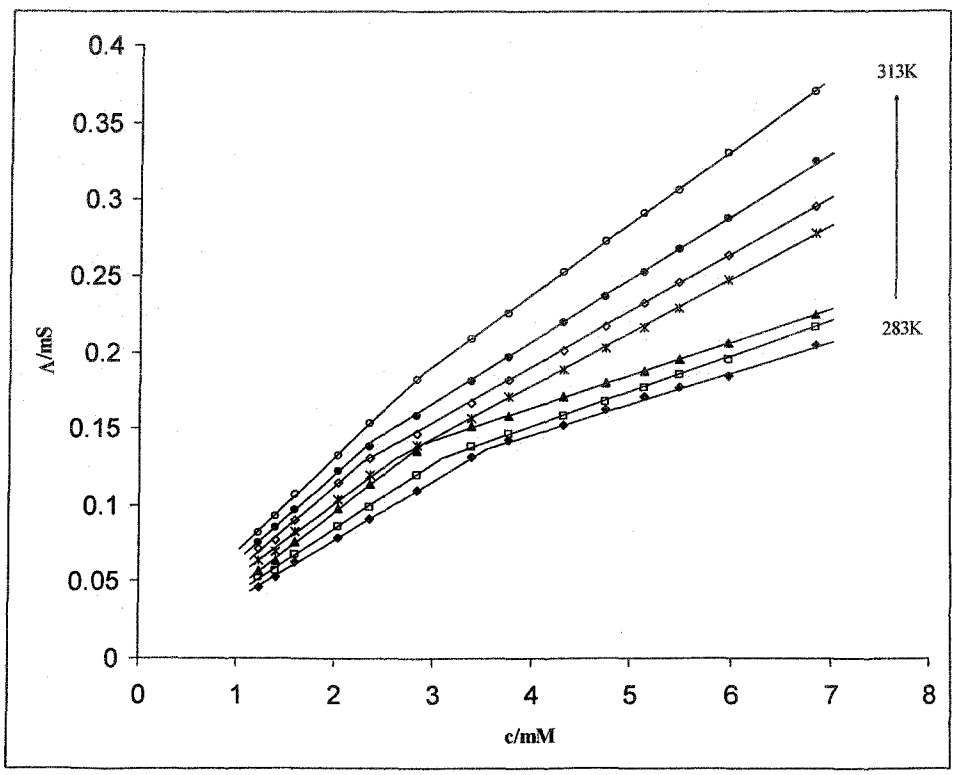

Figure 3.26: Conductance, Λ, of of AOT (sodium salt) in aqueous solution as a function of the surfactant concentration at different temperatures ranging 283K to 313K with 5K interval.

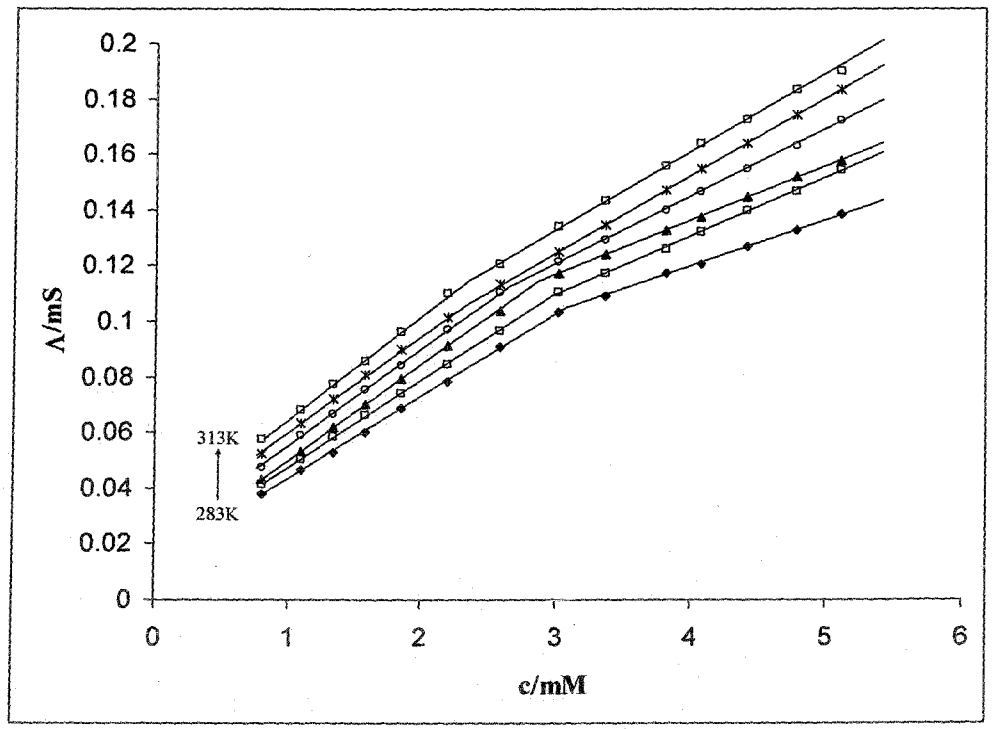

Figure 3.27: Conductance, Λ, of AOT (potassium salt) in aqueous solution as a function of the surfactant concentration at different temperatures ranging 283K to 313K with 5K interval.

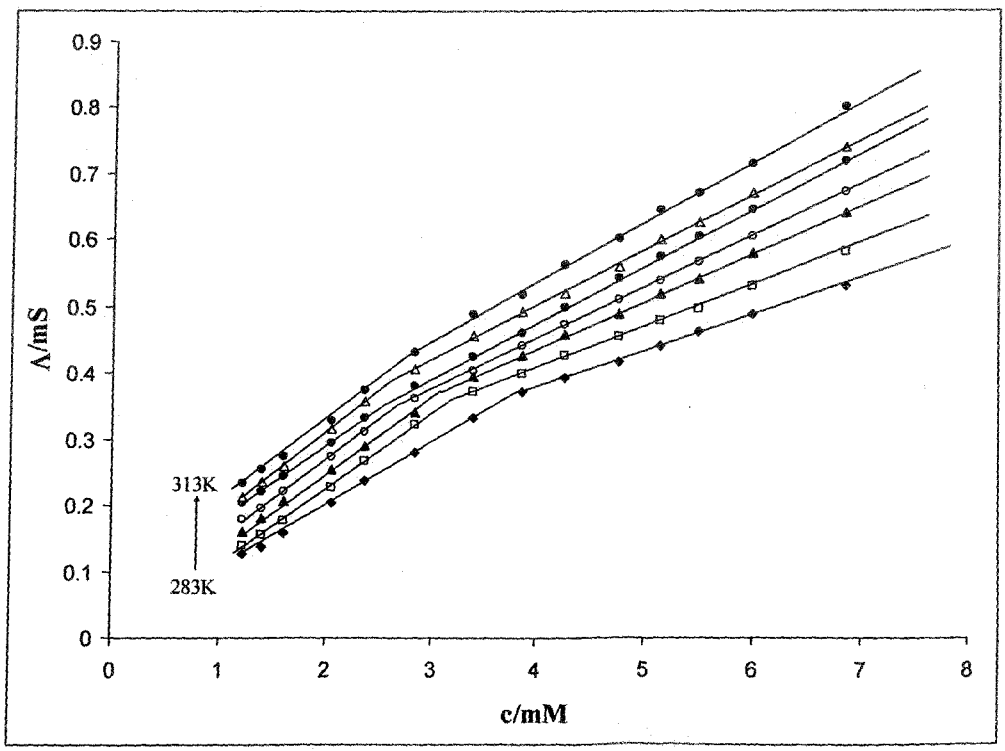

Figure 3.28: Conductance, Λ, of AOT (ammonium salt) in aqueous solution as a function of the surfactant concentration at different temperatures ranging 283K to 313K with 5K interval.

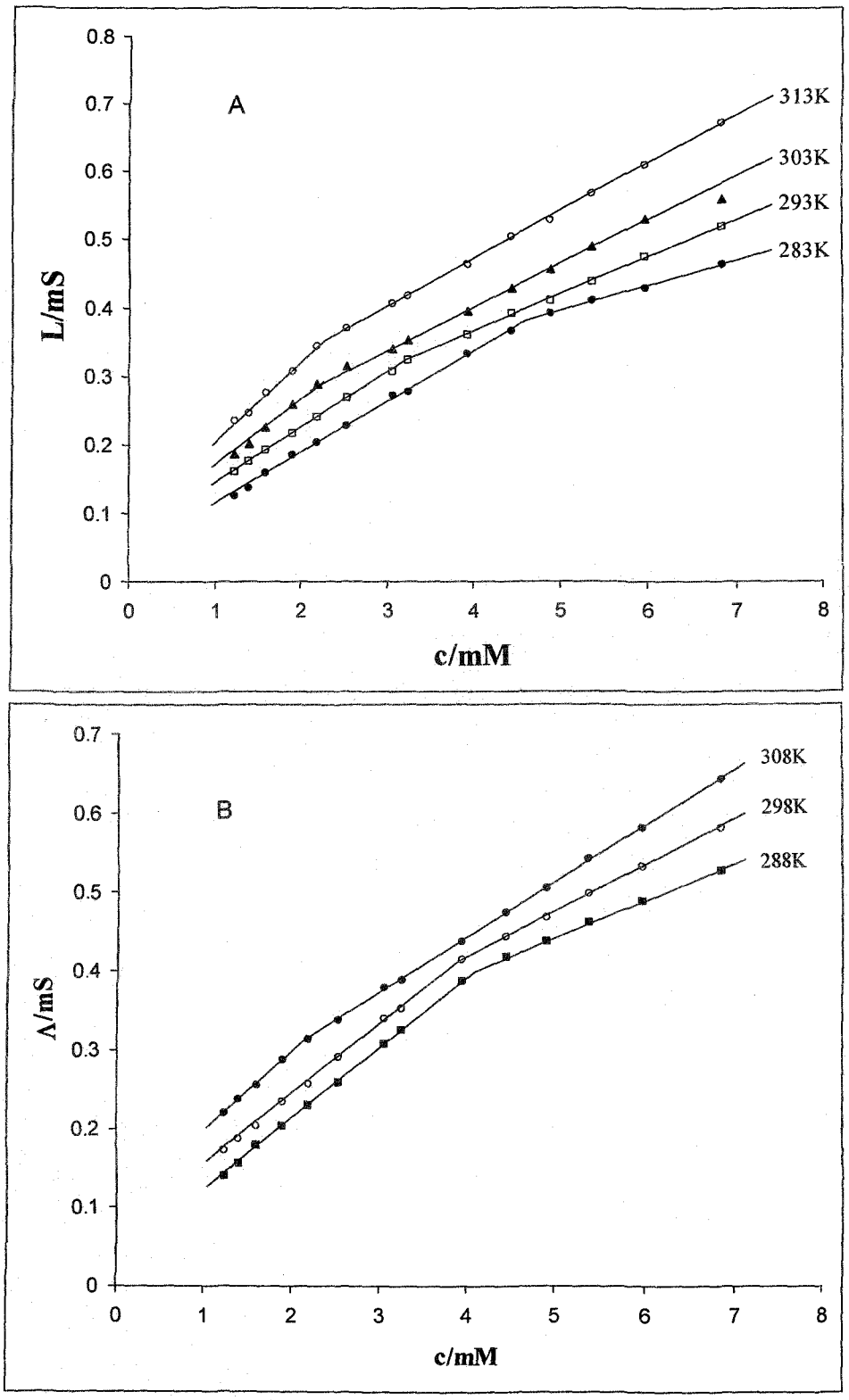

Figure 3.29: Conductance, Λ, of AOT (trtramethylammonium salt) in aqueous solution as a function of the surfactant concentration at different temperatures ranging 283K to 313K with 5K interval

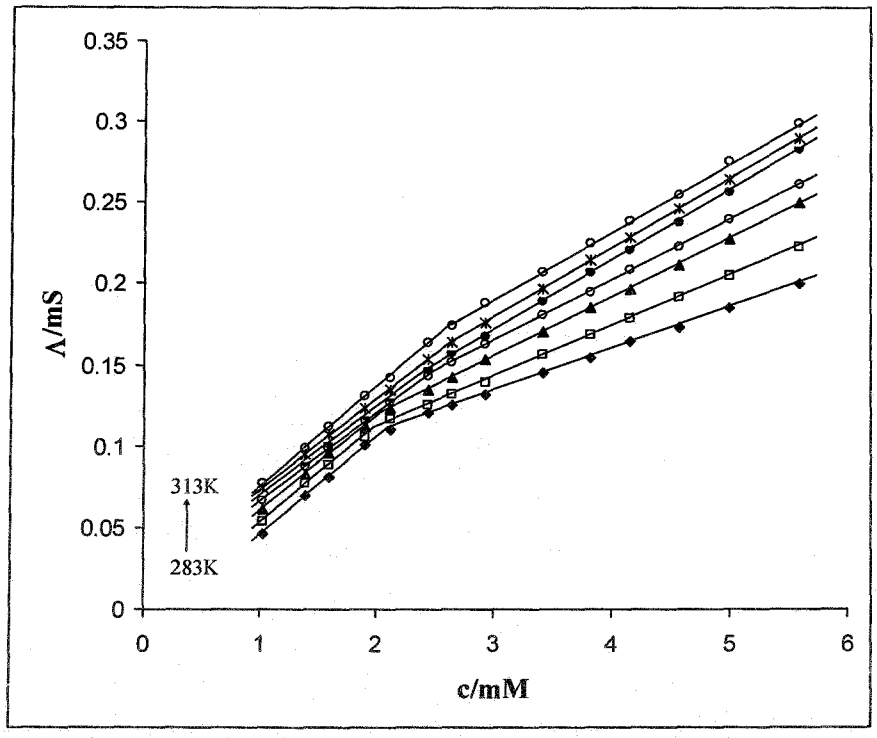

Figure 3.30: Conductance, Λ, of AOT (trtraethylammonium salt) in aqueous solution as a function of the surfactant concentration at different temperatures ranging 283K to 313K with 5K interval.

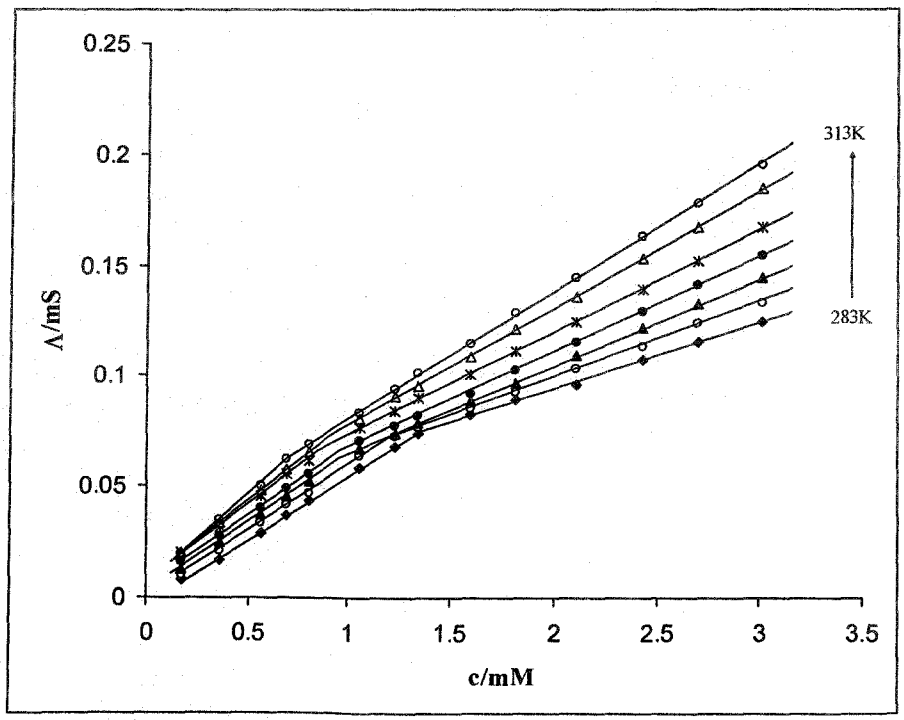

Figure 3.31: Conductance, Λ, of AOT (trtrapropylammonium salt) in aqueous solution as a function of the surfactant concentration at different temperatures ranging 283K to 313K with 5K interval

calculations of the hydration of micelles indicated a very small change in hydration during micellization [84]. This means that the hydration shell of cations limits the distance of closest approach. It seems apparent that the size of hydrated counter ion is important; bigger the size of counter ion i.e., low is its accessibility towards the head group, greater is the chance for micellization at lower concentration. The hydration number derived from the corrected ionic radii [87] along with the ionic and hydrated radius [88-90] of the above four ions are shown in the Table 3.9.

The larger the hydrated radius, the further the ion is located from the surface of the negatively charged surfactant head groups. Thus, NH_4^+ having the large ionic and hydrated radius cannot approach the highly charged surface of the micelle as close as smaller ions. Therefore, it can neither screen the charge at the surface of micelles nor reduce the surface potential as effectively as the smaller ions [91]. Dodecyl sulfate and AOT behaves differently towards micellization when Na^+ and Li^+ are present as counterion. Li^+ ion with its largest hydrated radius may modify slightly the internal structure of the double tailed AOT micelle which interacts with the hydrated Li^+ ion resulting lower cmc value. The K^+, however, gives anomalous result due to its strong tendency for ion pair formation in K-AOT.

It has been observed that in case of dodecyl sulfate and AOT having tetraalkylammonium counterions the cmc values follow the order $N^+(CH_3)_4$ > $N^+(C_2H_5)_4$ > $N^+(C_3H_7)_4$> $N^+(C_4H_9)_4$ (at temperature range <298K). It seems that the hydrodynamic size of the counterion plays an important role along with the hydrophobicity of tetraalkylammonium ions. Measurement of partial molar volumes [93,94] and calculation of hydration of micelles [95] by previous workers indicated that there was little loss of hydration water in this system during micellization. Therefore, the tightly bound hydration shell would limit the distance of closest approach. It is well known that the increase of the number of carbon atoms of hydrocarbon tail of a surfactant allows micellization to occur at a lower concentration due to increased hydrophobicity of the hydrocarbon tail [92]. But the increased ionic size from $N^+(CH_3)_4$ to $N^+(C_4H_9)_4$ enhances the micellization tendency and eventually reduces the cmc.

Table - 3.1

Surface properties of dodecyl sulfate having different alkyl counterions along with NH_4^+ ion at various temperatures (T/K): cmc, maximum surface excess concentration, minimum areas per molecule at the surface.

Counterion	T/K	cmc[a] /(mol $dm^{-3}\times10^3$)	Γ_{max}/ mol $cm^{-2}\times10^{10}$	A_{min}/ $nm^2\times10^2$	α
Li^+	283	9.11 (9.06)	3.22	0.52	0.30
	288	8.87 (8.92)	3.10	0.54	0.29
	293	8.52 (8.55)	2.98	0.55	0.31
	298	8.23 (8.18)	3.08	0.54	0.33
	303	8.43 (8.42)	2.94	0.56	0.34
	308	8.51 (8.52)	2.90	0.57	0.32
	313	8.47 (8.45)	2.91	0.57	0.33
Na^+	283	8.88 (8.96)	3.12	0.53	0.28
	288	8.15 (8.17)	3.01	0.55	0.30
	293	8.05 (8.01)	3.11	0.54	0.30
	298	7.96 (7.94)	2.90	0.57	0.32
	303	8.58 (8.62)	2.88	0.58	0.35
	308	8.65 (8.67)	2.78	0.60	0.32
	313	8.77 (8.80)	2.73	0.61	0.34
NH_4^+	283	9.21 (9.16)	3.21	0.52	0.27
	288	9.07 (9.10)	3.18	0.52	0.29
	293	8.88 (8.90)	3.11	0.53	0.28
	298	8.51 (8.62)	3.02	0.55	0.32
	303	8.39 (8.38)	2.93	0.57	0.30
	308	8.85 (8.76)	2.87	0.58	0.31
	313	8.92 (8.88)	2.88	0.58	0.28

[a]The values in the parenthesis represent cmc determined by conductivity method.

Table 3.2

Surface properties of dodecyl sulfate having different tetraalkylammonium counterions at various temperatures (T /K): cmc, maximum surface excess concentration, minimum areas per molecule at the surface.

Counterion	T/K	cmc[a] /(mol $dm^{-3}\times10^3$)	Γ_{max}/ mol $cm^{-2}\times10^{10}$	A_{min}/ $nm^2\times10^2$	α
$(CH_3)_4N^+$	283	5.92 (6.01)	3.34	0.50	0.21
	288	5.70 (5.66)	3.24	0.51	0.21
	293	5.58 (5.55)	3.18	0.52	0.23
	298	5.51 (5.52)	3.15	0.53	0.25
	303	5.49 (5.47)	3.20	0.52	0.22
	308	5.56 (5.60)	3.14	0.53	0.24
	313	5.80 (5.72)	3.08	0.54	0.23
$(C_2H_5)_4N^+$	283	4.08 (4.10)	3.28	0.51	0.20
	288	3.98 (3.97)	3.25	0.51	0.21
	293	3.92 (3.91)	3.19	0.52	0.23
	298	3.86 (3.86)	3.11	0.53	0.24
	303	3.82 (3.85)	3.18	0.52	0.24
	308	3.87 (3.88)	3.09	0.54	0.22
	313	3.85 (3.85)	2.99	0.56	0.23
$(C_3H_7)_4N^+$	283	2.32 (2.36)	3.35	0.49	0.20
	288	2.26 (2.30)	3.30	0.50	0.19
	293	2.22 (2.23)	3.22	0.51	0.20
	298	2.23 (2.24)	3.19	0.52	0.21
	303	2.18 (2.21)	3.20	0.52	0.21
	308	2.23 (2.20)	3.17	0.52	0.19
	313	2.22 (2.21)	3.11	0.53	0.19
$(C_4H_9)_4N^+$	283	1.34 (1.32)	3.33	0.50	0.19
	288	1.29 (1.28)	3.28	0.50	0.18
	293	1.22 (1.24)	3.20	0.52	0.20
	298	1.17 (1.15)	3.14	0.53	0.20
	303	1.18 (1.21)	3.09	0.54	0.18
	308	1.15 (1.17)	2.91	0.57	0.18
	313	1.10 (1.11)	3.01	0.55	0.17

[a]The values in the parenthesis represent cmc determined by conductivity method.

Table 3.3

Thermodynamic parameters of micellisation for Dodecyl sulfate with different alkyl counterions along with NH_4^+ at various temperatures: Standard Gibb's free energy, Enthalpy and Entropy.

Counterion	Temp./°C	$-\Delta G_m°$/ (kJ mol^{-1})	$\Delta H_m°$/ (kJ mol^{-1})	$\Delta S_m°$/ (J mol^{-1})
Li^+	283	34.9	27.2	219.2
	288	35.8	25.9	214.4
	293	36.2	24.1	205.7
	298	36.5	22.2	196.9
	303	36.8	20.3	188.3
	308	37.8	18.6	182.9
	313	38.2	16.3	174.2
Na^+	283	35.4	-9.4	91.8
	288	35.9	-14.3	75.1
	293	36.6	-19.6	57.8
	298	36.8	-25.0	39.5
	303	36.5	-30.4	19.8
	308	37.7	-37.4	1.2
	313	37.8	-43.5	-18.3
NH_4^+	283	35.4	-15.7	69.8
	288	35.7	-19.6	56.0
	293	36.6	-24.1	42.9
	298	36.6	-28.0	28.6
	303	37.7	-33.2	14.7
	308	37.8	-38.1	-0.9
	313	39.1	-44.3	-16.5

Table 3.4
Thermodynamic parameters of micellisation for Dodecyl sulfate with different tetraalkylammonium counterions at various temperatures: Standard Gibb's free energy, Enthalpy and Entropy.

Counterion	Temp./°C	$-\Delta G_m°$/ (kJ mol^{-1})	$\Delta H_m°$/ (kJ mol^{-1})	$\Delta S_m°$/ (J mol^{-1})
$(CH_3)_4N^+$	283	38.5	-2.3	128.1
	288	39.4	-6.1	115.7
	293	39.7	-10.0	101.4
	298	40.0	-14.0	86.9
	303	41.4	-18.9	74.2
	308	41.5	-23.4	58.6
	313	42.2	-28.7	43.2
$(C_2H_5)_4N^+$	283	40.3	19.0	209.8
	288	40.9	18.4	205.9
	293	41.2	17.6	200.6
	298	41.7	16.8	196.4
	303	42.5	16.0	193.0
	308	43.6	15.3	191.3
	313	44.1	14.3	186.5
$(C_3H_7)_4N^+$	283	42.7	21.1	225.4
	288	43.8	20.7	224.1
	293	44.4	20.0	220.0
	298	44.9	20.0	215.4
	303	45.8	18.6	212.3
	308	46.9	18.0	210.7
	313	47.7	17.1	207.1
$(C_4H_9)_4N^+$	283	45.3	14.0	209.4
	288	46.5	13.3	207.7
	293	47.0	12.3	202.6
	298	48.0	11.4	199.5
	303	49.3	10.6	197.7
	308	50.3	9.5	194.0
	313	51.6	8.3	191.4

Table 3.5

Micellization and surface parameters of AOT surfactants having different alkyl counterions along with NH_4^+ ion at various temperatures (T/K): cmc, maximum surface excess concentration, minimum areas per molecule and ionization degree.

Counterion	T/K	cmc[a] /(mol $dm^{-3}\times10^3$)	Γ_{max}/ mol $cm^{-2}\times10^8$	A_{min}/ $nm^2\times10^2$	α
Li^+	283	3.35 (3.40)	1.63	1.02	0.73
	288	2.98 (3.15)	1.60	1.04	0.51
	293	2.82 (2.90)	1.59	1.04	0.49
	298	2.66 (2.63)	1.59	1.44	0.58
	303	2.40 (2.37)	1.56	1.06	0.70
	308	2.24 (2.19)	1.61	1.03	0.68
	313	2.39 (2.23)	1.60	1.05	0.77
Na^+	283	3.55 (3.53)	1.42	1.17	0.61
	288	3.16 (3.20)	1.45	1.14	0.51
	293	2.88 (2.77)	1.49	1.11	0.46
	298	2.63 (2.40)	1.57	1.06	0.70
	303	2.24 (2.20)	1.76	0.94	0.69
	308	2.37 (2.26)	1.70	0.98	0.70
	313	2.80 (2.69)	1.71	0.97	0.67
K^+	283	2.97 (3.11)	1.84	0.90	0.74
	288	2.90 (3.01)	2.01	0.83	0.63
	293	2.82 (2.90)	2.22	0.75	0.58
	298	2.70 (2.62)	2.25	0.74	0.73
	303	2.44 (2.35)	2.30	0.72	0.85
	308	2.42 (2.32)	2.44	0.68	0.75
	313	–	–	–	–
NH_4^+	283	3.87 (3.85)	1.56	1.06	0.45
	288	3.31 (3.20)	1.58	1.05	0.58
	293	3.09 (3.12)	1.45	1.14	0.66
	298	2.70 (2.65)	1.55	1.07	0.68
	303	2.59 (2.52)	1.80	0.92	0.77
	308	2.65 (2.60)	1.72	0.96	0.66
	313	2.82 (2.75)	1.76	0.94	0.71

[a]The values in the parenthesis represent cmc determined by conductivity method.

Table 3.6

Micellization and surface parameters of AOT surfactants having different tetraalkyl-ammonium counterions at various temperatures (T/K): cmc, maximum surface excess concentration, minimum areas per molecule and ionization **degree.**

Counterion	T/K	cmc[a] /(mol $dm^{-3}\times10^3$)	Γ_{max}/ mol $cm^{-2}\times10^8$	A_{min}/ $nm^2\times10^2$	α
$(CH_3)_4N^+$	283	4.76 (4.61)	1.68	0.99	0.50
	288	3.82 (4.10)	1.65	1.01	0.51
	293	3.24 (3.40)	1.53	1.08	0.67
	298	2.90 (2.90)	1.60	1.04	0.74
	303	2.05 (2.35)	1.80	0.92	0.72
	308	2.10 (2.20)	1.72	0.96	0.76
	313	2.26 (2.31)	1.67	0.99	0.74
$(C_2H_5)_4N^+$	283	1.88 (2.10)	1.44	1.15	0.42
	288	1.78 (2.00)	1.33	1.25	0.56
	293	2.95 (1.85)	1.46	1.14	0.65
	298	2.45 (2.50)	1.43	1.16	0.67
	303	2.31 (2.43)	1.76	0.94	0.80
	308	2.37 (2.50)	1.31	1.27	0.69
	313	2.56 (2.63)	1.41	1.12	0.66
$(C_3H_7)_4N^+$	283	1.18 (1.34)	1.67	0.99	0.56
	288	1.05 (1.20)	1.71	0.97	0.69
	293	0.93 (0.98)	1.85	0.89	0.66
	298	0.97 (0.95)	1.71	0.97	0.65
	303	0.92 (0.85)	1.77	0.94	0.68
	308	0.87 (0.90)	1.69	0.98	0.75
	313	0.74 (0.80)	1.93	0.86	0.74
$(C_4H_9)_4N^+$	283	1.04 (1.11)	1.32	1.26	0.57
	288	0.87 (0.91)	1.40	1.18	0.58
	293	0.80 (0.83)	1.42	1.17	0.59
	298	0.77 (0.80)	1.63	1.02	0.76
	303	0.75 (0.78)	1.82	0.91	0.67

[a]The values in the parenthesis represent cmc determined by conductivity method.

Table 3.7
Thermodynamic parameters of micellization for AOT surfactants with different alkyl counterions at various temperatures: Standard Gibb's free energy, Enthalpy and Entropy.

Counterion	Temp./°C	$-\Delta G_m°$/ (kJ mol^{-1})	$-\Delta H_m°$/ (kJ mol^{-1})	$\Delta S_m°$/ (J mol^{-1})
Li^+	283	29.0	09.9	63.4
	288	35.1	12.1	80.0
	293	36.3	12.6	80.9
	298	34.9	12.3	76.0
	303	32.8	11.6	69.9
	308	34.3	12.3	71.5
	313	32.1	12.0	73.3
Na^+	283	44.4	23.5	73.8
	288	37.2	25.3	41.3
	293	37.0	25.4	39.7
	298	32.1	22.1	33.3
	303	33.5	23.1	34.1
	308	33.6	23.8	32.0
	313	34.2	24.3	34.4
K^+	283	29.2	5.7	83.4
	288	32.4	6.4	90.5
	293	34.1	6.8	93.2
	298	31.3	6.3	84.0
	303	29.2	5.9	76.8
	308	32.3	6.7	83.3
	313	–	–	–
NH_4^+	283	35.0	16.5	61.3
	288	33.0	15.6	56.9
	293	32.0	14.3	50.2
	298	32.5	15.9	56.6
	303	30.9	15.8	52.0
	308	34.1	16.0	50.0
	313	33.2	16.3	53.5

Table 3.8

Thermodynamic parameters of micellization for AOT surfactants with different tetraalkyl-ammonium counterions at various temperatures: Standard Gibb's free energy, Enthalpy and Entropy.

Counterion	T/C	$-\Delta G_m^\circ$/ (kJ mol^{-1})	$-\Delta H_m^\circ$/ (kJ mol^{-1})	ΔS_m°/ (J $K^{-1}mol^{-1}$)
$(CH_3)_4N^+$	283	33.0	29.1	13.7
	288	34.2	30.0	14.6
	293	31.7	27.9	13.3
	298	30.8	27.2	12.1
	303	33.0	28.6	14.5
	308	32.3	28.5	12.2
	313	33.1	29.0	12.8
$(C_2H_5)_4N^+$	283	35.0	12.2	80.6
	288	33.0	11.7	74.0
	293	32.0	12.2	67.6
	298	32.5	12.3	67.8
	303	30.9	11.9	62.7
	308	34.1	13.3	67.5
	313	35.2	13.7	67.7
$(C_3H_7)_4N^+$	283	36.4	8.5	98.7
	288	34.7	8.1	92.3
	293	35.8	8.5	93.3
	298	36.6	8.8	93.1
	303	36.6	8.9	91.2
	308	35.4	8.7	86.5
	313	36.8	8.8	90.6
$(C_4H_9)_4N^+$	283	36.6	14.4	78.4
	288	37.6	14.9	78.8
	293	38.2	15.3	78.2
	298	34.4	15.2	64.4
	303	37.7	15.5	73.3

Table 3.9
Ionic and Hydrated radius along with Hydration number of ions derived from corrected ionic radii.

Ion	Hydration Number	Ionic Radius (Å)	Hydrated Radius (Å)
NH_4^+	4.6	1.48	3.31
K^+	5.1	1.37	2.23
Na^+	6.5	0.99	2.76
Li^+	7.4	0.59	3.40

Here the hydrocarbon exterior of the tetraalkyl ions undergoes hydrophobic interactions with the exposed hydrocarbon of the micelle surface and overcome steric hindrance. However, such a phenomenon is little or absent in the set of counterions viz., $N^+(CH_3)_4$, NH_4^+ and Na^+. In the absence of any appreciable hydrophobic interaction, NH_4^+ and Na^+ ions interact with the micellar head groups more strongly than $N^+(CH_3)_4$ ions due to their smaller sizes. Eventually they lead to form micelle more readily via efficient charge screening than that of $N^+(CH_3)_4$ ions and the systems yield low cmc values. But in case of other tetraalkylammonium ions as the bulkiness of the ion increases due to the presence of large alkyl groups the hydrophobicity plays important role causing increasingly micellization to occur at lower concentrations as has already been mentioned.

The cmc in aqueous solution for a particular surfactant reflects the degree of binding of the counterion to the micelle. Increased binding of the counterion, in the aqueous system causes a decrease in the cmc of the surfactant. The extent of binding of the counterion increases also with increase in the polarizability and charge of the counterion and decreases with increase in its hydrated radius. Thus in aqueous medium, for anionic lauryl sulfates, the cmc decreases in the order $Li^+ > Na^+ > K^+ > Cs^+ > N^+(CH_3)_4 > N^+(C_2H_5)_4 > Ca^+, Mg^+$, which is same order as the increase in the degree of binding of the cation [78]. The depression of cmc from Li^+ to K^+ is small, but for other counter ions it is quite substantial. When the counterion is a cation of a primary amine, RNH_3^+, the cmc decreases with increase in the chain length of the amine [79].

On the other hand, when comparing surfactants of different structural types, the value of cmc does not always increase with decrease in degree of binding of the counterion. Thus although in the series $RN^+(CH_3)_3$ the degree of binding increases and the cmc decreases with increase in length of R, the decrease in cmc is due mainly to the increased hydrophobicity of the surfactant as a result of increase in alkyl chain length, and only to a minor extent due to the smaller area per head group.

It has been reported that in case of dodecyl sulfate (DS) cmc shows very little temperature dependency when a counter ion varies within different alkali metals viz. from lithium to cesium ion [96] and tetraalkylammonium ion [13]. Similar result is observed when the counterion is changed from Li^+ to tetrabutylammonium ion (TBA^+) for the present study of dodecyl sulfate (Table 3.1 and 3.2). It is observed that when Li^+, Na^+ and NH_4^+ are present as counterion the cmc of dodecyl sulfate show pronounced temperature dependency and passes through a shallow minimum at the temperature range 298 - 308K (Figure 3.32). But when tetraalkylammonium ion is present as counterion, the cmc of dodecyl sulfate show a little temperature sensitivity. On the other hand, in AOT the cmc values give more pronounced temperature dependency even when the counterion is tetraalkylammonium ion. Figure 3.33 represents the temperature dependency in cmc of AOT as a function of different counterions. The decrease in the cmc with temperature (at lower temperatures) is possibly due to the hydration of the monomers, whilst further temperature increase causes a disruption of the structured water around the hydrophobic groups that opposes micellization. In the case of K-AOT the cmc can't be determined at 40°C due to the very low solubility of the particular surfactant at that temperature which may be hardly sufficient to make micelle. The variation of cmc with temperature shows good agreement with the empirical equation given by La Mesa [100]:

$$\left(\mathrm{cmc} - \mathrm{cmc}^*\right) = \left|\left(T - T^*\right)/T^*\right|^{\gamma'} \qquad (3.10)$$

where cmc* is the minimum value of cmc and T^* the temperature at the minimum with $\gamma' = 1.74 \pm 0.03$. It should be mentioned that the exponent γ' has no obvious physical meaning, but, both cmc* and the related temperature in case of a particular surfactant are the measure of the hydrophobic-hydrophilic balance of micelle [46].

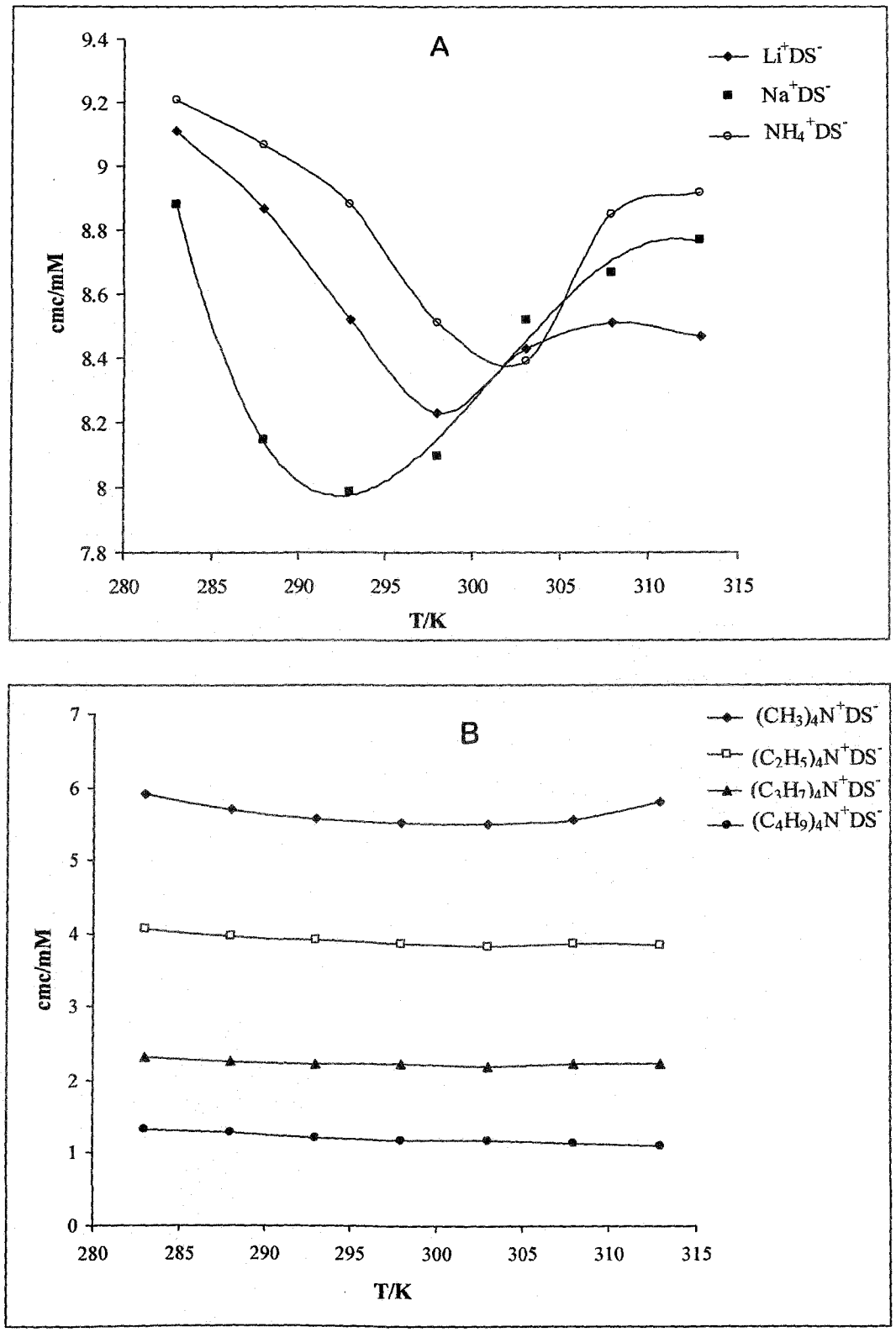

Figure 3.32: Variation of cmc with temperature (K) of dodecyl sulfate having different counterion.

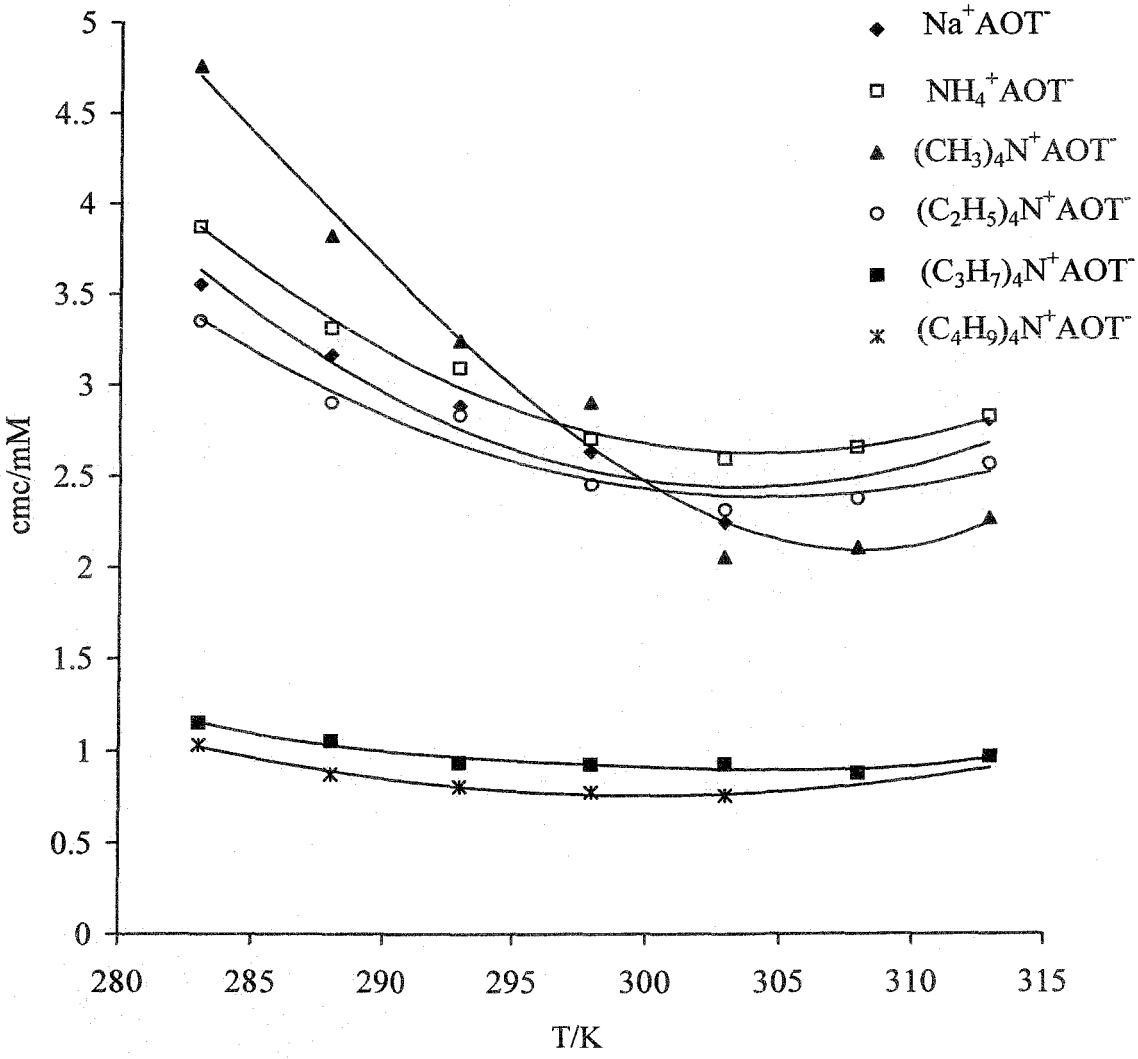

Figure 3.33: Variation of cmc with temperature (K) of AOT having different counter cation

The position of the minimum has thermodynamic significance also. The minimum in cmc represents minimum in free energy of micellization.

Thermodynamic Parameters:

The temperature dependency of dodecyl sulfate (DS) and AOT micelles having different counterions also enables to determine the corresponding thermodynamic parameters of micellization. According to mass action or phase separation model the standard free energy of micelle formation per mole of monomer of ionic uni-univalent surfactants is expressed by well-known equation [21a,69]:

$$\Delta G^0_m = (2 - \alpha)\, RT \ln X_{cmc} \qquad (3.11)$$

Here X_{cmc} is the cmc expressed in mole fraction scale and $\alpha = 1 - \beta = p/n$, is the ionization degree or counter ionic ionization constant of the micelle, where p and n are the effective charge and the aggregation number of the micelle respectively. The value of α can be determined from the ratio of the slope of the two linear fragments of conductivity-concentration plot above and below cmc [32,97]. The values of ΔG^0_m determined for each surfactant-counterion pair at different temperatures eventually give the standard enthalpy (ΔH^0_m) and entropy (ΔS^0_m) of micellization from the simple thermodynamic relations:

$$\Delta H^0_m = -(2 - \alpha)\, RT^2 \left(\partial \ln X_{cmc}/\partial T\right)_P \qquad (3.12)$$

The equation 3.12 is obtained from the well known Gibbs-Helmholtz relation and equation 3.11 assumes that α does not vary much with temperature. However, α is not strictly temperature independent and the more appropriate form of equation 3.12 should be

$$-\Delta H^0_m/T^2 = (2 - \alpha)\, R \left(\partial \ln X_{cmc}/\partial T\right)_P + R \ln X_{cmc} \left(\partial(2 - \alpha)/\partial T\right) \qquad (3.13)$$

Since the variation of α with temperature is not well defined and is devoid of any general trend, the quantity $\partial(2 - \alpha)/\partial T$ is difficult to find out experimentally [98]. Therefore, at least to gain qualitative information regarding the thermodynamics, equation 3.12 has been applied at the appropriate α.

$$\Delta S^0_m = (\Delta H^0_m - \Delta G^0_m)/T \quad (3.14)$$

The ln X_{cmc} vs T plot is not linear. To evaluate ΔH^0_m, following polynomial form of variation of $\ln X_{cmc}$ with temperature has been considered.

$$\ln X_{cmc} = a + bT + cT^2 \quad (3.15)$$

where a, b, c are respective polynomial constants.

Thus,

$$\left(\partial \ln X_{cmc}/\partial T\right) = b + 2cT \quad (3.16)$$

The polynomial constants b and c were evaluated from the fitting of experimental data. For all DS and AOT surfactants with different counterions the calculated thermodynamic parameters of micellization are listed in Table 3.2 and 3.4. Spontaneity of the micellization process is well explanatory from the large negative values of ΔG^0_m. Micelles containing the same amphiphile but different counterions show different values of thermodynamic parameters because of the different counterions could bind to an amphiphile to a different extent and with different energy. Micellization in aqueous medium usually leads to a positive entropy change, which is mainly due to the melting of the "flickering cluster" that arises out of the hydrophobic effect of amphiphilic part of the surfactant molecules [99]. During formation of a micelle, the endothermic melting of the ordered polar solvent molecules around the nonpolar tail of amphiphile is greater than the subsequent exothermic association of the molecules. The resulting disordered state is actually reflected in the positive entropy change. The variation of the standard thermodynamic parameters with different counter ions at a certain temperature can also be explained by the size and the hydration of the counter ion as has been already discussed. Like cmc, the ΔG^0_m and ΔH^0_m also show temperature dependency for all the surfactant-counterion systems.

A close look on the thermodynamic parameters (Table 3.3, 3.4, 3.7 and 3.8) support the view that in order to form micelle the gain in entropy is the major factor leading to negative change in Gibbs free energy [101-103] if the temperature is not very high. Conceptually, ΔG^0_m, may be imagined to be divided into an electric

contribution, F_{el}^0 arising from the ionic head groups and a hydrocarbon contribution F_{hc}^0

$$\Delta G^0_m = F_{el}^0 + F_{hc}^0 \tag{3.17}$$

where F_{el}^0 is positive and its contribution to the total ΔG^0_m value is generally small (about 3~4%). The F_{hc}^0 value may be divided into the free energy components $\Delta G^0_{-CH_2-}$ (contribution of $-CH_2-$ groups) and $\Delta G^0_{-CH_3}$ (contribution of terminal $-CH_3$ groups). $\Delta G^0_{-CH_3}$ is constant, however, $\Delta G^0_{-CH_2-}$ depends upon the chain length. For ionic surfactants in aqueous solution, the reported [4,103] value of $\Delta G^0_{-CH_2-}$ is approximately 2.93~3 kJ.mol^{-1}. However, the fact that though the free energy changes are not very different, the enthalpy change is significantly higher and the entropy changes are much lower for $N^+(CH_3)_4$ counterion containing AOT compared to all other systems. This leads one to interpret that the enthalpy contributes major driving force in micellization. Loosely bound water dipole with the $N^+(CH_3)_4$ ion may cause lower contribution of ΔS^0_m in aggregation process. Similarly, for other counterions in both DS and AOT systems ΔH^0_m and ΔS^0_m contribute differently to get similar ΔG^0_m. However, like a variety of processes such as oxidation-reduction, hydrolysis, protein unfolding, etc., micellization process also exhibit a linear relationship between the enthalpy and entropy change which is known as enthalpy-entropy compensation [20,104,105]. This is important in connection with the hydrophobicity of surfactant which leads to stable micelle formation. In general, the compensation phenomenon between the enthalpy change, ΔH^0_m and the entropy change, ΔS^0_m in various processes can be described in the form of [106]

$$\Delta H^0_m = \Delta H^*_m + T_c \Delta S^0_m \tag{3.18}$$

In a plot of ΔH^0_m vs ΔS^0_m, the slope T_c has a dimension of temperature and is known as compensation temperature. This can be interpreted as a measure of desolvation part of micellization, that means a characteristic of solute-solute and solute-solvent interaction, and the intercept characterizes the solute-solute interaction. Present experimental results also show a good agreement with the enthalpy-entropy compensation linearity for all AOT surfactants having different

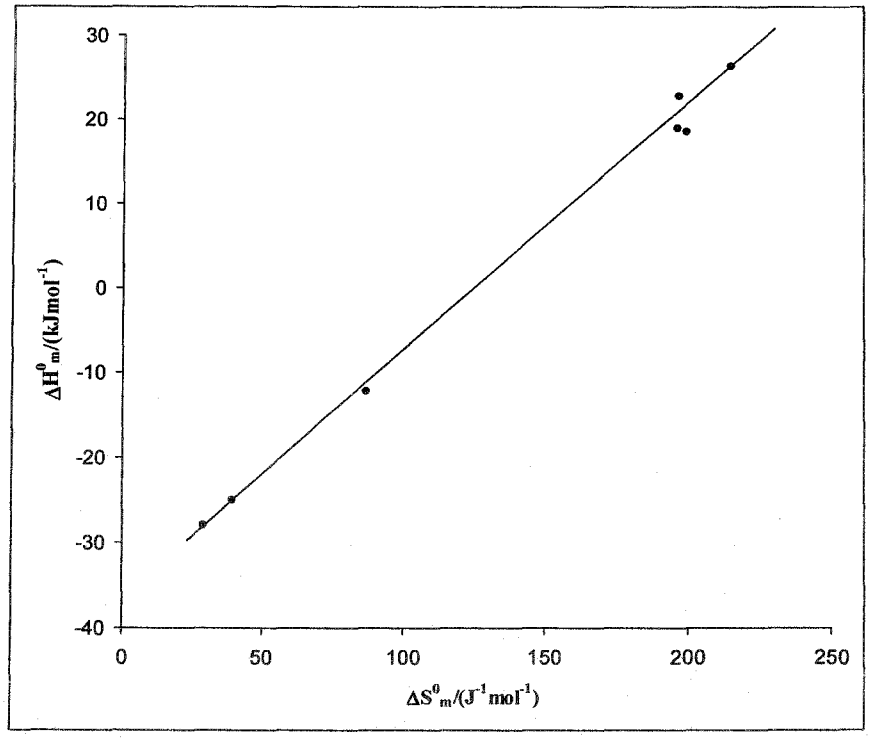

Figure 3.34: Enthalpy–entropy compensation plots for dodecyl sulfate having different counterions at 298 K

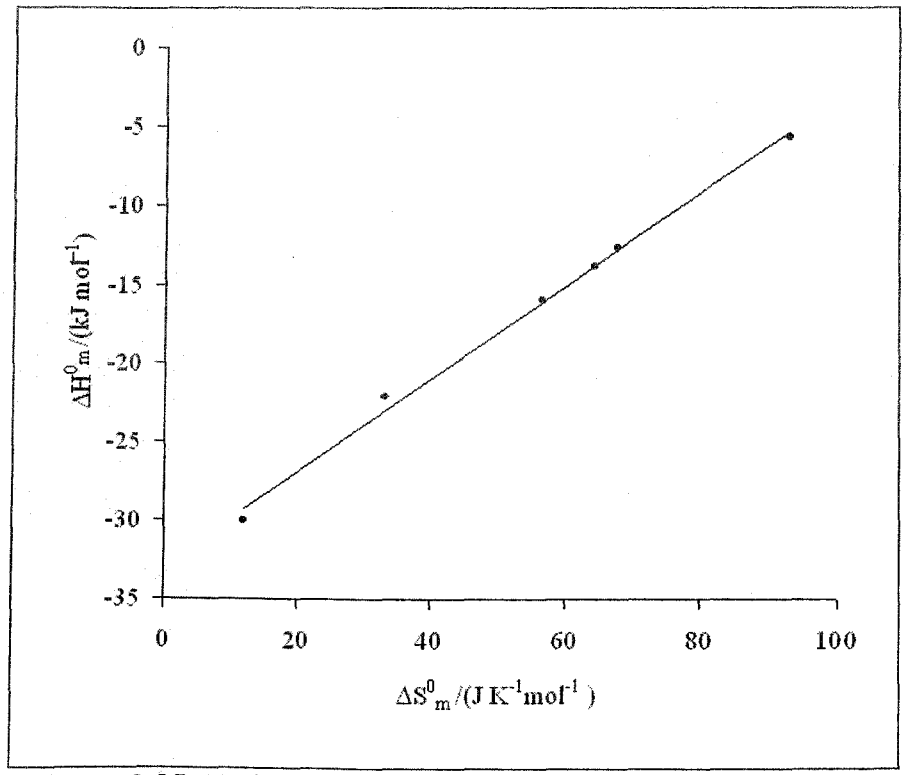

Figure 3.35: Enthalpy–entropy compensation plots AOT surfacta having different counterions at 298 K

counterions. Figure 3.34 and Figure 3.35 represent the enthalpy-entropy compensation plots at 298K for DS and AOT. The calculated compensation temperature value of 303.2 K for DS and 295.6 K for AOT satisfactorily follows the characteristic range of other ionic surfactants [20,78,105]. The intercept, ΔH^*_m, has been calculated as -37.8 kJmol^{-1} and -32.8 kJmol^{-1} for DS and AOT respectively which correspond to the driving force of micellization where the entropy does not contribute the process at that particular temperature.

It is well known that the air-solution interface of a surfactant solution is well populated by the adsorbed molecules. The maximum surface excess concentrations (Γ_{max}) in the aqueous-air interface are calculated by using common Gibbs adsorption equation. For 1:1 ionic surfactant in the absence of any other solutes, Γ_{max} may be expressed by the following relation [107-109]:

$$\Gamma_{max} = (1/2.303n'RT)(-\partial\gamma/\partial \log C) \qquad (3.19)$$

where γ expresses the surface tension, C and n′ are the molar concentration and number of particles per molecule of the surfactant respectively. Since in aqueous solution at concentrations less than cmc, both dodecyl sulfate and AOT behave like a uni-univalent electrolyte, the thermodynamic treatment requires n′ = 2, states an equimolar ratio of surfactant anion and counterion in the interface. Similar to analysis of $\ln X_{cmc}$ vs T plot, γ vs lnC plot was also fitted to a second order polynomial to measure Γ_{max}. The area per molecule at the interface provides information on the degree of packing and the orientation of the adsorbed surfactant molecule when compared with the dimensions of the molecule as obtained by the use of molecular models. From the surface excess concentration the minimum area per molecule (A_{min}) at the interface in square nanometer is calculated from the relation:

$$A_{min} = 10^{14}/(N\Gamma_{max}) \qquad (3.20)$$

where N is the Avogadro's number and Γ_{max} is in mol/cm^2.

The surface excess concentration at surface saturation Γ_{max}, is a useful measure of the effectiveness of adsorption of the surfactant at air-solution interface, science it is the maximum value that adsorption can attain. It is well known that for

both nonionic [108] and anionic [109] surfactants, Γ_{max} values slightly decreases with temperature while in some other cases an increase of the surface excess quantity has been reported [110] in presence of additives. With increasing temperature Γ_{max} for dodecyl sulfate follow more or less general trend as expected, which presumably due to increased thermal motion with a consequent decrease in the effectiveness of adsorption. But in the case of AOT surfactant with six different counter ions, the change of Γ_{max} does not follow a regular trend. A critical examination of Table 3.5 and 3.6 show a slight increment in Γ_{max} with temperature for all the counter ions, which may be due to the effect of lower hydration of the sulfosuccinate part of AOT at higher temperature and hence an increasing tendency to move to the air-liquid interface [45,46]. While in case of dodecyl sulfate Γ_{max} decreases with temperature (Table 3.1 and 3.2), and this suggests greater salvation of the amphiphilic molecules at higher temperature, where salvation energy overcome the so called dehydration process. It is quite obvious that the standard state for the adsorbed surfactant is a hypothetical monolayer at its minimum surface area per molecule, but at zero surface pressure. The typical double chain of the amphiphile may also partially be responsible for this result causing 'steric inhibition' during adsorption. The moderate increase in the effectiveness of adsorption at the air-water interface with temperature is due to increased thermal motion, and therefore, A_{min} display an inverse trend with temperature, as expected. With increasing bulkiness of the counterions of the amphiphiles the increase of Γ_{max} are quite noticeable. At a particular temperature, Γ_{max} shows anomalous behaviour as the counter ion of the surfactant changes. It may be attributed to the enhanced hydrophobicity of the anionic part of the surfactant molecules depending upon accessibility of their corresponding counter ions. A study of the behaviour of tetramethylammoniumdodecyl sulfate at the air-solution interface indicated to a penetration of a part of the $N^+(CH_3)_4$ ions in the dodecyl sulfate layer [111]. A similar phenomenon may also partially be responsible for the observed surface behaviour in the present systems.

3.3 Effect of Alcohols on the Aggregation Properties of Micellar systems in Aqueous Medium

The hydrophobic and electrostatic forces among ionic surfactant molecules play an essential role for the self-association and formation of micelles. One of the

most interesting aspects of these heterogeneous micelles is their ability to accommodate organic molecules [112–115]. An increased flexibility of the micellar membrane and thereby an improved ability to solubilize hydrophobic molecules can be achieved by adding alcohols [116]. The size and shape of micelle aggregates containing commonly used surfactants and co-surfactants have been investigated earlier [117,118]. Many researchers are interested in mixed alcohol-water systems particularly due to their importance in the preparation of microemulsions [119,120]. Reports of Onori et at. [121-123] showed that the effects due to alcohols on two very different systems and processes, the thermal denaturation of t-RNA (transfer ribonucleic acid) and the micellization of several surfactant molecules were strikingly similar and were closely paralleled in simpler properties of alcohol-water mixtures themselves. These results support the hypothesis that the dominant mechanism by which an alcohol affects this process is through its effect on structure of water. At higher concentrations some other effects like the alteration in the dielectric constants of the solvent or the partition of the alcohol molecules between bulk and the micellar phase may be more important. The behaviour of sodium dodecyl sulfate (SDS) micelles in the presence of *n*-alcohols was extensively investigated by many researchers [45,56,57,124,125]. Micellization studies with hydrophilic alcohols and diols with the same number of carbons but different molecular structure have also been carried out [126, 127]. Carnero Ruiz [141] reported the thermodynamics of micellization in tetradecyltrimethylammonium bromide in a dihydric alcohol, ethylene glycol-water binary mixtures, and showed that with increasing the percentage of alcohol in the solvent both the cmc and counter ion dissociation constant (α) increased to a considerable extent. But in case of other progressively long chain alcohols, (e.g. n-heptanol to n-decanol) opposite observations were reported recently [115]. Similar reports are available for middle and short chain alcohols also [45,50,142]. It was suggested that for ionic surfactants, the cmc is related by the following equation [103]:

$$\log(\mathrm{cmc}) = Z(1-\beta)\left[\log\frac{2000\pi\sigma^2}{\varepsilon_r RT} - \log c_i\right] + \left[\frac{\Delta G_{(-CH_2-)}}{2.303RT}\right]n + B \qquad (3.21)$$

where Z is the charge of the surfactant ion, β is the fraction of counter ions bound by the micelle in the case of ionic surfactants, σ is the surfactants charge

density on the micelle, ε_r is the dielectric constant of the solvent, c_i is the concentration of counter ions in the polar solution, n is the carbon number of the surfactant and B is an arbitrary constant depending upon the system.

Equation 3.21 suggests that it is difficult to predict the effect of temperature on the cmc. But an increase in temperature may also decrease β, so the overall effect for an increase in temperature is to increase the cmc. When the β parameter of the system increases with an increment in carbon number of alcohol, it also indicates that the cmc of surfactant will also decrease.

But when the fraction of long-chain alcohol increases, the extent of counterion binding to the micelle also increases and as a result lowering of cmc will be observed. But due to the presence of alcohol the dielectric constant of the solvent decreases considerably, which suggest an easier denaturation of micelles and the cmc of the surfactant should be increased. In general all the factors mentioned above are reflected in the resulting cmc and related thermodynamic values of micellization in water-alcohol binary mixtures. As mentioned earlier ethylene glycol (EG) showed the reverse effect than the other alcohols which may be explained by its higher dielectric constant, small hydrophobic surface and greater capability of hydrogen bond formation. Sjöberg [133] also observed that in strong polar solvents, such as formamide and EG, mocelles are found with qualitatively the same features as in water. It was found that the cmc of hexadecyl -trimethylammonium bromide (C_{16}TAB) is much higher in formamide (100 mM) than water (1mM) at 333K temperature. It is a general feature, also exemplified by smaller micelle radii and aggregation numbers, that self-assembly is much less co-operative in alternative polar solvents.

In this connection the influence of very common short chain alcohols, viz. ethanol, 1-propanol and 2-propanol on the micellization of SDS and AOT in aqueous medium are studied in the present investigation within the temperature range of 298-313K. Though it is said that the highly water-soluble alcohols such as methanol, ethanol and propanol dissolve mainly in the aqueous bulk solution [57,128], there are number of reports [129-130] supporting the influence of these short chain alcohols on micellization. The results of the investigation are relevant to several applied topics in colloids where micelles and microemulsions in alcohol–water mixtures have been used as an elution medium in micellar liquid chromatography [134]. 2-propanol is

also used in studies of photohydrogen abstraction by ketones in both homogeneous and micellar solutions [135].

3.3.1 Experimental Section

As discussed earlier, to investigate the micellization properties conductivity measurements of the solutions containing different proportion of alcohols and surfactants are performed within the temperature range of 298K to 313K. The temperature was maintained in a thermostated double-glass water jacket by the flow of constant temperature with in ±0.01K. All the alcohols (Merck) associated in the experiments are used after necessary distillation as described elsewhere [136].

3.3.2 Results and Discussion

Similar to the previous measurements the cmc values of the SDS and AOT solutions in the presence of hydrophilic alcohols were determined by the 'break points' of the concentration versus conductance plots. The cmc and the other related thermodynamic parameters of SDS and AOT are given in Table 3.10 and 3.11 respectively. All the thermodynamic parameters including cmc are determined by similar procedure as described in the previous section (section 3.2.2). As expected, the cmc decreases upon addition of short chain alcohols, but the decrease is less than in case of a medium chain alcohol such as *n*-butanol [114,127]. For SDS-propanol systems the calculated cmc and α values are well similar to the reported [50] values determined spectroscopically. At alcohol concentrations higher than 1M, the determination of the cmc becomes more difficult because the change in conductivity is less pronounced. As mentioned above to explain the deviations observed in the micellization parameters two factors, viz., lowering of dielectric constant with addition of alcohol and the effective hydrophobic area of the alcohol molecule must be considered. In all cases the process of micelle formation is energetically favoured which can be supported by effective negative value of ΔG_m^0. The other two thermodynamic parameters viz. ΔH_m^0 and ΔS_m^0 also show their necessary contribution in favour of micellization process.

Based on the relation between cmc and the thermodynamic functions the effect of alcohols on micellizatin can also be well explained. Table 3.10 suggests that in aqueous-alcohol medium relatively greater negative values of ΔH^0_m (-22.1 ~ -38.2

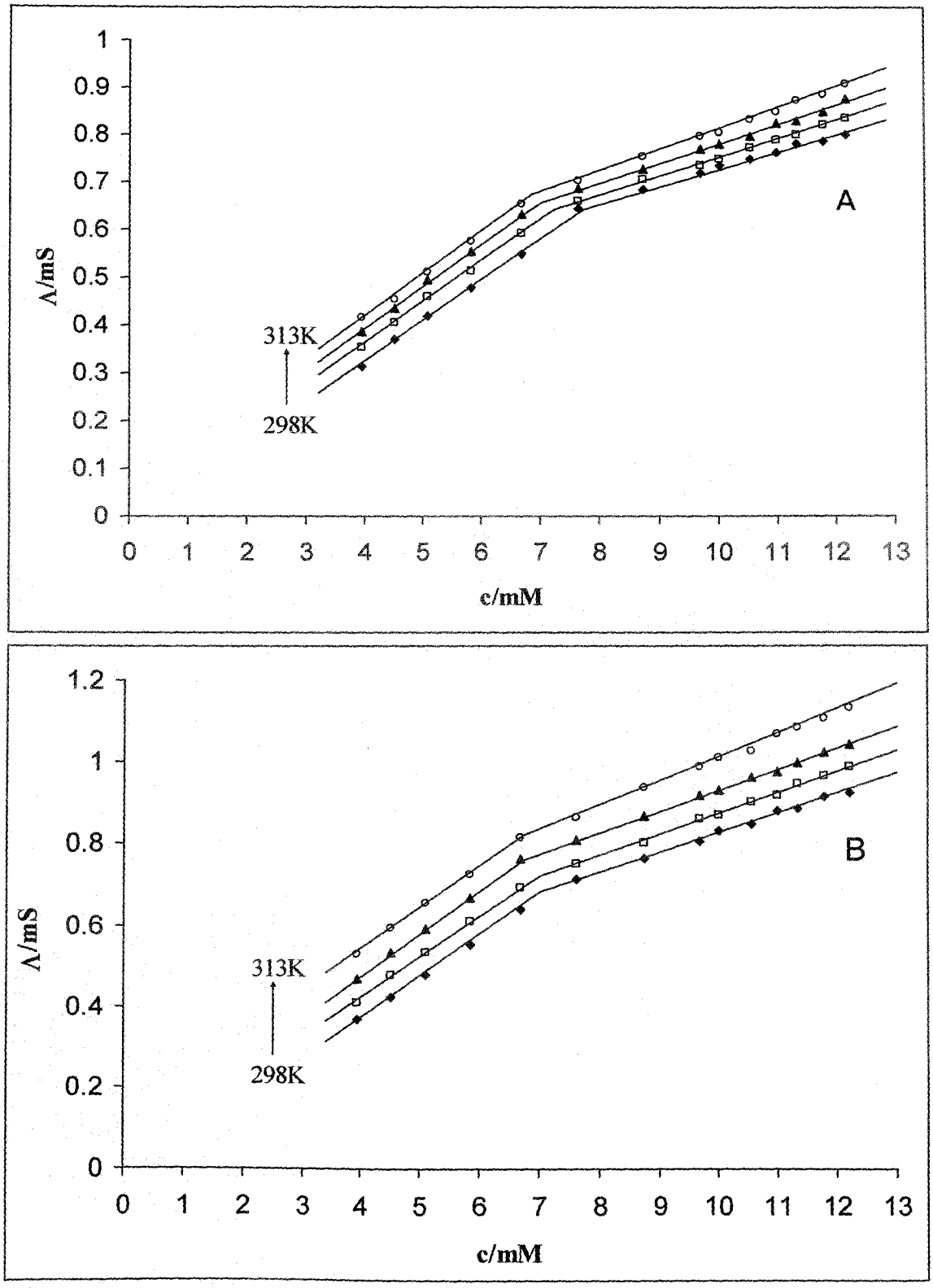

Figure 3.36 : Variation of conductance, Λ, with concentration of SDS having different proportion of ethanol (A: 0.4M ethanol; B: 0.7M ethanol)

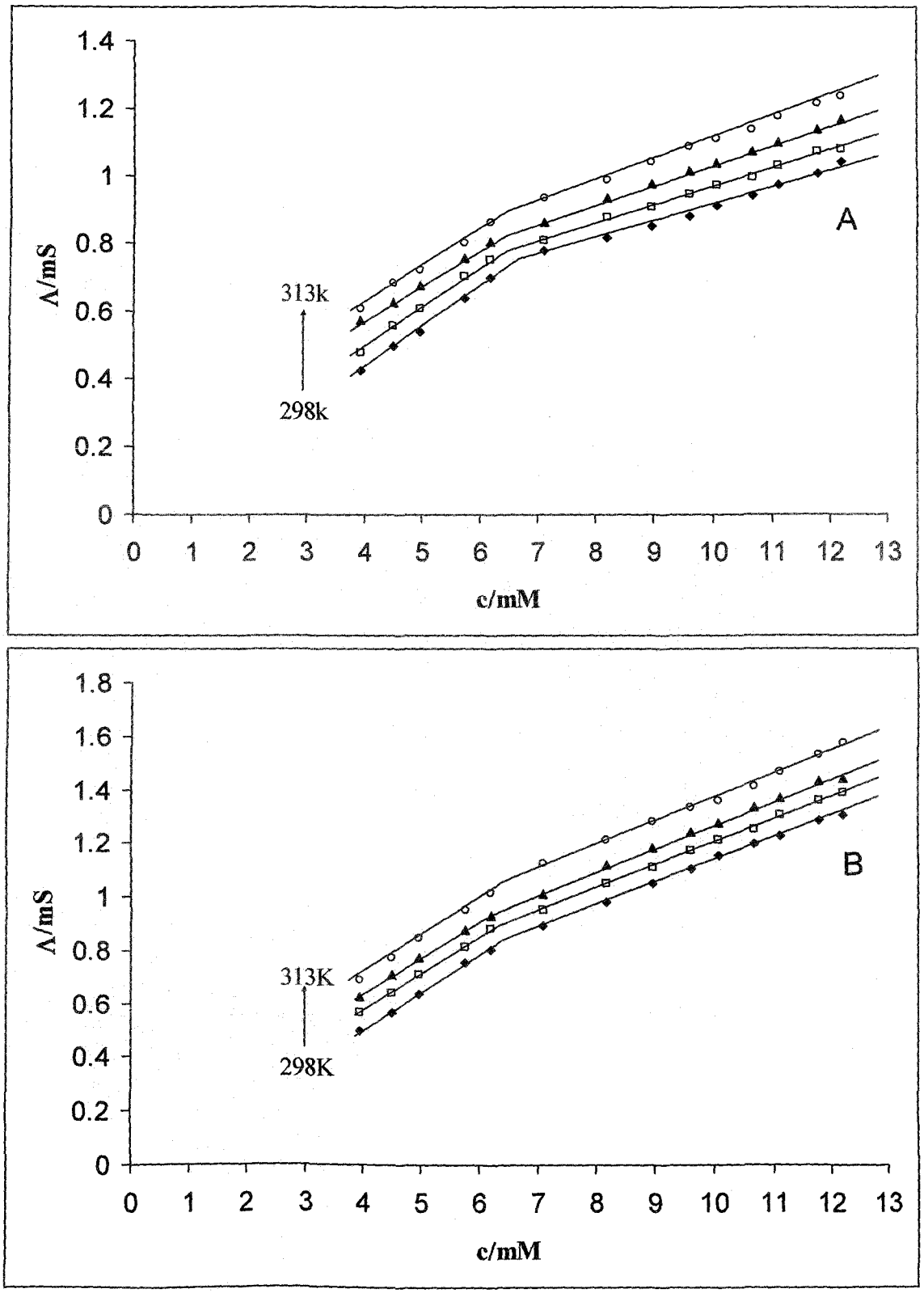

Figure 3.37: Variation of conductance, Λ, with concentration of SDS having different proportion of ethanol (A: 1.0M ethanol; B: 1.4M ethanol)

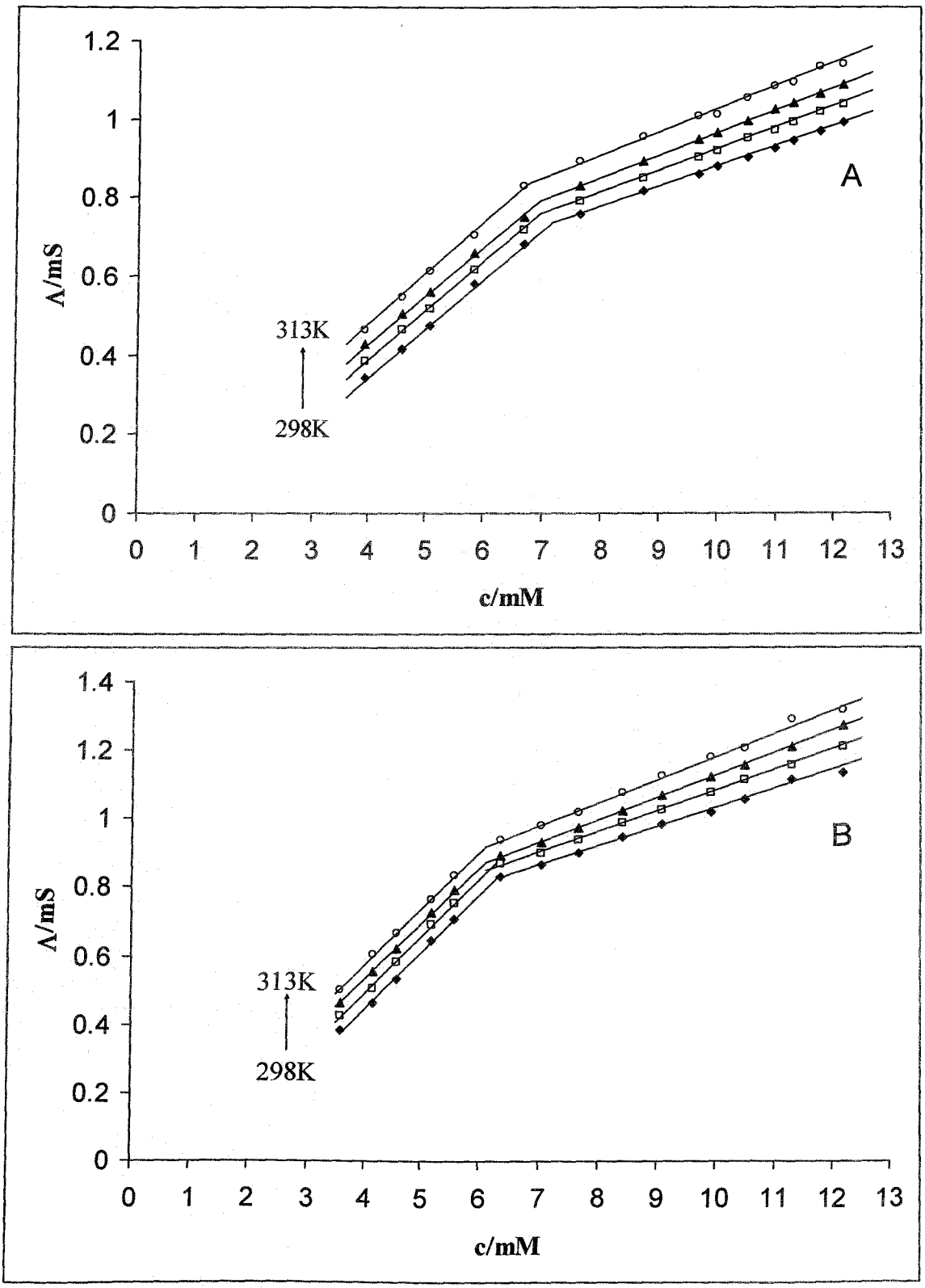

Figure 3.38: Variation of conductance, Λ, with concentration of SDS having different proportion of 1-propanol (A: 0.2M 1-propanol; B: 0.4M 1-propanol)

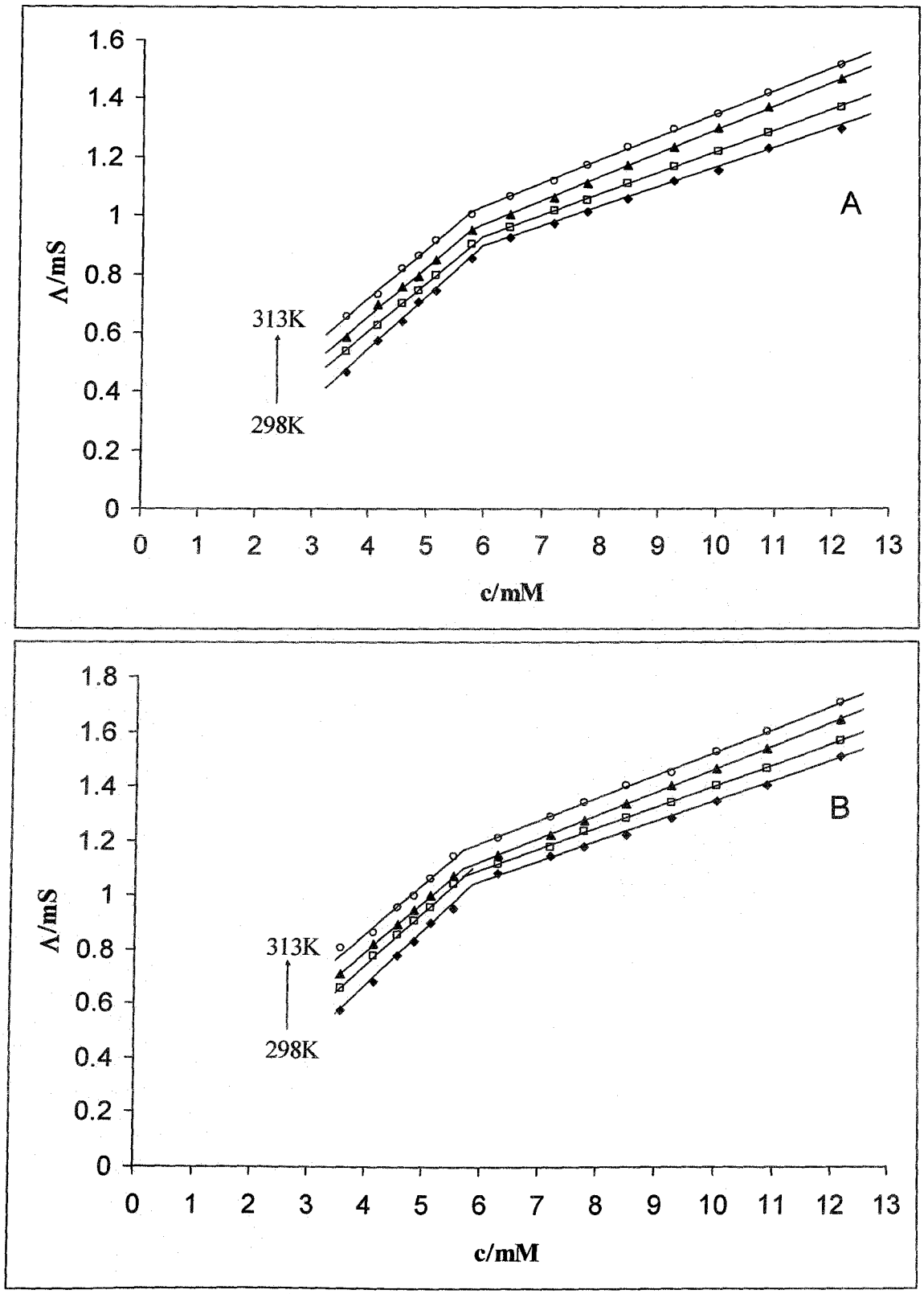

Figure 3.39: Variation of conductance, Λ, with concentration of SDS having different proportion of 1-propanol (A: 0.6M 1-propanol; B: 0.8M 1-propanol)

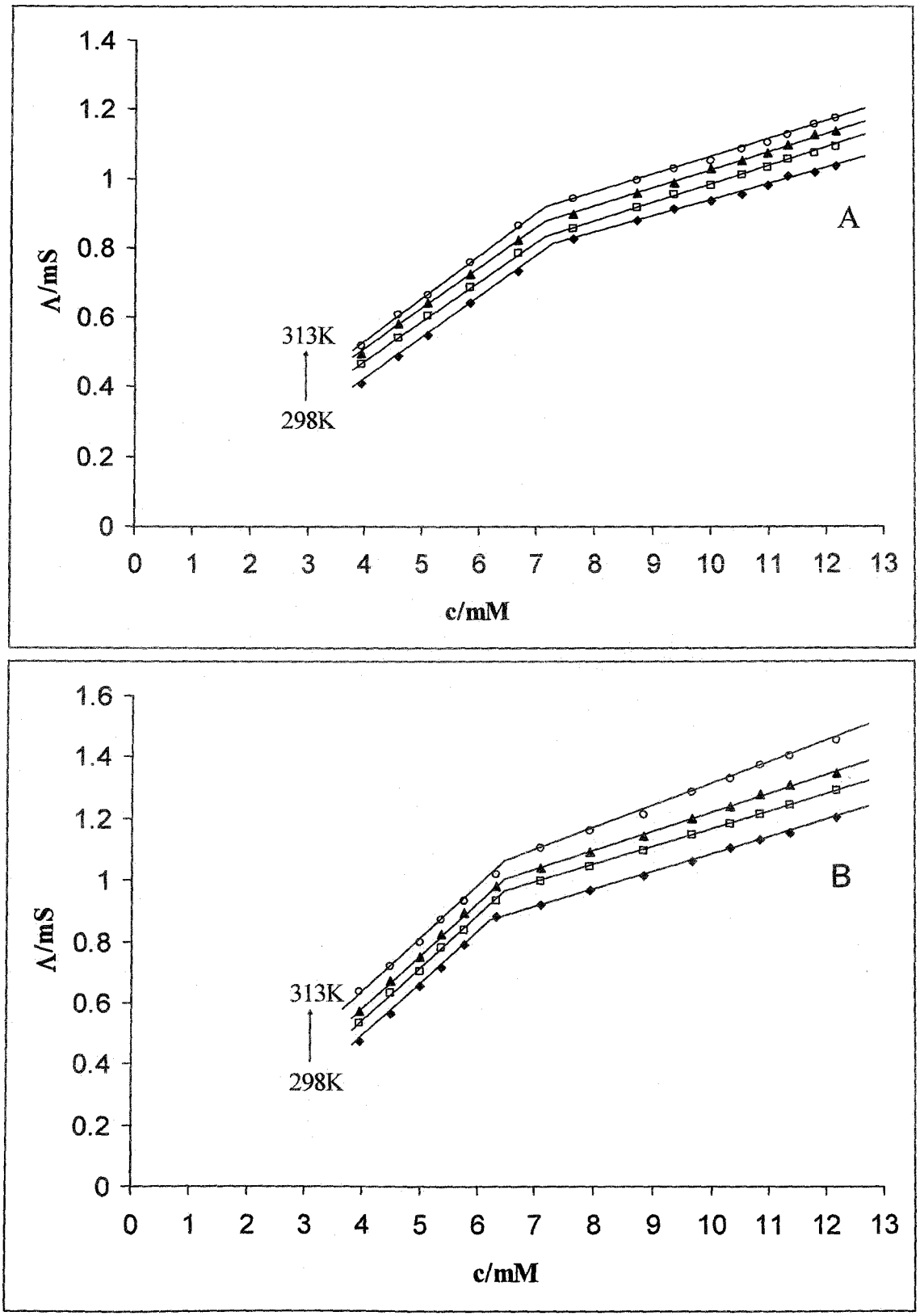

Figure 3.40: Variation of conductance, Λ, with concentration of SDS having different proportion of 2-propanol (A: 0.2M 2-Propanol; B: 0.4M 2-Propanol)

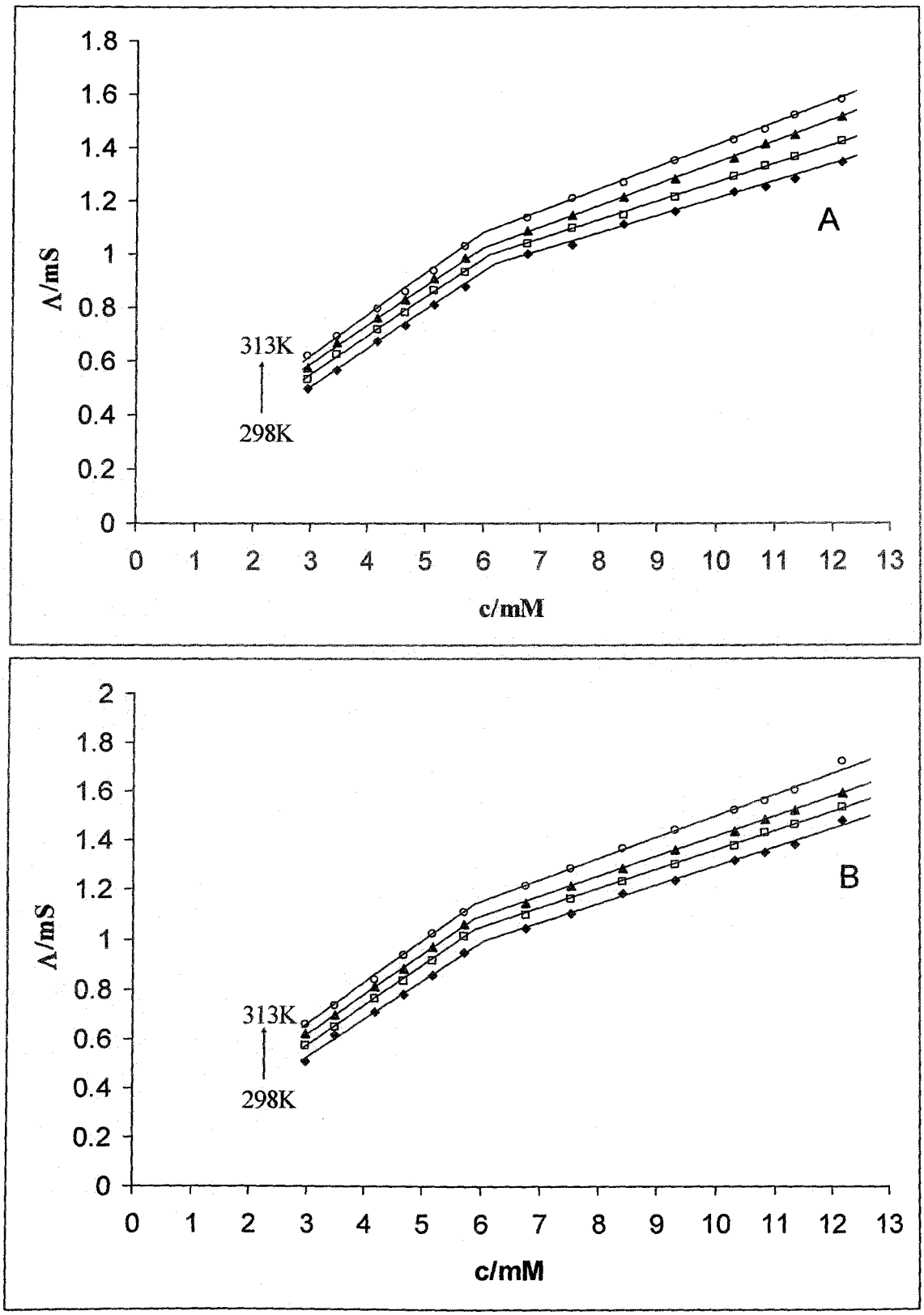

Figure 3.41: Variation of conductance, Λ, with concentration of SDS having different proportion of 2-propanol (A: 0.6M 2-Propanol; B: 0.8M 2-Propanol)

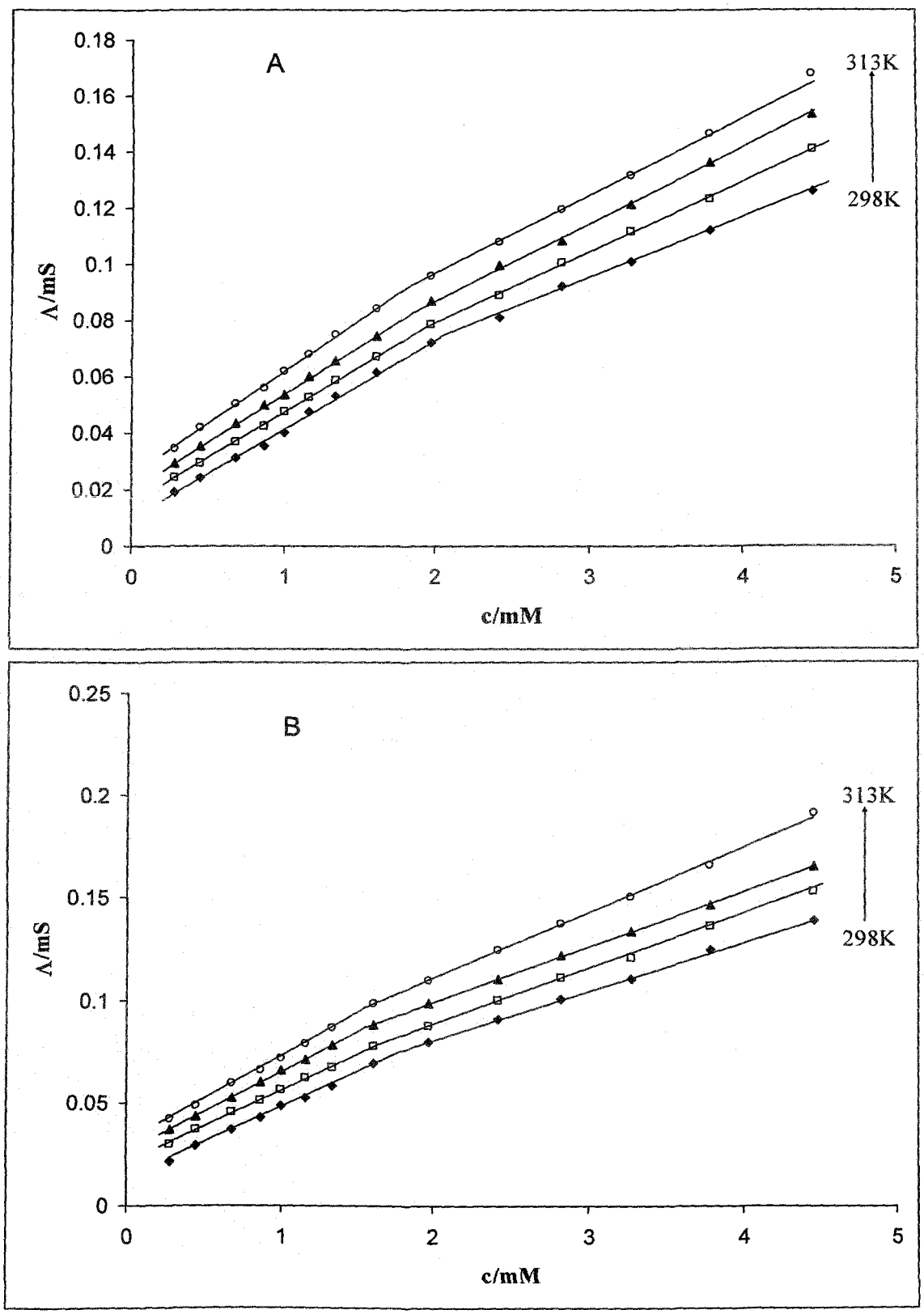

Figure 3.42: Variation of conductance, Λ, with concentration of AOT having different proportion of Ethanol (A: 0.4M Ethanol; B: 0.7M Ethanol).

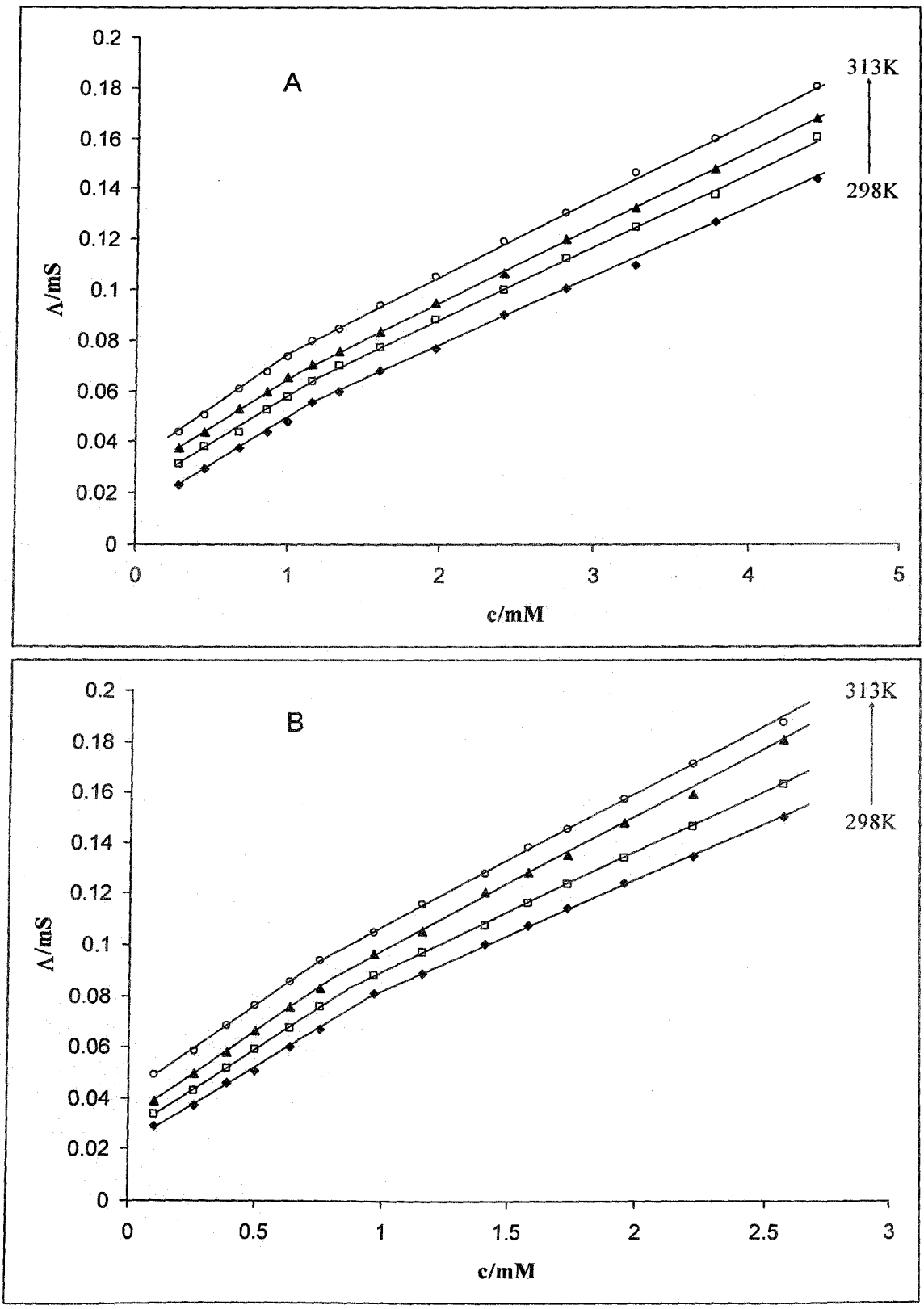

Figure 3.43: Variation of conductance, Λ, with concentration of AOT having different proportion of 1-Propanol (A: 0.6M 1-Propanol; B: 0.8M 1-Propanol).

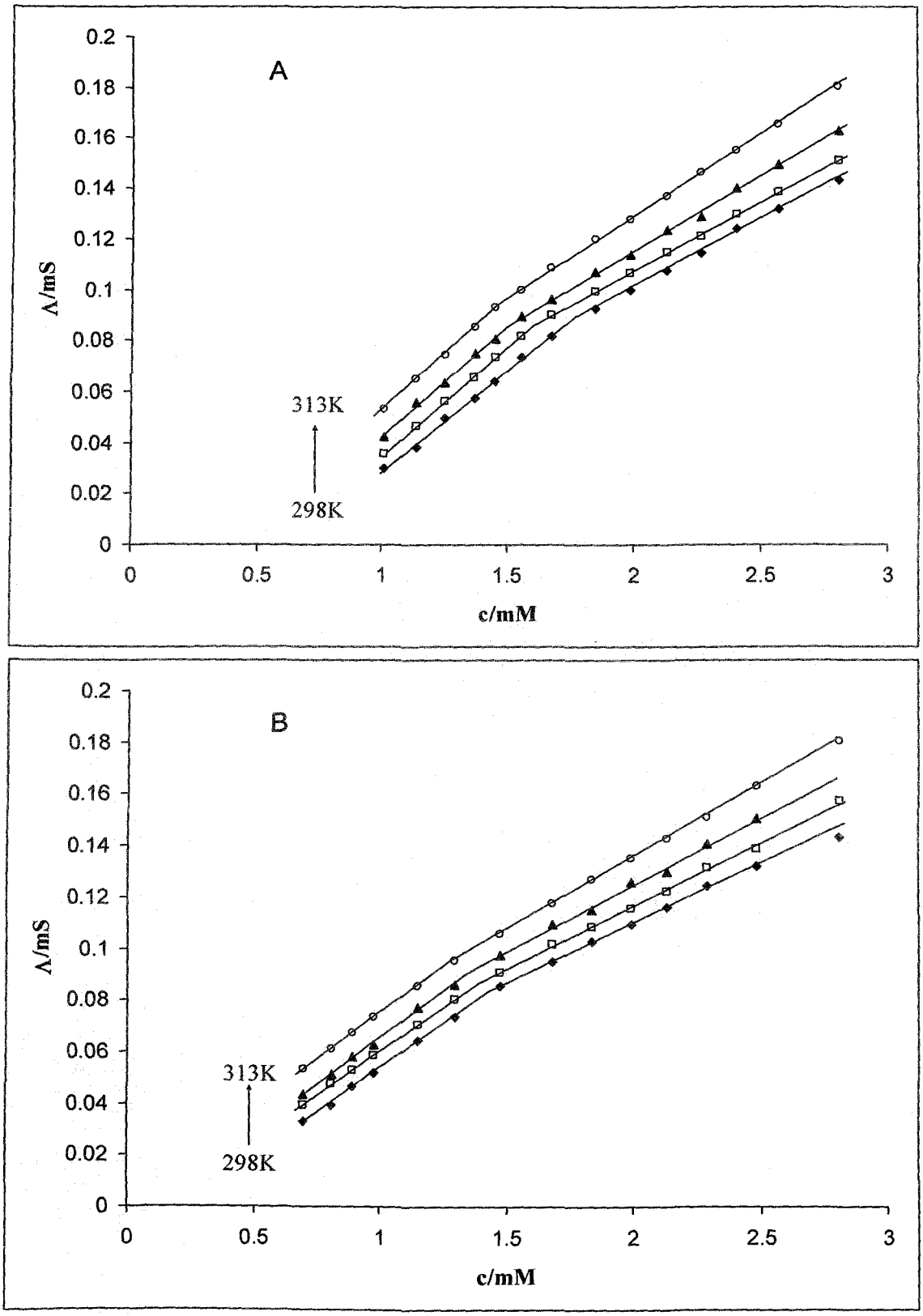

Figure 3.44: Variation of conductance, Λ, with concentration of AOT having different proportion of 2-Propanol (A: 0.2M 2-Propanol; B: 0.4M 2-Propanol).

$kJmol^{-1}$) contributes to the negative ΔG^0_m (-31.0 ~ -39.6$kJmol^{-1}$) for the micellization of SDS when compared with aqueous neat medium (Table 3.3). But for AOT this phenomenon is somehow less pronounced due to its more hydrophobic double strand molecular moiety. The effect of alcohol on the micellization process, given by ΔG^0_t, is calculated using the following equation:

$$\Delta G_t^0 = \Delta G^0_{m(alcohol-water)} - \Delta G^0_{m(water)} \tag{3.20}$$

It may be noted that for AOT, micellization process is less favourable in water-alcohol binary mixture than SDS, which is well supported by the all positive values of ΔG^0_t. For SDS, on the other hand, ΔG^0_t gives both positive and negative values depending upon the temperature and the proportion of alcohols present in the solvent.

MacManus et. al. [137] showed that the position of the solubilized alcohol depends on the alkyl chain length. More hydrophobic alcohols seem to penetrate deeper into the hydrocarbon interior of the micelles than the hydrophilic ones. The solubilization of alcohol leads to a decrease in the electrostatic interaction between the surfactant head groups, and makes the surfactant molecules more energetically favorable for being a part of the micelles. Although the short-chain alcohols are highly hydrophilic, they undergo partitioning between the micellar pseudophase and the aqueous phase which can be supported by enhancement of the degree of ionization, α with addition of alcohols. The decrease of local polarity of the micelle was reported [138] upon addition of allyl alcohol may also favors micellization at the lower concentration of surfactants.

In order to quantify the solubilization or association of alcohol in the micelles, the fraction (a) of alcohol which is present in the micellar pseudophase may be expressed with self-diffusion coefficients [139]:

$$D_A = (1-a)D_A^{free} + aD_A^{mic} \tag{3.19}$$

where D_A is the measured self-diffusion coefficient of the alcohol, D_A^{free} is the self-diffusion coefficient of the free alcohol molecules, and D_A^{mic} is the self-diffusion coefficient of the alcohol molecules bound in the micelles. In solutions where the cmc is low and the concentration of the surfactant is large compared to the cmc, the D_A^{mic} may be considered equal to the measured self-diffusion coefficient of the surfactant.

Table 3.10

Micellization parameters of SDS having different proportion of alcohols

Alcohol /(mol dm^{-3})	T/ (K)	cmc /(mol $dm^{-3} \times 10^3$)	α	$-\Delta G_m^o$/ (kJ mol^{-1})	$-\Delta H_m^o$/ (kJ mol^{-1})	ΔS_m^o/ (J $K^{-1} mol^{-1}$)
			Ethanol			
0.4	298	7.81	0.31	37.1	25.2	40.0
	303	7.21	0.32	37.9	31.0	22.8
	308	6.90	0.33	38.5	35.1	11.0
	313	6.85	0.32	39.4	32.1	23.3
0.7	298	7.03	0.43	34.9	23.4	38.6
	303	6.90	0.45	35.1	28.6	21.5
	308	6.82	0.44	36.0	34.7	0.4
	313	6.79	0.47	35.9	34.1	0.6
1.0	298	6.66	0.52	33.1	22.1	36.9
	303	6.56	0.55	33.0	26.8	20.5
	308	6.49	0.56	33.4	31.5	6.2
	313	6.48	0.60	33.0	31.8	3.8
1.4	298	6.40	0.62	31.0	20.6	34.9
	303	6.34	0.63	31.3	25.3	19.8
	308	6.29	0.62	32.1	30.7	4.5
	313	6.21	0.64	32.2	31.0	3.8
			1-Propanol			
0.2	298	7.22	0.33	37.0	24.9	40.6
	303	7.02	0.35	37.3	30.5	22.4
	308	6.90	0.37	37.5	36.2	4.2
	313	6.78	0.36	38.5	37.4	3.5
0.4	298	6.34	0.37	36.7	23.4	44.6
	303	6.21	0.39	36.9	28.6	27.4
	308	6.17	0.41	37.1	34.7	7.8
	313	6.17	0.41	37.7	34.9	8.9
0.6	298	6.01	0.43	35.5	23.4	40.6
	303	5.95	0.45	35.7	28.6	23.4
	308	5.81	0.44	36.6	34.7	6.2
	313	5.80	0.47	36.5	35.0	4.8
0.8	298	5.88	0.48	34.5	22.7	39.6
	303	5.76	0.48	35.1	28.1	23.1
	308	5.68	0.51	35.1	33.1	6.5
	313	5.65	0.47	36.6	34.0	8.3
			2-Propanol			
0.2	298	7.30	0.29	37.9	25.5	41.6
	303	7.22	0.31	38.1	31.2	22.8
	308	7.16	0.33	38.3	37.1	3.9
	313	7.16	0.30	39.6	38.2	4.5
0.4	298	6.62	0.33	37.3	24.9	41.6
	303	6.55	0.32	38.4	31.0	24.4
	308	6.50	0.34	38.5	36.9	5.2
	313	6.47	0.37	38.4	37.1	4.1
0.6	298	6.21	0.37	36.7	24.3	41.6
	303	6.17	0.38	37.2	29.9	24.1
	308	6.11	0.41	37.1	35.4	5.5
	313	6.05	0.40	38.0	37.0	3.2
0.8	298	6.03	0.41	36.0	23.7	41.3
	303	5.94	0.42	36.4	29.2	23.8
	308	5.92	0.45	36.3	34.5	5.8
	313	5.88	0.46	36.7	35.1	5.1

Table 3.11

Micellization parameters of AOT having different proportion of alcohols

Alcohol /(mol dm^{-3})	T/ (K)	cmc /(mol $dm^{-3} \times 10^3$)	α	$-\Delta G_m^o$/ (kJ mol^{-1})	$-\Delta H_m^o$/ (kJ mol^{-1})	ΔS_m^o/ (J $K^{-1} mol^{-1}$)
			Ethanol			
0.4	298	2.03	0.67	33.7	19.8	46.4
	303	1.95	0.70	32.2	24.0	27.1
	308	1.83	0.72	32.4	28.5	12.8
	313	1.80	0.71	33.2	31.5	5.4
0.7	298	1.78	0.72	32.8	19.1	46.1
	303	1.63	0.72	33.7	23.6	33.0
	308	1.56	0.73	34.1	28.2	18.9
	313	1.56	0.74	34.4	33.0	4.2
1.0	298	1.41	0.75	32.8	18.6	47.4
	303	1.34	0.73	34.0	23.5	34.8
	308	1.30	0.75	34.1	27.8	20.5
	313	1.20	0.74	35.2	33.0	6.9
1.4	298	1.01	0.76	33.5	18.5	50.5
	303	1.00	0.79	33.3	22.3	36.1
	308	0.92	0.77	34.7	27.3	23.7
	313	0.88	0.80	34.5	31.5	9.7
			1-Propanol			
0.2	298	1.78	0.70	33.3	19.4	46.8
	303	1.66	0.72	33.6	23.6	32.8
	308	1.53	0.72	34.4	28.5	19.3
	313	1.52	0.71	35.3	33.8	4.6
0.4	298	1.50	0.73	33.1	18.9	47.5
	303	1.51	0.73	33.6	23.4	33.6
	308	1.39	0.72	34.7	28.5	20.3
	313	1.35	0.74	34.8	33.0	5.7
0.6	298	1.23	0.74	33.5	18.8	49.2
	303	1.20	0.73	34.4	23.5	36.0
	308	1.09	0.75	34.7	27.8	22.4
	313	1.01	0.75	35.5	32.8	8.7
0.8	298	0.94	0.75	34.0	18.6	51.6
	303	0.88	0.75	34.8	23.1	38.7
	308	0.80	0.77	35.1	27.4	25.2
	313	0.73	0.77	36.0	32.2	11.9
			2-Propanol			
0.2	298	1.77	0.69	33.6	19.5	47.2
	303	1.60	0.70	34.2	24.0	33.7
	308	1.50	0.72	34.5	28.5	19.5
	313	1.47	0.72	35.1	33.6	4.9
0.4	298	1.43	0.72	33.5	19.1	48.4
	303	1.38	0.73	33.9	23.5	34.5
	308	1.35	0.73	34.6	28.4	20.5
	313	1.25	0.74	35.1	33.0	6.5
0.6	298	1.15	0.73	33.9	18.9	50.3
	303	1.07	0.73	34.7	23.4	37.2
	308	0.99	0.75	35.0	27.8	23.4
	313	0.88	0.75	36.0	32.8	10.1
0.8	298	0.80	0.75	34.5	18.6	53.3
	303	0.77	0.77	34.7	22.7	39.4
	308	0.69	0.76	35.9	27.6	26.9
	313	0.70	0.77	36.1	32.2	12.3

Table 3.12
Effect of alcohol on micellization

SDS			AOT		
Alcohol /(mol dm^{-3})	T/ (K)	ΔG^0_t	Alcohol (mol dm^{-3})	T/ (K)	ΔG^0_t
		Ethanol			
	298	0.3		298	1.6
0.4	303	1.4	0.4	303	-1.3
	308	0.8		308	-1.2
	313	1.6		313	-1.0
	298	-1.9		298	0.7
0.7	303	-1.4	0.7	303	0.2
	308	-1.7		308	0.5
	313	-1.9		313	0.2
	298	-3.7		298	0.7
1.0	303	-3.5	1.0	303	0.5
	308	-4.3		308	0.5
	313	-4.8		313	1.0
	298	-5.8		298	1.4
1.4	303	-5.2	1.4	303	-0.2
	308	-5.6		308	1.1
	313	-5.6		313	0.3
		1-Propanol			
	298	0.2		298	1.2
0.2	303	0.8	0.2	303	0.1
	308	-0.2		308	0.8
	313	0.7		313	1.1
	298	-0.1		298	1.0
0.4	303	0.4	0.4	303	0.1
	308	-0.6		308	1.1
	313	-0.1		313	0.6
	298	-1.3		298	1.4
0.6	303	-0.8	0.6	303	0.9
	308	-1.1		308	1.1
	313	-1.3		313	1.3
	298	-2.3		298	1.9
0.8	303	-1.4	0.8	303	1.3
	308	-2.6		308	1.5
	313	-1.2		313	1.8
		2-Propanol			
	298	1.1		298	1.5
0.2	303	1.6	0.2	303	0.7
	308	0.6		308	0.9
	313	1.8		313	0.9
	298	0.5		298	1.4
0.4	303	1.9	0.4	303	0.4
	308	0.8		308	1.0
	313	0.6		313	0.9
	298	-0.1		298	1.8
0.6	303	0.7	0.6	303	1.2
	308	-0.6		308	1.4
	313	0.2		313	1.8
	298	-0.8		298	2.4
0.8	303	-0.1	0.8	303	1.2
	308	-1.4		308	2.3
	313	-1.1		313	1.9

References

1. Hiementz, P.C.; Rajagopalan, R. *Principles of Colloidal and Surface chemistry,* Third edition, New York, 1997.

2. (a) Bellare, J.R.; Kaneko, T.; Evans, D.F. *Langmuir* **1988**, *4*, 1066. (b) Hoffmann, H. *J. Phys. Chem.* **1994**, *98*, 1433.

3. Paul, M.; Holland, Donn, N.; Rubingh, *Mixed Surfactants System, ASC symposium series 501,* American chemical society, Washington, DC, P1-43, 1992.

4. (a) Hartley, G.S. *Aqueous Solutions of Paraffin Chain Salts,* Hermann and Cie, Paris, 1936. (b) Attwood, D.; Florence, A.T. *Surfactant System,* Champan and Hall Ltd. USA, 1985.

5. Jakobi, G.; Lohr, A. *Detergent and Textile Washing,* VCH publisher, Germany, P 49-63, 1987.

6. (a) Bales, B.L.; Benrraou, M.; Zana, R. *J. Phys. B* **2002**, *101*, 9033. (b) Zana, R. *Colloid Interface Sci.* **1980**, *78*, 330.

7. Evans, D.F.; Wennerström, *The Colloidal Domain. Where Physics, Chemistry, Biology and Technology Meet,* Wiley-VCH, New York, 1994.

8. Saha, S. K.; Jha, M.; Ali, M.; Chakraborty, A.; Bit, G.; Das, S. K. *J. Phys. Chem. B* **2008**, *112*, 4642.

9. Israelachvili, J.N. *Intermolecular and Surface Forces,* Academic Press, London, 1985.

10. Gruen, D. W. R. *Prog. Colloid Polym. Sci.* **1985**, *70*, 6.

11. Paul, A.; Griffiths, P.C.; Pettersson, E.; Stilbs, P.; Bales, B.L.; Zana, R.; Heenan, R.K. *J. Phys. Chem. B* **2004**, *108*, 3810.

12. Bales, B.L. *J. Phys. Chem. B* **2001**,*105*, 6798.

13. Benrraou, M.; Bales, B.L.; Zana, R. *J. Phys. Chem. B* **2003**, *107*, 13432.

14. Shimizu, S.; Pires, P.A.R.; El Seoud, O.A. *Langmuir* **2004**,*20*, 9551.

15. Pisárčik, K.; Devínsky, F.; Lacko, I. *Acta Facult. Pherm. Univ. Comenianae* **2003**,*50*, 119.

16. Lah, J.; Bešter-Rogač, M.; Perger, T.-M.; Vesnaver, G. *J. Phys. Chem. B* **2006**, *110*, 2379.

17. Chatterjee, A.; Moulik, S.P.; Sanyal, S.K.; Mishra, B.K.; Puri, P.M. *J. Phys. Chem. B* **2001**, *105*, 12823.

18. Stigter, D. *J. Phys. Chem.* **1974**, *78*, 2480.

19. Kresheck, G. C. *J. Phys. Chem. B* **1998**, *102*, 6596.

20. Chatterjee, A.; Moulik, S. P.; Sanyal, S. K.; Mishra, B. K.; Puri, P. M. *J. Phys. Chem. B.* **2001**, *105*, 12823.

21. (a) González-Pérez, A.; Czapkiewicz, J.; Del Castillo, J.L.; Rodríguez, J.R. *Colloid Polym. Sci.* **2004**, *282*, 1359. (b) Asakawa, T.; Kitano, H.; Ohta, A.; Miyagishi, S. *J. Colloid Interface Sci.* **2001**, *242*, 284.

22. (a) Rehage, H.; Hoffmann, H. *Mol. Phys.* **1991**, *74*, 933. (b) Iijima, H.; Kato, T.; Soderman, O. *Langmuir* **2000**, *16*, 318.

23. Hoffmann, S.; Rauscher, A.; Hoffmann, H. *Ber. Bunsen-Ges. Phys.Chem.* **1991**, *95*, 153.

24. Malliaris, A.; Lang, J.; Zana, R. *J. Chem. Soc., Faraday Trans. 1* **1986**, *82*, 109.

25. Lindman, B.; Puyal, M-C.; Kamenka, N.; Rymden, R.; Stilbs, P. *J. Phys. Chem.* **1984**, *88*, 5048.

26. Bales, B.L.; Benrraou, M.; Tiguida, K.; Zana, R. *J. Phys. Chem. B* **2005**, *109*, 7987.

27. Shikata, T.; Imai, S.-I.; Morishima, Y. *Langmuir* **1997**, *13*, 5229.

28. Appell, J.; Porte, G.; Khatory, A.; Kern, F.; Candau, S. J. *J. Phys.II (Fr.)* **1992**, *2*, 1045.

29. Sepulveda, L.; Cortes, J. *J. Phys. Chem.* **1985**, *89*, 5322.

30. Gaillon, L.; Lelievre, J.; Gaboriaud, R. *J. Colloid Interface Sci.* **1999**, *213*, 287.

31. Corkill, J.M.; Goodman, J.F.; *Trans. Faraday Soc* **1962**,. *58*, 206.

32. Mukerjee, P. *Adv. Colloid Interface Sci.* **1967**, *1*, 241.

33. Baumuller, W.; Hoffmann, H.; Ulbricht, W.; Tondre, C.; Zana, R. *J. Colloid Interface Sci.* **1978**, *64*, 418.

34. Satake, I.; Iwamatsu, I.; Hosokawa, S.; Matuura, R. *Bull. Chem. Soc. Jpn.* **1963**, *36*, 204.

35. Wang, Y.; Dubin, P.L.; Zang, H. *Langmuir* **2001**, *17*, 1670.

36. Oda, R. Narayanan, J.; Hassan, P.A.; Manohar, C.; Salkar, R.A.; Kern, F.; Candau, S. *Langmuir* **1998**, *14*, 4364.

37. Soldi, V.; Keiper, J.; Romsted, L.S.; Cuccovia, I.M.; Chaimovich, H. *Langmuir*, **2000**, *16*, 59.

38. Frahms, J.; Diekmann, S.; Haase, A. *Ber. Bunsen-Ges. Phys. Chem.* **1980**, *84*, 566.

39. Liu, Y. C.; Chen, S. H.; Itri, R. *J. Phys.: Condens. Matter* **1996**, *8*, A169.

40. Missel, P. J.; Mazer, N. A.; Carey, M. C.; Benedek G. B. *J. Phys. Chem.* **1989**, *93*, 8354.

41. Packter, A.; Donbrow, M. *J. Pharm. Pharmacol.* **1963**, *15*, 37.

42. Z.-J. Yu; Zhang, X.; Z. Zhou; G. Xu *J. Phys. Chem.* **1990**, *94*, 3675.

43. Mukerjee, P., *Solution Chemistry of Surfactants 1* (K.L. Mittal, Ed.). Plenum, New York, 1979.

44. Yiv, S.; Zana, R.; Ulbrich, W.; Hoffmann, H. *J. Colloid Interface Sci.* **1981**, *80*, 224.

45. Chakraborty, A.; Chakraborty, S.; Saha, S.K. *J. Dispersion Sci. Technol.* **2007**, *28*, 984.

46. Chakraborty, A.; Saha, S.K.; Chakraborty, S. *Colloid Polym. Sci.* **2008**, *286*, 927.

47. Shinoda, K.; Friberg, S.; *Adv. Colloid Interface Sci.* **1976**, *4*, 281.

48. Robinson, B.H., *Chemistry in Britain* **26**(4), April 1990.

49. Moroi, Y., *Micelles: Theoretical and Applied Aspects*, Plenum, New York, 1992.

50. Romani, A.P.; Gehlen, M.H.; Lima, G.A.R.; F.H. Quina. *J. Colloid Interface Sci.* **2001**, *240*, 335.

51. Chen, S.H.; *Annl. Rev. Phys. Chem.* **1986**, *37*, 351

52. Hayashi, S.; Ikeda, S. *J. Phys. Chem.* **1980**, *84*, 744.

53. Backlund, S.; Rundt, K.; Birdi, K.S.; Dalsager, S.; *Colloid Polym. Sci.* **1981**, *259*, 1105.

54. Rubio, D.; Zanette, D.; Nome, F.; Bunton, C.A. *Langmuir* **1994**, *10*, 1151.

55. Stephany, S.M.; Kole, T.M.; Fisch, M.R.; *J. Phys. Chem.* **1994**, *98*, 11126.

56. Førland, G.M.; Samseth, J.; Høiland, H.; Mortensen, K. *J. Colloid Interface Sci.* **1994**, *164*, 163.

57. Leung, R.; Shah, D.O. *J. Colloid Interface Sci.* **1986**, ***113***, 484.

58. Lianos, P.; Zana, R. *J. Colloid Interface Sci.* **1984**, ***101***, 587.

59. Bostrom, G.; Backlund, S.; Blokhus, A.M.; Hoeiland, H. *J. Colloid Interface Sci.* **1989**, *128*, 169.
60. Souza, S.M.B.; Chaimovich, H.; Politi, M. *Langmuir* **1995**, ***11***, 1715.

61. Attwood, D.; Mosquera, V.; Perez-Villar, V. *J. Colloid Interface Sci.* **1989**, *127*, 532.

62. Boström, G.; Backlund, S.; Blokhus, A.M.; Høiland, H. *J. Colloid Interface Sci.* **1989**, *128*, 169.

63. McGreevy, R. J., and Schechter, R. S., *J. Colloid Interface Sci.* **1989**, *127*, 209.

64. Stilbs, P. *J. Colloid Interface Sci.* **1982**, *89*, 547.

65. Blandamer, M.J.; Cullis, P.M.; Soldi, L. G.; Engberts, J.B.F.N.; Kacperska, A.; van Os, N.M.; Subha, M.C.S. *Adv. Colloid Interface Sci.* **1995**, *58*, 171.

66. Blankschtein, D.; Shiloach, A.; Zoeller, N. *Current Opinion Colloid Interface Sci*, **1997**, *2*, 294.

67. Hines, J.D. *Current Opinion Colloid Interface Sci*, **2001**, 6, 350.

68. Zana, R., *Adv. Colloid Interface Sci.*, **1995**, *57*, 1.

69. Zana, R. *Langmuir* **1996**, *12*, 1208.

70. Gao, H-W.; Zhao, J-F. *J. Anal. Chem.* **2003**, *58*, 322.

71. Watanabe, K.; Imai, S.; Mori, Y.H. *Japan.Chemical Engineering Science* **2005**, *60*, 4846.
72. Apostolos, G.; Evangelos, G.; Antigoni, S. *Disalination* **2007**, *211*, 249.

73. Paul, B.K.; Moulik, S.P. *Ind. J. Biochem. Biophys.* **1991**, *28*, 174.

74. Paul, B.K.; Moulik, S.P. *Adv. Colloid Interface Sci.* **1998**, *78*, 99.

75. Eastoe, J.; Robenson, B.H.; Heenan, R.K. *Langmuir*, **1993**, *9*, 2820.

76. Temsamani, M.B.; Maeck, M.; Hassani, I.E.; Hurwitz, H.D. *J. Phys. Chem. B* **1998**, *102*, 3335.

77. Acosta, E.; Bisceglia, M.; Fernandez, J.C. *Colloids Surfaces A* **2000**, *161*, 417.

78. Shugihara, G.; Nakano, T.Y.; Sulthana, S,B.; Rakshit, A.K. *J. Oleo. Sci.* **2001**, *50*, 29.

79. Robb, I.D.; Smith, R. *J. Chem. Soc. Faraday Trans. 1* **1974**, *70*, 187.

80. Z.-J. Yu; G. Xu *J. Phys. Chem.* **1989**, *93*, 7441.

81. Tsubone, K.; Arkawa, Y.; Rosen, M.J. *J. Colloid Interface Sci.* **2003**, *262*, 516.

82. Tsubone, K.; Ogawa, T.; Mimura, K. *J. Surfactants Detergents* **2003**, *6*, 39.

83. Tsubone, K.; Rosen, M.J. *J. Colloid Interface Sci.* **2001**, *244*, 394.

84. Van Os, N.M.; Haak, J.R.; Rupert, L.A.M. *Physicochemical properties of Anionic, Cationic and Nonionic Surfactants*; Elsevier: New York, 1993.

85. Mukerjee, P.; Mysels, K.J.; Kapauan, P. *J. Phys. Chem.* **1967**, *71*, 4166.

86. Romsted, L.S.; Yoon, C.O. *J. Am. Chem. Soc.* **1993**, *115*, 989.

87. Marcus, Y. *Ion Solvation*, Wiley-Interscience, New York, 1985.

88. Lide, D.R., Ed. *Handbook of Chemistry and Physics*, 79th ed.; CRC Press: Boca Raton, 1998.

89. Israelatchvili, J.N. *Intermolecular and Surface Forces*, 2nd ed.; Academic: New York, 1992.

90. Volkov, A.G.; Paula, S.; Deamer, D.W. *Bioelectrochem. Bioenergetics* **1997**, *42*,153.

91. Frahms, J.; Diekmann, S.; Haase, A. *Ber. Bunsen-Ges. Phys. Chem.* **1980**, *84*, 566.

92. Nakagaki, M.; Handa, T. ACS Symposium Series, **1984**, *253*, 73.

93. Moroni, M.A.; Minardi, R.M.; Schulz, P.C.; Puig, J.E.; Rodríguez, J.L. *Colloid Polym. Sci.* **1998**, *276*, 738.

94. Stokkeland, I.; Skauge, A.; Høiland, H. *J. Soln. Chem.* **1987**, *16*, 45.

95. Heuvelsland, W.J.M.; de Visser, C.; Somsen, G. *J. Phys. Chem.* **1978**, *82*, 29.

96. Mukerjee, P. *Adv. Colloid Interface Sci.* **1961**, *1*, 242.

97. Mukhim, T.; Ismail, K. *J. Surface Sci. Technol.* **2005**, *21*, 113.

98. Kang, K.; Kim, H.; Lim, K. *Colloids Surfaces A*, **2000**, *189*, 113.

99. Tanford, C. *The Hydrophobic Effect: Formation of Micelles and Biological Membrens*, Vol. 2, Wiley, New York, 1980.

100. La Mesa, C. *J. Phys. Chem.* **1990**, *94*, 323.

101. Weckström, K.; Hanu, K.; Rosenholm, J.B. *J. Chem. Soc., Faraday Trans.* **1994**, *90*, 733.
102. Morori, A. *Micelles: Theoretical and Applied Aspects*, Planum Press, New York, 1992.
103. Rosen, M.J. *Surfactants and Interfacial Phenomena*, Wiley-Interscience, New York, 2004.

104. Bedo Zs, Berecz E, Laktos I (1992) Colloid Polym Sci 270:799

105. Galán, J.J.; González-Pérez, A.; Rodríguez, J.R. *J. Therm. Anal. Cal.* **2003**, *72*, 465.
106. Carnero Ruiz, C.; Díaz-López, L.; Aguiar, J. *J. Colloid Interface Sci.* **2007**, *305*, 293.
107. Umlong, I.M.; Ismail, K. *J. Colloid Interface Sci.* **2005**, *291*, 529.

108. Rosen, M.J.; Cohen, A.W.; Dahanayake, M.; Hua, X. *J. Phys. Chem.* **1982**, *86*, 541.

109. Oh, S.G.; Shah, D.O. *J. Phys. Chem.* **1993**, *97*, 284.

110. Sulthana, S.B.; Bhat, S.G.T.; Rakshit, A.K. *Langmuir* **1997**, *13*, 4562.

111. Su, T.J.; Lu, J.R.; Thomas, R.K.; Penfold, J. *J. Phys. Chem. B* **1997**, *101*, 937.

112. Das, D.; Ismail, K. *J. Colloid Interface Sci.* **2008**, *327*, 198.

113. Jalali, F.; Shamsipur, M.; Alizadeh, N. *J. Chem. Thermodynamics* **2000**, *32*, 755.

114. Gunaseelan, K.; Ismail, K. *J. Colloid Interface Sci.* **2003**, *258*, 110.

115. Zhang, H-L.; Kong, Z.; Yan, Y-M.; Li, G-Z.; Yu, L.; Geng, F. *J. Dispersion Sci. Technol.* **2007**, *28*, 958

116. Moroi, Y. *Micelles: Theoretical and Applied Aspects*, Plenum, New York, 1992.

117. Chen, S.H.; *Ann. Rev. Phys. Chem.* **1986**, *37*, 351.

118. Hayashi, S.; Ikeda, S. *J. Phys. Chem.* **1980**, *84*,744.

119. Sjöblom, J.; Lindberg, R.; Friberg, S.E. *Adv. Colloid Interface Sci.* **1996**, *95*, 125.

120. Schwunger, M.J.; Stickdorn, K.; Shomäcker, R. *Chem. Rev.* **1995**, *95*, 849.

121. Onori, G.; Passeri, S.; Cipiciani, A. *J. Phys. Chem.* **1989**, *93*, 4306.

122. Cipiciani, A.; Onori, G.; Savelli, G. *Chem. Phys. Letters* **1988**, *143*, 505.

123. Beneventi, S, Onori, G. *Biophys. Chem.* **1986**, *25*, 181.

124. Akhter, M.S. *Colloids Surf. A* **1999**, 157, 203.

125. Zhou, M.F; Rhue, R.D. *J. Colloid Interface Sci.* **2000**, *228*, 18.

126. McMahon, C. A.; Hawrylak, B.; Marangoni, D.G.; Palepu, R., *Langmuir* **1999**, *15*, 429.

127. Chauhan, M.S.; Kumar, G.; Kumar, A.; Chauhan, S. *Colloids Surf. A* **2000**, *166*, 51.

128. Christian, S.D.; Scamehorn, J.F., Eds. *Solubilization in Surfactant Aggregates, Part VI*, Dekker, New York, 1995.

129. Brinchi, L.; Di Profio, P.; Germani, R.; Savelli, G.; Spreti, N. *J. Colloid Interface Sci.* **2002**, *247*, 429.

130. Zana, R.; Yiv, S.; Strazielle, C.; Lianos, P.; *J. Colloid Interface Sci.* **1981**, *80*, 208.

131. Yadav, S.K.; Kumar, A.; Yadav, O.P. *Indian J. Chem.* **1999**, *38A*, 529.

132. Javadian, S.; Gharibi, H.; Sohrabi, B.; Bijanzadeh, H.; Safarapour, M.A.; Behjatmanesh-Ardakani, R. *J. Mol. Liq.* **2008**, *137*, 74.

133. Sjöberg, M. *Ph. D. Thesis*, Department of Physical Chemistry, The Royal Institute of Technology, Stockholm, Sweden, 1992.

134. Lopez-Grio, S.; Baeza, B.J.J.; Alvarez-Coque, M.C.G. *Chromatographia* **1998**, *48*, 655.

135. Nakagawa, K.; Tajima, K. *Langmuir* **1998**, *14*, 6409.

136. Armarego, W.L.F.; Perrin, D.D. *Purification of Laboratory Chemicals*, 4th Ed. Butterworth-Heinemann, Oxford, 1996.

137. McManus, H.J.D.; Kang, Y.S.; Kevan, L. *J. Chem. Soc. Faraday Trans.* **1993**, *89*, 4085.

138. Kalyanansundaram, K.; Thomas, J.K.; *J. Am. Chem. Soc.* **1977**, *99*, 2039.

139. Stilbs, P.; *J. Colloid Interface Sci.* **1982**, *87*, 385

140. Huang, J.-B.; Mao, M.; Zhu, B.-Y. *Colloid Surf. A* **1999**, *155*, 339.

141. Carnero Ruiz, C. *Colloid Polym. Sci.* **1999**, *277*, 701.

142. Safarpour, M.A.; Rafati, A.A.; Gharibi, H.; Rezaie Sameti, M. *J. Chin. Chem. Soc.* **1999**, *46*, 983.

Chapter 4

Studies on Physico-chemical Characteristics of Progressively Alkylated Thiazine Dyes in Micellar and Microemulsion Media

4.1 Introduction and Review of the Previous Work

In aqueous solution, micelle formation is usually detected by some change in the physical properties of the solution, such as surface tension, conductivity, viscosity and e.m.f. or some optical or spectroscopic property of the solution [1-3]. Hartley [4] first noticed that the colour of sulphonaphthalein indicators changed on the addition of detergents, and this effect occurred only when the charge on the detergent aggregate was opposite in sign to that of the dissociated indicator molecule. This behaviour proved to be quite general, as azo [5] triphenyl methane [6] and merocyanine dyes [7] all exhibited the same effect.

At concentrations below the cmc addition of a surfactant to a dye solution may bring about the formation of colloidal dye surfactant submicellar aggregates (mixed micelles) or insoluble dye surfactant salts, ion pair, molecular complex, dye-rich induced micelles, induced self-aggregates of dye, aggregation of dye-surfactant complex and change in chromophore microenvironment [8-14]. The actual species formed depends mainly on the nature of the dye and their own tendency to form the aggregate [15,16].

Formation of an insoluble salt between ionic dyes and oppositely charged detergents is most common, but is not a completely general phenomenon. In fact, some dyes, such as phenol red [17] or 8-hydroxy quinoline-5-sulphonic acid produce neither turbidity nor precipitation [18] along with the spectral change induced by addition of the cationic surfactant.

Dyes are also amphiphiles, in the sense that bulky non-ionic moieties are attached to the ionic or analytical groups, but as they lack long-chain alkyl groups they have weak surface activity and do not form micelles in water. Depending on the balance between the hydrophobic and hydrophilic tendencies of any particular dye, increase in dye concentration can lead to stepwise aggregation i.e. the formation of dimers, trimers, polymers and finally colloids [19].

If a surfactant is added to such a dye solution at submicellar concentrations, both the surfactant monomer and the dye aggregates can interact to form a special kind of micelle (mixed micelle) [20] at concentrations far below the normal cmc, characteristic of the surfactant. This dye-surfactant interaction accounts for the often observed fact that the so-called 'spectroscopic probe method' [21] does not provide a true cmc value. In fact in such cases, the change in absorbance or fluorescence

intensity of a dye probe in the presence of increasing surfactant concentrations may not reflect the formation of micelles of the surfactant (homomicelles) but that of mixed micelles or dye-surfactant salts. But there are also many reports in the literature where these spectroscopic methods [22-24] have been used to determine the cmc of both ionic and non-ionic surfactants. García-Río et al. [2] recently discard the possibility in a cmc change due to the presence of dye. They however, got the same result by measuring the cmc of SDS conductometrically with and without the presence of crystal violet (CV)

Once the surfactant concentration has reached a value close to or above the cmc neither turbidity nor precipitation is observed. Solubilization of the dye-surfactant 'salt like' ion pairs in the micellar phase and/or the final incorporation of the dye into the micelles (homomicelles) takes place. Many of the features observed in the spectral behaviour of dye-surfactant systems having opposite charge can often be extended to general sensitized reactions in micellar media [25,26].

In past, Mukherjee and Mysels [27] using spectrophotometric and electrical conductivity measurements of the pynacyanolsodium dodecyl sulphate system identified the presence of two types of dye-surfactant aggregates : (i) below the cmc a dye-surfactant salt which formed a coarse (visible suspension) stable slurry in the presence of more than a stoichiometric amount of surfactant and (ii) dye-rich micelles, at below and around the cmc which solubilized the water-insoluble dye-detergent salt. Malik et al. [28,29] reported that spectral changes for several dyes are due to electrostatic forces involving interactions between the anionic (or cationic) surfactant and the basic (or acidic) dye. They claimed that chemical interaction giving a stoichiometric dye-surfactant complex was very improbable.

Guha et al. [30] attributed the changes in the absorption spectra and the decrease in fluorescence intensity of thionine to the formation of a dye-surfactant complex at SDS concentration below the cmc. At concentration above the cmc the appearance of the dye absorption spectrum with a small red shift and increased extinction co-efficient, was interpreted as due to the incorporation of the dye into the micelles.

The existence of true ion-association complexes formed below the cmc between ionic surfactants and dyes with opposite charge is supported by most of the

published data [6,31,32]. These complexes are electrically neutral and often poorly soluble in water but readily extractable by low-polarity solvents. They have stoichiometric surfactant ratios. At surfactant concentrations equal to the cmc value and above, the solubilizing effect of the micelles begins to be important and the ion-association complexes are incorporated into the micelles.

Electrostatic interaction of anionic dyes with the surface of cationic surfactant micelles takes place through the negatively charged groups of the dye (e.g. - SO_3^-, - COO^-). However, this kind of electrostatic interaction could not explain by itself the spectral changes observed during the interaction. In fact, bulky non-micelle forming species such as the diphenylguanidinium or tetra ethyl ammonium ion have no effect *per se*. Moreover, simple ion-pairing between a negative group such as -SO_3^-, or - COO^-, of the dye and a quaternary ammonium ion does not perturb the chromophore [32]. In the presence of cationic surfactants, aromatic compounds with sulphonic [33] or carboxylic acid groups [34] do not act simply as counterions, but are incorporated into the water-rich stern layer of the micelle in a sandwich arrangement. This permits not only the hydration of the hydrophilic -SO_3^- (or - COO^-) group, but also the solvation of the aromatic ring of the dye by the -$N(CH_3)_2$ group and the participation of vander Waals interaction between adjacent surfactant chains and the dye organic moiety (hydrophobic forces). In this situation, the micro-environment of the chromophore has clearly changed, from that existing in the bulk aqueous phase, and this change is the cause of the spectral shifts observed. Since dyes based on aromatic rings are widely used in spectrophotometry and fluorimetry, this picture can be considered general and is probably operative in most analytical dye-surfactant systems at concentration above the cmc.

The proton release occurring during the reaction between an anionic dye and a cationic surfactant produces a change in the spectrum which is similar to that observed on increasing the pH of the dye solution. Such pKa shifts for solubilized indicators have been attributed to the influence of the surface potential of micelles [35,36]. The pKa changes also appear to be related to the reduction of the difference in free energy between the acidic form of the dye and its anion in the micelle [34,37]. Extensive incorporation of an anionic dye into a cationic micelle implies that the free

energy of the anionic form decreases more than that of the un-ionized form, as the anion is more polarizable and firmly attached to the positive end groups of neighboring surfactant molecules [38].

There is multiple binding in these associated miceller species; evidence has been produced indicating that hydrophobic interaction, not charge compensation, plays the main role in binding between dyes and surfactants. The exact nature of this interaction, however, has not yet been satisfactorily explained. Chiang et al. [39] reported that their result on the interaction between 2-p-toluidinylnaphthalene-6-sulphonate and SDS micelles suggest that the binding force is hydrophobic. Analogously, Birdi et al. [37] claimed that the interaction of SDS micelles with 1-anilinonaphthalene-8-sulphonate is hydrophobic in nature. The interaction between some mono-azo dyes with a series of non ionic surfactants has been shown [40] to be hydrophobic in nature and occurs between dyes and the ethylene oxide chains of the non-ionic surfactant. Minch [7] showed, from spectral changes of merocyanine dyes in cationic and anionic micelle, that in all cases the spectra were red-shifted when the dye was incorporated into micelles and that the magnitude of the shift increased with more hydrophobic dyes. Biedermann and Datyner [41] also suggested that the interactions of some azo dyestuffs with SDS micelles increased with increasing lipophilicity of the dyes.

According to Dill et al. [42] the inclusion of a dye molecule within a micelle is not strictly akin to placing it in a hydrophobic region in the micellar core, but is more likely placing it in a hydrophobic environment where it is exposed to water. A consideration of hydrocarbon chains in micelles as disordered structures could explain why the nature of the dye may determine its binding site within the micelle assembly [41]. In other instances, the factors responsible for the spectral changes have been ascribed to the deaggregation of the dye molecules by association with micelles [43] to the joint effect of deaggregation and the change in the molecular environment [44,45] or to the localization of the chromaphore within the hydrophobic micellar interior [46]. Micelles are sensitive to small changes in the ionic strength of the aqueous solution. The change in the cmc of cetyl pyridinium bromide (CPB) in aqueous solution with electrolyte concentration [46] reveal two

trends, one occurring at low and the other at high concentrations of the added salt. Addition of salts to ionic micelle solutions reduces the mutual electrostatic repulsions of charged head groups [47].

Owing to electrostatic repulsion, the interaction between anionic dye ions and the head-groups of anionic surfactants should produce neither new spectral bands nor changes in absorbance or fluorescence intensity. Similar results are also observed in case of interaction between cationic dye ions and head groups of cationic surfactants. However, as mentioned earlier, lipophilicity may often be the driving force for interaction, rather than the electrostatic interaction [7,37,39,41] and some spectral changes can be explained in this way. A similar explanation can also be given for the effect of non-ionic surfactants on the spectral behaviour of dyes. Coomassie brilliant blue G-250 does not show any spectral shift with anionic detergents such as sodium dodecyl sulphate or sodium deoxycholate, but does with non-ionic surfactants, probably owing to transfer of the dye from a hydrophilic to a hydrophobic micellar environment [48]

If a charge-type effect can combine with the classical hydrophobic interactions then both kinds of interactions, electrostatic and hydrophobic, seem to act concurrently, bringing about the largest spectral changes, as shown for anionic dye-cationic surfactant complexes by Savvin et al. [32] or for metal chelate – cationic surfactant species by Sanz-Medel et al. [18,49]. In any case, it seems clear that the surfactant character has the decisive role in determining the observed spectral changes, since bulky ions, which are non-micelle-forming (e.g., tetraethylammonium) do not give rise to effects similar to those observed in the presence of micelle-forming agents [32,50]. The implications of a model for the interactions in micelles are significant not only for micelles in water but also for related assemblies, since the principles of organization are thought to be quite general [51]

The surfactant interactions in non-aqueous media have been investigated [52] less than those in aqueous surfactant systems. The surfactant aggregates in organic solvents are described as having a 'reverse micellar structure', in which the

hydrocarbon tails are in contact with the solvent and the polar head groups form the micellar core.

The aggregation number in such reverse micelles is relatively small, e.g. less than 10 for alkyl ammonium carboxylates, compared with up to 100 for aqueous micelles [53]. It is supposed that these systems would exhibit an experimentally determinable cmc. Although many of the common methods for cmc determination in aqueous solution are not applicable to reverse micellar systems, because of the low degree of aggregation and because ionic surfactants do not ionize in organic media, the 'spectral change method' has been proposed for determination of the cmc of Aerosol-OT (sodium bis-(2-ethyl hexyl) sulphosuccinate) [54] with the dye 7,7,8,8-tetracyano quinodimethane (TCNQ). Breaks in the plots of absorbance against surfactant concentration were interpreted as corresponding to the surfactant cmc. However, as the concept of cmc as explained for normal micelles is no longer applicable in these systems and is still subject to controversy. Reverse micelles alter the micro-environment of solubilized reactants and thus affect their stereochemistry, dissociation constants, redox potentials and reactivities [55]

4.1.1 Dye-Surfactant Interaction in Sub-Micellar Concentrations of Surfactant

There has been an increasing interest in the study of interaction of dyes with surfactants as the knowledge of dye-surfactant interaction is of great value in understanding the chemical equilibrium, mechanism and kinetics of surfactant sensitized colour and fluorescence reactions [49]. Many researchers had noticed the change in colour of the ionic dyes when they were dissolved in oppositely charged ionic micelles [44,56-62]. Most of the previous studies on dye-surfactant interaction were carried out with the concentration of the surfactants above the cmc and the colour changes have been explained on the basis of the interaction between the surfactant micelles and the dyes and the equilibrium between conjugate acid and base forms of the dye. However, there is not much information available regarding the nature and mechanism of the interaction between dyes and surfactants when the concentrations of the surfactants are much below the cmc. Dutta and Bhatt [63] carried out systematic spectroscopic and thermodynamic investigations in order to understand the nature of this interaction between ionic dyes and oppositely charged

surfactants of very low concentrations i.e., far below their cmc's. They have investigated interactions of cationic dyes viz. phenosafranin (PSF), safranine O (SFO) and safranine T (SFT) with anionic surfactants, viz. sodium dodecyl sulfate (SDS) and sodium octyl sulphate (SOS) in submicellar concentration ranges. The interaction has been shown to be an induced protonation of the dye in the dye-surfactant ion pair. Even though the opposite charges on the dye and the surfactant are the primary requirements for the ion pair formation, it is the hydrophobicity of the surfactant as well as of the dye which induces the protonation.

As the concentration of SDS is slowly increased from 1.6 x 10^{-4}M (the lowest concentration at which there was detectable decrease/increase in absorbance of PSF bands) to 3 x 10^{-3}M, λ_{max} of PSF band gradually shifted from 520 to 528 nm with a gradual decrease in intensity of the λ_{max} band, accompanied by an increase in absorbance in the longer wavelength region of ca λ 550 to ca 700 nm. The red shift of the PSF band from 520 to 528 nm was attributed partly to a change in the environment of the chromophore of PSF and partly to the overlapping of the 520 nm band with the new band in the longer wave length region. Increasing the concentration of SDS up to 4 x 10^{-4} M, for a fixed concentration of PSF (2.13 x 10^{-5} M) gives a series of spectra that go through a sharp isobestic point at 550 nm.

It was observed that the spectra of PSF in low concentration of SDS were similar to those of PSF in strong acidic media. Gopidas and Kamat [64] had reported that PSF^+ in HCl (2M) has absorption band at 580 nm which can be attributed to $HPSF^{2+}$. They had noticed that with the increase in concentration of strong acids, e.g., H_2SO_4, $HClO_4$ etc. PSF gave rise to three bands viz. at 580, 625 and 690 nm. Similarly, with the increase of BF_3 in ether the absorption maxima of PSF were at 578, 622 and 688 nm successively. The appearance of a new band at ca. 582 nm which increases with the increase in concentration of SDS (up to ca. 3 x 10^{-3}M) and decreases with increase in temperature, and the presence of an isobestic point indicate of the presence of an equilibrium between the free PSF, SDS and complexed PSF (an interaction product of PSF and submicellar SDS). With the increase in concentration of SDS above cmc (6.0x10^{-3} M in presence of 2.2x10^{-5} M PSF), the 520 nm band shifts to higher wave length, viz., 531 nm which is attributed to the association of the dye

with the surfactant micelles. There was hardly any change in the position and intensity of this band with further addition of SDS.

The colour change observed in many dyes on the addition of very small amount of oppositely charged surfactant has been attributed to ion pair formation [60], dye-surfactant salt formation [27], the formation of dye dimer or higher aggregates [65], micelle and mixed micelle formation [44,62], etc. However, in the case of cationic dyes, like phenazinium and thiazinium dyes, the dimerizations are known to cause hypsochromic shifts in the spectra [66]

No interaction of the phenazinum dyes with N-hexadecyl pyridinium chloride (a cationic surfactant) and triton X - 100, $(CH_3)_3CCH_2C(CH_3)_2$-C_6 H_4 $(OCH_2CH_2)_{10}OH$ (a non ionic surfactant), in the submicellar concentration range was observed [63]. This indicates that the opposite charge on the dye and the surfactant is the primary requirement for this interaction. Therefore it can be suggested that as the oppositely charged ions, viz., PSF^+ and DS^- (anionic part of SDS), come closer to each other due to electrostatic attraction, the hydrophobic nature of the large organic ions and hydrogen-bonded water structure enforce them to form closely associated ion pairs, PSF^+DS^- [60,67,68].

It is clear that some more changes, in addition to the ion pair formation, occurs to the chromophore to affect the large shift of the absorption band. Gopidas and Kamat [64] reported that PSF gets protonated and gives a band at 583 nm when it is bound to H^+ -Nafion, a polymer which exhibits a strong acidic environment to the dye in aqueous solution [68]. It has been shown that the PSF absorption band remains unperturbed even on lowering of the pH of aqueous PSF solution to 1.2. Only below pH of 1.2, the 580 nm band of PSF appears. On the other hand, in the entire experimental submicellar concentration range of SDS, the pH's of the aqueous SDS solutions were 6.5. Therefore, it seems that the 582 nm band of PSF in submicellar SDS may also be due to the protonated PSF, viz., $HPSF^{2+}$ caused by a strong acidic environment exhibited by monomeric DS^- bound to PSF^+ in the hydrophobic ion pair of PSF^+DS^- [63].

The SOS has a shorter hydrocarbon chain than SDS and therefore it is expected to show weaker interactions with cationic dyes (due to lesser

hydrophobicity) [69] than that of SDS. From the equilibrium constants and other thermodynamic parameters it is evident that the interaction of cationic dyes with SOS is much weaker compared to that with SDS. The slightly lower value of ΔS for PSF - SDS may be due to more ordering of the protonated ion pair in water, as SOS is relatively less hydrophobic compared to SDS.

SFO is a 2,8-dimethyl derivative of phenosafranin and SFT is a positional isomer of SFO. Both of these dyes have absorption maxima at 520 nm in the visible range. The spectral changes in the aqueous solutions of SFO and SFT on addition of SOS were similar to those of PSF - SDS and PSF - SOS. It seems apparent that hydrophobicity of the surfactant plays an important role in the ion pair formation as well as in induced protonation of the dye in the ion pair.

4.1.2 Dye-Surfactant Interaction in Super Micellar Concentrations of Surfactant

As has already been discussed that changes in the colour of ionic dyes in the presence of oppositely charged ionic surfactants in aqueous solution have been observed by many workers [27,70,71] and these changes have been explained by proposing dimer and multimer formation of dye molecules in the surfactant micelle. Hayashi [72] studied the interaction of congo red dye with cetyltrimethylammonium bromide (CTAB) and p-t-octylphenoxypolyoxyethanol, TX-100 (Triton X-100) and interpreted the spectrophotometric data in terms of formation of a 1:2 dye surfactant complex. Matibinkov et al. [73] studied the effect of sodium lauryl sulphate (SLS) on xanthane dyes and observed shifts in their visible absorption maxima at lower surfactant concentrations. Recently the results of spectrophotometric studies on phenosafranin dye, a cationic phenazine dye, in aqueous solutions containing three different types of surfactants such as CTAB, SLS and triton X-100 were reported [61]. While the formation of 1:1 dye Triton X-100 and dye-SLS complexes were observed, there was no interaction of phenosafranin with CTAB. The thermodynamic and spectrophotometric properties of these complexes suggest that phenosafranin forms strong charge transfer (CT) complex with triton X-100 whereas the interaction with SLS is coulombic in nature. This conclusion was claimed to be confirmed by photogalvanic and photoconductivity measurements of phenosafranin in these surfactants. The interaction of triton X-100, a good electron donor [74,75] with cationic phenosafranin dye is CT in nature, it is therefore interesting to see if other

cationic dyes would also form CT complexes with triton X-100. The spectrophotometric data of the cationic dyes (rhodamin B, fuchsin and crystal violet) shown 1:1 complex. The equilibrium constant (K) and the molar extinction coefficient can be determined using Ketelaar's equation [76] or Scott equation [77]. The data presented [78] provide direct 'spectrophotometric evidence' of molecular interactions between the cationic dyes and triton X -100.

In the neutral surfactant micelle of triton X-100 a cationic dye can penetrate the micelle to form a strong molecular complex at a polar site, the interaction may occur either at phenoxy group or at the polyoxyethylene chain. The absorption spectra of phenosafranin in acetonitrile, water, dioxane, acetone, ethanol and glycol exhibit absorption maxima at 518, 520, 525, 526, 532 and 535nm respectively. The position of absorption maximum of phenosafranin - triton X-100 complex in aqueous medium occurs at 537.5 nm. These results suggest that the positive centre of the dye molecule within the micelle is associated not with the lone pair electron on ether oxygen atom but with the lone pair electron on the oxygen of the hydroxyl group.

However, there is no indication of hydrophobic interaction between the dyes and triton-X-100 in non aqueous media as the absorption spectra of the dyes do not show any characteristic change in the absorption maxima in non-aqueous media containing triton X-100. This molecular interaction between the dyes and triton X-100 in aqueous media is considered to be charge transfer (CT) interaction. This is confirmed by the fact that absorption spectra of the dye-surfactant systems in the presence of small amount of NaCl are not affected.

Progressively alkylated thiazine dyes are structurally similar to phenosafranin; the former dyes are the substituted phenothiazines, while the latter is the substituted phenazine. It is, therefore, expected that thiazine dyes behave similarly to phenosafranin towards triton X-100. The thionine shows an absorption maximum at 597 nm. A spectacular change is noticed when the triton X-100 concentration is above the cmc, where all spectra show shifted absorption band at longer wave length, 608 nm, being a function of the concentration of triton X-100. The visible absorption spectra of other thiazine dyes (such as azure A, azure B, azure C and methylene blue) in aqueous solution of triton X-100 behave similarly. Spectrophotometric data were employed to calculate the thermodynamic as well as spectrophotometric properties of dye surfactant interaction. For 1:1 complex, the

equilibrium constant (K) and molar extinction co-efficient (ε) can be determined using the Benesi Hildebrand equation [79] or Scott equation [77].

From the thermodynamic and spectrophotometric properties of these complexes, the abilities of dyes to accept an electron are in the order azure C > thionine > azure A > azure B > methylene blue, where the values of K, ΔG^0, ΔH^0 and ΔS^0 are found to vary from 21.16 to 52.63 lit mol^{-1}, 7.61 to 9.88 $kJmol^{-1}$, 19.00 to 29.25 $kJmol^{-1}$, and 38.22 to 65.00 $Jmol^{-1}$ deg^{-1} respectively for these dyes. Using Scatchard [80] and Scott [77] equations, almost identical values of K and ε were obtained. Triton X-100 in carbon tetrachloride solution can not even solubilize the dye; it is expected that the hydrophilic part of triton X-100 interacts with the dye whereas there is no hydrophobic interaction between the dyes and triton X-100. The absorption spectra of thionine in different solvents such as acetonitrile, water-dioxane, acetone, ethanol, and tert-butanol exhibit absorption maxima at 593, 597, 520, 598, 600 and 607 nm respectively. Although the absorption maximum of thionine-triton X-100 complex appears at 612 nm, the shifted band of thionine in Triton X-100 solution exhibits at 608 nm. These results suggest that the positive centre of the dye molecules within the micelle is associated not with the lone pair electron on the ether oxygen atom, but with the lone pair of electron on the oxygen of the hydroxyl group for comparatively higher electron density. This molecular interaction between the dyes and Triton X-100 in aqueous medium is again considered to be a CT interaction.

The visible absorption spectra of Thionine along with the difference spectra of mixed solutions with a fixed concentration of Thionine and varying concentrations of Tween-80 in aqueous media at 298K were studied [81]. Thionine shows an absorption maximum at 597 nm. A remarkable change was noticed when the Tween-80 concentration was above the cmc, where the difference spectra showed shifted absorption band at longer wave length, i.e. 616 nm with an isobestic point at 600 nm, the magnitude of the absorbance at 616 nm being directly proportional to the concentrations of Tween-80. The visible absorption spectra of thionine in aqueous solutions of others surfactants except CTAB, above their cmc behaved similarly. In the presence of CTAB, the Thionine spectra were not perturbed at all, indicating no interaction between thionine and CTAB, whereas the presence of sharp isobestic point and spectral shift in other cases indicated 1:1 molecular complex formation between thionine and the surfactants. The equilibrium constant (K) as well as, molar

extinction coefficient of the thionine-surfactant interaction, were evaluated using the Benesi-Hildebrand equation [79].

Mukhopadhyay et al. [81] have shown the spectra for the thionine-tween-80 complex at three different temperatures (287, 298, 313K) and calculated the equilibrium constant and other thermodynamic parameters also. They have recorded the spectra of thionine (Th)-Tw-60, Th - Tw-40, Th - Tw-20, Th - Tx-100 and have determined the thermodynamic parameters.

The cationic dye thionine is expected to form a strong complex with anionic surfactant SLS. Mukhopadhyay et al. [81] have shown that thionine forms stronger complexes with all the non-ionic surfactants compared to SLS. The nature of interaction of this dye with the non ionic surfactants is therefore different than that with SLS. The thermodynamic and spectrophotometric parameters, ΔH^0, and ΔS^0 for thionine complexes with non-ionic surfactants are also higher. Since all these surfactants can not even solubilize the dye in carbon tetrachloride solution, it is plausible that the hydrophilic part of surfactants interacts with the dye in aqueous medium. A cationic dye can penetrate the non- ionic micelles to form a strong molecular complex at a polar site on the oxygen of the hydroxyl group for having comparatively higher electron density. The molecular interaction between the thionine and non ionic surfactants in aqueous medium is considered to be CT interaction. On the other hand, with the negatively charged micelles of SLS, the cationic dye will be held in the stern region due to coulombic interaction, and the dye will be repelled by the positively charged micelles of CTAB [82].

According to Mulliken's CT theory [82] the CT complex for the present system may be represented by a resonance hybrid of a non ionic ground state structure and an ionic excited state structure. For thionine (Th) and non-ionic surfactant (S), these two states are represented as Th ..... S and $Th^-.....S^+$. The excited or CT state is formed by the transfer of an electron from the non ionic surfactant, an electron donor to the dye, an electron acceptor on light absorption of suitable energy. It is shown that upon light excitation of the dye–non ionic surfactant systems, the primary charge separation takes place, forming a negatively charged dye and a positively charged surfactant and this charge separation causes photovoltage development when the illuminated and dark compartments of the cell containing dye-surfactant are connected to the electrometer. In the case of thionine-SLS system,

the interaction is ionic in nature, so no new ionic species are generated when the system is illuminated. The prominent interaction of thionine with surfactants above their cmc in aqueous medium indicates that the charged surface formation in micelle is a necessary criterion for complex formation. The interfaces (micelle/water) catalyze the CT complex formation due to absorption of thionine from solution and thus increase the concentration of CT complex. Mukhopadhyay et al. [81] concluded that the electron donating abilities of the non ionic surfactants towards the dye are in the order: tween-80 > tween-60 > tween-40 > tween-20 > triton X-100 and this is in accordance with the increasing alkyl hydrocarbon chain length, which in turn, increases the electron density at the electron-donating centre of the molecule, due to inductive effect. The presence of an aryl group in triton X-100 results in an opposite effect. They concluded that the nature of interactions of thionine with different types of surfactants is different. Thionine undergoes CT interaction with non-ionic surfactants, ionic interaction with negatively charged SLS, and no interaction with positively charged CTAB.

The absorption spectra of methyl violet, a cationic dye, were investigated in aqueous solution containing anionic, non-ionic and cationic surfactants above their cmc. The dye forms 1:1 electron donor acceptor or charge transfer complexes with different non ionic surfactants. The dye acts as the electron acceptor and the surfactants as the electron donors. The length of the alkyl hydrocarbon chain of the non-ionic surfactants influences the stability of the complex [83]. Recently association constant for the formation of cresyl violet–surfactant complex and the binding constant for the micellization of the dye, both in absence and in the presence of electrolyte have been determined. In these experiments, the dielectric constant experienced by cresyl violet within the SDS micelles has been found to decrease due to micellization process. The environment around cresyl violet in the anionic micelle of SDS is highly polar and electrostatic attraction between cresyl violet and anionic micelle favour location of dye close to the head groups of the micelle [84].

Investigations of photo-induced electron transfer reactions in surfactant solutions are not only inherently interesting and relevant to the understanding of photobiology but they are also potentially important for efficient energy conversion and storage. Surfactant solutions help to achieve the separation of photoproducts by

means of hydrophilic-hydrophobic interaction between the products and the interface [85-88].

4.1.3 Dye-Surfactant Interaction in Microemulsion Media

Microemulsions as discussed in chapter 1, differ from micelles by the complex composition and larger sizes of the particles as they contain compartmentalized water with surfactants and alcohols having medium hydrocarbon chains (e.g. n-hexanol, n- heptanol, etc.), generally called co-surfactant along with a nonpolar solvent. They are, therefore, characterized by a higher micro heterogeneity of interfaces and a higher solubilizing capacity of organic molecules and can also be treated as analogical model of biologically functioning systems [51], which are the basis of living matter. Apart from different synthetic applications [89,90] it is also used in the removal of dyes from water [91]. Solubilization of water in microemulsion (or reverse micelle) systems has been found to be dependent on various factors involving the rigidity of the interfacial film, which in turn depends upon the size of the polar head group and the hydrocarbon moiety of surfactant, the type of oils, the presence of electrolyte, the nature and valance of counterion, the temperature, etc [92]. The structure of the interfacial water of microemulsion systems is somehow different from bulk water. In the micro-encapsulated domain, the presence of amphiphilic head groups and the counterion (in case of ionic amphiphile) may significantly affect the water mobility [93,94]. Because of the peculiar chemical and physical properties [95] of the polar interior of reverse micellar aggregates, substantial efforts have been focused on the investigation of the state of water in the pool. To explore the properties of water in the compartmentalized states as in microemulsion different absorption and fluorescence probes, viz. TCNQ [96], acridine orange [97], pyrene [98] and cyanine [99] derivatives, etc have been commonly used. In past, Oldfield et al. [100] and Fletcher [101] analyzed their spectral data on the acid-base equilibrium of both interfacially as well as bulk located dyes to illustrate their behavior in microemulsions. They examined differences in properties of interfacial and bulk water in the water-pool of microemulsions obtained by using the surfactant AOT. The interfacial water molecules can interchange H^+ ion with the Na^+ ion of AOT and thus affecting the pH of the vicinal water. Though fluorescence [102] and ^{31}P-NMR [103] techniques have been used to

estimate the pH of microemulsions, but the extent of pH change of a buffer medium in the compartmentalized condition is still debatable mostly because the exact location of the probe molecule in the water-pool remains uncertain. The dielectric constant of the compartmentalized water can also be altered by changing the dimension of microemulsion [104]. These factors can alter the dissociation equilibrium of an indicator dye along with there corresponding absorption coefficient. Observations of many researchers [99-102] on dye-surfactant interactions in reverse micellar media suggests the formation of dye-surfactant salt, ionpair, molecular complex and changes in microenvironment in dye chromophore.

It is well known that when the molecular forms of a dye are electronically neutral or have same charge with the surfactant in micellar systems, the form of the dye with less or no charge is preferentially associated to the micelles [112-114,116,117]. However, the preferential location of the dye as well as the reasons for the preference among oil-water interface, bulk oil and bulk water, which determine the spectral behavior of the dyes in microemulsions are not clearly understood. Although there are many reports on the interaction of dye molecules with non ionic [99,107,108] as well as oppositely charged ionic [99,109-111] surfactants in microemulsion, such studies of molecular interactions of dye molecules in microemulsions of surfactants with similar charge is rare. If the dye molecules with similar charges as that of surfactants are present in the aqueous pool of the microemulsion, the model offers an ideal situation for monitoring the effect of compartmentalized water on the molecular interactions because chances of finding the dye molecules in the interfacial region becomes rare, and the question of uncertainty on the actual location of the probe does not arise. The presence of cosurfactant makes the situation even more complicated. In this connection it has been reported that organic dyes including azure A changes their properties by molecular encapsulation [115].

Spectral changes on increasing concentration of an aqueous solution of many dyes which have larger planer hydrophobic skeleton with hydrophilic substituents have been known for a long time. It is now well accepted that these spectral changes are mainly due to the aggregation of such molecules. Aggregation can bring about drastic changes in physical and chemical properties of the dyes, specially their photophysics. The photophysics and photochemistry of dyes in general are of

considerable interest in the observation of various phenomena such as fluorescence, phosphorescence, long range and short range excitation energy transfer and electron transfer and other modes of quenching, as probes for liquid structures for mixed solvents and various relaxation processes in solution [118]. Certain concentration effect is also observed during the study of photophysical and photochemical properties of ionic dyes including methylene blue (one of the thiazine dyes), which leads to enquire into the molecular states of these dyes in solution [119].

The strength of dye aggregation is strongly dependant on the structure of the dye molecules, nature of solvent and temperature. A number of physical descriptions of this phenomenon have been proposed to account for the changes in the dye spectrum but none is found superior than others. In this chapter attempt have been made to understand the nature of dye-surfactant interaction in aqueous medium and dye-dye aggregation and the effect of progressive alkylation of dye molecule in the water-pool of microemulsion media. The nature of dye-dye aggregation in the compartmentalized water of microemulsion has been discussed in terms of 'molecular exciton theory'.

4.1.4 Aggregation of Organic Dyes

Interests in dye aggregates have been generated afresh recently due to its role in light energy conversion devices along with photography and xerography. Of particular interest is their ability to sensitize large band gap semiconductor material such as silver bromide nanocrystals in colour photography. Because of their practical importance, several research groups have done experiments to investigate the excited state behavior and electron transfer reactions of dye aggregates [120-130]. Moreover, discovery of lyotropic liquid crystalline phases, which are known as 'chromonics' has added considerably to the present interest on the aggregation of organic dye systems [131-133]. Spontaneous occurrence of chirality of some squarine [134], cyanine [135,136], and porphyrine [137] dye aggregates, although made up by non-chiral molecules, have also been shown recently.

Most of the basic dyes in solution show deviations from the Beer's law at higher concentrations. This behavior has been attributed to the formation of dimers and higher aggregates of the dyes [138,139]. In general, the dimerization constants are in the range of 100-10000, corresponding to free energies ~ 8 –22kJ mol^{-1}. These

are of the order of the magnitude of formation of hydrogen bonds [140], as well as, of other types of interactions such as hydrophobic [141,142], vander Waals or $\pi-\pi$ interactions, dispersion forces [142], all of which are presumed to be present when dyes undergo self aggregation in solution. Remarkable changes in the spectral characteristics with increasing concentrations, and the effect of temperature on this have been studied to unravel the nature of the forces involved in dye aggregation. Aggregates of the above type are also formed at lower concentration in the presence of some natural or synthetic polymers [143,144] or polyelectrolytes [145,146]. In these cases the equilibrium constants are, at least, a factor 10 higher, so that aggregation can be observed at concentrations which are well behaved in the absence of the additives [147]. Bergman and O'Konski [148] described a spectroscopic study of methylene blue adsorbed on Na-bentonite. Spectral changes were found to follow with the changes in the amount of methylene blue (MB) adsorbed on the clay surface. Due to the fact that these changes are similar to the spectral shifts accompanying dimerization and polymerization of MB in aqueous solution, these shift also attributed to dye-dye interaction on the surface of the montmorillonite and the corresponding dimer dissociation constant was determined as 1.7×10^{-4} mol lit^{-1} at 25^{0}C. West and Pearce [149] examined the dimeric state of cyanine dyes and showed that the stability of the dimers, as measured by the free energy of dimerization, increase steadily with chain length. Authors showed that if a solution in which 95% of the dye is present as monomer is regarded as tolerable approximation to a solution of the pure monomer, the concentration at which this conditions prevailed was found to vary from 2.8×10^{-5} M (for $K=10^{-3}$) to 2.8×10^{-8}M (for $K = 10^{-6}$).

Baranova and Levshin [150] reported that Rhodamine 6G forms aggregates upto dimerization stage at concentration below 2×10^{-3}M, but higher aggregates are formed at higher concentrations. The change in the spectrum of an aqueous solution of 3,6 -diamino acridine dye with the increase in concentration was not very large, reliable results could not be obtained by Mataga [151]. However, the degree of aggregation and log K_n were determined by means of Zanker's method [152]. Hida and Sanuki [153] opined that the maximum slope method for evaluating dimerization parameters was more reliable over some other methods viz, Zanker's method. These authors also found the dependence of dimerization constants of a

number of dyes in neutral salt concentrations. In 1972, Selwyn and Steinfeld [154] presented a very convincing and detailed account of the absorption spectra of laser active dyes rhodamine B, rhodamine 6G and acridine red in aqueous, ethanolic and EPA (2 parts ethanol : 5 parts isopentane : 5 parts ethylether by volume) solutions as a function of concentration and temperature. The observed absorbance of the aqueous solutions of rhodamine B and rhodamine 6G was analyzed in terms of monomer-dimer equilibrium. The dissociation constants, $K = C^2_{monomer}/C_{dimer}$ were 6.8×10^{-4} and 5.9×10^{-4} mol/lit at 22°C for aqueous rhodamine B and rhodamine 6G solutions respectively. The absorption spectra of pure monomer and dimer were obtained for these two systems. Acridine red in H_2O was shown to be monomeric up to 3.38×10^{-5} M. Rhodamine B in ethanol formed dimers for which the equilibrium constant for dissociation was 1.1×10^{-4} mol/lit at 62°C and 4.9×10^{-5} mol/lit at 22°C. At -78.5°C higher aggregates are formed in ethanolic rhodamine B solutions whereas rhodamine 6G solutions (2×10^{-4} M) show no evidence for the formation of aggregates in ethanol, even at -78.5°C. Small amount of dimer was noted in acridine red-ethanol solution under the same conditions. Solutions of rhodamine B in EPA are totally dimeric at -196°C. At 22°C the equilibrium constant was 6.2×10^{-5} mol/lit, at -78.5°C it was 3.1×10^{-5} mol/lit. The low value of ΔH (3.36 kJ/mol) in this solvent gives a strong support to the hypothesis that hydrogen bonding is important in dimer formation. Rhodamine 6G-EPA failed to aggregate even when cooled to -196°C. Acridine Red - EPA is predominantly monomeric at 22°C; at -78.5°C an equilibrium constant for the dissociation of dimer of 4.4×10^{-4} mol/lit was calculated. James and Robinson [155] studied the self-aggregation of N(10)-alkyl derivative of acridine orange and their interactions with cationic and anionic surfactants. The dimerization of the dyes in aqueous solution was enhanced relative to acridine orange when the alkyl substituent has more than six carbon atoms. A temperature jump study of the dimerization equilibrium of the octyl and dodecyl derivatives shows the greater stability of the dimer which is reflected in lower rate constant for dissociation. This study further shows a variation of dimerization constant of acridine orange derivatives from 1.05×10^4 to $(79 \pm 52) \times 10^4$ lit/mol for variation of the number of carbon atoms in the alkyl group from 0 to 16. Kamat and Litchin [156] examined the electron transfer in the quenching of protonated triplet methylene blue by ground state molecule of the dye. They determined the extent of dimerization of methylene

blue spectrophotometrically and found to be negligible in solvents containing 50% (vol/vol) or more organic component. Association was found to be significant in neat water and they had taken the value of dimerization constants at 25°C with μ< 0.001M, as 2.5 x 10^{-3} lit/mol from the work of Zadoroznnaya et al. [157]. From these data, monomer amount in a solution with $[MB^+]_{stoich}$ = 2 x 10^{-4} M was calculated as ~ 83%. Arbeloa found changes in the shapes of visible absorption spectra of the fluorescein dianion when the concentration was increased, due to the formation of aggregates [158]. The absorption spectra of dilute dye solutions did not change remarkably with temperature. The variations produced in the spectra of the concentrated solutions with an increase in temperature were due to the dissociation of aggregates. The author applied an iterative method in computing the formation constants of aggregation of the dyes. In the concentration range between 5 x 10^{-6} and ca. 10^{-1}M, the dimerization constant (K_d) does not change appreciably. At the higher concentration the K_d value increases due to the non-negligible existence of other aggregates. The average dimerization constant at 20°C for concentration up to 10^{-1} M was 5.0 ± 0.2 (Standard concentration 1 mol lit^{-1}). The dimer formation enthalpy (ΔH_d), entropy change (ΔS_d), and Gibbs potential (ΔG_d), were found to be -28 ±1 kJ mol^{-1}, -82 ± 5 J $mol\text{-}K^{-1}$ and -3.9± 0.1 kJ mol^{-1} respectively. At higher concentrations, possibility of trimer formation was considered and examined in considerable detail. Arbeloa and Rohatgi-Mukherjee [159] determined the formation constants and absorption spectra of the dimer and trimer of phenosafranin in aqueous solutions. Using two different iterative methods [149,158], the two average dimerization constants at room temperature (28°C) with solutions of concentration smaller than 4 x 10^{-3} M were calculated as 42 ± 2 and 44 ± 2 lit mol^{-1} respectively. Thermodynamic functions for the dimerization process have also been determined. The enthalpy of dimerization, (ΔH_0), was found to be -17 ± 1 kJ mol^{-1}. The standard free energy change and entropy variations of the dimer formation were -9.4 ± 0.1 $kJmol^{-1}$ and -25 ± 5 $J.mol^{-1}K^{-1}$ respectively, at 28°C. The calculated enthalpy change was smaller than the usual values found for hydrogen bond i.e., about -20 kJ mol^{-1}. It has been proposed that besides the possible participation of hydrogen bond, contribution of vander Waals and London forces, which are temperature dependent to some extent, were also important in the dimer formation. The formation constant and absorption spectrum of the trimer were determined assuming that the trimer hypochromism H_t

is equal to H_d^2. The average trimerization constant at 28°C, thus calculated was 65 ± 10 lit.mol^{-1}, which is greater than the dimerization constant. Values of ΔG^0, ΔH^0 and ΔS^0 were -9.4 ± 0.1, -17 ± 1 and -25 ± 5 kJ/mol respectively for the trimerization process suggest that the forces responsible for aggregation are changing from an enthalpy directed one to an entropy directed one. The contribution of hydrogen bonding in the association process is decreased and that of the vander Waals force is increased. The increased hydrophobic interactions justify the substantial increase in the entropic contribution in higher aggregates presumably due to the breaking of water structure. Neumann et al. [160] examined the formation of mixed dimers in solutions of basic dyes. Mixed dimer equilibrium constants for various dyes were estimated to be between 1.4 x 10^2 and 4.9 x 10^4 lit/mol. However, the mixed dimer formation equilibrium constants are larger than those for self dimers. These are ascribed to a charge transfer contribution to the interaction as a result of the difference in the electron densities of different dyes.

4.1.5 The Molecular Exciton Model

The molecular exciton model offers a theoretical method for treating the resonance interaction of excited states of weakly coupled composite systems [161]. The types of problems which have been dealt with on the basis of molecular exciton model among others include spectra of dimers and polymers consisting of molecules held together by weak intermolecular forces (hydrogen bond, vander Waals forces etc.) and the electronic transitions of composite molecules (polyenes, parapolyphenyles and others), considered as resulting from the interaction of excited unit chromophores. In the weakly coupled composite systems for which the molecular exciton model offers a satisfactory approximation for the treatment of excited states, intermolecular (or interchromophore) electron overlap and electron exchange are negligible. In such systems the optical electrons associated with individual component molecules (or chromophoric units) are considered localized, and the molecular units (or chromophoric units) preserve their individual characteristics in the composite (aggregate) system, with relatively slight perturbation. The mathematical formalism then takes the form of a state interaction theory, with the omission of details of atomic orbital composition usual in molecular

electronic theories. The electronic states of the aggregate are then expressed in terms of the electronic states of the component light absorbing units.

Thus, the spectral properties of a molecular aggregate are related to the spectral properties of the component molecules by theoretical expressions involving observable experimental parameters: intermolecular distance, mutual intermolecular orientation and geometry, and intensity (oscillator strength) of light absorption by component molecules. Although the spectral effects of aggregation are small enough to satisfy the use of a quantum mechanical perturbation method, nevertheless these effects are extremely characteristics and may be understood on the basis of the quantum mechanical resonance of excited states. Thus, blue shifts, red shifts, or spectral splitting may be observed, depending on the geometry of the aggregate, accompanied by characteristic changes in polarization properties. Spectral absorption intensity changes may also be observed for the aggregate, and luminescence properties may be affected profoundly compared with those for the component molecules.

The exciton concept was introduced by J. I. Frenkel in 1931 in connection with the theory of transformation of electromagnetic radiation into heat in argon crystal. In 1948, A. S. Davydov applied the molecular exciton model to the problem of electronic states of naphthalene crystals. Since then, a host of researches have appeared exploring all aspects of the model. Davydov's "Theory of Molecular Excitons" [162] summarizes his results, and contains bibliographies of the research literature in this field. Simpson [163] explored underlying elements of the model under the title "Independent Systems Approach" in his "Theories of Electrons in Molecules". McClure's review [164] on the interpretation of the spectra of molecular crystals on the basis of exciton theory is a standard reference. Kasha, on the other hand, emphasized in applications of the molecular exciton model to non crystalline molecular aggregate systems. In a first paper, the distinction between atomic excitons and molecular excitons was stressed, together with the non conductive nature of exciton bands [165]. In a second paper, diverse spectral effects for various coupling strengths were described. The quasi-classical electrostatic vector model was developed as an aid in understanding exciton band formation and various mechanisms of excitation migration were elaborated on [166].

Molecular Exciton Wave Functions:

The starting point of the molecular exciton model treatment will be singlet electronic energy states and their corresponding electronic state wave functions for a component molecule of the aggregate. It is assumed that the electronic signlet state energies E_0, E_1, E_2 ..... and wave functions ψ_0, ψ_1, ψ_2 ..... are known, satisfying the individual molecule Schrödinger equation:

$$H_n\psi_n = E_n\psi_n \tag{4.1}$$

In general, each problem will involve only a pair of states and wave functions, so these may be designated as G and E for ground and excited singlet state energy, and ψ_u and $\psi_u^\dagger$ for corresponding state wave functions for molecule u. It is a very great abstraction to represent an entire molecule in an electronic state by ψ_u or $\psi_u^\dagger$. But these are the starting states for the model.

Molecular Dimers:

The ground state wave function for a molecular dimer consisting of two identical molecules will be (Figure 4.1).

$$\Psi_G = \psi_u\psi_v \tag{4.2}$$

where, ψ_u and ψ_v are wave functions associated with molecule u and v respectively. This is the unique ground state wave function of the dimer; it is totally symmetric with respect to all symmetry operations of the dimer.

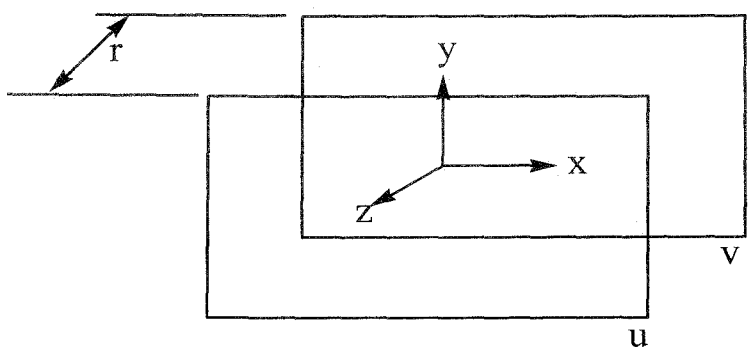

Figure 4.1 Structure and co-ordinate of parallel or card-pack dimer

The first excited state of the dimer can be described equally well by two possible wave functions,

$$\Phi_1 = \psi_u \psi_v^{\dagger} \qquad \text{and} \qquad \Phi_2 = \psi_u^{\dagger} \psi_v$$

These are degenerate and do not describe stationary states of the system. The correct zeroth order wave functions are,

$$\left.\begin{aligned} \Psi_I &= \frac{1}{\sqrt{2}}(\Phi_1 + \Phi_2) = \frac{1}{\sqrt{2}}(\psi_u \psi_v^{\dagger} + \psi_u^{\dagger} \psi_v) \\ \Psi_{II} &= \frac{1}{\sqrt{2}}(\Phi_1 - \Phi_2) = \frac{1}{\sqrt{2}}(\psi_u \psi_v^{\dagger} - \psi_u^{\dagger} \psi_v) \end{aligned}\right\} \tag{4.3}$$

Interchange of molecular levels u, v indicates that the first function is totally symmetric and the second is antisymmetric. In both of the stationary exciton states Ψ_I, Ψ_{II}, the excitation is on both molecules, u and v, i.e., the excitation is collective or delocalized. The node corresponding to minus sign in the exciton wave function is an excitation node not an electron orbital node. At an excitation node the phase relation between transition moments on the respective molecular centers changes sign.

The Intermolecular Perturbation Potential

The energy states and wave functions of molecular aggregate are determined by adding to the total Hamiltonian for the collection of unperturbed molecules a term $\sum_{l,k<l} V_{kl}$ where V_{kl} is the intermolecular interaction operator acting between molecules k and l, and the summation is carried over all pairs of molecules. This is essentially an intermolecular coulombic potential term, giving the interactions between charged particles (electron and nuclei) on the two molecules. However, the use of an exact coulombic potential, V_{coul}, would involve $1/r_{kl}$ as an operator (r_{kl} is the kl intermolecular distance), which would make simplification of the interaction integrals impossible. Accordingly, a point-multipole expansion can be used:

$$V_{coul} \cong V_{mono\text{-}mono} + V_{mono\text{-}di} + V_{di\text{-}di} + \ldots\ldots \tag{4.4}$$

For neutral total charge distribution the monopole interactions are zero. For allowed electric-dipole transitions, the dipole-dipole potential term becomes the leading one and higher multipoles are neglected. Thus, for strong absorption bands, corresponding to allowed electric dipole transitions

$$V_{coul} \cong V_{dipole-dipole} = -\frac{e^2}{r_{kl}^3}\sum_{i,j}\left(2z_k^i z_l^j - x_k^i x_l^j - y_k^i y_l^j\right) \tag{4.5}$$

where in the classical dipole-dipole potential r_{kl}, is the distance between the point dipoles in molecules k and l, and x_k^i is the x coordinate of the i th electron on molecule k, x_l^j is the x coordinate of the j th electron on molecule l, and so forth, the coordinate system being chosen with the z axis parallel to the line of molecular centers, and the summation is over all electrons in each molecule. Thus, an approximation may be introduced, which allows the physical interpretation that the excited state resonance splitting comes about from the electrostatic interaction of transition electric dipoles on neighboring or nearly neighboring molecules (the interaction falling off as the inverse cube of the intermolecular distance). Moreover, in most cases electron displacement along only one coordinate is effected by light wave causing the excitation at a particular frequency, so that in general only one term in the dipole-dipole interaction may remain, e.g., for the upper state of an x-polarized transition in a dimer consisting of two molecules u and v, whose transition moments are both parallel to the x-axis, the perturbation potential reduces to

$$V_{uv} = \frac{e^2}{r_{uv}^3}\sum_{i,j}\left(x_u^i x_v^j\right) \tag{4.6}$$

The Exciton Splitting in a Simple Dimer:

The application of the quantum mechanical molecular exciton formalism to the problem of spectral properties of vander Waals' dye aggregates was made by Simpson et al. for the case of pyridocyanine parallel or card-pack dimers [167]. The application to dimers of diverse geometries, especially for hydrogen bonded molecular pairs [168,169] was made by EL-Bayoumi and Kasha. The application to benzoic acid dimers was made by Nagakura et al. [170] considering the parallel card-pack dimer of Figure 4.1 to understand the spectral properties of such a molecular dimer, one must evaluate the excited state interaction energy to measure the exciton splitting, and the transition moment in order to determine the selection rules.

The Exciton Band Width

In evaluating the excited state interaction energy one should examine merely the exciton splitting for simplicity. The energy of interaction will be given by the

expectation value of the interaction potential with respect to the degenerate excited states of the dimer.

$$\mathscr{E} = \iint \psi_u \psi_v^{\dagger} V_{uv} \psi_u^{\dagger} \psi_v d\tau_u d\tau_v \tag{4.7}$$

where V_{uv} is the intermolecular interaction operator acting between molecules u and v. Inserting the form of V_{uv} appropriate to an x-polarized electric-dipole transition in molecules u and v (cf. Figure 4.1)

$$\mathscr{E} = \frac{e^2}{r_{uv}^3} \iint \psi_u \psi_v^{\dagger} \left(\sum_{i,j} x_u^i x_v^j \right) \psi_u^{\dagger} \psi_v d\tau_u d\tau_v \tag{4.8}$$

where x_u^i is the x co-ordinate of the i th electron on molecule u and x_v^j is the x co-ordinate of the j th electron on the molecule v. Because of the form of V_{uv}, this equation may be factored to yield.

$$\mathscr{E} = \frac{1}{r_{uv}^3} \left[\int \psi_u \left(\sum_i ex_u^i \right) \psi_u^{\dagger} d\tau_u \right] \left[\int \psi_v^{\dagger} \left(\sum_j ex_v^j \right) \psi_v d\tau_v \right] \tag{4.9}$$

where r_{uv} is the distance between the point dipoles in molecules u and v. One recognizes immediately that each of the integrals is now precisely the transition moment integral for the excitation of the individual (monomer) molecules u and v,

$$M_u = \int \psi_u \left(\sum_i ex_u^i \right) \psi_u^{\dagger} d\tau_u \tag{4.10}$$

At this point an arbitrary feature regarding the phase factor of the transition moment enters the picture. We must choose a phase relationship such that a lowering of energy or stabilization of the dimer excited state occurs for the exciton stationary state wave function Ψ_I chosen to lie lowest (cf. Figure 4.2).

Thus, in order to make the exciton stationary state wave function ψ_1 correspond to a lowering of energy $\mathscr{E}$, we can choose the phase factors so that

$$M_u = -M_v \tag{4.11}$$

This phase factor is an entirely arbitrary one. If we choose to define $M_u = +M_v$, then the stationary state exciton function Ψ_{II} of Figure 4.2 would lie lowest for the parallel dimers of Figure 4.1. The expression for the energy lowering or interaction energy for the parallel dimer of Figure 4.1 becomes

$$E = -\frac{M_u^2}{r_{uv}^3} \tag{4.12}$$

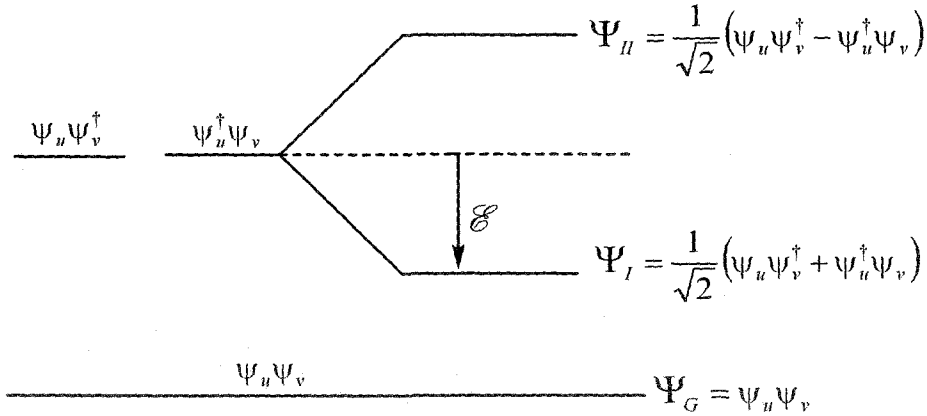

Figure 4.2 Schematic energy level diagram showing exciton splitting in molecular dimers (Displacement term omitted)

The exciton band width will be twice this value or $2\mathscr{E}$.

Thus, we see that the energy lowering for the simple dimer case at hand (Figure 4.1) is given by the monomer transition moment squared i.e., is proportional to the probability or intensity of the electric dipole allowed transition in the monomer, divided by the inter molecular distance cubed. Thus, the stronger the absorption band, the greater will be the exciton band splitting. One observes also that the r-dependence makes this a comparatively long range interaction.

For a dimer with arbitrary mutual orientations of molecular axes with respect to an x, y, z co-ordinate frame (Figure 4.1) the energy of interaction is given by

$$\mathscr{E} = -\frac{M_u^2}{r_{uv}^3}\left(2\cos\theta_u^z\cos\theta_v^z - \cos\theta_u^x\cos\theta_v^x - \cos\theta_u^y\cos\theta_v^y\right) \qquad (4.13)$$

Where again M_u represents the transition moment in a free molecule, and $\cos\theta_u^x$, $\cos\theta_u^y$, $\cos\theta_u^z$ represent the cosines of the angles which the transition moment M_u for molecule u makes with the x, y, z axes.

Selection Rules:

Although in the molecular dimer two exciton states theoretically result from the exciton splitting, both of these may not necessarily be observed as allowed spectral transitions. In fact, which exciton stationary states may be reached by electric dipole transitions from the ground state is a strictly geometry-determined problem.

Let us examine the spectral selection rules by evaluating the matrix elements of the electric dipole operator between the ground state and the stationary exciton states of the dimer. Thus, the transition moment vector of the dimer is given by

$$M^{I} = \iint \Psi_G (\mathscr{M}_u + \mathscr{M}_v) \Psi_I d\tau_u d\tau_v$$
$$M^{II} = \iint \Psi_G (\mathscr{M}_u + \mathscr{M}_v) \Psi_{II} d\tau_u d\tau_v \qquad (4.14)$$

Where $\mathscr{M}_u$, $\mathscr{M}_v$ are the electric dipole operators corresponding to the molecular electronic co-ordinates of molecules u and v. Evaluating these, and because of orthogonality and normalization properties of the intramolecular state wave functions following values of transition moments are obtained.

$$M^{I} = \frac{1}{\sqrt{2}}(M_v + M_u)$$

and (4.15)

$$M^{II} = \frac{1}{\sqrt{2}}(M_v - M_u)$$

For the card-pack dimer we had defined as required phase relations for the wave functions Ψ_I and Ψ_{II}, $M_u = -M_v$. Therefore, for the parallel or card-pack dimer of Figure 4.1, the transition moments corresponding to the stationary exciton states of Figure 4.2 are:

$$M^{I} = \frac{1}{\sqrt{2}}(M_v - M_v) = 0$$

and (4.16)

$$M^{II} = \frac{1}{\sqrt{2}}(M_v + M_v) = \frac{2M_v}{\sqrt{2}}$$

Thus, the transition moments for the dimer are given as super positions of the transition moments for the individual molecules. According to the above equation the oscillator strength (f) for electric dipole transitions between singlet states of the dimer Ψ_G and Ψ_1 is zero. For the transition to singlet state Ψ_{II} since

$f \propto (M^{II})^2 = 2 M_v^2$ or $f_{II,\,dimer} = 2f_{monomer}$

an allowed transition with no change of intensity per monomer is predicted.

4.1.6 Spectral Properties of Dimer in terms of Exciton Theory:

Three characteristics of vander Waals dye molecule parallel dimers have been recognized in the literature. These are (a) The absorption spectrum characteristically blue shifts by 2000-4000cm^{-1} in these dimers, (b) the prominent fluorescence of the monomer is invariably quenched, and (c) the relatively inefficient phosphorescence of the monomer becomes the predominant luminescence in the dimer. Simpson et al. [167] and McRae and Kasha [171] have interpreted these properties in dye molecule dimers and polymers on the basis of the molecular exciton splitting and selection rules in the dimer. In the monomer, absorption to the lowest singlet excited state is strongly allowed, and the very rapid fluorescence emission competes with excitation of the lowest molecular triplet state. In the dimer, the allowed exciton state is at significantly higher energy than the singlet excited state of the monomer: a blue shift is thus accounted for in case of the card-pack, or parallel dimer. However, collisions rapidly deactivate the excited dimer to its lower singlet exciton stationary state. But this state is a metastable signlet state with an improbable fluorescence capacity. Further deactivation of the dimer to the triplet state becomes the most probable path for the excitation. Thus the fluorescence is quenched, and a very strong triplet state to ground singlet state emission is observed. Reference [171], contains a general bibliography of the various experimental observations on spectral consequences of dye dimerization. The parallel or card-pack structure probably fits quite well to vander Waals dimers consisting of large planar dye molecules. However, numerous other dimer structures are possible, and the exciton model permits a qualitative and semi-quantitative discussion of such dimers as well. These have been described in references [166,168-170]. In particular, for head-to-tail orientation of transition moments in the dimer, a strong red shift is predicted, with the upper exciton component forbidden in the dimer; whereas, in the oblique dimer, with mutual angle between molecular transition moments between 0 and π, both exciton components are observed with a spectral splitting as the characteristic result. These general dimer results may be gleaned from the linear polymer exciton model treated by McRae and Kasha [171]. Rohatgi and Mukhopadhyay [172] studied the dimer spectra of fluorescein and some of its halogen derivatives in aqueous solution. From the splitting observed in the spectra, the inclination of the component molecules in a dimer has been obtained on application of the theory of exciton interaction. The

distance r between the two component molecules in the dimer was also calculated for various geometries. In other series of publication Arbeloa [158,173] studied molecular structures of the dimeric and trimeric states of fluorescein dianion. The absorption spectra of the dimer and trimer of the dye molecule in aqueous solution were evaluated. The geometric structures of both aggregates were determined using the exciton theory. The nature of the association forces was also studied. Evidence was presented for the formation of Eosin Y dimer as the highest aggregates of complexes between eosin Y and poly-L-lysin, poly (1-xylyl viologen) or cetyl-pyridium [174]. The absorption spectra of these complexes have been obtained free from contamination by Eosin Y monomer spectrum and were fitted with Gaussian band model, using a non-linear least square fitting computer program. Using such models, exciton theory had been employed to calculate parameters such as orientation and molecular separation of the components of the Eosin Y dimer. Where appropriate, these parameters have been compared with the dimensions of the repeating unit and the possible conformations of the polymer [174]. Basu et al. [175] studied concentration effects on the absorption and emission properties of Ni (II) and Zn(II) tetra(p-venyl phenyl) porphyrins in benzene solutions. Whereas exciton splitting of the soret band was observed for the Ni (II) complex, only a hypochromic effect is observed for the Zn(II) complex. The exciton parameters were calculated for Ni complexes. Arbeloa et al. [159] also studied the excitonic interaction and the nature of bonding in the aggregation of phenosafranin from concentration dependent spectral changes.

By applying simple exciton theory in zero order an attempt has also been made to study the geometric structure of the trimer, as has been accomplished for xanthene aggregates [158,159]. Molecular model showed that the angle θ between the chromophore groups of the monomers is due to the steric effect between the phenyl groups. Newmann et al. [160] put forward evidences of the formation of mixed dimers of basic dyes, which shows spectroscopic properties in accordance with exciton theory. The bands of these dimers can be found at wave lengths shorter and longer than those of the forming dyes, with higher and lower excited states, respectively. These bands correspond to the transitions of both the in-phase (high energy) and out-of-phase (low energy) transition moment geometries, none of which are prohibited.

In a recent publication Horng and Quitevis [176] observed that expanding the scope of analysis to include dye aggregation and exciton theory enhances the pedagogical value of studying the visible absorption spectra of conjugated dyes in the physical chemistry curriculum. As has been already mentioned, the exciton theory of dipole-dipole coupling can be used to relate the distance and relative orientation of monomeric dye molecules, cyanine and Merocyanine dyes are known to form aggregates in concentrated, aqueous solution exhibiting a strong spectral shift of absorption band toward longer wave lengths with respect to the monomer absorption. These assemblies have been named J-aggregates. In other cases the absorption band is shifted upon aggregation toward smaller wavelength and the corresponding assemblies have been termed H-aggregates [177] Practically, the J-aggregates has served as an important spectral sensitizer in silver halide photographic material as the electronically excited J-aggregates can effectively inject photo-electron into the conduction band of silver halide and its sharp absorption band allows easier control over the spectral sensitivity of the photo imaging system [178].

Progressively alkylated thiazine dyes are known to show interesting spectral characteristics in solution and have been used in photogalvanic and photochemical studies [116,179,180]. They can also be often designated as azures (Figure 1.4c-e in Chapter 1) and are also acted as useful photosensitizes [181]. Hence, they have been have selected for the present study. The absorption UV-Vis spectroscopy is one of the most suitable methods for quantitative study of the aggregation properties of the dyes as a function of concentration in both aqueous and microemulsion media.

4.2 Experimental

Five progressively alkylated thiazine dyes viz. thionine (Th), azure A (AzA), azure B (AzB), azure C (AzC) and methylene blue (MB) were supplied by Aldrich Chemical Co., USA. The structure of all thiazine dyes are shown in Figure 1.4 of Chapter 1. N-Cetylpyridiniumbromide (≥97.0 %, Fluka, Switzerland), Chloroform, n-heptane, (E-mark) used are analytical in grade. Chloroform and n- heptane were distilled for further purification by usual method [182]. CPB was used as received. Source and purification of other two surfactants, viz. SDS and AOT are mentioned in chapter 3. All the five dyes were found to contain colured impurities. They were

purified over a chromatographic column of silica gel using chloroform-methanol mixture as elutent. AzC was extracted efficiently with 8:2 chloroform-methanol mixture whereas, azure A was extracted with 7:3 solvent mixture. All other dyes were eluted by less polar solvent mixtures than that used for AzA. Finally they were recrystallised and dried at 50^0C under vacuum. Purity of the dye samples were checked by TLC using 8:2 water-acetic acid mixtures as the mobile phase and purity of all dyes except AzC were found to be excellent. The commercial AzC contained high percentage of insoluble materials in addition to other coloured impurities. Even after repeated chromatographic treatment it gave faint additional spot on the TLC plate indicating the presence of a small amount of impurity. However, although the purification of this dye was not up to the level of other dyes, various analyses (spectral and analytical) showed that final purity of the dye was satisfactory. Except thionine all dyes supplied as chloride salts and are highly soluble in aqueous medium. Thionine was also being changed to its corresponding chloride from acetate salt by passing through the ion exchange column (Amberlite IRA 400, BDH, England) containing chloride ion. Doubly distilled water having conductivity 2 μS cm^{-1} was used throughout experiment.

With in the dye solutions (of order 10^{-5} M) appropriate amount of SDS and AOT were added to investigate the influence dye on micellar aggregation at a fixed temperature of 303K.

Microemulsions were obtained by adding water in solution of CPB in 1:1 (v/v) chloroform and n-heptane and mixing them well until the mixtures become totally transparent by using a micropipette. By varying the proportion of water and CPB, the [water]/[CPB] mole ratio, ω was varied. Chloroform was used for preparing microemulsion for increasing the polarity of the oil phase to some extent so that large amount of surfactant can be dissolved in the mixture to produce larger water-pool.

Absorption spectra were recorded on a double beam Jasco V-530 UV/vis spectrophotometer (Japan). The spectra were recorded with a quartz cell having 1 cm and 1mm optical path length. The temperature of the whole experiment was maintained at 303K with a thermostatic arrangement coupled with the spectro-photometer.

4.3 Results and Discussion

4.3.1 Interaction of Thiazine Dyes with SDS and AOT in Aqueous Media

The representative visible absorption spectra of all thiazine dyes (1.17×10^{-5} – 2.10×10^{-5}M) in aqueous media with and without SDS and AOT were recorded. The spectra taken in a cell of 1 cm path length are shown in Figure 4.3 – 4.12. As the concentration of SDS is increased from 4.0×10^{-3} M to 2.82×10^{-2} M in each thiazine – SDS system, which essentially covers both pre and post micellar concentrations of SDS (cmc of SDS in aqueous solution = 8.6×10^{-5} M at 303K [183]), the intensity of spectra is increased significantly. In the visible region the dyes (10^{-5} mol.dm^{-3}) viz. Th, AzA, AzB, AzC and MB have absorption bands λ_{max} of 598, 634, 646, 620 and 661 nm with extinction coefficients of 6.16×10^4, 5.18×10^4, 6.90×10^4, 4.96×10^4 and 7.20×10^4 respectively in aqueous solution (Table 4.3). But in presence of submicellar concentration of SDS the spectral absorbance decreased markedly in case of thionine. The band shape also changed with the shifting of λ_{max} to 634 nm with a large shoulder at 520 nm. From the spectral feature it can be said that there must exist some dye-surfactant interactions.

It was reported that the degree of shifting of λ_{max} of a dye which form self-aggregation depends on the number of monomer involved in the aggregation process and on the geometry of the aggregates as has already been mentioned [184]. The planer dyes such as acridine orange and methylene blue aggregate in stacked manner and exhibit blue shifted metachromasia [184,185], where as nonplaner dyes such as pseudoisocyanine aggregate in a staggered way and depict a red shift of λ_{max} [186]. Figure 4.3 shows the effect of different concentrations of SDS on the absorption spectrum of thionine. Datta and Bhat [187,188] proposed the formation of "water-structure-enforced ion pairs in which the head groups of the surfactant molecule is attached to the sulfonate group of methyl orange (MO)" in order to explain the large blue shift in the spectrum of MO upon addition of small amount of a cationic amphiphile. Although the dye and the surfactant molecules are individually hydrated in the solution, long range electrostatic and short range hydrophobic forces may cause the formation of dye-surfactant complexes. Values of calculated monomer suggest that all the thiazine dyes in the concentration range $1\sim2 \times 10^{-5}$ M are present mostly in the monomeric form [193]. On the other hand, the dye-surfactant complex is formed involving electrostatic interaction between the negative charge of anionic

surfactant and positively charged dye molecule (particularly with the $-NH_2^+$ group), with the alkyl chain of the surfactant in close contact with the rest of the dye molecule. Some of these complexes can aggregate and precipitate in the solution which is in equilibrium with the precipitates. The loss of absorbance of dye solution in submicellar concentration region of a surfactant may be to some extent due to the precipitation of dye in the solution. However, in the present systems, hydrophobic forces do not play any significant role in the interaction of dyes with surfactants because dyes are highly water soluble and only coulombic interactions may be important. Similar premicellar aggregates were reported upon the interaction of oppositely charged 3,3'-diethylthiacarbocyuanine (DTC) and SDS at [SDS] $\geq 10^{-5}$M [189]. This kind of interaction registers a drop of fluorescence quantum yield over the premicellar concentration range of surfactant as was reported by Tatikolov and Costa [99]. These authors used cetyltrimethylammonium chloride (CTAC) as the surfactant and a synthetic cyanine as the oppositely charged dye. However, in the present investigation, further addition of SDS (>cmc) to the thionine-SDS solution leads to a small red shift of about 3nm (λ_{max} = 601nm) relative to that of aqueous solution (λ_{max} = 598nm) [representative spectra are shown in Figure 4.3]. Shape of the spectral band also appears very much similar to that of the spectra in aqueous solution. It is obvious that as the concentration of SDS micelles increased, the solubility of dye is also increased via the formation of dye-micelle aggregates in aqueous solution, resulting in a slight red shift in the spectrum with an increase in intensity of the absorption. It may also be mentioned that in post micellar concentration range, dye molecules remain in the interface of the micelles due to coulombic attractive force. Change of polarity of the associated water molecules in the vicinity of the micellar surface may be responsible for the small shift of the spectral peak. In this connection it should be noted that Tatikolov et al. [99] found only weak interaction between TX-100 and cyanine dye due to absence of any significant electrostatic attraction. Concentration of TX-100 at below and somewhat above cmc (cmc = 2.6 x 10^{-4}M) did not yield any effective change of photophysical parameters of the dye. The authors observed a slight red shift in the dye fluorescence spectrum only in presence of high surfactant concentrations ([TX-100] $\approx 10^{-3}$M), and this shifting was found to increase with surfactant concentration slowly.

All the other four thiazine dyes also behave similarly when treated separately with SDS. However, marked change of the spectral feature in submicellar concentration of surfactant was observed as a function of degree of alkylation of thiazine dyes (viz., AzA, AzB, AzC and MB). The dyes give much intense shoulder in the lower wavelength region like thionine. This observation also supports the fact that the alkylated planer thiazine dyes having comparatively larger hydrophobic moieties stacked firmly with the surfactant molecule, while the hydrophobic interactions along with the coulombic attraction play important role in the formation of the dye-surfactant complex.

Similar experiments were also carried out with another important anionic surfactant viz., AOT (Figure 4.8 – 4.12). Due to its double strand hydrophobic chain AOT has marvelous surface activity. Within a wide range of premicellar and postmicellar concentration of AOT, the λ_{max} of the spectral band does not show any significant shift. However, just like SDS, an intense shoulder appears at 564 nm in premicellar concentration of AOT. Among other dyes, Azure B gives an extra peak at 593 nm when treated with AOT in its submicellar concentration range. The characteristics of the spectral features observed due to the interaction of dye with AOT are well explanatory on the basis of intense ion-pair formation in submicellar media followed by dye-micelle interaction in the higher concentration (>cmc) ranges of the surfactant. Some of the spectral characteristics of progressively alkylated thiazine dyes in aqueous solution in presence of SDS and AOT in pre and postmicellar concentration are listed in Table 4.1.

4.3.2 Determination of cmc of Surfactants and Dye-surfactant Association Constant

Organic dyes may provide a simple and rapid method for the cmc determination of a surfactant owing to the large change in their spectrophotometric properties that accompanies micelle formation [191]. However, in many cases the apparent cmc varies with the dye's charge and concentration [191] and is in disagreement with values obtained by other physical methods, such as conductance and surface tension measurements. Samsonoff et al. [24] have successfully used UV-vis spectroscopy to determine the cmc of anionic, cationic, zwitterionic and nonionic surfactants by using

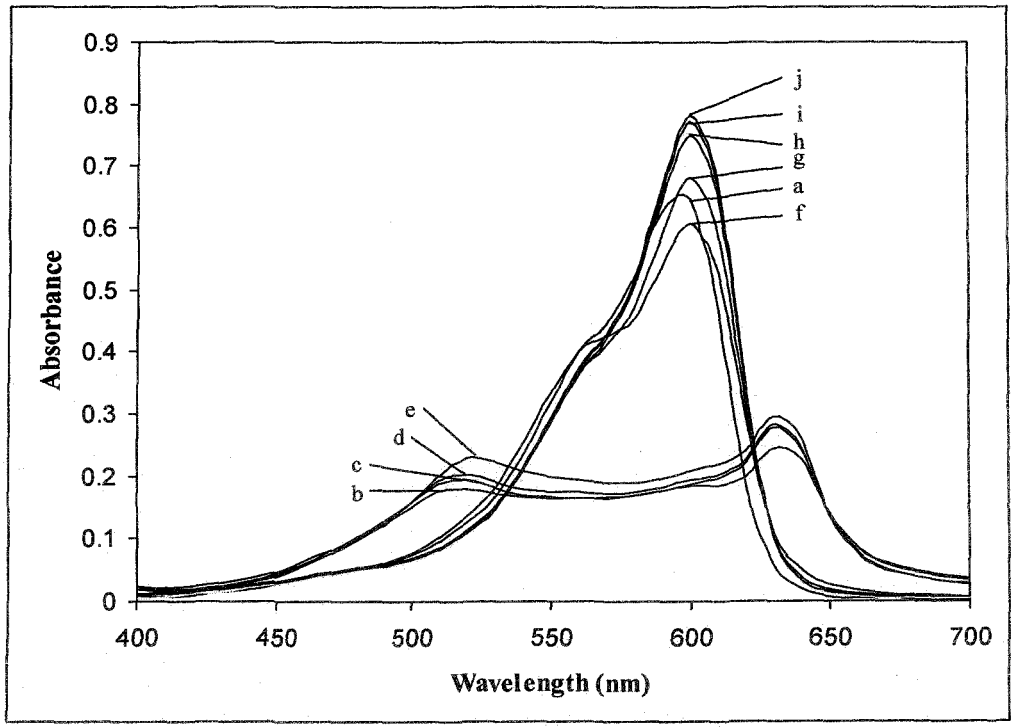

Figure 4.3 UV-Vis Spectra of Thionine (1.50×10^{-5}M) in aqueous solutions of various concentrations of SDS at 303K. [SDS]/10^{-3}M: (a) 0.00, (b) 4.00, (c) 4.96, (d) 5.93, (e) 7.04, (f) 8.00, (g)11.57, (h) 12.50, (i) 15.70, (j) 20.02, (k) 25.01.

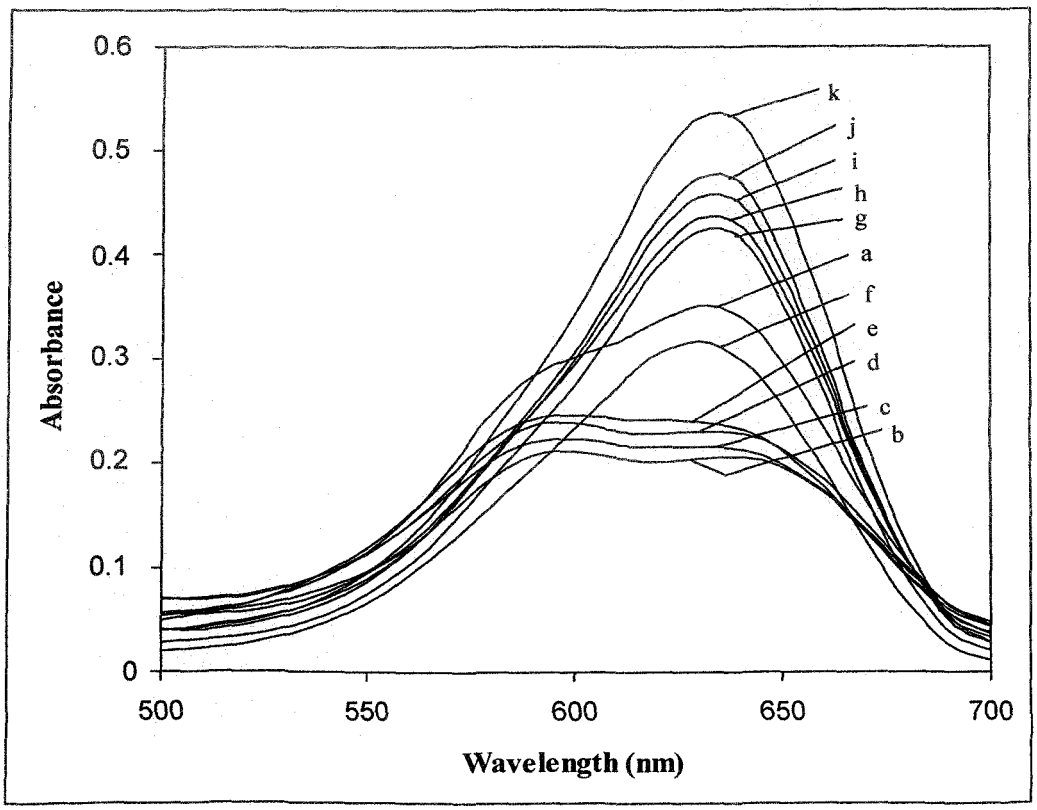

Figure 4.4 UV-Vis Spectra of Azure A (2.10×10^{-5}M) in aqueous solutions of various concentrations of SDS at 303K. [SDS]/10^{-3}M: (a) 0.00, (b) 4.00, (c) 4.96, (d) 5.93, (e) 7.04, (f) 10.50, (g)11.57, (h) 12.50, (i) 15.70, (j) 20.02, (k) 25.01.

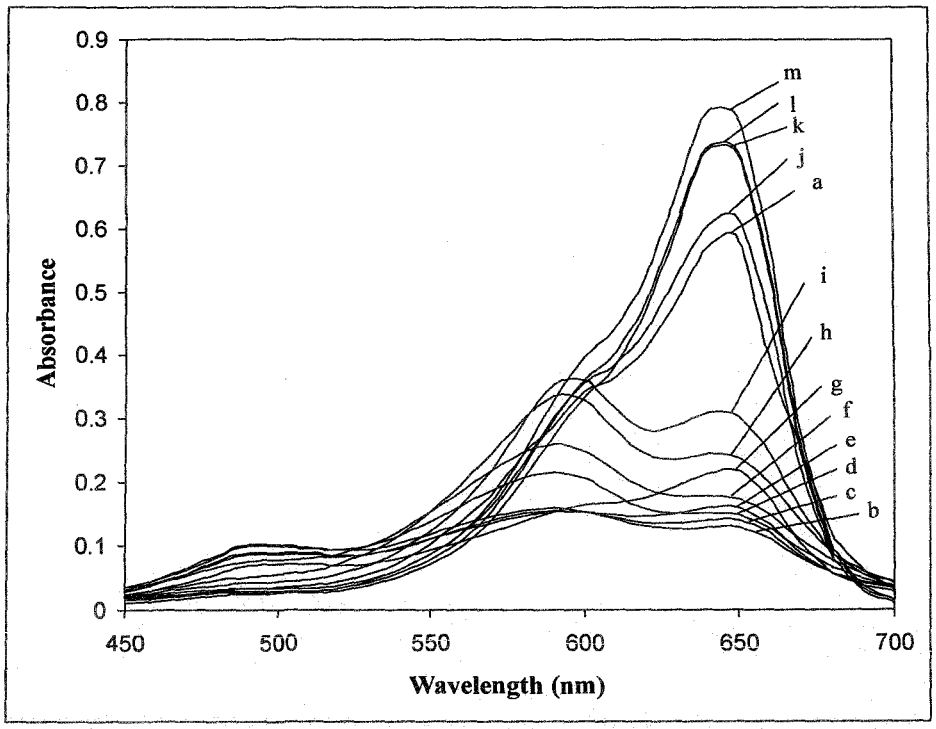

Figure 4.5 UV-Vis Spectra of Azure B (1.20×10^{-5}M) in aqueous solutions of various concentrations of SDS at 303K. [SDS]/10^{-3}M: (a) 0.00, (b) 4.00, (c) 4.96, (d) 5.93, (e) 7.04, (f) 7.55, (g) 8.02, (h) 12.50, (i) 15.70, (j) 20.02, (k) 22.03, (l) 25.01, (m) 28.2.

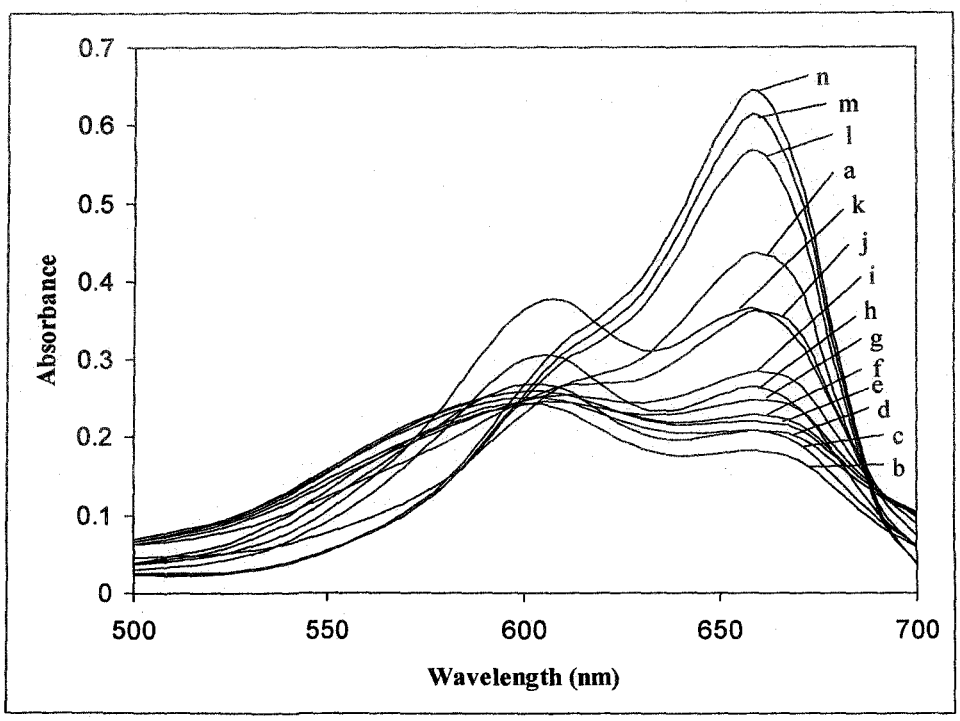

Figure 4.6 UV-Vis Spectra of Methylene Blue (1.17×10^{-5}M) in aqueous solutions of various concentrations of SDS at 303K. [SDS]/10^{-3}M: (a) 0.00, (b) 4.00, (c) 4.96, (d) 5.93, (e) 6.50, (f) 7.00, (g) 8.02, (h) 8.50, (i) 7.55, (j) 9.02, (k) 14.30, (l) 22.01, (m) 25.2, (n) 28.2

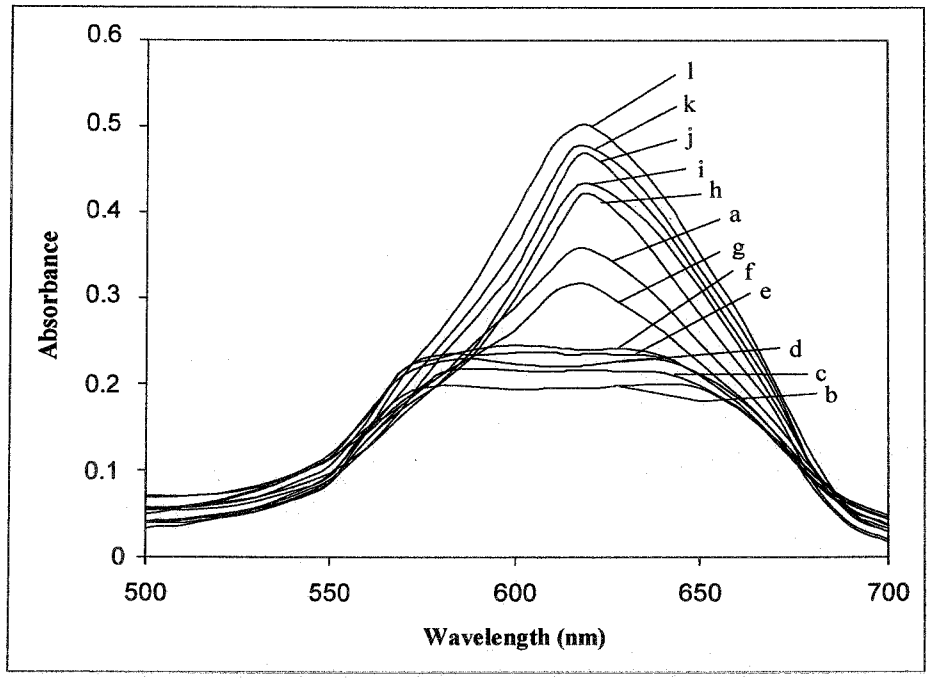

Figure 4.7 UV-Vis Spectra of Azure C (1.24×10^{-5}M) in aqueous solutions of various concentrations of SDS at 303K. [SDS]/10^{-3}M: (a) 0.00, (b) 4.00, (c) 4.96, (d) 5.93, (e) 7.04, (f) 8.00, (g) 9.23, (h) 12.50, (i) 15.70, (j) 20.02, (k) 22.3, (l) 25.01.

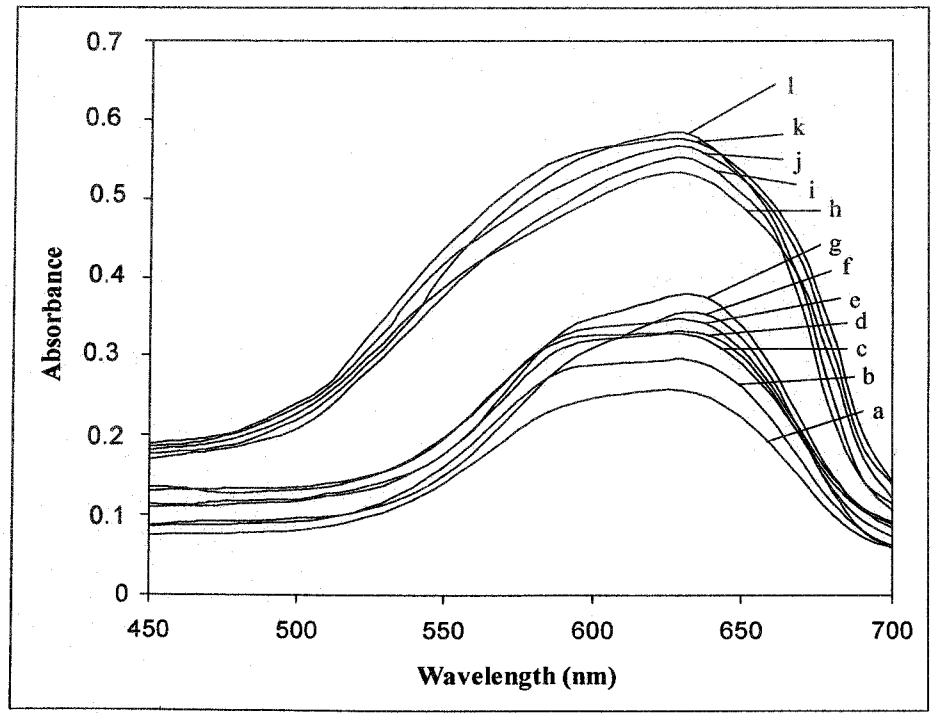

Figure 4.8 UV-Vis Spectra of Azure A (2.10×10^{-5}M) in aqueous solutions of various concentrations of AOT at 303K. [AOT]/10^{-4}M: (a) 4.00, (b) 6.02, (c) 7.28, (d) 8.80, (e) 10.01, (f) 15.06, (g) 19.80, (h) 23.96, (i) 27.00, (j) 60.23, (k) 70.30, (l) 80.51

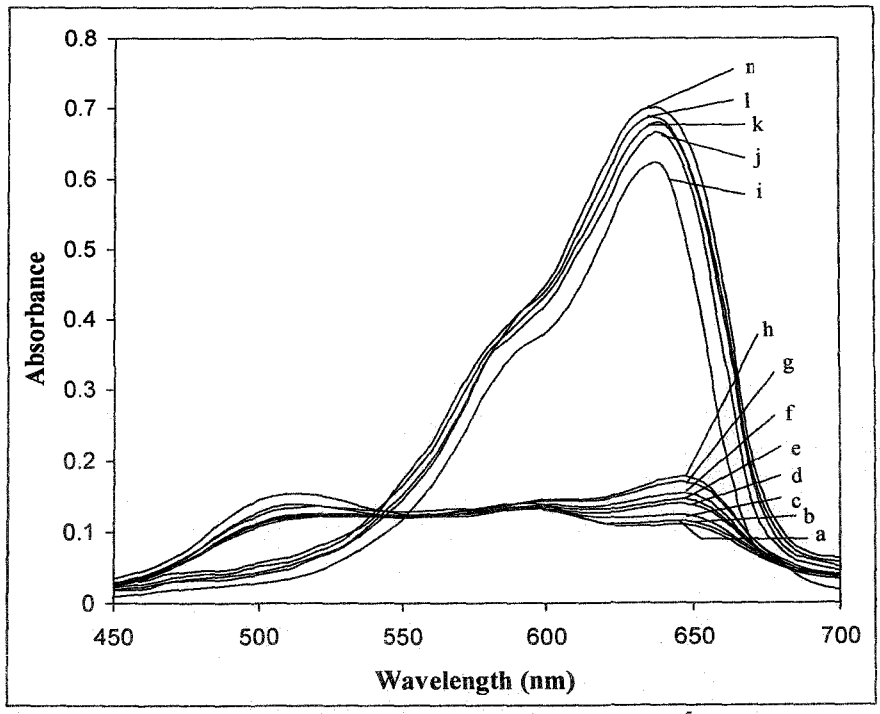

Figure 4.9 UV-Vis Spectra of Azure B (1.20×10^{-5}M) in aqueous solutions of various concentrations of AOT at 303K. [AOT]/10^{-4}M: (a) 4.00, (b) 6.02, (c) 7.28, (d) 8.80, (e) 10.01, (f) 15.06, (g) 19.80, (h) 23.96, (i) 27.00, (j) 60.23, (k) 70.30, (l) 80.51, (m) 92.30.

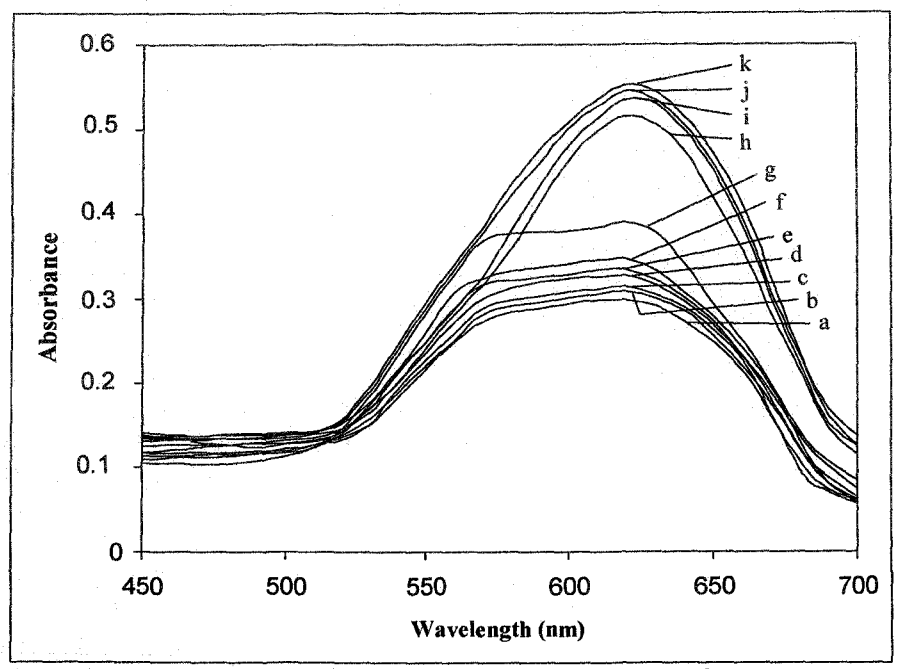

Figure 4.10 UV-Vis Spectra of Azure C (1.50×10^{-5}M) in aqueous solutions of various concentrations of AOT at 303K. [AOT]/10^{-4}M: (a) 4.00, (b) 6.02, (c) 7.28, (d) 8.80, (e) 15.01, (f) 20.06, (g) 25.80, (h) 40.96, (i) 50.00, (j) 60.23, (k) 70.30,

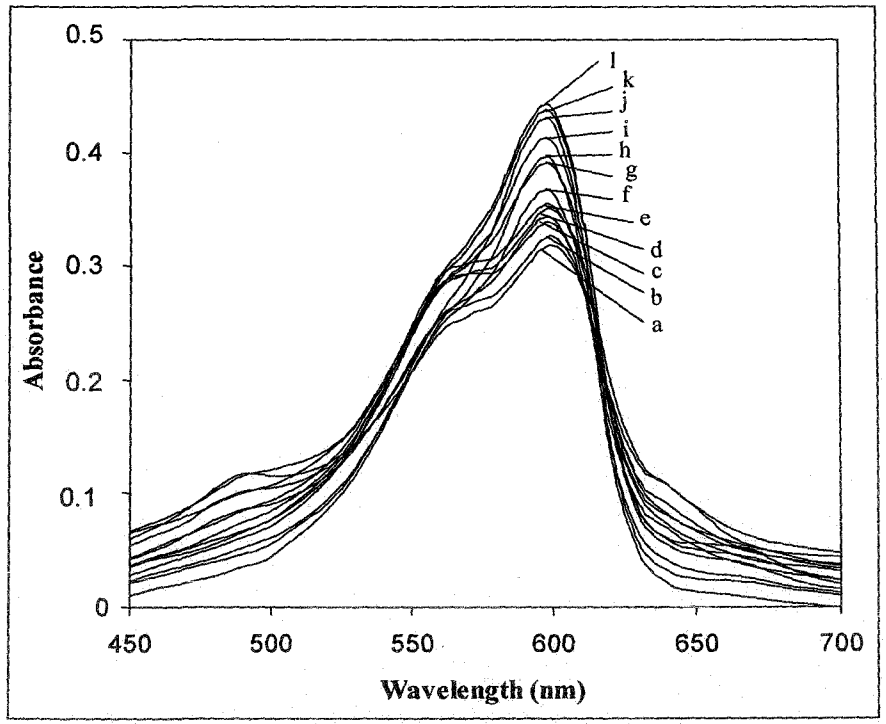

Figure 4.11 UV-Vis Spectra of Thionine (1.50×10^{-5}M) in aqueous solutions of various concentrations of AOT at 303K. [AOT]/10^{-4}M: (a) 4.00, (b) 6.02, (c) 7.28, (d) 8.80, (e) 15.01, (f) 20.06, (g) 25.80, (h) 40.96, (i) 50.00, (j) 60.23, (k) 70.30, (l) 80.51

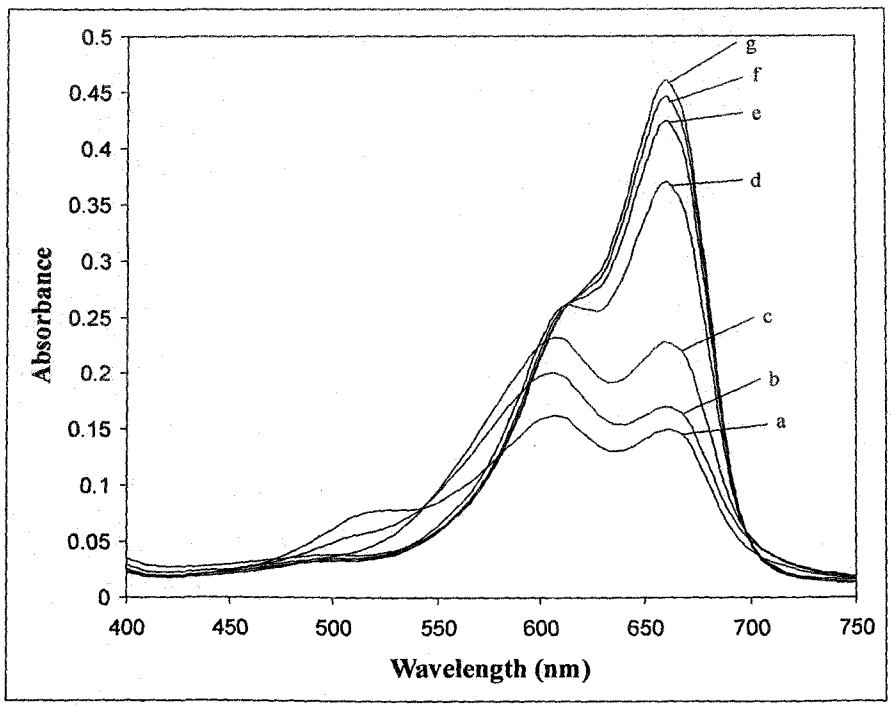

Figure 4.12 UV-Vis Spectra of Methylene Blue (1.17×10^{-5}M) in aqueous solutions of various concentrations of AOT at 303K. [AOT]/10^{-4}M: (a) 8.10, (b) 10.01, (c) 15.06, (d) 19.80, (e) 27.00, (f) 60.23, (g) 70.30.

Table 4.1

Some of the Spectroscopic Characteristics of Dyes in Aqueous Solution in pre-micellar and post-micellar concentration of SDS and AOT at 303K

Dye	Pre-micelle				Post-micelle		
	λ_{max} (nm)	λ_1(nm) (shoulder)	$\Delta\lambda$ (nm) = $\lvert(\lambda_{max}[aq] - \lambda_{max}[mic])\rvert$	λ_{max} (nm) (aqueous)	λ_{max} (nm)	λ_1 (nm)	$\Delta\lambda$ (nm) = $\lvert(\lambda_{max}[aq] - \lambda_{max}[mic])\rvert$
			SDS				
Thionine	634	520	36	598	601	564	3
Azure C	620	570	0	620	620	–	0
Azure A	634	593	4	630	634	–	0
Azure B	648	591	2	646	645	600	1
Methylene Blue	661	604	0	661	658	612	3
			AOT				
Thionine	598	564	0	598	598	564	0
Azure C	618	570	2	620	618	–	2
Azure A	634	591	4	630	634	591	4
Azure B	646	512	0	646	646	580	0
Methylene Blue	661	608	0	661	661	614	0

Coomassie brilliant blue G-250 (CBB) dye as a probe. They found the cmc values very close to the other literature values. Huang et al. [23] also described a method of cmc determination by measuring surfactant catalyzed redox reaction rate between H_2O_2 and bromopyrogallol red (BPR), a triphenylmethane dye. They used two cationic surfactant, viz. cetylpyridinium bromide (CPB) and cetyltrimethylammonium bromide (CTAB) for their experiment.

The association of a substrate or a probe (dye) molecule with a surfactant micelle can be described by the following equilibrium [190]:

$$D_w + S_m \underset{}{\overset{K_{ass}}{\rightleftharpoons}} D_m \qquad (4.17)$$

for which the equilibrium or association constant, K_{ass} is given by the expression

$$K_{ass} = \frac{[D_m]}{[D_w][S_m]} \qquad (4.18)$$

where $[D_w]$ and $[D_m]$ denote the concentrations of probe in aqueous and micellar phase respectively, and $[S_m]$ is related to the total surfactant concentration, $[S_t]$ by the relation

$$[S_m] = [S_t] - \text{cmc} \qquad (4.19)$$

It has been already pointed our that the shape of the visible absorption spectra of thionine dyes are greatly influenced in the presence of submicellar concentration of SDS and AOT due to strong electrostatic interaction between the surfactant and dye molecule. However, when the surfactant concentration reaches cmc value, at the onset of homogeneous micelle formation, the spectral feature is restored, but the absorbances at λ_{max} is greatly enhanced as compared to the values observed in the pure aqueous solution of the corresponding dye. From this marked change in the spectral intensity of the dye below and above cmc of the surfactant, the dye-surfactant association constant (K_{ass}) and critical micelle concentration (cmc) of SDS and AOT at 303K have been determined based on the methods of Nigam et al [190] and Datta et al. [192]. Considering the equilibrium 4.18 and the mass balance variation 4.19 one can easily derive the following equation [22,192]:

$$\frac{(d_0 - d)}{(d - d_m)} = -K_{ass}.cmc + K_{ass}[S_t] \qquad (4.20)$$

where d_0, d and d_m are the absorbances of the dye in absence of surfactant, in presence of post-cmc surfactant concentration $[S_t]$, and in excess of surfactant respectively at a fixed wavelength of the band where absorbance increases with the concentration of the added surfactant. A plot of $(d_0 - d)/(d - d_m)$ versus $[S_t]$ is linear with slop equal to K_{ass} and the intercept of the abscissa equal to cmc. The plots of $(d_0 - d)/(d - d_m)$ vs. $[S_t]$ for different dye surfactant systems are shown in Figures 4.13 - 4.21.

Table 4.2

Spectroscopically determined cmc of SDS and AOT with Gibbs free energy (ΔG^0) and the corresponding association constant (K_{ass}) of dye-surfactant at 303K

Surfactant	Dye	cmc /(mol.dm^{-3}×10^3)	K_{ass} /(dm^{-3}.mol)	$-\Delta G^0$ /(kJ.mol^{-1})
SDS	Thionine	8.82 (7.60)	285.2	14.24
	Azure C	8.72 (8.40)	173.6	12.99
	Azure A	9.02 (8.20)	121.4	12.09
	Azure B	8.80 (8.50)	109.0	11.82
	Methylene Blue	8.40 (8.50)	96.5	11.51
AOT	Thionine	2.65 (2.80)	90.6	11.35
	Azure C	2.82 (2.60)	70.3	10.71
	Azure A	2.87 (2.50)	60.1	10.32
	Azure B	3.01 (3.00)	50.1	9.86
	Methylene Blue	2.85 (3.10)	48.3	9.77

The plots are linear which indicates the validity of the equation (4.20). Present method yields cmc values much easily compared to other spectroscopic methods using probes [191]. The values of $[S_t]$ corresponding to the point where the straight line meets the abscissa, gives cmc of the surfactant. The points for $[S_t]$ below cmc fall on the abscissa due to the absence of micelles in the system. The inflexion points of the plots of absorbances as a function of surfactant concentrations (Figure 4.22 - 4.27) also correspond very nearly (but not exactly) to the cmc value of the surfactants. The

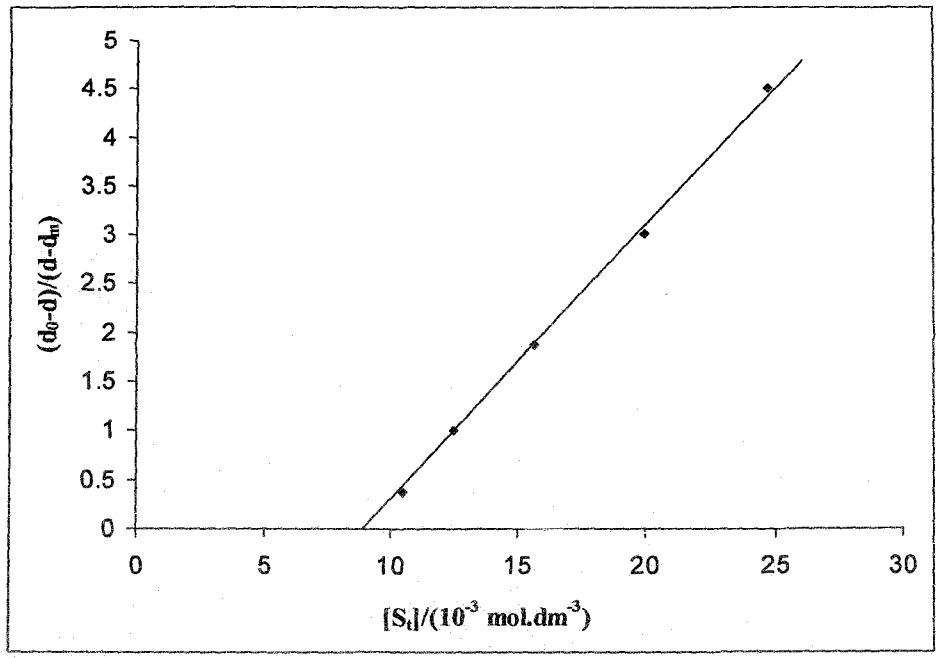

Figure 4.13 $(d_0-d)/(d-d_m)$ vs. concentration (SDS) for Thionine-SDS system having dye concentration 1.50 x 10^{-5}(M) at 303K.

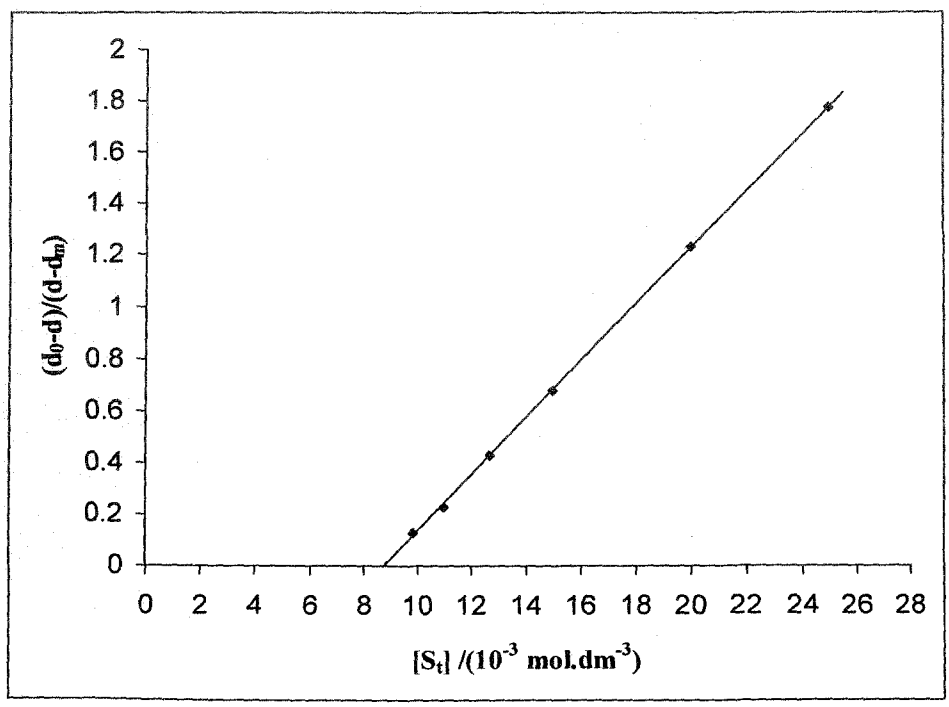

Figure 4.14 $(d_0-d)/(d-d_m)$ vs. concentration (SDS) for Azure B-SDS system having dye concentration 1.20 x 10^{-5}(M) at 303K.

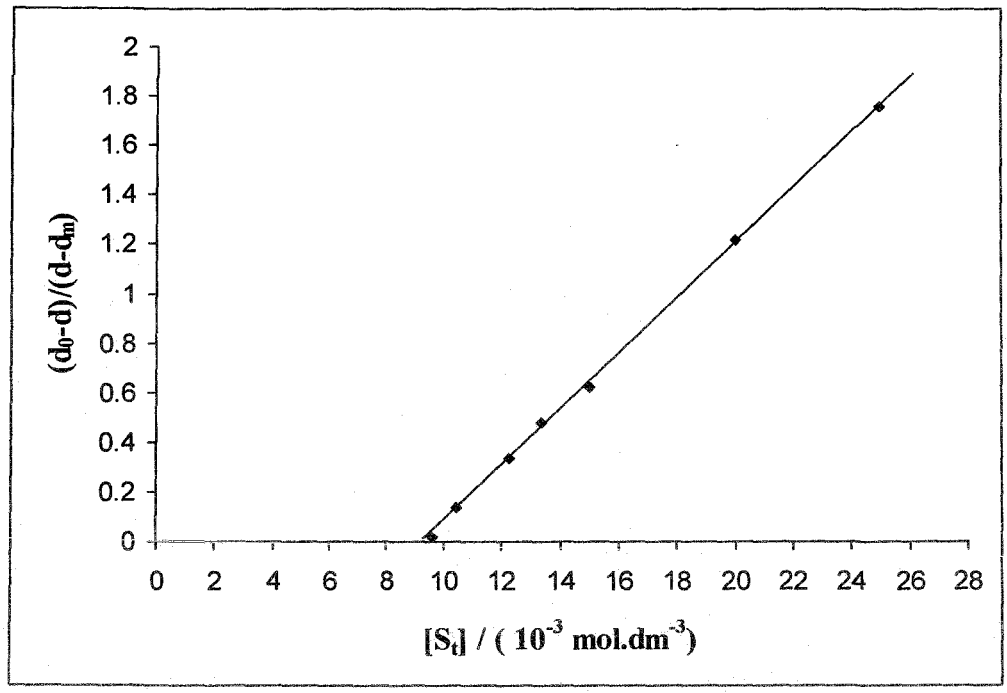

Figure 4.15 (d_0-d)/(d-d_m) vs. concentration (SDS) for Azure A-SDS system having dye concentration 2.1 x 10^{-5}(M) at 303K

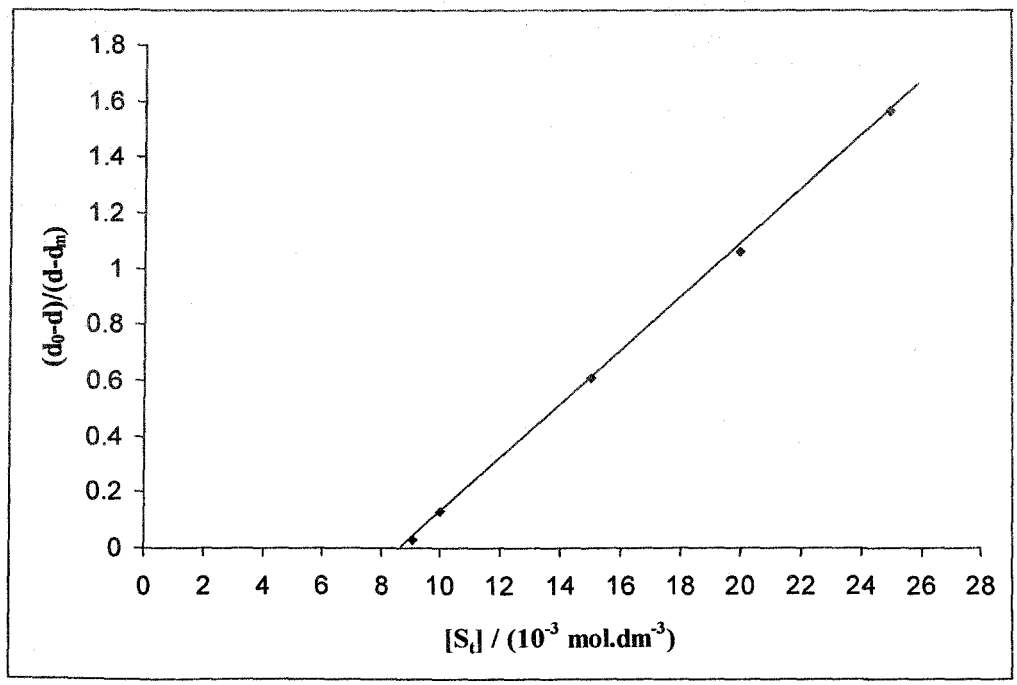

Figure 4.16 (d_0-d)/(d-d_m) vs. concentration (SDS) for Methylene Blue-SDS system having dye concentration 1.17 x 10^{-5}(M) at 303K.

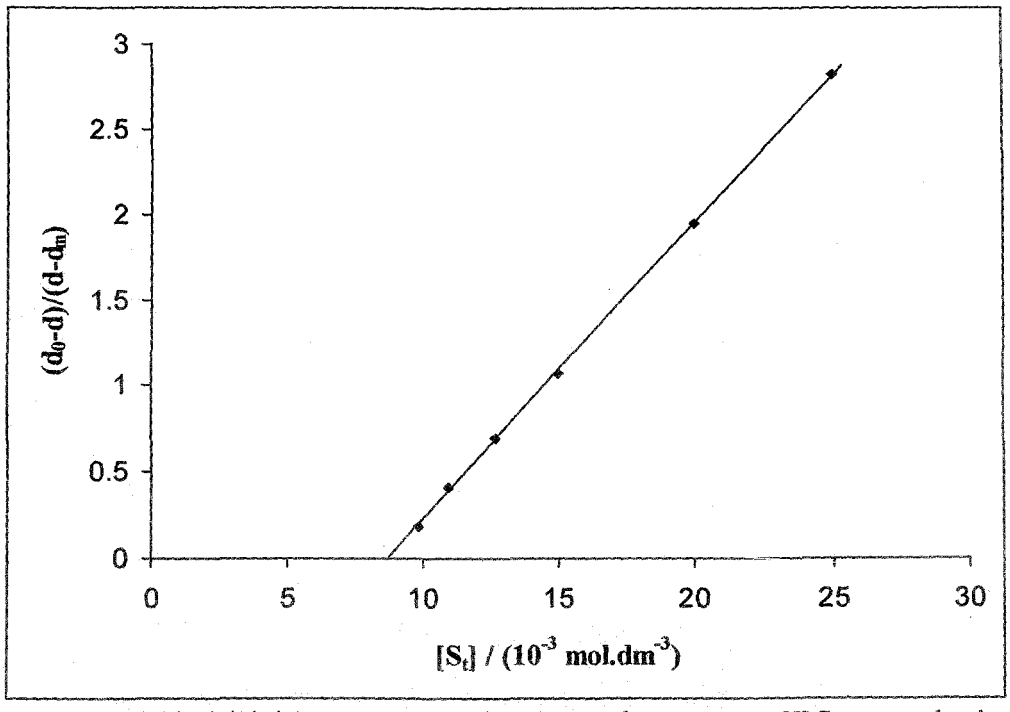

Figure 4.17 $(d_0-d)/(d-d_m)$ vs. concentration (SDS) for Azure C-SDS system having dye concentration 1.50 x 10^{-5}(M) at 303K.

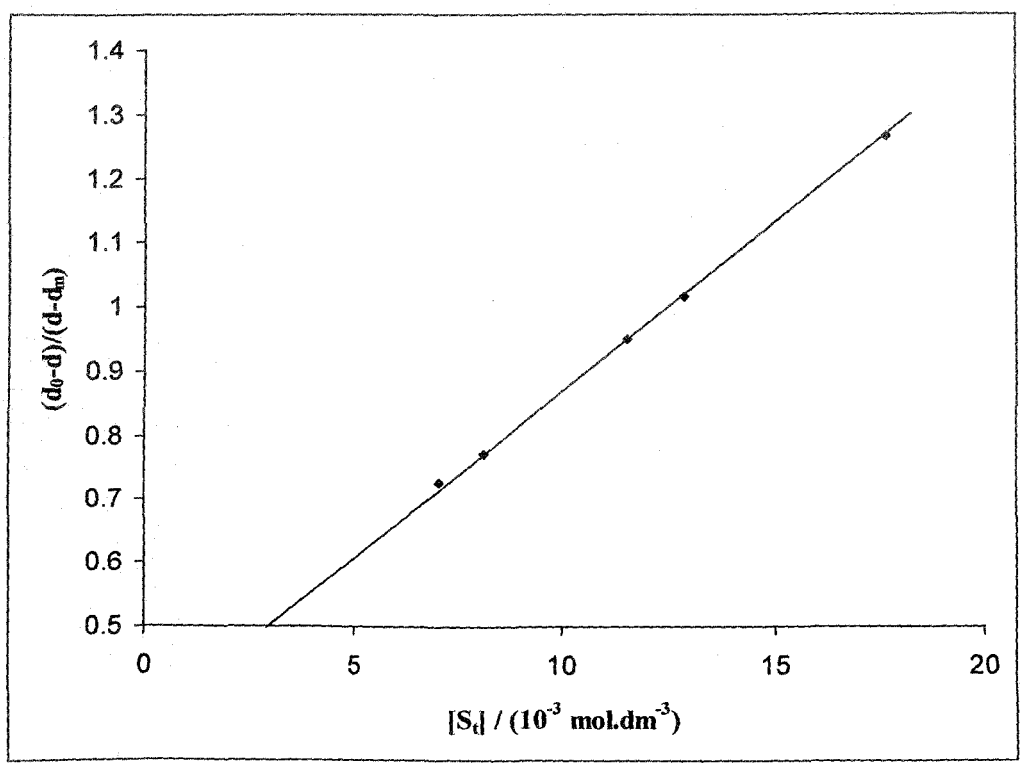

Figure 4.18 $(d_0-d)/(d-d_m)$ vs. concentration (AOT) for Azure B-AOT system having dye concentration 1.20 x 10^{-5}(M) at 303K.

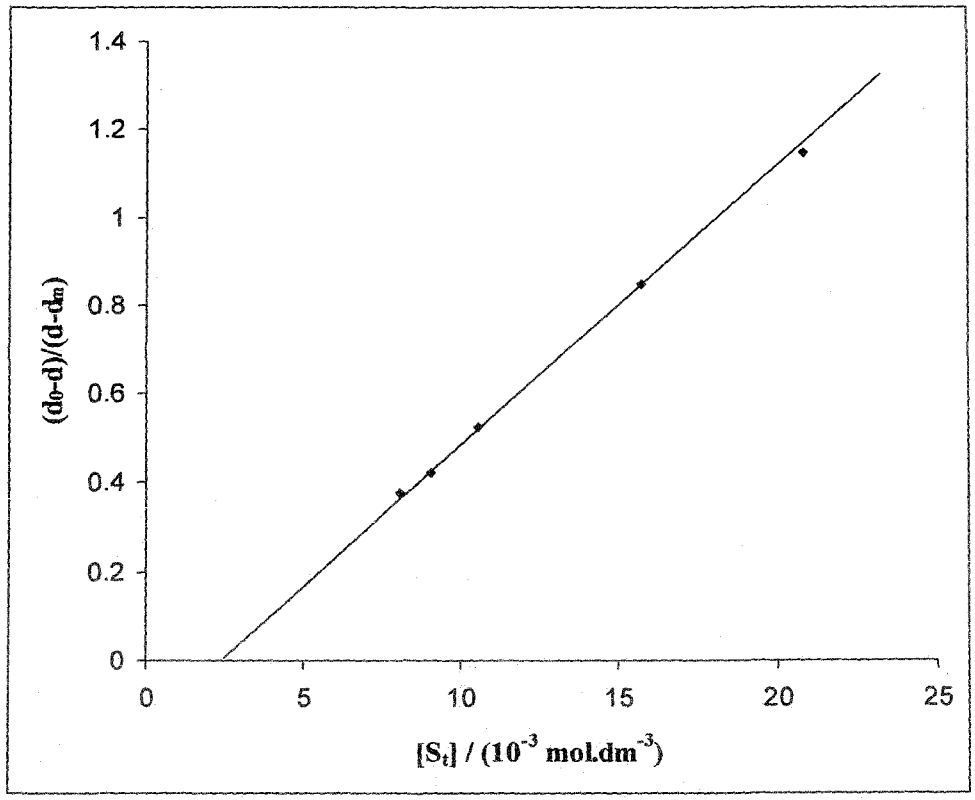

Figure 4.19 $(d_0-d)/(d-d_m)$ vs. concentration (AOT) for Azure A-AOT system having dye concentration 2.10 x 10^{-5}(M) at 303K.

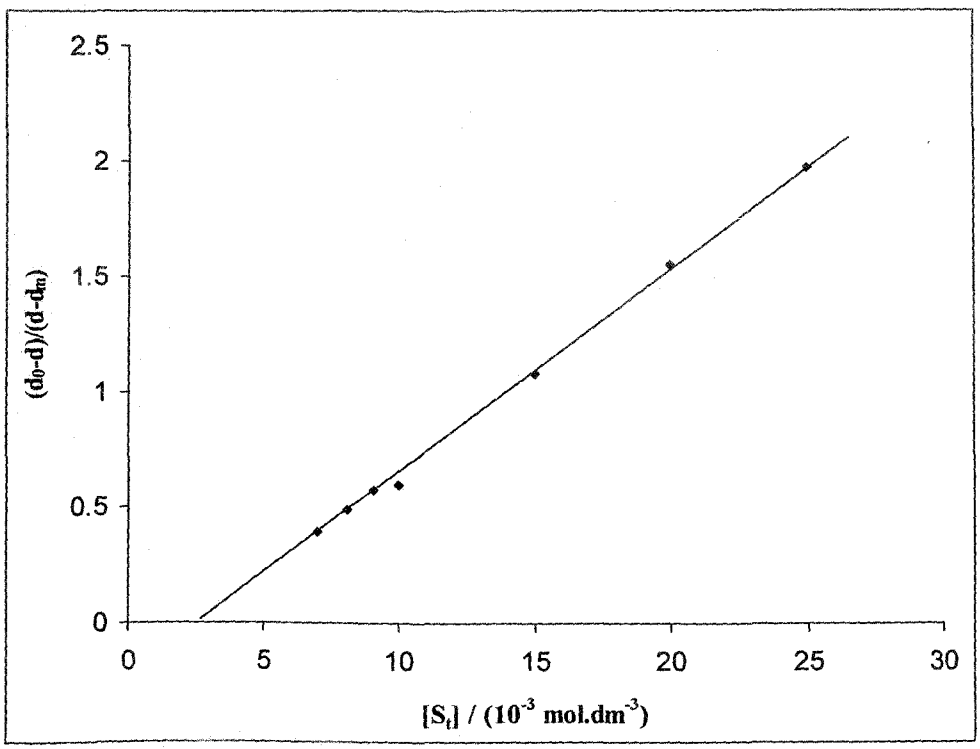

Figure 4.20 $(d_0-d)/(d-d_m)$ vs. concentration (AOT) for Thionine-AOT system having dye concentration 1.50 x 10^{-5}(M) at 303K.

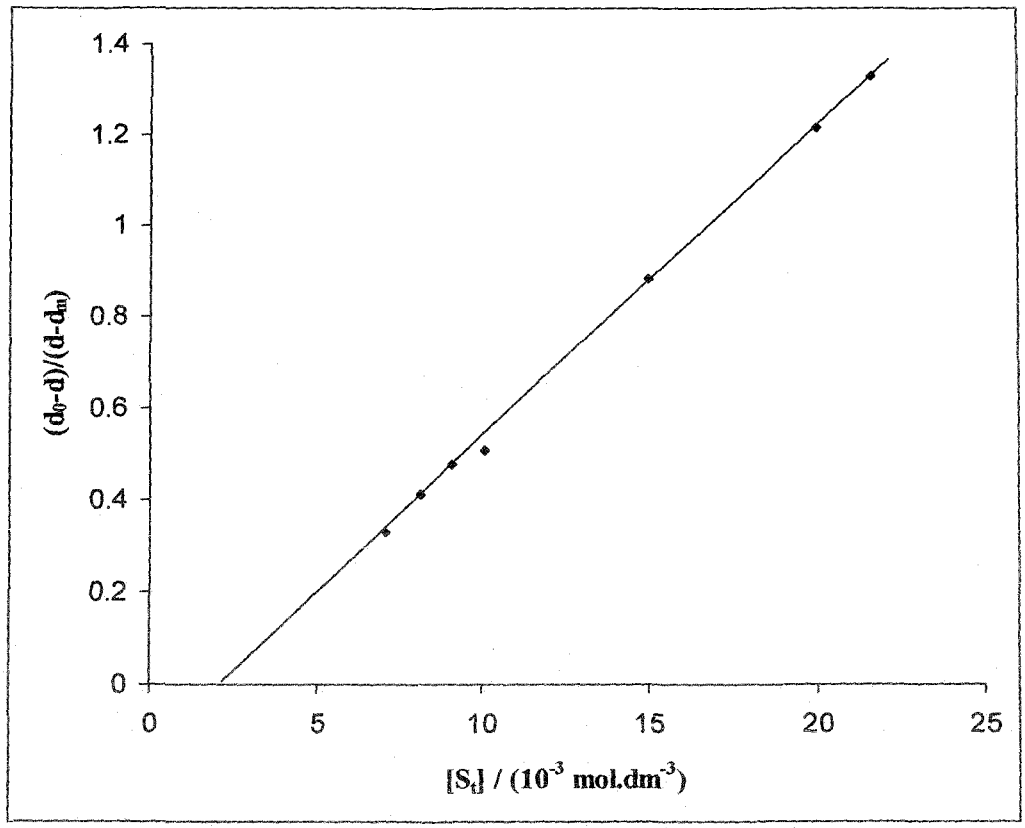

Figure 4.21 $(d_0-d)/(d-d_m)$ vs. concentration (AOT) for Azure C-AOT system having dye concentration 1.24 x 10^{-5}(M) at 303K.

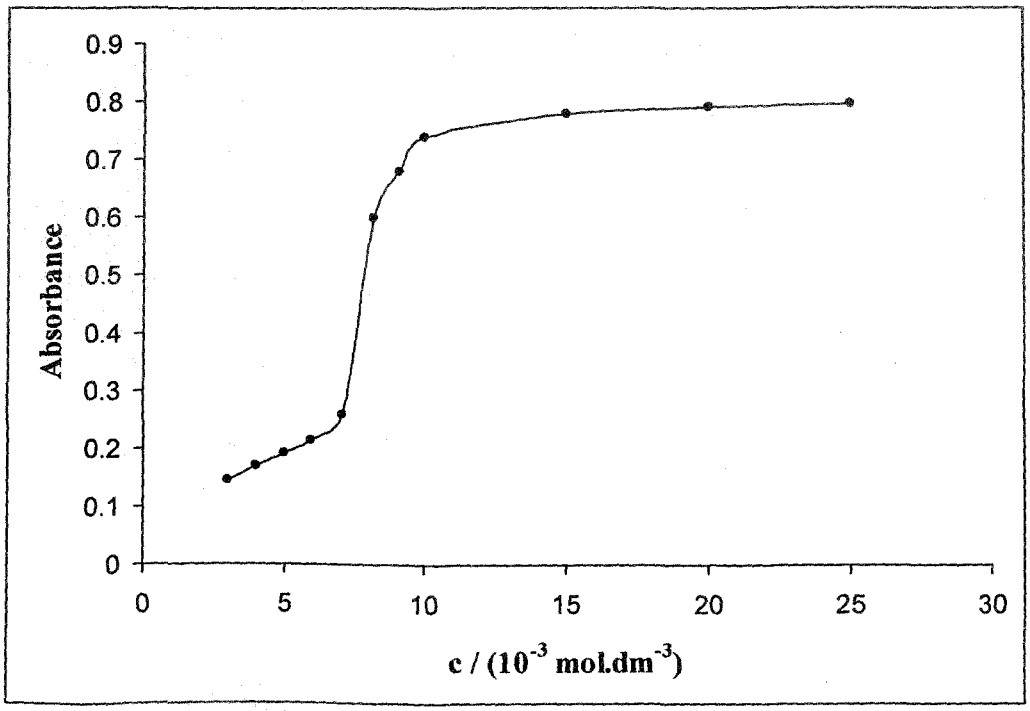

Figure 4.22 Absorbance (λ = 600 nm) vs. concentration (SDS) for Thionine-SDS system with the dye concentration 1.50 x 10^{-5}(M) at 303K.

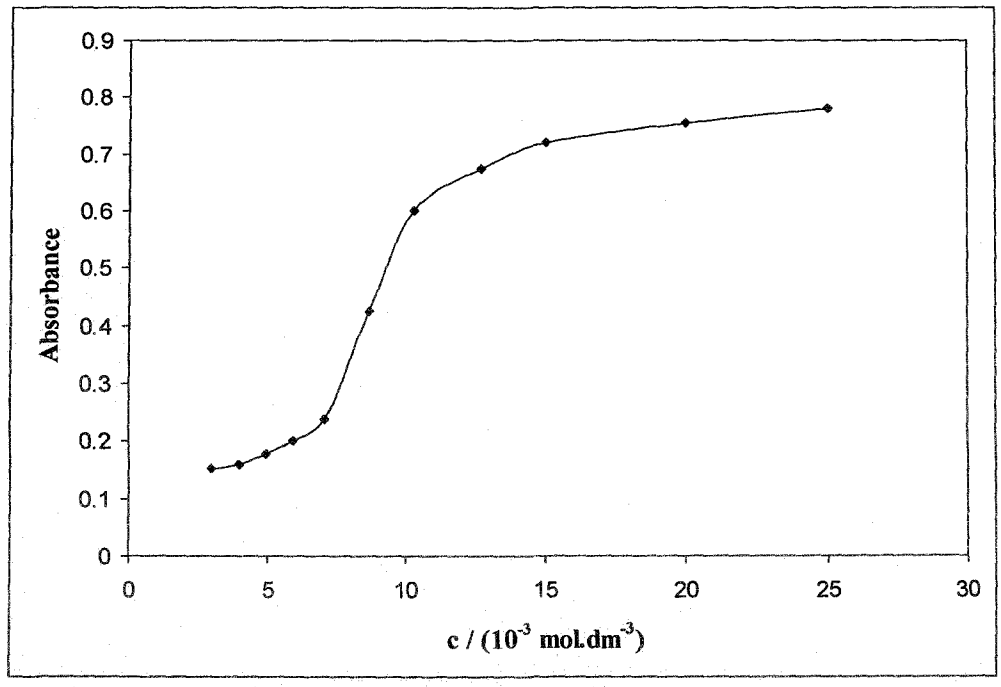

Figure 4.23 Absorbance (λ = 645 nm) vs. concentration (SDS) for Azure B-SDS system having dye concentration 1.20 x 10^{-5}(M) at 303K.

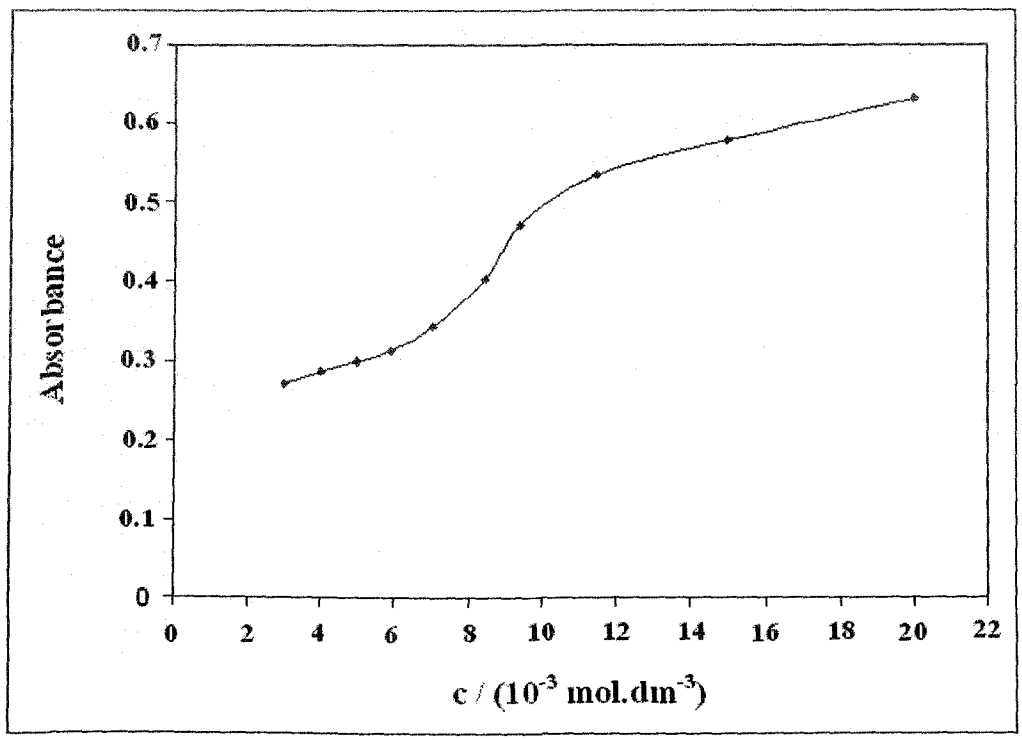

Figure 4.24 Absorbance (λ = 634 nm) vs. concentration (SDS) for Azure A-SDS system having dye concentration 2.10 x 10^{-5}(M) at 303K.

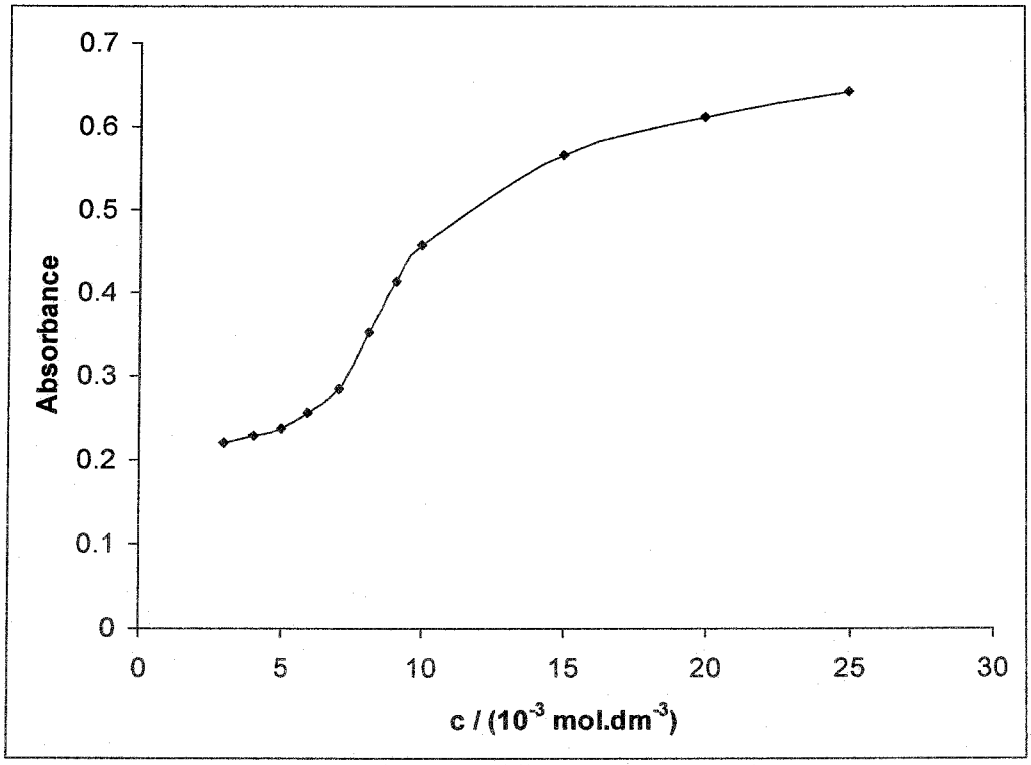

Figure 4.25 Absorbance (λ = 660 nm) vs. concentration (SDS) for Methylene Blue-SDS system having dye concentration 1.17 x 10^{-5}(M) at 303K.

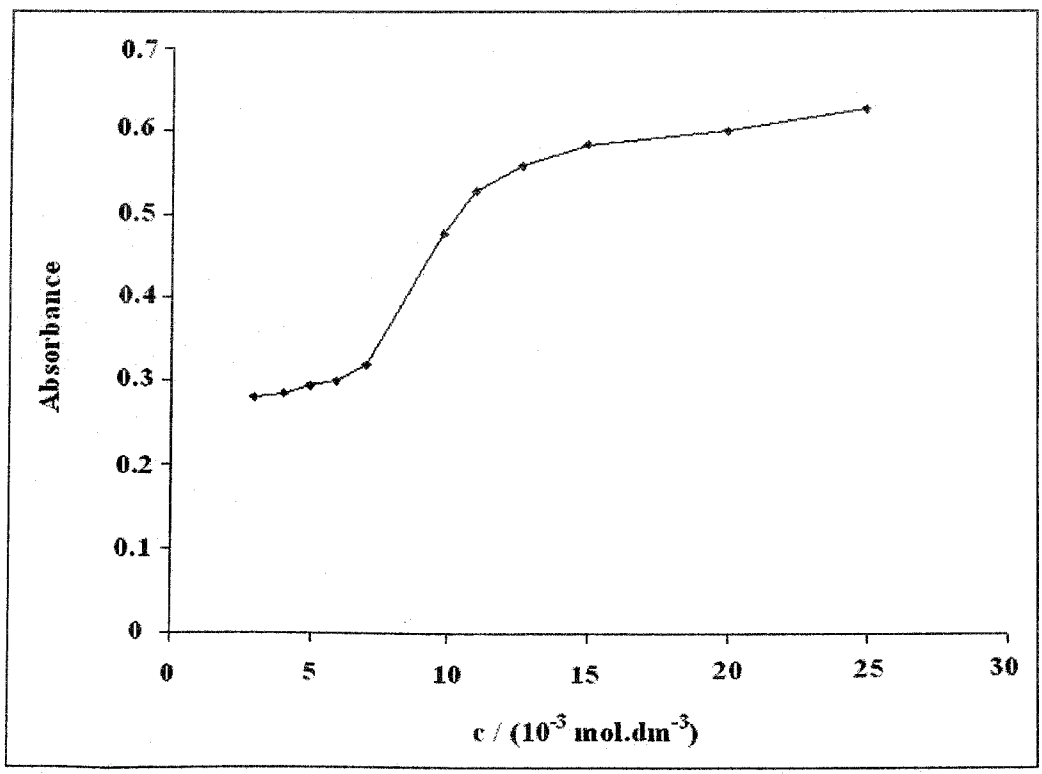

Figure 4.26 Absorbance (λ = 620 nm) vs. concentration (SDS) for Azure C-SDS system having dye concentration 1.24 x 10^{-5}(M) at 303K.

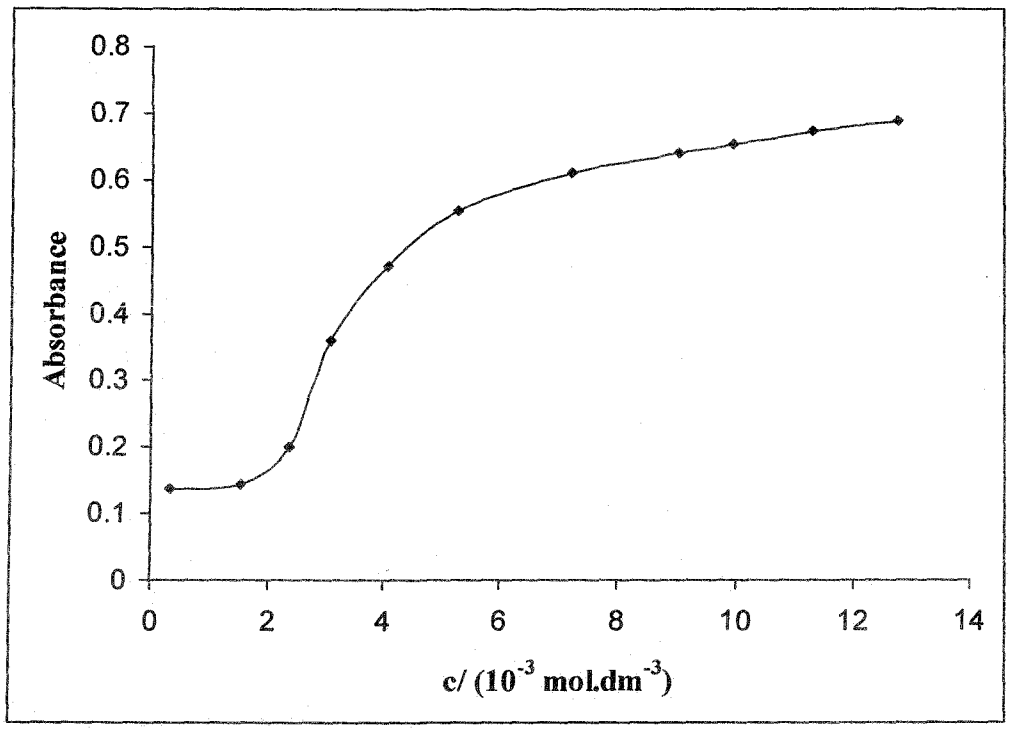

Figure 4.27 Absorbance (λ = 646 nm) vs. concentration (AOT) for Azure B-AOT system having dye concentration 1.20x 10^{-5}(M) at 303K.

inflexion points of these plots are shown in Table 4.2 in the brackets against the corresponding cmc values measured from the plot of equation 4.20. The cmc values obtained by the present method are slightly different from those obtained by other methods as shown in chapter 3. However, it should be noted that premicellar interaction between dye molecules and the surfactant unimers must affect the experimental cmc as determined above and this has already been discussed.

The free energy change, ΔG^0 for the dye-surfactant interaction is determined from the thermodynamic relation, $\Delta G^0 = - RTlnK_{ass}$. It was previously reported that K_{ass} was dependent on the pH, therefore in the present study pH is mentained constant throughout. Measured values of cmc, K_{ass} and ΔG^0 for different dye-surfactant systems are summarized in Table 4.2. Though García-Río et al. [2] claimed exactly same value of cmc of SDS by UV-vis spectrophotometry with crystal violet (CV), as compared other standard methods, it should be noted that apart from the submicellar dye-surfactant interaction the charged dye particle may also change the microenvironment of micellar pseudo-phase resulting in the slight modification of cmc value. The association constants for each pair of dye-surfactant system shows a general trend. It has been observed from Table 4.2 that thionine stacked most strongly with each of the two surfactants followed by other dyes in the order AzC> AzA> AzB >MB. It suggests that the dye-surfactant coulombic interaction between the charged part of the dye molecule and the ionic head of the amphiphile plays a key role in the interaction at the postmicellar concentration of surfactant along with the hydrophobic interaction between the micellar core and the aromatic moiety of the dye. The large negative ΔG^0 values also support the view in favour of the above electrostatic interaction.

4.3.3 Studies on Monomer-dimer Equilibrium of Progressively Alkylated Thiazine Dyes in Aqueous and Microemulsion Media

As discussed in the experimental section the microemulsions are prepared with a cationic surfactant, cetylpyridinium bromide (CPB) in a 1:1 (volume/volume) mixture of n-heptane and chloroform by mixing appropriate amount of water. The reason for choosing the particular microemulsion for the present study is two fold. Firstly, the cationic surfactant like CPB, restricts the possibility of the entry of cationic thiazine dyes in the interfacial region of the microemulsion and ensures the location

in the water-pools. Secondly, in the presence of dye molecules above microemulsion offers a very stable and well-behaved system for studying monomer-dimer equilibrium in water-pools of microemulsion. Further, it can be said that in microemulsion the compartmentalized water dipoles must be firmly associated with the positively charged inner surface of the aggregate. Dyes used for the present study are highly soluble in water but completely insoluble in both chloroform and n-heptane. When dissolved in microemulsion, optically clear solutions are obtained. It is also obvious that due to strong columbic repulsion between the dye molecules and charged monolayer of the interior of microemulsion, the dyes essentially exist in the water-pool.

The representative spectra of five thiazine dyes in microemulsion (recorded in 1 mm path length cell) are shown in Figure 4.28 – 4.32. As expected, the spectra show considerable changes with the variation of dye concentrations in microemulsion water-pool due to the presence of aggregation equilibrium. With the change of concentration of dye in the compartmentalized water for a particular system the dimension of the pool (ω) also change to some extent. It is, however, assumed that in the present experiments, small variation of ω value (22.0 – 38.3) does not affect the microenvironment of the pool to any great extent. Relatively large water-pools of the microemulsion offer an ideal media (size variation is small) to study the aggregation equilibria of dyes in microemulsion media where confinement of dye molecules in the pool is ensured by electrostatic interactions between dye molecules and the interface as already pointed out. To avoid the possibility of formation of trimer and higher aggregates the concentrations are kept within a narrow range (1.35×10^{-4} to 7.28×10^{-4}) for each dye.

Depending upon the pH of the system the thiazine dyes can exists in two forms, viz. Th^+, AzA^+, AzB^+, AzC^+, MB^+ and their corresponding protonated forms in aqueous solution [195]. Different researchers have also calculated the equilibrium constants of acid and basic form of dyes [195-197]. However, when these dyes are dissolved in water the pH of the solution remains within a small range 6.8 ± 0.5 where the dyes exist as their cationic form. In the present investigation spectra of each dye (Figure 4.28 – 4.32) show a clear isobestic point when recorded as a function of concentration. This supports the existence of two chemical species in each of dye system viz., monomer and the dimer species. Thionine shows an isobestic point at

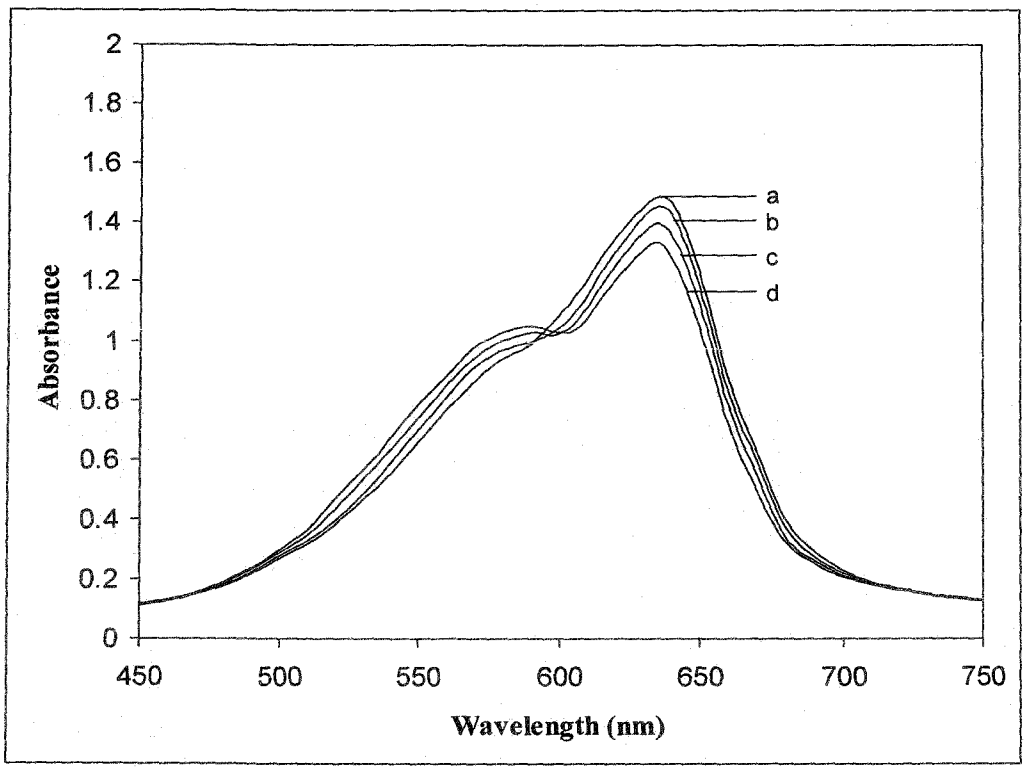

Figure 4.28 Absorption spectra of Azure A [(a) 5.34 x 10^{-4}, (b) 5.75 x 10^{-4}, (c) 6.03 x 10^{-4}, (d) 6.56 x 10^{-4} M] in microemulsion (water-in-oil) at 303K.

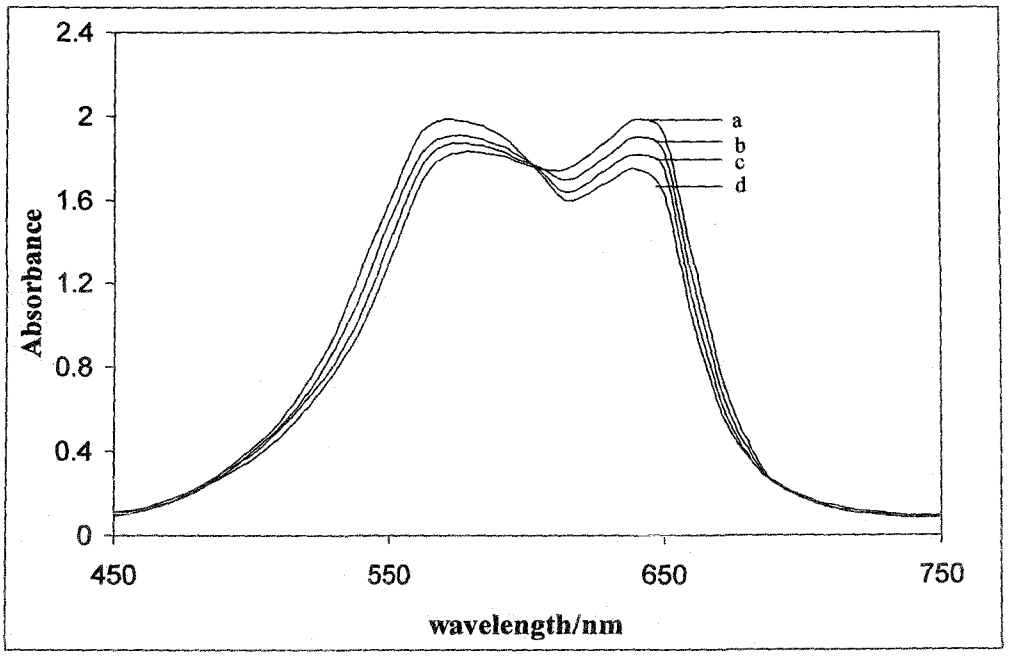

Figure 4.29 Absorption spectra of Azure B [(a) 5.00 x 10^{-4}, (b) 5.65 x 10^{-4}, (c) 6.13 x 10^{-4}, (d) 6.70 x 10^{-4} M] in microemulsion (water-in-oil) at 303K.

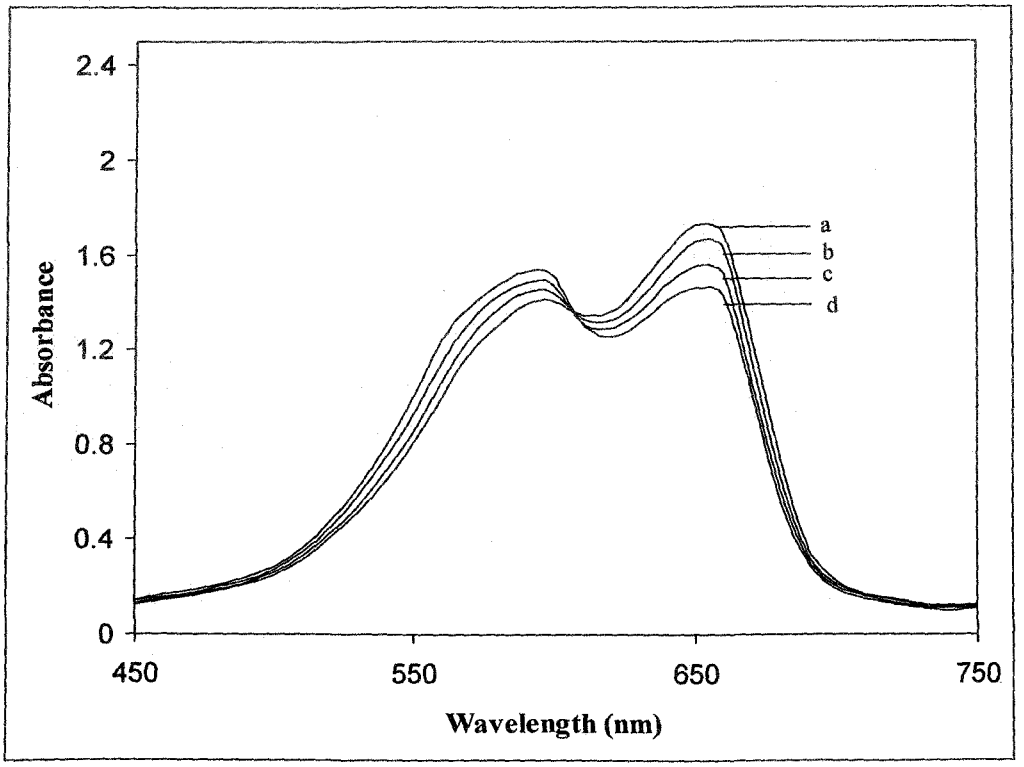

Figure 4.30 Absorption spectra of Methylene Blue [(a) 6.20 x 10^{-4}, (b) 6.55 x 10^{-4}, (c) 6.90 x 10^{-4}, (d) 7.23 x 10^{-4} M] in microemulsion (water-in-oil) at 303K.

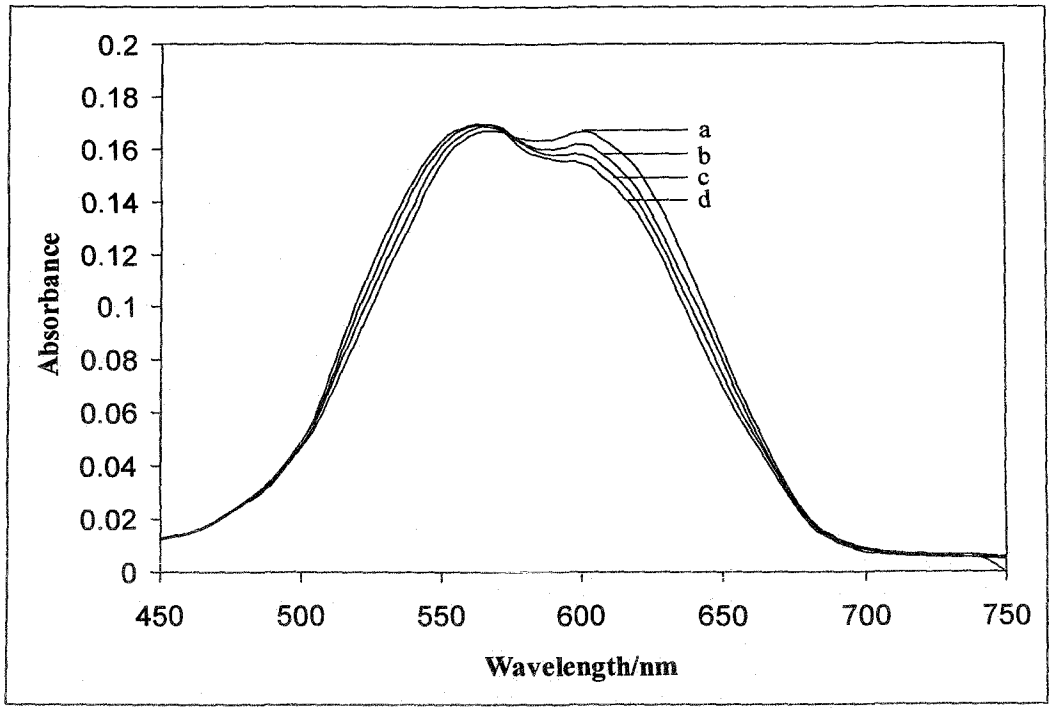

Figure 4.31 Absorption spectra of Thionine [(a) 1.35 x 10^{-4}, (b) 1.67 x 10^{-4}, (c) 1.90 x 10^{-4}, (d) 2.56 x 10^{-4} M] with different sizes of microemulsion (water-in-oil) at 303K

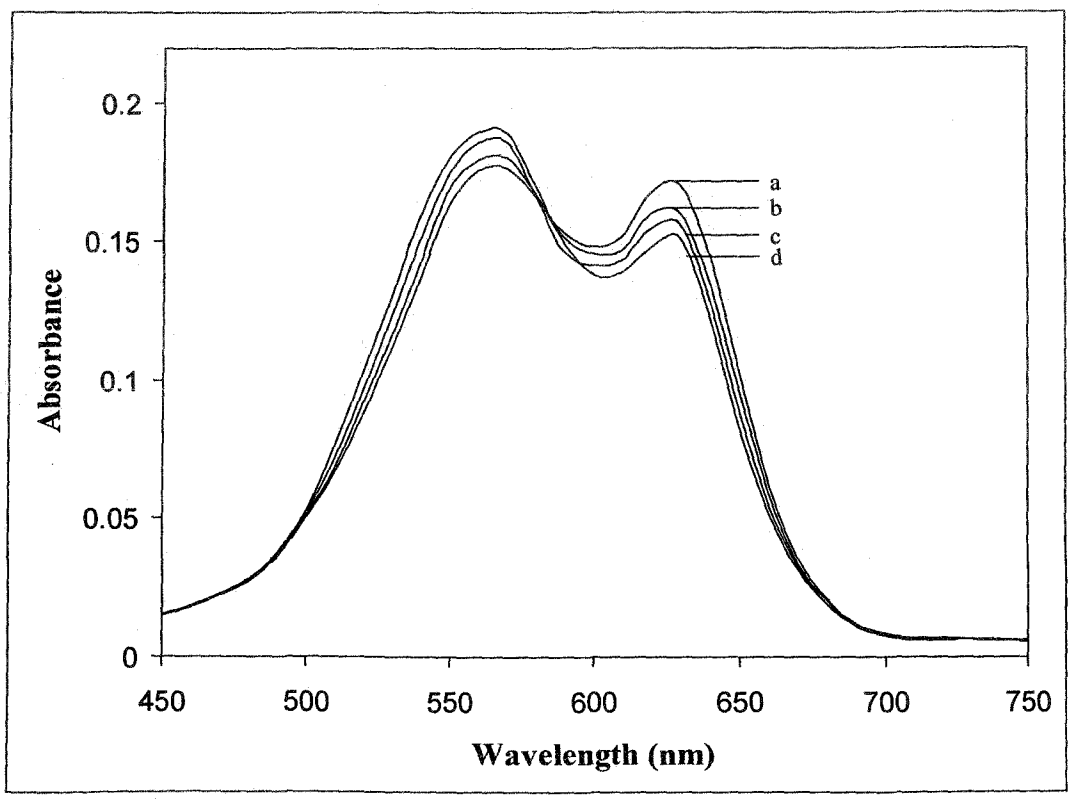

Figure 4.32 Absorption spectra of Azure C [(a) 5.45 x 10^{-4}, (b) 5.63 x 10^{-4}, (c) 5.90 x 10^{-4}, (d) 6.32 x 10^{-4} M] with different sizes of microemulsion (water-in-oil) at 303K

576 nm and the other dyes, viz, AzA, AzB, AzC and MB display their isobestic points at 600, 605, 585 and 606 nm respectively. These two species viz., monomer and the dimer species correspond to those appeared in the aqueous phase also because the spectra obtained in present microemulsion system are apparently similar to those observed in the aqueous solution; the only difference is in their absorbance intensity.

The dimension of microemulsions bearing water-pools of the microemulsion depends upon the [water]/[CPB] mole ratio, ω. For the present systems, CPB is present at a fixed concentration of 0.1512M with appropriate amount of water to prepare microemulsions such that ω may have values within a range of 22.0 to 38.3. For each dye, the spectra show an intense peak in similar wavelength as observed in case of pure dilute aqueous solution. It is well known that the compartmentalized water in microemulsion is much different in character compared to bulk water with respect to the physical nature, viz. polarity, viscosity, acidity etc. [200,201] due to its restricted mobility and very low dielectric constant at the interface. It has been observed that in the absence of the complication of highly polarisable groups such as ester, amides, nitriles and aromatic moieties in the solvent, the spectra of dyes may be correlated directly with the dielectric constant of the surrounding medium [202].

Interpretation of measurements on micellar solutions is largely predicted on the oil-drop picture of a micelle, with a hydrocarbon-like interior of local dielectric constant ~2. There must be a transition between that small value and that of the bulk solvent, approximately 80, as the head group region is traversed. Indeed a radically varying dielectric constant, highly dependant upon position and microenvironment is anticipated, and this is suggested by the discrepancies between the results of various types of solubilized probe studies on identical micellar solution. The value of dielectric constant also shows temperature dependency for every surfactant. In case of CPB the dielectric constant at 303K was measured as 24.0 at the micelle-water interface [203].

However, it was observed that in microemulsion at low water levels ($\omega < 7$-10), the radii of inner water-pools are typically 0.8-1.6 nm, and most of the water molecules are utilized to form the hydration sphere around the polar surfactant head groups and counter-ions [204]. Beyond $\omega > 10$, the radii of the inner water-pools increase substantially and the properties of the inner water-pool tend towards those of ordinary bulk water. However, for the present purpose as the concentration of dye

increases, the peak that supports the presence of monomer, shows lower absorbance while another peak (supports the existence of aggregates) increases. The dimerization constant of monomer-dimer equilibrium for each system is calculated by using the technique of Sabaté et al. [205]

The monomer-dimer equilibrium of dye molecules in aqueous or microemulsion media may be represented as follows:

$$M + M \rightleftharpoons D \tag{4.21}$$

where M and D stands for monomer and the dimer respectively. This equilibrium may be described by the dimerisation constant K_D, which is given by the ratio between the molar concentrations of dimers, C_D, and the monomers, C_M, at equilibrium at a constant temperature and can be expressed as

$$K_D = \frac{C_D}{C_M^{\,2}} \tag{4.22}$$

Thus, it is necessary to know the value of C_D and C_M, which can be determined from the molar absorptivity obtained from the spectral bands of monomeric and dimeric species.

The total absorbance (A_λ) of a dye solution at a given wavelength λ is

$$A_\lambda = \varepsilon_M(\lambda).C_M + \varepsilon_D(\lambda).C_D \tag{4.23}$$

where ε_M and ε_D represent the molar absorption coefficients of monomeric and dimeric species respectively of any band at a wavelength λ.

Considering the mass balance of dye in the dispersed volume the monomer and dimer concentrations can be calculated from equation 4.22

$$C = C_M + 2C_D \tag{4.24}$$

where C is the total analytical concentration of dye.

Replacing C_M and C_D with the total concentration term, equation 4.23 can be rewritten as:

$$A_\lambda = \varepsilon_D(\lambda)\left(\frac{C}{2} - \frac{-1 \pm \sqrt{1+8CK_D}}{8K_D}\right) + \varepsilon_M(\lambda)\left(\frac{-1 \pm \sqrt{1+8CK_D}}{4K_D}\right) \tag{4.25}$$

Now, from the plot of the measured absorbances as a function of dye concentration at any wavelength, the molar absorption coefficient of monomers, $\varepsilon_M(\lambda)$ and dimers, $\varepsilon_D(\lambda)$ along with the dimerisation constant K_d, are calculated using a nonlinear least-square fitting routine (Microsoft Excel Solver) [205]. The resolved monomer and dimer spectra are drawn for the corresponding values of $\varepsilon_M(\lambda)$ and $\varepsilon_D(\lambda)$ as a function of λ.

Spectral features of progressively alkylated thiazine dyes applied in the present study in aqueous medium were reported by previous researchers [179,206]. The deconvoluted monomer and dimer absorption spectra, calculated using the equation 4.25, of all the five dyes both in aqueous and in microemulsion, are shown in Figures 4.33 - 4.42. Some charecterestic features of monomer resolved spectra in aqueous and microemulsion media are listed in Tables 4.3 and 4.5 respectively. The resolved dimer spectra are, however composed of two bands of monomer with their maxima at greater and smaller energy than the monomer maximum respectively [173]. Some of the characteristics of dimer spectra along with their respective dimerization constants are listed in Table 4.4 and 4.6. If we compare the charecterestics of monomer spectra in aqueous media with that of microemulsion media it is seen that the absorption peak (λ_{max}) are more or less remain unaltered except thionine and azure C. The λ_{max} of visible absorption spectra of thionine and azure C are red shifted through 7.0 and 5.0 nm respectively. However, the molar absorptivities (ε's) of resolved monomer spectra have displayed a very great change for all the five thiazine dyes. In the water-pools of microemulsion the molar absorptivities of the monomer are decreased to a great extent relative to bulk water.

Under the present experimental conditions (303K temperature), in aqueous medium, the K_d values obtained, are 1.761×10^3, 2.350×10^3, 3.381×10^3, 6.258×10^3 and 3.658×10^3 lit/mol for Th, AzC, AzA, AzB and MB respectively in aqueous medium. The K_d values indicate that the increased hydrophobicity in the dye molecule upon methylation increases dimerization tendency, which in turn minimizes the contact area of the dyes with water. In case of methylene blue, steric hindrance is probably very high and the dimerization constant is less. In microemulsion media, on the other hand, the K_d values are 2.214×10^3, 1.760×10^3,

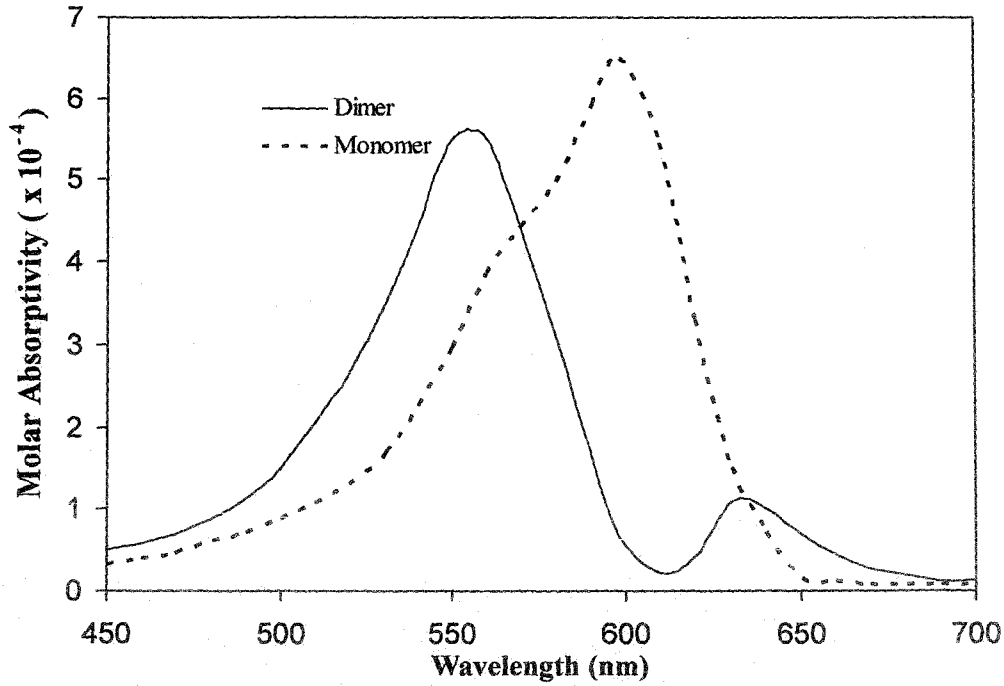

Figure 4.33 Absorption spectra of Thionine in water

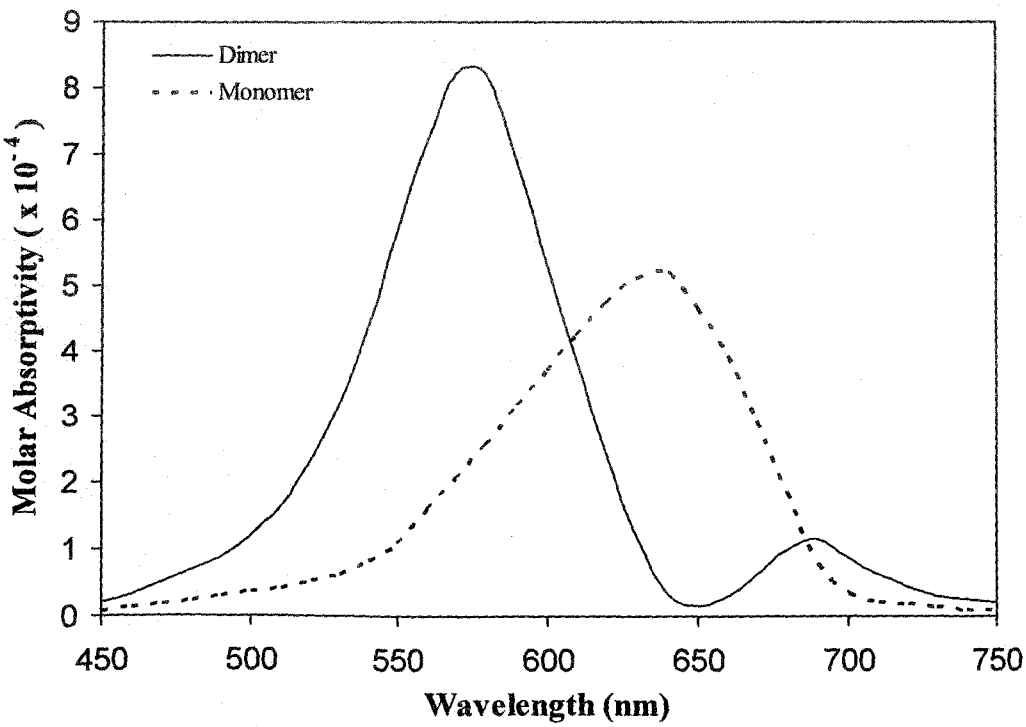

Figure 4.34 Absorption spectra of Azure A in water

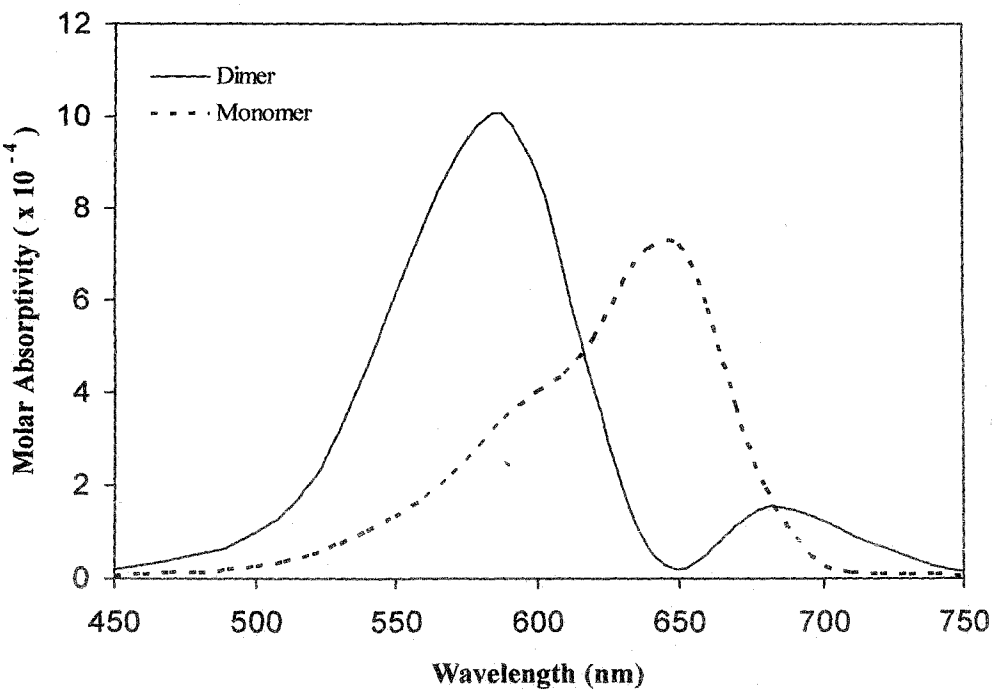

Figure 4.35 Absorption spectra of Azure B in water

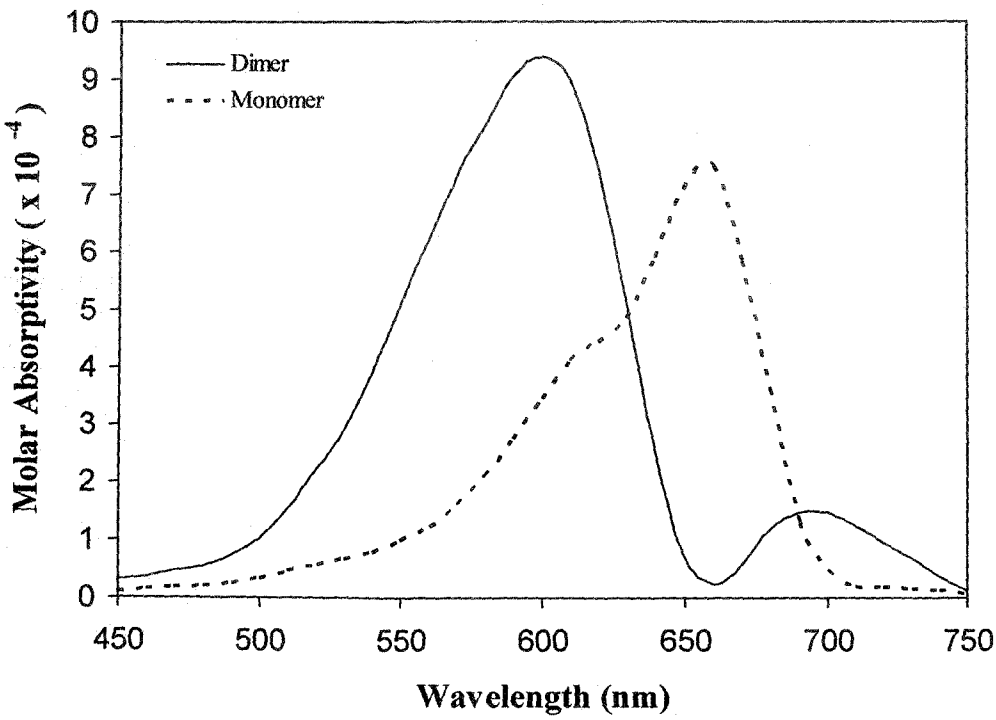

Figure 4.36 Absorption spectra of Methylene Blue in water

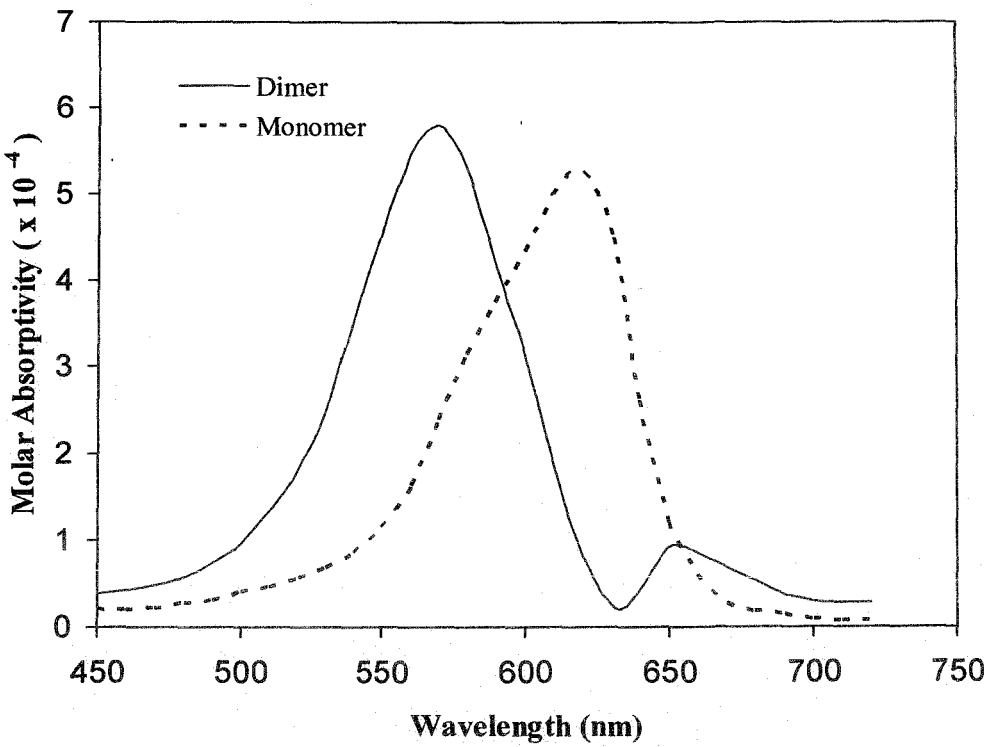

Figure 4.37 Absorption spectra of Azure C in water

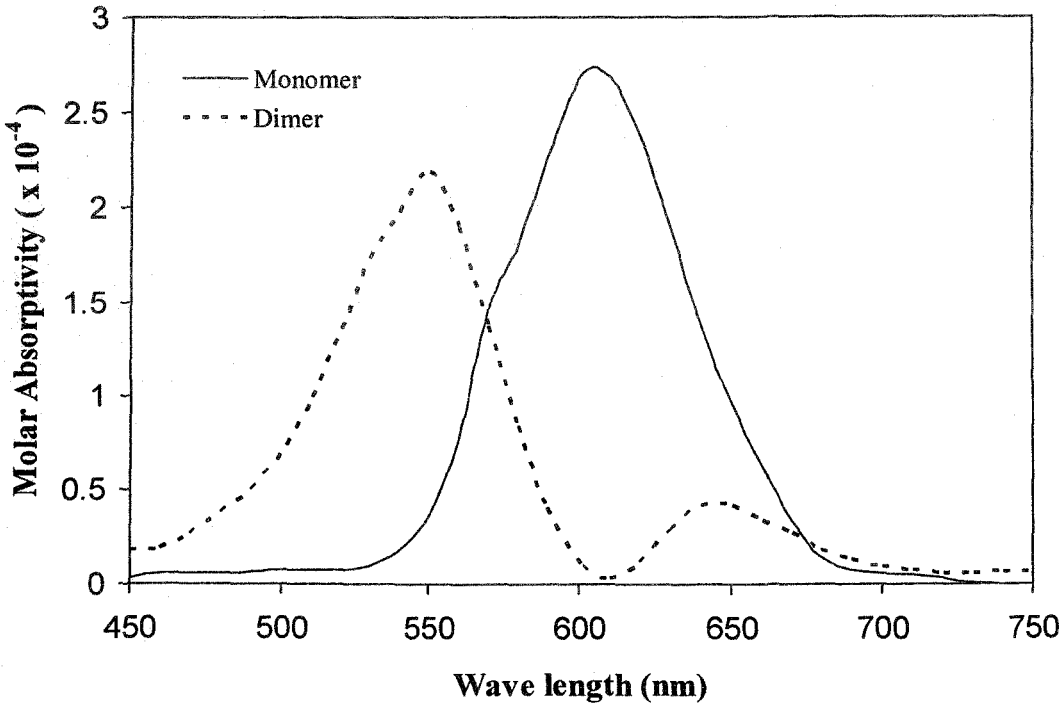

Figure 4.38 Absorption spectra of Thionine in microemulsion

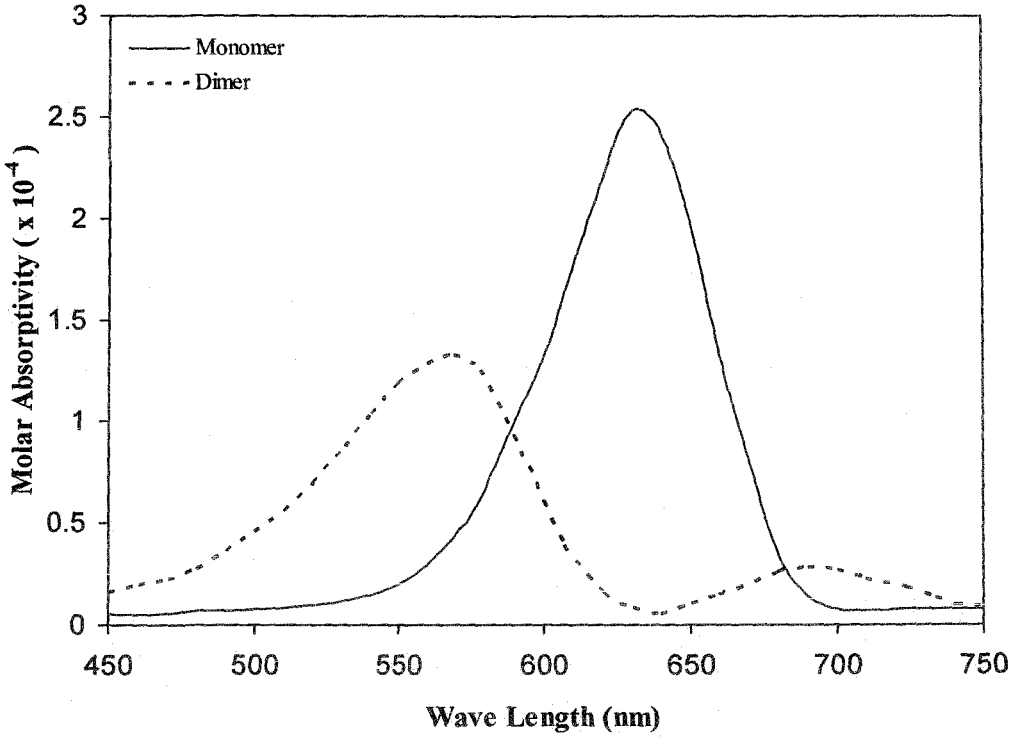

Figure 4.39 Absorption spectra of Azure A in microemulsion

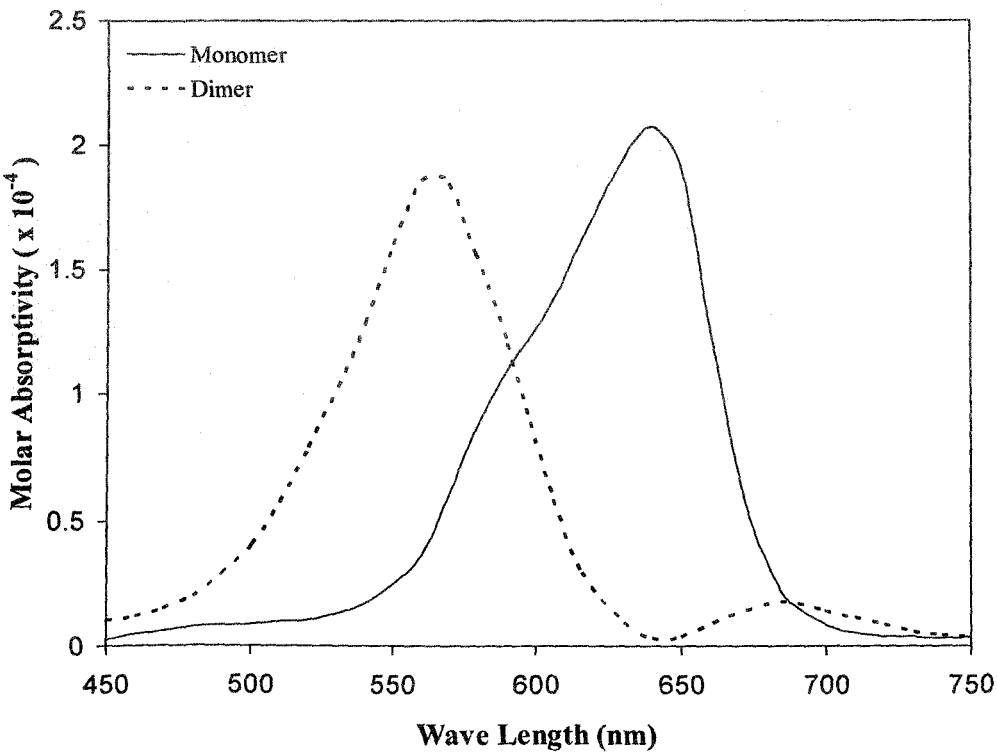

Figure 4.40 Absorption spectra of Azure B in microemulsion

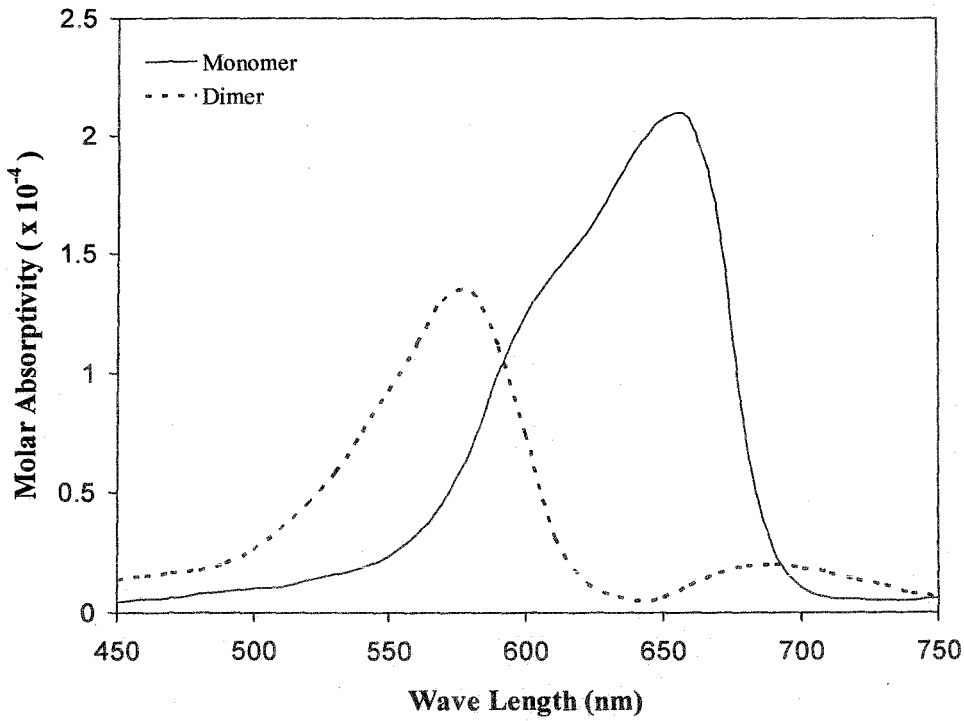

Figure 4.41 Absorption spectra of Methylene Blue in microemulsion

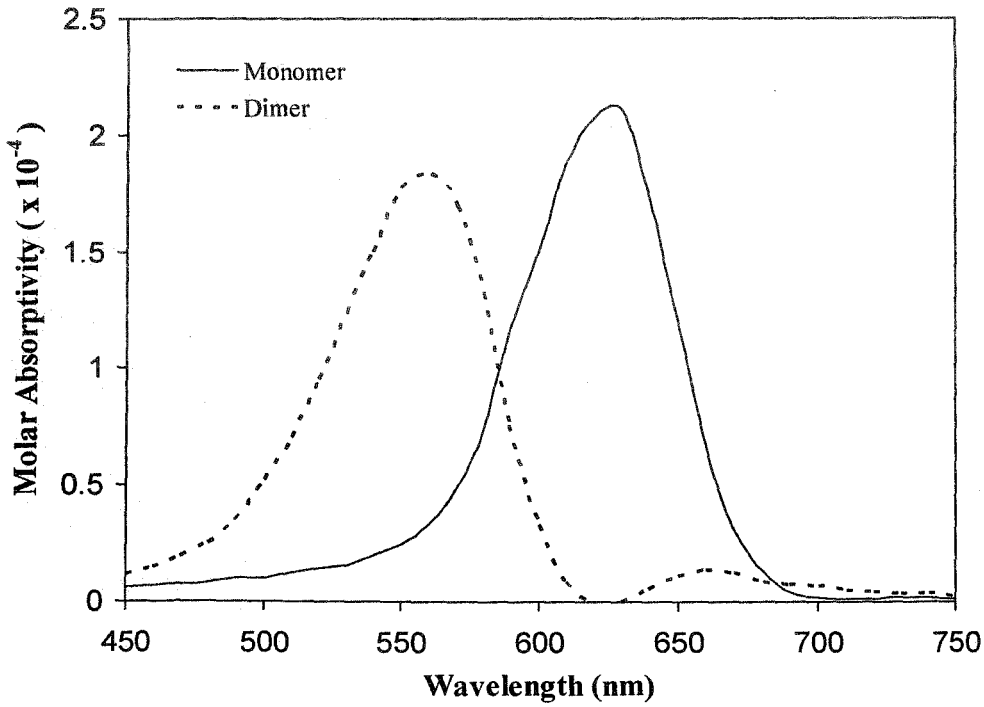

Figure 4.42 Absorption spectra of Azure C in microemulsion

Table 4.4

Dimerizatin parameters (K_d, ΔG^0) and some characteristics of dimer spectra of the dyes in aqueous solution

Dye	$K_d \times 10^{-3}$ (lit.mol^{-1})	$-\Delta G^0$ (kJ.mol^{-1})	λ_1(nm)	λ_2(nm)	$\varepsilon_1 \times 10^{-4}$	$\varepsilon_2 \times 10^{-4}$
Thionine	1.761	18.83	555	630	5.64	1.11
Azure C	2.350	19.56	571	651	5.75	0.96
Azure A	3.381	20.47	575	687	8.17	1.16
Azure B	6.258	22.02	588	682	10.11	1.50
Methylene Blue	3.658	20.67	600	691	9.27	1.03

Table 4.3

Some characteristics of monomer spectra of the dyes in aqueous solution

	Thionine	Azure C	Azure A	Azure B	Methylene Blue
λ_{max}(nm)	598	620	634	646	661
$\varepsilon \times 10^{-4}$	6.16	4.96	5.18	6.90	7.20

Table 4.5

Some characteristics of monomer spectra of the dyes in microemulsion

	Thionine	Azure C	Azure A	Azure B	Methylene Blue
λ_{max}(nm)	605	625	634	646	661
$\varepsilon \times 10^{-4}$	2.71	0.71	2.54	2.07	2.10

3.504 x 10^3 and 4.112 x 10^3, 1.501 x 10^3 lit/mol for Th, AzC, AzA, AzB and MB respectively, which do not follow the regular trend like that in aqueous medium. It is therefore evident that along with the structure of the dye molecules, nature of the solvent along with the electrostatic interactions (repulsion) between the similarly charged dye molecules and the inner phase of microemulsion may also play important role on the strength of aggregation. The ΔG^0 for dimerization processes of five thiazine dyes are negative and do not differ very much upon progressive methyl substitution. As expected there is no general trend but in most cases, ΔG^0 displays slightly higher negative value on methylation in aqueous and micro-emulsion media.

Table 4.6

Dimerizatin parameters (K_d, ΔG^0) and some characteristics of dimer spectra of the dyes in microemulsion

Dye	$K_d \times 10^{-3}$ (lit.mol^{-1})	$-\Delta G^0$ (kJ.mol^{-1})	λ_1(nm)	λ_2(nm)	$\varepsilon_1 \times 10^{-4}$	$\varepsilon_2 \times 10^{-4}$
Thionine	2.214	19.40	550	640	2.18	0.41
Azure C	1.760	18.83	559	660	0.61	0.05
Azure A	3.504	20.56	570	690	1.33	0.28
Azure B	4.112	20.96	563	684	1.86	0.18
Methylene Blue	1.501	18.42	580	685	1.34	0.21

4.3.4 Analysis of Monomer Spectra in Aqueous and Microemulsion Media in terms of Vibronic Exciton Model

The monomer spectra of five thiazine dyes at 303K, as resolved from deconvolution calculations are shown in Figures 4.33 - 4.42. Monomers which are present in equilibrium with dimers in aqueous and microemulsion media have shown some striking features depending upon the medium. All the monomer spectra were analyzed in detail in terms of their vibronic bands in order to understand these features. In this analysis, it is assumed that the force constant of the ground and excited states are same and the vibronic transition can be described satisfactorily by a Gaussian band shape. The simplest physical model in dealing with a vibronic progression is that of a displaced harmonic oscillator with Gaussian bands of constant band width requiring five adjustable parameters. Background of the method of such an analysis is given below [208,209].

Molecules of many atoms posses a number of vibrational modes and their electronic transition may be accompanied by simultaneous changes in the vibrational quanta of various fundamentals. However, of the large number of possible "vibronic bands" only a few will occur with large probability, in general. Application of Born-Openheimer approximation and symmetry considerations show that an allowed electronic transition is dominated by totally symmetric vibrational progressions. For aromatic molecules the dominant totally symmetric vibration is the ring "breathing". Moreover, since vibrational spacings are of the order of 1000 cm^{-1}, the number of vibrationally excited molecules at room temperature is negligibly small. It follows

that an allowed electronic transition of large planner (aromatic) molecule in solution may be taken to consist of a single progression in absorption spectrum.

In the present investigation, the spectra of the five thiazine dye monomers have been analyzed in terms of their vibronic bands b_g adopting the following assumption.

(i) Only one fundamental vibrational mode need to be considered.

(ii) The difference in the force constants of the ground state and excited state oscillators may be disregarded;

(iii) The harmonic approximation applies;

(iv) The vibronic transition may be described satisfactorily by a Gaussion band shape;

The assumptions lead to single formulae for analyzing the absorption spectra of the monomers. The simplest physical model as described, to apply in dealing a vibronic progression is that of a displaced harmonic oscillator with Gaussian bands of constant band width requiring just five adjustable parameters in accordance with the formulae

$$I(\bar{\nu}) = I_{00}\sum_{m}\frac{X^m}{m!}\left(1+\frac{mV}{\bar{\nu}_{00}}\right)\exp\left\{\left(-\frac{4\ln 2}{b_g^2}\right)(\bar{\nu}-\bar{\nu}_{00}-mV)^2\right\} \qquad (4.26)$$

where , I_{00} is the intensity, $\bar{\nu}_{00}$ is the position of the (0,0) band, b_g is the Gaussion band width, X is the ratio of (1,0) to (0,0) band intensities and ν, the separation between the bands.

In general intensity distribution within an electronic band is represented well by Gaussion model. It is described accordingly, each vibronic band, (m,0) by the formula.

$$I_m(\bar{\nu}) = A_{m_1}\exp\left(-A_{m_3}\left(\bar{\nu}-A_{m_2}\right)^2\right) \qquad (4.27)$$

Where $I_m(\bar{\nu})$ is the band intensity at wave number $(\bar{\nu})$, Am_1 is the peak height, Am_2 is the position of the band centre, and $A_{m_3} = \ln 2/b_g^2$ with $2b_g$ as the

width of the band at half maximal intensity. The band width may be taken to be constant within a progression, so that one writes $A_{m_3} = A_3$

It is also assumed that the ground and excited states are adequately described as displaced harmonic oscillators with the same force constant which has the following consequences:

i) the band centers are separated by a constant distance V, so that

$$Am_2 = Ao_2 + mV$$

ii) the intensity of the band obey a modified poisson distribution.

In particular, in the case of Gaussian bands the integrated intensities are proportional to the peak height Am_1 and these are related to one another through a parameter X which, in turn, is a measure of the displacement of the normal co-ordinate of vibration(s)

$$Am_1 = \frac{X^m}{m!} A_{ol} \frac{A_{m2}}{A_{o2}} \tag{4.28}$$

The complete progression may thus be defined in terms of five molecular parameters x, v, Ao_1, Ao_2 and A_3 as follows

$$I(\bar{\nu}) = \sum_m \frac{X^m}{m!} Ao_1 \left(1 + \frac{mV}{Ao_2}\right) \exp\left\{-A_3^2(\bar{\nu} - Ao_2 - mV)^2\right\} \tag{4.29}$$

Replacing the symbols of the above parameters by more common symbols and after minor rearrangement the equation 4.29 takes the form of equation 4.26, as already described.

The $\varepsilon(\lambda)$ values recovered were plotted as a function of wave number $(1/\lambda)$ are shown in Figure 4.43 - 4.52 reproduce the experimental monomer spectra and the fitted monomer spectra ($\varepsilon(\lambda)$ vs. wave number, $1/\lambda$) of five thiazine dyes both in aqueous and microemulsion media. The spectra were fitted to the above 'five parameter Gaussion equation'. This has been done on a computer by means of a general non-linear curve-fitting program, KINFIT (updated) [209] properly adopted in the present system. Satisfactory results were obtained by truncating the summation after six bands. Results of fitting indicate that the present physical model describing a vibronic progression of a displaced harmonic oscillator with Gaussian

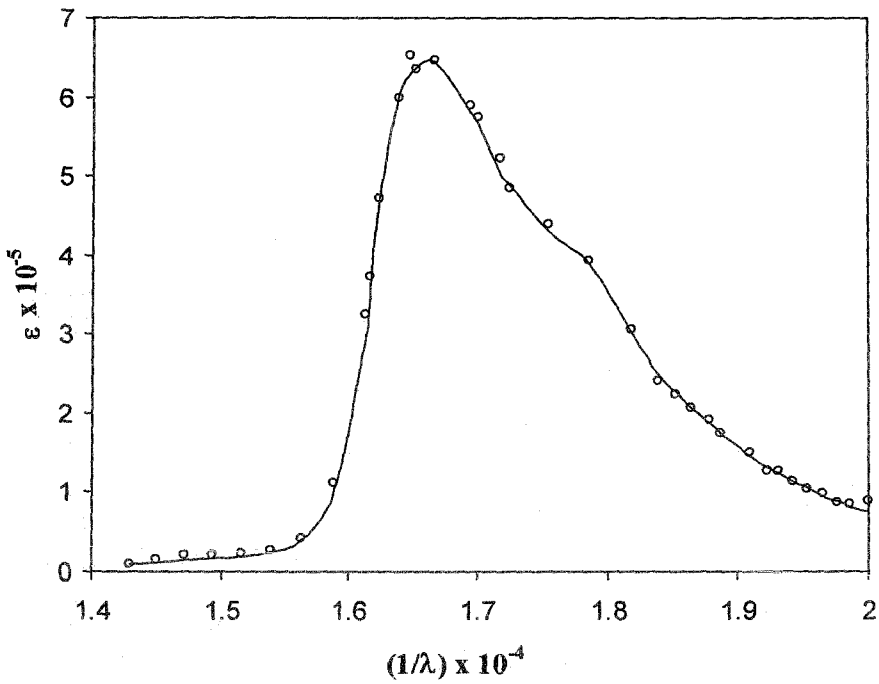

Figure 4.43 Absorption spectra of Thionine monomer in aqueous medium. Solid line represents the experimental spectrum and circles correspond to calculated points.

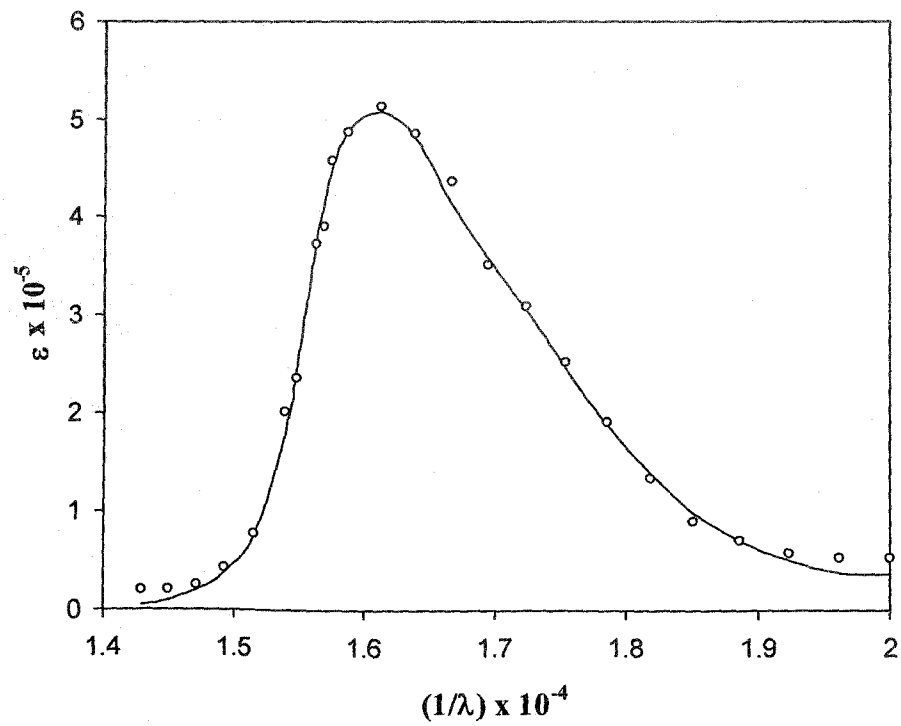

Figure 4.44 Absorption spectra of Azure C monomer in aqueous medium. Solid line represents the experimental spectrum and circles correspond to calculated points.

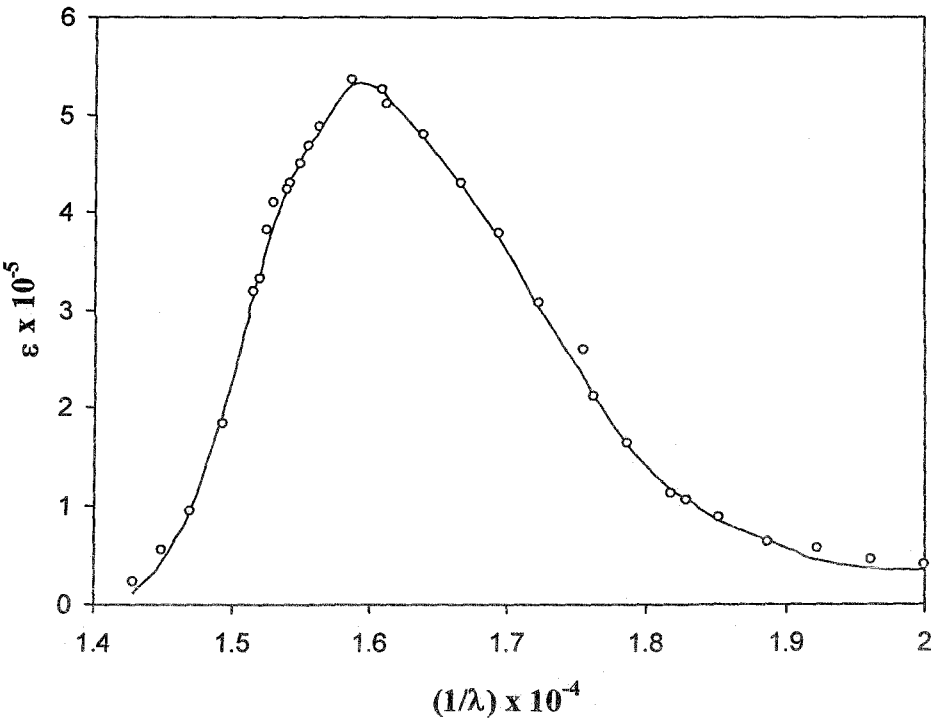

Figure 4.45 Absorption spectra of Azure A monomer in aqueous medium. Solid line represents the experimental spectrum and circles correspond to calculated points.

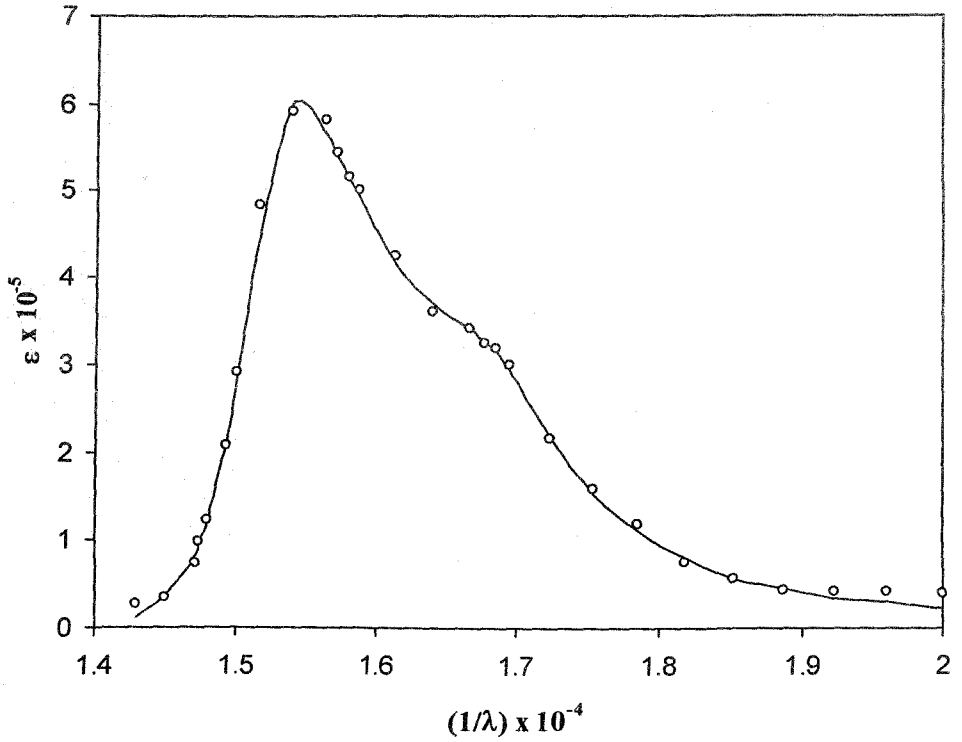

Figure 4.46 Absorption spectra of Azure B monomer in aqueous medium. Solid line represents the experimental spectrum and circles correspond to calculated points.

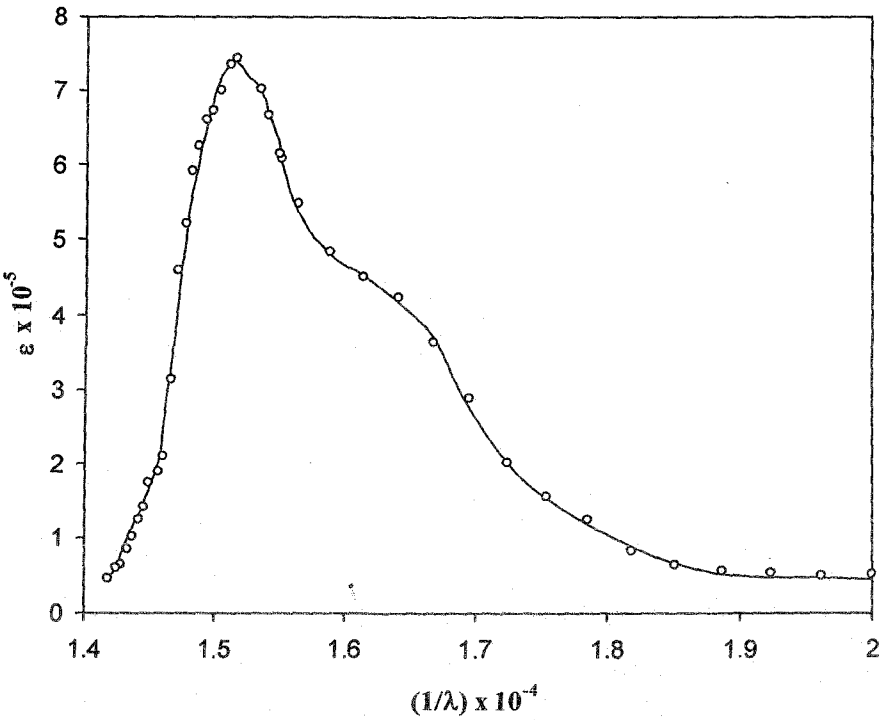

Figure 4.47 Absorption spectra of Methylene Blue monomer in aqueous medium. Solid line represents the experimental spectrum and circles correspond to calculated points.

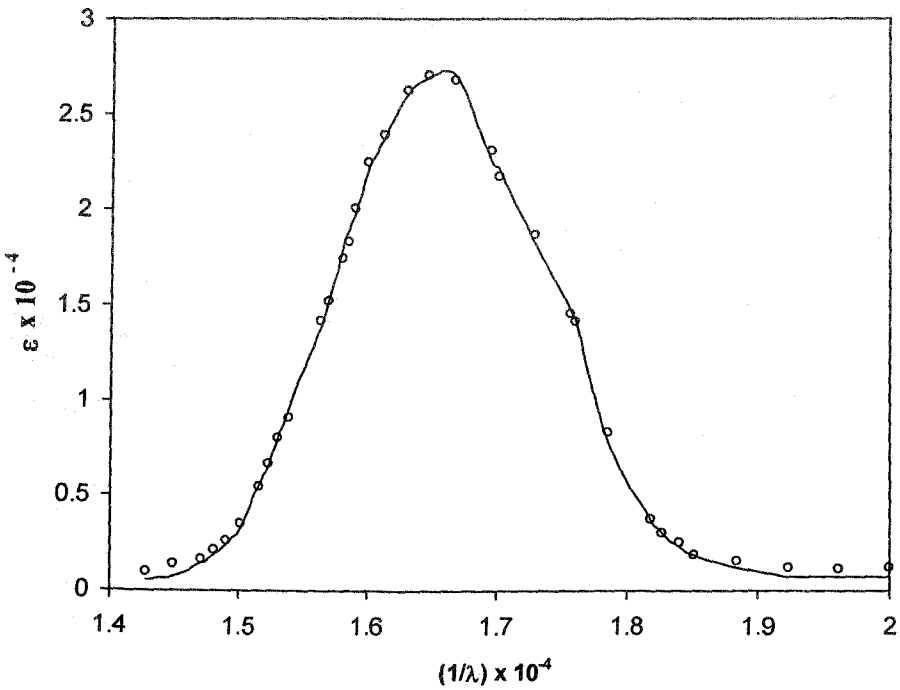

Figure 4.48 Absorption spectra of Thionine monomer in microemulsion. Solid line represents the experimental spectrum and circles correspond to calculated points.

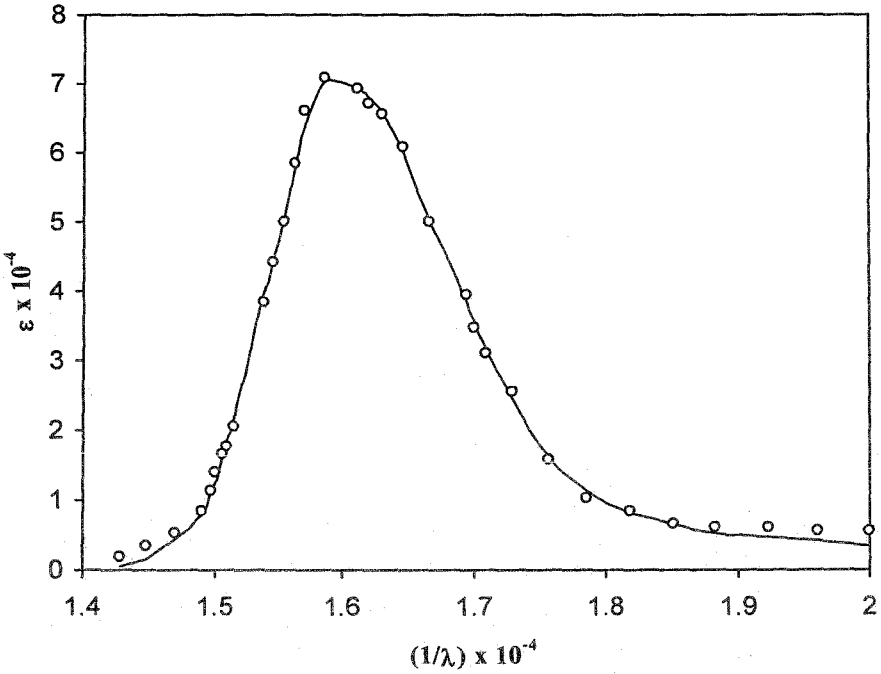

Figure 4.49 Absorption spectra of Azure C monomer in microemulsion. Solid line represents the experimental spectrum and circles correspond to calculated points.

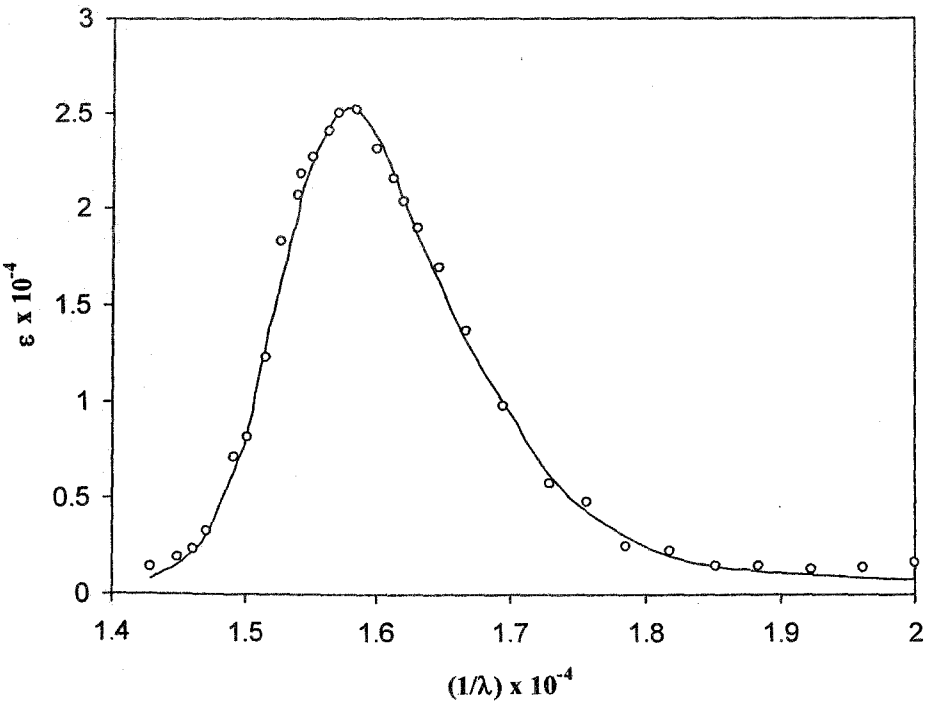

Figure 4.50 Absorption spectra of Azure A monomer in microemulsion. Solid line represents the experimental spectrum and circles correspond to calculated points.

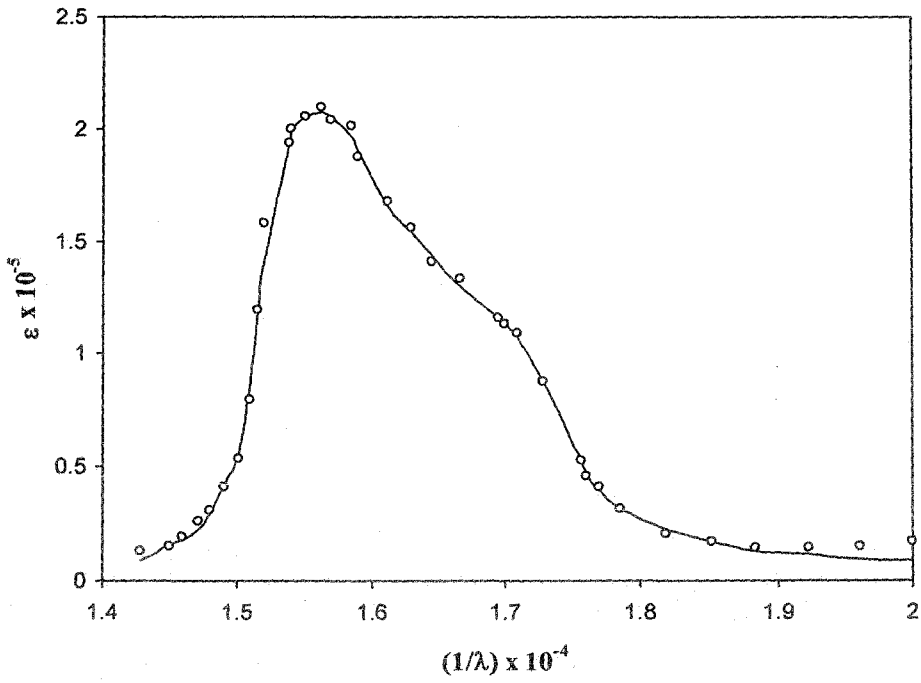

Figure 4.51 Absorption spectra of Azure B monomer in microemulsion. Solid line represents the experimental spectrum and circles correspond to calculated points.

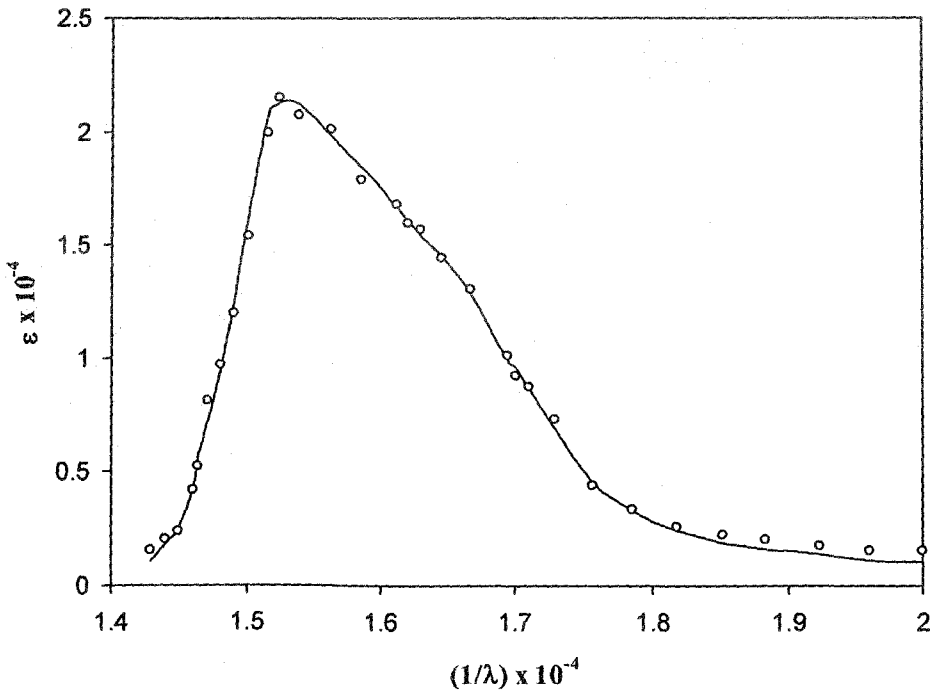

Figure 4.52 Absorption spectra of Methylene Blue monomer in micro-emulsion. Solid line represents the experimental spectrum and circles correspond to calculated points.

bands of constant band width is well applicable in the present systems under investigation.

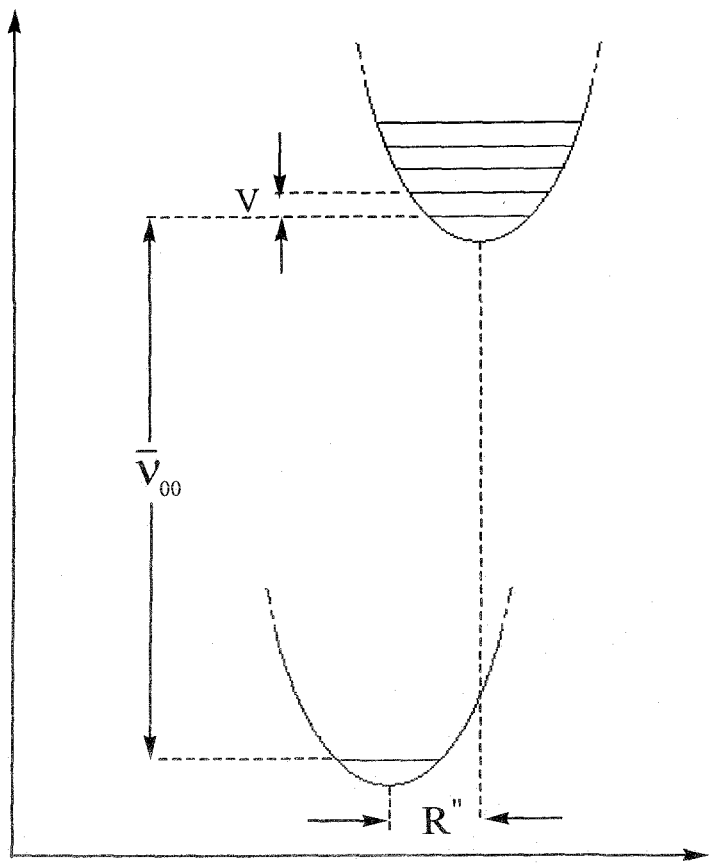

Figure 4.53 Schematic potential energy diagram in absorption

The parameter X which is the ratio of the (1, 0) to (0, 0) band intensities is related to the equilibrium nuclear conformation in the two electronic states. It is thus related to the displacement of the normal coordinate of vibration R, through the formula $X = (2\pi^2 c' V\mu) R^2$, where μ is the reduced mass of the oscillator, c' is the velocity of light and R is the displacement of normal coordinate of vibration, i.e., change in bond lengths between the atoms of the aromatic ring system.

Values of all five parameters of the progressively alkylated thiazine dyes in aqueous and microemulsion are listed in Table 4.7 and 4.8 respectively. Substantial change in the intensity I_{00} and the ratio of (1,0) to (0,0) band intensities i.e. X in most of the dyes have been observed which are intriguing. As has been mentioned above there are some evidences and justification in favour of an assertion that the parameter I_{00} and X are correlated. While the exact reason for the observed variation

of V with progressive methylation of dye or with the salvation media is not certain, above variation must have influenced vibronic characteristics of the dye molecules.

Table 4.7

Monomer (in aqueous solution) parameters for the five thiazine dyes with standard deviation

Dye	I_{00}	ν_{00} (cm^{-1})	V (cm^{-1})	X	b_g (cm^{-1})
Thionine	28424±913	16669±26	1072±47	0.587±0.038	1171±45
Azure C	26130±780	16065±25	1190±43	0.533±0.036	1173±46
Azure A	25584±984	15705±39	1361±52	0.626±0.056	1120±49
Azure B	23520±732	15522±19	1053±35	0.547±0.028	1162±36
Methylene Blue	24560±836	15288±54	1078±19	0.649±0.014	1143±34

Table 4.8

Monomer (in microemulsion) parameters for the five thiazine dyes with standard deviation

Dye	I_{00}	ν_{00} (cm^{-1})	V (cm^{-1})	X	b_g (cm^{-1})
Thionine	25205±880	16265±11	1193±36	0.403±0.031	1011±31
Azure C	24750±750	15920±57	1228±71	0.396±0.066	969±11
Azure A	24525±525	15739±23	1261±36	0.298±0.034	1134±68
Azure B	20760±480	15600±17	1019±30	0.470±0.028	1019±35
Methylene Blue	21980±520	15384±33	1068±57	0.620±0.052	1065±52

The rationale behind the observed variation of X for the thiazine dyes lie in the fact that though both the salvation media are water, the difference in physical characteristics (water mobility, dielectric constant, etc.) of bulk water with that of the water-pool of miocroemulsion also influences dimer geometry in solution and that in presence of a dynamic equilibrium which exists between monomers and the dimers, the electronic distribution of dye molecules are influenced and which is manifested in the variation in X value. This point will be discussed further during considering dimer spectra of the thiazines. The I_{00} values i.e., intensity of (0,0) band

also experience considerable loss in moving the medium from bulk water to microemulsion water-pool.

4.3.5 Analysis of Dimer Spectra in terms of Molecular Exciton Model

An important theoretical tool by which different types of dye aggregates (H, J or intermediate) could conveniently be analyzed is the molecular exciton theory of dipole-dipole coupling. According to this model, parallel aggregates (H - aggregates) absorb at shorter wave length and head to tail aggregates (J aggregates) show absorption at longer wave lengths compared to monomer. Intermediate geometries give rise to band splitting, where the monomer units are thought to be arranged parallely (Model I) or obliquely (Model II). In the above geometries the excited states of the dimer are described by exciton states in which the excitation is delocalised over both monomer units. This model describes the resonance interaction of excited states of molecular aggregate systems and neglect vibronic interactions. The model thus applies to aggregates of molecules which have intense or strongly allowed singlet-singlet interaction, with strong 0-0 vibronic bands. On the other hand, Fulton and Gouterman [211] described a model where the degenerate exciton interaction in the dimer corresponds to the vibronic coupling phenomena. Kurucsev applied the model of Fulton and Gouterman to dimer species of a number of dyes [212-214]. Although the vibronic exciton model has been claimed to be based on more recent development in exciton theory, the so called "non-vibronic" model is simpler and works surprisingly well in explaining dimer spectra of many organic dye systems. The splitting of dimer spectra for the so called "intermediate geometries" leads to compute the angle θ between monomer units and intermolecular separation of the monomer molecules in the dimer.

Resolved dimer spectra of dyes are shown in Figures 4.33 - 4.42. As expected each dimer spectrum is decomposed into two bands characteristics of which are given in Table 4.4 and 4.6 in both aqueous and microemulsion media. The decomposition of the dimer spectrum into two bands shows that the monomer visible spectrum corresponds to an electronic transition with two vibronic bands and not two electronic transitions. As mentioned earlier in the exciton model the point dipole - point dipole approximation of the point multiple expression of the theory of moleculer exciton coupling can be extended and applied to all thiazine dimers in

concentrated solutions. Briefly, using the values of the oscillators' strength of the low (f_1) and high (f_2) frequency components (the J-band and H-band respectively) of the dimer spectra, the angle θ between the main oscillators of the two molecules can be determined by the expression [215].

$$f_1/f_2 = \tan^2\{(180-\theta)/2\} \tag{4.30}$$

On the other hand, the distance (R) betweens the centers of the two molecules can be calculated from the resonance interaction energy, U, (a term which is equal to half the separation between the electronic band maxima of the splitted dimer spectrum).

(U has been designated as $\mathscr{E}$ in Figure 4.2)

The relationship between the interaction energy, strength of transition dipole and the geometry of the dimer is given by the general equation

$$U = \frac{|M|^2}{R^3}\left(\cos\theta + 3\cos^2\phi\right) \tag{4.31}$$

Where $|M|^2$ is the square of the transition moments of the monomer, θ is the angle between polarization axes for the monomer and ϕ is the angle between the polarization direction and the line joining the centers of the two component molecules. The following equation can be used directly to determine oscillator strength of a derivative spectrum.

$$f = 4.32 \times 10^{-9} \int \varepsilon(\nu)\, d\nu \tag{4.32}$$

However, it is more convenient to modify the equation to make it easier to analyze spectra measured a function of a wave length instead of frequency. If the dispersion relationship $C = \lambda\nu$ is used to substitute for ν in the above equation, the alternative relationship

$$f = (0.0432 / \lambda_0^2) \int \varepsilon\ (\lambda)\, d\lambda. \tag{4.33}$$

may be derived. In this expression $\varepsilon(\lambda)$ has units of lit/mol-cm and λ in nm, λ_0 is the wave length at the peak of a smoothed envelops containing the spectrum.

The angle θ calculated for the dimers are presented in Table 4.11 and 4.12. For the calculations of f_1 and f_2 values for each dimer spectrum, measurement of the area

under the J and H-bands of the spectra was done by using Microcal Origin 6.0 software. The transition moment M is calculated using the relationship

$$f = 4.704 \times 10^{29} \bar{\nu} M^2 \tag{4.34}$$

in cm^{-1} of the dimer at maximum ε in the dimer spectrum.

The distance (R) between monomers in a dimer is model dependent, i.e., it depends on the geometric disposition. To explain dimer band splitting, two models allowing the two transitions are possible. In model I, the monomers are in parallel planes with a twist angle θ while in model II, they are in the same plane forming angle θ. The interaction energy in these models is as follows [158,159].

Model I: ($\theta = \theta$ and $\phi = 90^0$; Sandwitch dimer with a Twist angle θ)

$$U = -\frac{|M|^2 \cos\theta}{R_I^3} \tag{4.35}$$

Model II: ($\theta = \theta$ and $\phi = \theta$; Co-planar inclined angle dimer)

$$U = -\frac{|M|^2}{R_{II}^3}\left(\cos\theta + 3\cos^2\phi\right) = -\frac{|M|^2}{R_{II}^3}\left(\cos\theta + 3\sin^2\theta/2\right) \tag{4.36}$$

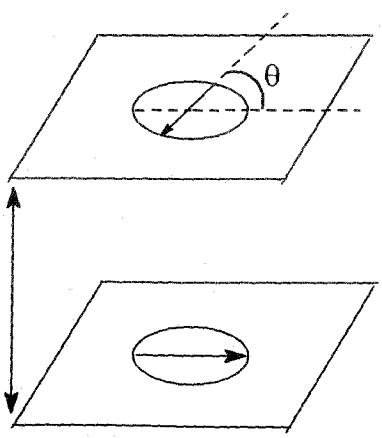

Model - I

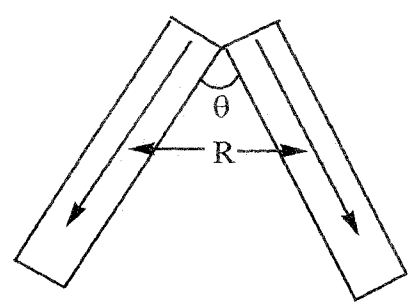

Model - II

Where R_I and R_{II} are the distances between the monomers in the dimers in model I and II respectively. Model I refers to the case of non-planar transition dipoles where the molecules are arranged in a sandwich dimer (card pack) oriented with angle θ the angle of skew between the polarization direction of the absorption oscillators of each dye molecule. Model II refers to the "coplanar inclined angle dimer" of the

"oblique" arrangement where θ is the angle between the planes of the aromatic ring. The twist angles θ (for model I) and the oblique angle θ (for model II) and the distance (R) between the centers of the monomer units in a dimer have been calculated for all the thiazine dyes under investigation.

The calculated oscillators strength of the dimers are listed in Table 4.9 and 4.10. The excitonic parameters of thiazine dimers and values of transition moments and twist angles are shown in Table 4.11 and 4.12 respectively in aqueous and microemulsion media.

Table 4.9

Oscillators strength in aqueous medium

Dye	Oscillator strength of monomer (f_m)	Oscillator strength of the low frequency band (J-band) f_2 of dimer)	Oscillator strength of the high frequency band (H-band) f_1 of dimer
Thionine	0.603	0.048	0.532
Azure C	0.451	0.043	0.581
Azure A	0.552	0.050	0.863
Azure B	0.641	0.075	0.980
Methylene Blue	0.610	0.073	0.972

Table 4.10

Oscillators strength in microemulsion medium

Dye	Oscillator strength of monomer (f_m)	Oscillator strength of the low frequency band (J-band) f_2 of dimer)	Oscillator strength of the high frequency band (H-band) f_1 of dimer
Thionine	0.382	0.032	0.307
Azure C	0.101	0.025	0.280
Azure A	0.202	0.029	0.250
Azure B	0.280	0.030	0.299
Methylene Blue	0.191	0.024	0.231

The twist angle for the thionine (34.8^0) is found to be largest among all the dyes and Az C shows smallest twist angle of 28.4^0 when dimers are formed in aqueous medium. But in microemulsion Az B gives the least value of twist angle among all the dyes. As discussed earlier the variation of physico-chemical characteristics of the

water in the water-pool to that of the bulk water also plays important role to the dimer geometry.

Table 4.11

Excitonic parameters of the dimers of thiazine dyes in aqueous media

Dye	Twist angle (θ /deg.)	Square of the transition moments $\left(\|M\|^2 x10^{36}\right)$ /esu	Interaction energy (U /cm^{-1})	Intermolecular distance (Å)	
				R_I	R_{II}
Thionine	34.8	56.23	1072.5	6.01	6.61
Azure C	28.4	63.20	1076.5	6.38	6.80
Azura A	28.5	67.23	1417.5	5.95	6.75
Azura B	30.2	59.96	1172.0	6.06	6.65
Methylene Blue	31.7	78.81	1097.5	6.76	7.30

Table 4.12

Excitonic parameters of the dimers of thiazine dyes in microemulsion media

Dye	Twist angle (θ /deg.)	Square of the transition moments $\left(\|M\|^2 x10^{36}\right)$ /esu	Interaction energy (U /cm^{-1})	Intermolecular distance (Å)	
				R_I	R_{II}
Thionine	35.7	35.89	1515.1	3.70	5.59
Azure C	28.1	29.57	1465.9	4.65	5.88
Azura A	30.9	30.19	1541.0	4.42	5.35
Azura B	25.3	23.69	1682.2	4.12	5.01
Methylene Blue	28.2	33.43	1374.3	4.97	6.26

While the twist angles displayed by all the five dyes are close to each other, no systematic variation is observed on progressive alkylation of the dye molecule. However, except methylene blue, progressive alkylation decreases the twist angle to some extent. It seems apparent that apart from the steric effect due to the addition of successive methyl groups in the dye molecule, hydrophobic as well as electron donating nature of methyl groups are also involved. Apparently the increased hydrophobic interaction due to methyl substitution as well as for their electron donating nature, a stronger field is created such that the dipoles tend towards parallel alignment resulting in decrease in θ upon introduction of methyl groups successively in the thionine molecule. In other wards a better $\pi-\pi$ interaction

between two monomer molecules as a result of successive addition of methyl groups may cause the observed alignment. Further substitution of methyl groups probably increase stetric hindrance resulting in the increase of the angle, θ, between dipoles in the case of methylene blue. But in microemulsion due to the effective electrostatic repulsion between the similarly charged dimers and inner layer of microemulsion, the dimers give relatively lower twist angle between the dipoles when compared to that in bulk water.

It should be mentioned in this context that the angle between the transition moments of two monomers of methylene blue as reported by Bergmann and O'Konski [147] was only 13^0. The twist angle calculated for the present study is much higher than that reported by above authors. However, the present analysis is based on more recently developed theories, which showed consistency in recent study for a number of dye systems [216]

On the other hand, intermolecular distance between two monomer molecules in a dimer as calculated according to model I varies from 5.59 to 6.76 Å; while the same varies from 6.61 to 7.30 Å when calculated according to model II for aqueous medium. In microemulsion media, however the distance lie between 3.70 to 4.97 Å for model I and 5.01 to 6.26 Å for model II.

It is interesting to note that due to the location of dyes in the relatively confined space and also due to the electrostatic interactions and low dielectric constant of the medium, distance between monomers in the dimer is decreased considerably in water-pools of microemulsion. This is due to stronger excitinic band splitting of dimer spectra in microemulsion relative to bulk water. The distances between the transition dipoles in the dimers as revealed in the present systems are somewhat higher than observed previously for fluorescein and rhodamine dyes. But the values calculated according to model I are somewhat less. In view of this and the observation of the previous workers on a number of dyes it may be argued that model I might be appropriate. On the other hand, more recent work argued in favour of model II [209]. However, these models represent only the ideal cases and the real structure may only approximate to one of them. It is noteworthy that although the exciton theory as applied in the present systems is over simplification for the problem of dye aggregation, the interdipole distances computed therefrom appears to be reasonable if proper geometry of the aggregate is taken into consideration.

References

1. Rafati, A.A; Gharibi, H.; Rezaie Sameti M. *J. Mol. Liq.* **2004**, *111*, 109.
2. García-Río, L.; Hervella, P.; Mejuto, J.C.; Parajó, M. *Chem. Phys.* **2007**, *335*, 164.
3. Tehrani Bagha, A.R.; Bhrami, H.; Movassagh, B.; Arami, M.; Menger, F.M. *Dyes Pigments* **2007**, *72*, 331.
4. Hartley, G.S. *Trans. Faraday Soc.* **1934**, *30*, 44.
5. Savvin, S.B.; Chernova, R.K.; Shtykov, S.N. *Zh. Analit. Khim.* **1978**, *33*, 865.
6. Rosendorfova, J.; Cermakova, L. *Talanta* 1980, *27*, 705.
7. Minch, M.J. and Sadiq-Shah, S. *J. Org. Chem.* **1979**, *44*, 3253.
8. Buwalda, R.T., Engberts, J.B.F.N. *Langmuir* **2001**, *17*, 1054.
9. Karukstis, K.K.; Savin, D.A.; Loftus, C.T.; D'Angelo, N.D.; *J. Colloid Interface Sci.* **1998**, *203*, 157.
10. He, Q.; Chen, H.; Fresen, J. *Anal. Chem.* **2000**, *367*, 270.
11. Sarkar, M.; Poddar, S. *J. Colloid Interface Sci.* **2000**, *221*, 181.
12. Oliveira, C.S.; Bastos, E.L.; Durate, E.L.; Itri, R.; Baptista, M.S. *Langmuir* **2006**, *22*, 8718.
13. Junqueira, H.C.; Severino, D.; Dias, L.G.; Gugliotti, M.S.; Baptista, M.S. *Phys. Chem. Chem. Phys.* **2002**, *4*, 2320.
14. Chibisov, A.K.; Prokhorenko, V.I.; Gorner, H. *Chem. Phys.* **1999**, *250*, 47.
15. Robinson, B.H.; Löffler, A.; Schwarz, G.; *J. Chem. Soc., Faraday Trans. I* **1973**, *69*, 56.
16. Braswell, E.H. *J. Phys. Chem.* **1984**, *88*, 3653.
17. Rosendorfova, J.; Cermakova, L. *Talanta* **1980**, *27*, 705.
18. Sanh-Medel, Garcia Alonso, A.J.I.; Blanco Gonzalez, E. *Anal.Chem.* **1985**, *57*, 1681.
19. Reeves, R.L.; Maggio, M.S.; Harkaway, S. A. *J. Phys. Chem.* **1979**, *83*, 2359.
20. Kali, K.M.; Cussler, E.L.; Evans, D.F. *J. Phys. Chem.* **1980**, *84*, 593.
21. Corrin, M.L.; Harkins, W.D. *J. Am. Chem. Soc.* **1974**, *96*, 679.
22. Saikia, P.M.; Kalita, A.; Gohain, B.; Sarma, S.; Datta, R.K. *Colloid Surf. A* **2003**, *216*, 21.
23. Huang, X.; Jinghe, Y.; Zhang, W.; Zhang, Z.; An, Z. *J. Chem. Edu.* **1999**, *76*, 93.

24. Samsonoff, C.; Daily, J.; Almog, R.; Berns, D.S. *J. Colloid Interface Sci.* **1986**, 109,325.

25. Sanz-Medel,A.; Camara Rica, C.; Perez Bustamante, J.A. *Anal. Chem.* **1980**, *52*, 1035.

26. Garcia Alonso, J.I.; Sanz-Medel, A. *Quim Anal.* **1986**, *5*, 428.

27. Mukherjee, P.; Mysels, K.J. *J. Am. Chem. Soc.* **1955**, *77*, 2937.

28. Malik, W.V.; Haque, R. *J. Am.Chem. Soc.* **1963**, *67*, 2082.

29. Malik,; W.V.; Jhamb, O.P. *J. Electroanal Chem.* **1970**, *27*, 151.

30. Guha, S.N.; Moorthy, P.N.; Rao, K.N. *Proc. Indian Acad. Sci.* **1982**, *91*, 73.

31. Skarydova, V.; Cermakova, L. *Collection Czech. Chem. Commun.* **1982**, *47*, 776.

32. Savvin, S. B.; Marov, I. N.; Chernova, R.K.; Shtykov, S.N.; Sokolov, A.B. *Zh. Analit. Khim.* **1981**, *36*, 850.

33. Bunton, C.A.; Minch,M. J.; Hidalgo, J.; Sepulveda L. *J. Am. Chem. Soc.* **1973**, *95*, 3262.

34. Bunton, C.A.; Minch, M.J. *J. Phys. Chem.* **1974**, *78*, 1490.

35. Fernandez, M.S.; Fromjertz, P. *J. Phys. Chem.* **1977**, *81*, 1755.

36. Funasaki, N. *J. Phys. Chem.* **1979**, *83*, 1998.

37. Birdi, K.S.; Singh, H.N.; Dolsager, S.V. *J. Phys. Chem.* **1979**, *83*, 2733.

38. Minch, M.J.; Giaccio, M. and Wolff, R. J.Am.Chem.Soc. **97**, 3766, 1975.

39. Chiang, H.C.; Lukton, A. *J. Phys. Chem.* **1975**, *79*, 1935.

40. Stevenson, D.M.; Duff, D.G.; Kirkwood, D.J. *J. Soc. Dyers Colour* **1981**, 97, 13.

41. Biedermann, W.; Datyner, A. *J. Colloid Interface Sci.* **1981**, *82*, 276.

42. Dill, K.A.; Koppel, D.E.; Cantor, R.S.; Dill, J.D.; Bendedouch, D.; Chen, S.H. *Nature*, **1984**, *309*, 42.

43. Kapoor, R.C.; Mishra, V.N. *J. Ind. Chem. Soc.* **1976**, *53*, 965.

44. Sato, H.; Kawasaki, M.; Kasatani, Y.; Kusumoto, N.; Nakashima, N. Yoshihara, K. *Chem. Lett.* **1980, 12**, 1529.

45. Humphry, R.; Baker.; Gratzel, M.; Steiger, R. *J. Am. Chem. Soc.* **1980**, *102*, 847.

46. Wolff, T.; Bunsenges, B. *J. Phys. Chem.* **1981**, *85*, 145.

47. Diaz Garcia, M.E.; Sanz-Medel, A. *Talanta* **1986**, *33*, 255.

48. Rosenthal, K.S.; Koussali, F. *Anal. Chem.* **1983**, *55*, 1115.

49. Garcia Alonso, J.J.; Diaz Garcia, M.E.; Sanz-Medel, A. *Talanta* **1984**, *31*, 361.

50. Diaz Garcia, M.E.; Blanco Gonzalez, E.; Sanz-Medel, A. *Microchem. J.* **1984**, *30*, 211.
51. Tanford, C. *The Hydrophobic Effect: Formation of Micelles and Biological Membranes*, Wiley-Interscience, New York, 1980.
52. Fendler, J.H. *Acc. Chem. Res.* **1976**, *9*, 153.
53. Fendler, J.H.; Fendler, E.J. *Catalysis in Micellar and Macromolecular Systems*, Academic Press, New York, 1975.
54. Muto, S. and Meguro, K. *Bull. Chem. Soc. Japan* **1973**, 46, 1316.
55. O'Connor, C. J.; Lomax, T.D.; Ramage, R.E. *Adv. Colloid Interface Sci.* **1984**, *20*, 21.
56. Mandal, A.K; Pal, M.K. *J. Colloid Interface Sci.* **1997**, *192*, 83.
57. Gokturk, S.; Tuncay, M. *Spectrochemica Acta,, Part A* **2003**, *59*, 1857.
58. Hinze, W.L. *Solution Chemistry of Surfactants*, Mittal, K.L. (Ed.), Vol.-I, pp. 79-127, Plenum Press, New York, 1979.
59. Kapoor, R.C. *J. Ind. Chem. Soc.* **1986**, *63*, 541.
60. Callaham, J.H.; Cook, K.O. *Anal. Chem.* **1984**, *56*, 1632.
61. Rohatgi-Mukherjee, K.K.; Choudhuri, R.; Bhowmik, B.B. *J. Colloid Interface Sci.* **1985**, *106*, 45.
62. Reeves, R.L.; Harkaway, S.A. *Solution-Chemistry of Surfactants*, Mittal, K.L. (Ed.), Plenum Press, New York, p.819, 1979.
63. Dutt, R.K.; Bhat, S.N. *Bull. Chem. Soc. Jpn.* **1992**, *65*, 1089.
64. Gopidas, K.R.; Kamat, P.V. *J. Phys. Chem.* **1990**, *94*, 813.
65. Colichmann, E.L. *J. Am. Chem. Soc.* **1951**, *73*, 1795.
66. Ghosh, A.K.; Mukherjee, P. *J. Am. Chem. Soc.* **1970**, *92*, 6408.
67. Diamond, R.N. *J. Phys. Chem.* **1963**, *67*, 2513.
68. Weir, D.; Scaiano, J.C. *Tetrahedron* **1987**, *43*, 1617.
69. Tanigushi, M.; Yamagichi, A.; Iwamoto, T. *J. Phys. Chem.* **1990**, *94*, 2534.
70. Hiskey, C.P.; Downey, T.A. *J. Phys. Chem.* **1954**, *58*, 835.
71. Cockbain E.G. *Trans Fraday Soc.* **1954**, *49*, 104.
72. Hayashi M. *Bull. Chem. Soc. Japan* **1961**, *34*, 119.

73. Matibinkov, M.A.; Namaka, D. Varkevich, N.M.; Kaskov, B.N.; Monkher, D. Vest Akad Navak Belarus SSR 35R Ser Fiz Mat Naruk, **1973**, *87*, *Chem. Abstr.* 80, 101, 9447, 1974.

74. Rohatgi-Mukherjee, K.K.; Bhattacharya, S.C.; Bhowmik B.B. *Ind. J. Chem.* **1983**, *22A*, 911.

75. Bhowmik, B.B.; Bhattacharya, S.C.; Rohatgi-Mukherjee K.K. *Indian J. Chem.* **1986**, *25A*, 126.

76. Ketelaar, J.A.A.; Vande Stolpe, C.; Gersmann, H.R. *Rec. Trav. Chim.* **1952**, *70*, 499.

77. Scott, R. L. *Rec. Trans. Chim.* **1956**, *75*, 787.

78. Bhowmik, B.B.; Chaudhury, R.; Rohatgi-Mukherjee, K.K. *Ind. J. Chem.* **1987**, *26A*, 95.

79. Benesi, H A.; Hildebrand, J.H. *J. Am. Chem. Soc.* **1949**, *71*, 2703.

80. Scatchard, G.; Aun, N.Y. *Acad. Sci.* **1949**, *51*, 660.

81. Mukhopadhyay, M.; Sen Verma, C.; Bhowmik, B.B. *Colloid Polym. Sci.* **1990**, *268*, 447.

82. Mulliken, R.S. Person, W.B. *Molecular Complexes*, Wiley, New York, 1969.

83. Sarkar, M.; Poddar, S. *Spectrochimica Acta A*, **1999**, *55*, 1737.

84. Gawndi, V.B.; Guha, S.N.; Priyadarshini, K.I.; Mohan, H. *J. Colloid, Inf. Sci.* **2001**, *242*, 220.

85. Kalyanasundaram, K. *Chem. Soc. Rev.* **1978**, *7*, 453.

86. Moroi, Y.; Baraun, A.M.; Gratzel, M. *J. Am. Chem. Soc.* **1979**, *101*, 567.

87. Moroi, Y.; Infelta, P.P.; Gratzel, M. *J. Am. Chem. Soc.* **1979**, *101*, 573.

88. Turro, N. J.; Gratzel, M.; Baraun, A.M. *Angrew Chem. Int. Ed. Engl.* **1980**, *19*, 675.

89. Kawait, T.; Yasuda, Y.; Kon-no, K. *Bull. Chem. Soc. Jpn.* **1995**, *68*, 2175.

90. Mittal, K.L. *Micellization, Solubilization and Microemulsions*, Vols. 1 and 2, Plenum, New York, 1977.

91. Pandit,P.; Basu, S. *Environ. Sci. Technol.* **2004**, *38*, 2435.

92. Moulik, S.P.; Paul, B.K. *Adv. Colloid. Interface. Sci.* **1998**, *78*, 99.

93. Haandrikman, G.; Daane, G.J.R.; Kerkhof, F.J.M.; Van Os, N.M.; Rupert, L.A.M. *J. Phys. Chem.* **1992**, *96*, 9061.

94. Moran, M.; Bowmaker, G.A.; Cooney, R.P. *Langmuir* **1995**, *11*, 738.
95. Fendler, H.J.; *Membrane Mimetic Chemistry*, Wily, New York, 1982.
96. Harada, S.; Schelly, Z.A. *J. Phys. Chem.* **1982**, *86*, 2098.
97. Herrmann, U.; Schelly, Z.A. *J. Am. Chem. Soc.* **1979**, *101*, 2665.
98. Verbeeck, A.; Galade, E.; DeSchryver F.C. *Langmuir* **1982**, *2*, 448.
99. Tatikolov, A.S.; Costa, S.M.B. *Photochem. Photobiol. Sci.* **2002**, *1*, 211.
100. Oldfield, C.; Robinson, B.H.; Freedman, R.B. *J. Chem. Soc. Faraday Trans.* **1990**, *86*, 833.
101. Fletcher, P.D.I. *J. Chem. Soc. Faraday Trans. 1* **1986**, *82*, 2651.
102. Neimeyer, E.D.; Bright, F.V. *J. Phys. Chem. B* **1998**, *102*, 1474.
103. Fujii, H.; Kawai, T.; Nishikawa, H.; Ebert, G. *Colloid Polym. Sci.* **1998**, *260*, 697.
104. Belletete, M.; Durocher, G. *J. Colloid Interface Sci.* **1990**, *134*, 289.
105. Ishchenkoa, A.A.; Shapovalov, S.A. *J. Appl. Spectrosc.* **2004**, *71*, 605.
106. Gohain, B.; Saikia, P.M.; Sarma, S.; Bhat, S.N.; Datta, R.K. *Phys. Chem. Chem. Phys.* **2002**, *4*, 2617.
107. Pramanick, D.; Mukherjee, D. *J. Colloid Interface Sci.* **1993**, *157*, 131.
108. Zhu, D.; Schelly, Z.A. *Langmuir* **1992**, *8*, 48.
109. Foley, M.S.C.; Beeby, A.; Parker, A.W.; Bishop, S.M.; Phillips, D. *J. Photochem. Photobiol. B: Biol.* **1997**, *38*, 18.
110. Mackay, R.A.; Lai, W.-C. *Colloid Surfaces A: Physicochem. Eng. Aspects* 254, **2005**, 115.
111. Biswas, S.; Bhattacharya, S.C.; Bhowmik, B.B.; Moulik, S.P. *J. Colloid Interface Sci.* **2001**, *244*, 145.
112. Hung, H.C.; Chang, G.G. *J. Chem. Soc. Perkin Trans.* **1999**, *2*, 2177.
113. Hazarika, R.; Datta, R.K.; Bhat, S.N. *Indian J. Chem.* **1993**, *32A*, 239.
114. Dakiky, M.; Manassra, A.; Kareem, M.A.; Jhmean, F.; Khamis, M. *Dyes Pigments* **2004**, *63*, 101.
115. Arunkumar, E.; Forbes, C.C.; Smith. B.D. *Eur. J. Org. Chem.* **2005**, *19*, 4051.
116. Jana, N.R.; Pal, T. *J. Surf. Sci. Technol.* **2001**, *17*, 191.
117. Simončič, B.; Kert, M. *Dyes Pigments* **2002**, *54*, 221.
118. Rohatgi-Mukherjee, *Ind. J. Chem.* **1992**, *28*, 721.

119. Antonov , L.; Gergov, G.; Petrov, V.; Kubista, M.; Nygren, J. *Talanta* **1999**, *49*, 99.

120. Pagfeldt, A.; Graetzel, M. *Chem. Rev.* **1995**, *95*, 49.

121. West, W.; Gilman, P.B.Jr. in *The Theory Of The Photography Process*, 4th Ed.; James, T.H. Ed. Macmillan; New York, 1997.

122. Kemnitz, K.; Yoshihara, K.; Ohzeki, K ; *J. Phys. Chem.* **1990**, *94*, 3099.

123. Spitler, M.T. *J. Imaging Sci.* **1991**, *35*, 351.

124. Law, K.Y. *Chem. Rev.* **1993**, *93*, 449.

125. Kamat, P.V. *Chem. Rev.* **1993**, *93*, 267.

126. Parkinson, B.A.; Spitler, M.T., *Electrochim. Acta* **1992**, *37*, 943.

127. Das, S.; Thomas, K.G.; Kamat, P.V.; George M.V. Proc. *Ind. Acad. Sci. (Chem. Sci.)* **1993**, *105*, 513.

128. Chau, L.K.; Arbour, C.; Collins, G.E.; Nebesuy, K.W.; Lee, P.A.; England, C.D. Armstrong, N.R.; Parkinson, B.A. *J. Phys. Chem.* **1993**, *97*, 2690.

129. Taguchi, T.; Hirayama, S.; Okamoto, M. *Chem. Phys. Lett.* **1994**, *231*, 561.

130. Kim, Y.S.; Liang, K; Law, K.Y; Whitten, D.C. *J. Phys. Chem.* **1994**, *98*, 984.

131. Harrison, W.J.; Mateer, D.L.; Tiddy, G.J.T. *J. Phys. Chem. B.* **1996**, *100*, 2310.

132. Lydon, J.E. *Curr. Opin., Colloid Interface Sci.* **1998**, *3*, 458.

133. Lydon, J.E.; in *Hand Book Of Liquid Crystals*, vol. 2B; Demus, D.; Goodby, J.; Gray, G W; Spies, H.W.; Vill, V.; Eds. Willy. VCH, Weinheim, pp. 981-1007, 1998.

134. Kock-Yec Law, H.C.; Peristein, J.; Whitten, D.G. *J. Am. Chem. Soc.* **1995**, *117*, 7257.

135. Von. Berlepsch. H.; Bottcher, C.; Ouart, A.; Burger, C.; Dahne, S.; Kirstein, S. *J. Phys. Chem. B* **2000**, *104*, 5255.

136. Spitz, C.; Dahne, S.; Quart, A.; Abraham, H.W. *J. Phys. Chem. B* **2000**, *104*, 8664.

137. Rubires, R.; Farrera, J.A.; Ribo, J.M. *Chem. Eur. J.* **2001**, *7*, 436.

138. Burdett. B.C. *Aggregation Process in Solution*, Ed. Jones, E.W.; Gormally, J. (Elsevier, Armsterdam, 1983) Chap. 10, p. 241.

139. Aquilera, O.; Neckers, D.C. *Acc. Chem. Res.* **1989**, *171*, 22.

140. Rohatgi-Mukherjee, K.K. and Singhal, G.S. *J. Phys. Chem.* **1960**, *70*, 1695.

141. Mukherjee, P.; Ghosh, A.K. *J. Am. Chem. Soc.* **1970**, *92*, 6419.

142. Rabinson, B.H.; Loffler, A.; Schawarz, G. *J. Chem. Soc. Faraday Trans. 1* **1973**, *69*, 56.

143. Schubert, M.; Levine, A. J. Am. Chem. Soc., **77**, 4197, 1955.

144. Turner, R.; Cowmann, M.K. *Arch. Biochem. Biophys.* **1985**, *237*, 253.

145. Vitagliano, V. in *Aggregation Processes in Solution*, Eds. Jones, E.W.; Gormally, J. (Elsevier, Armsterdam, 1983) Chap. 11, p. 271.

146. Shirai, M.; Dhyabu, M.; Ono, Y.; Tanaka, M.; *J. Polym. Sci. Chem.* **1982**, *19*, 555.

147. Newmann, M.G.; Hioka, N. *J. Appl. Polym. Sci.* **1987**, *34*, 2829.

148. Bergmann, K.; O'Konsky, C. T. *J. Phys. Chem.* **1963**, *67*, 2169.

149. West, W.; Pearce, S. *J. Phys. Chem.* **1965**, *69*, 189.

150. Baranova, E.G.; Levshin, V.L. *Optica. Spetrokopia.* **1961**, *10*, 182.

151. Mataga, N. *Bull. Chem. Soc. Japan* **1957**, *30*, 375.

152. Zanker, V. *Z. Physik. Chem.* **1952**, *200*, 250.

153. Hida, M.; Sanuki, T. *Bull. Chem. Soc. Japan*, **1970**, *43*, 2291.

154. Selwyn, J.E.; Steinfeld, J.I. *J. Phys. Chem.* **1972**, *76*, 762.

155. James, A.D.; Rabinson, B.H. *Adv. Mol. Relax. Process B* **1976**, *8*, 287.

156. Kamat, P.V.; Lichtin, N.N. *J. Phys. Chem.* **1981**, *85*, 814.

157. Zadoroznnaya, E.M.; Nabinvanets, B.I.; Maslei, N.N. *Zh. Anal. Khim.* **1974**, *29*, 993.

158. Arbeloa, I.L. *J. Chem. Soc. Faraday Trans. 2*, **1981**, *77*, 1725.

159. Arbeloa, I.L.; Rohatgi-Mukherjee, K.K. *Spectrochemica Acta.* **1988**, *44A*, 423.

160. Newmann, M.G.; Gessner, F.; Olivelra, V.A. *J. Chem. Soc. Faraday Trans.* **1990**, *86*, 3551.

161. McRae, E.B.; Kasha, M. *Physical Processes in Radiation Biology*, Augenstein, L.; Rosenberg, B.; Mason, R. Ed., Acad. Press , N.Y., p. 23, 1964.

162. Davydov, A.S. *Theory of Molecular Excitons* (Translated by Kasha, M and Oppenheimer, M. Jr.) Mc Graw-Hill, N.Y., 1962.

163. Simpson, W.I. *Theory of Electrons in Molecules*, Prentice Hall, Englewood Cliffs, New Jersey, 1962.

164. McClure, D.S. *Solid State Phys.* **1959**, *8*, 1.

165. Kasha, M. *Rev. Mod. Phys.* **1959**, *31*, 162.

166. Kasha, M. *Radiation Res.* **1963**, *20*, 55.

167. Levinson, G.I.; Simpson, W.T.; Curtis, W. *J. Am. Chem. Soc.* **1957**, *79*, 3414.

168. Kasha, M.; EL-Bayoumi, M.A.; Rhodes, W. *J. Chem. Phys.* **1961**, *58*, 916.

169. EL-Bayoumi, M.A., *Exciton Theory: Application to H-Bonded Complexes*, Doctoral Thesis, Florida State University, Tallahssea, Florida, 1961.

170. Hosoya, H.; Janaka, J.; Nagakura, S. *J. Mol. Spectry.* **1962**, *8*, 257.

171. MacRay, E,G,; Kasha, M. *J. Phys. Chem.* **1958**, *28*, 721.

172. Rohatgi-Mukherjee, K.K.; Mukhopadhyay, A.K. *J. Phys. Chem.* **1972**, *76*, 3970.

173. Arbeloa, I.L. *J. Chem. Soc. Faraday Trans. 2*, **1981**, *77*, 1735

174. Jones, G.R.; Duddell, D.A.; Murry, D.; Cundall, R.B. *J. Chem. Soc. Faraday Trans. 2*, **1984**, *80*, 1181.

175. Basu, S.; Rohatgi-Mukherjee, K.K.; Arbeloa, I.L. *Spectrochemica Acta.* **1986**, *42A*, 1355.

176. Horng, M-L.; Quitevis, E.L *J. Chem. Edu.* **2000**, *77*, 637.

177. Berlepsch, H.V.; Bottcher, C.; Dahne, L. *J. Phys. Chem. B.* **2000**, *104*, 8792.

178. Kawasaki, M.; Sato, T. *J. Phys. Chem. B.* **2001**, *105*, 796.

179. Ahmed, S.; Saha, S.K. *Can. J. Chem.* **1996**, *74*, 1896.

180. Kartal, Ç.; Akbaş, H. *Dyes Pigments* **2005**, *65*, 191.

181. Jirsa, M.; Jirsa Jr, M.; Kubát, P. *J. Photochem. Photobiol. B* **1996**, *36*, 99.

182. Armarego, W.L.F.; Perrin, D.D. *Purification of Laboratory Chemicals*, 4th Ed. Butterworth-Heinemann, Oxford, 1996.

183. Benrraou, M.; Bales, B.L.; Zana, R. *J. Phys. Chem. B* **2003**, *107*, 13432.

184. Pal, M.K.; Schubert, M. *J. Am. Chem. Soc.* **1962**, *84*, 4384.

185. Pal, M.K.; Schubert, M. *J. Phys. Chem.* **1963**, *67*, 1821.

186. Pal, M.K.; Mandel, M. *Biopolymers* **1977**, *16*, 33.

187. Datta, R.K.; Bhat, S.N. *Bull. Chem. Soc. Jpn.* **1993**, *66*, 2457.

188. Datta, R.K.; Bhat, S.N. *Colloids Surf. A* **1996**, *106*, 123.

189. Vinogradov, A.M, Tatikolov, A.S.; Costa, M.B. *Phys. Chem. Chem. Phys.* **2001**, *3*, 4325.

190. Nigam, S.; Belletête, M.; Sarpal, R.S.; Durocher, G. *J. Chem. Soc. Faraday Trans.* **1995**, *91*, 2133.

191. (a) Mukherjee, P.; Mysels, K.J. Critical Micelle Concentrations of Aqueous Surfactant Systems, US-NBS, No. 36, US. GPO, Washington DC, 1971. (b) Hait, S.K.; Majhi, P.R.; Blume, A.; Moulik, S.P. *J. Phys. Chem. B* **2003**, *107*, 3650.

192. Datta, R.K.; Chowdhury, R.; Bhat, S.N. *J. Chem. Soc. Faraday Trans. 1* **1995**, *91*, 681.

193. Ahmed, S. *Ph. D. Thesis*, University of North Bengal, 1996.

194. F. Tavčer, *Dyes Pigments* **2004**, *63*, 181.

195. Havelcová, M.; Kubát, P.; Němcová, I. *Dyes Pigments* **2000**, *44*, 49.

196. Gak, V.Y.; Nadtochenko, V.A.; Kiwi, J. *J. Photochem. Photobiol. A* **1998**, *116*, 57.

197. Lang, K.; Luňak, S.; Sedlák, P.; Kubát, P.; Zeit, J. *J. Phys. Chem.* **1995**, *190*, 203.

198. Drummond, C.J.; Grieser, F.; Healy, T.W. *J. Chem. Soc. Faraday Trans.1.* **1989**, *85*, 561.

199. Rao, N.V.; Narayana, R.L. *Indian J. Chem.* **1982**, *21A*, 995.

200. Wormuth, K.R.; Cadwell, L.A.; Kaler, E.W. *Langmuir* **1990**, *6*, 1035.

201. Keh, E.; Valeur, B. *J. Colloid Interface Sci.* **1981**, *79*, 465.

202. Drummond, C.J.; Grieser, F.; Healy, T.W. *Faraday Discuss. Chem. Soc.* **1986**, *81*, 95.

203. Warr, G.G.; Evans, D.F. *Langmuir* **1988**, *4*, 217.

204. Zinsli, P.S. *J. Phys. Chem.* **1979**, *83*, 3223.

205. Sabaté, R.; Gallardo, M.; de la Maza A.; Estelrich, J. *Langmuir*, **2001**, *17*, 6433.

206. Havelcová, M.; Kubát, P.; Němcová, I. *Dyes Pigments* **2000**, *44*, 49.

207. Siu, H.; Duhamel, J. *J. Phys. B* **2008**, DOI: 10.1021/jp801105q.

208. Kurucsev, T. *J. Chem. Edu.* **1978**, *55*, 128.

209. Adhikari, R.; Saha, S.K. *Z. Phys. Chem.* **2005**, *219*, 1373.

210. Dye, J.L.; Nicely, V.A. *J. Chem. Edu.* **1971**, *48*, 443. (The program has been updated in 1992)

211. Fulton, R.L.; Gouterman, M. *J. Chem. Phys.* **1964**, *41*, 2280.

212. Fornasiero, D; Kurucsev, T. *J. Chem. Soc., Faraday Trans, 2*, **1986**, *82*, 15.

213. Gianneschin, L.P.; Kurucsev, T. *J. Chem. Soc. Faraday Trans, 2*, **1976**, *72*, 209.

214. Gianneschin, L.P.; Cant., A; Kurucsev, T. *J. Chem. Soc. Faraday Trans 2*, **1977**, *73*, 664.

215. Valdes-Aguilera, O.; Neckers, D.C. *J. Phys. Chem.* **1988**, *92*, 4286.

216. Rohatgi-Mukherjee, K.K *Ind. J. Chem.* **1992**, *31*, 500.

Chapter 5

Electrochemical Studies of Progressively Alkylated Thiazine Dyes on the Glassy Carbon Electrode

5.1 Introduction and Review of the Previous Works

Cyclic voltammetry (CV) is perhaps the most powerful electroanalytical technique for the study of electroactive species. Various electrochemical aspects of photogalvanic solution during the photochemical reaction have been studied successfully by many workers with the aid of this technique. The ease of the measurement has also resulted in extensive use of the technique.

Electrochemical properties of rhodamine B by cyclic voltammetry at fixed and rotating disk electrode were studied in past by Austin et al. [1]. During electrode modification, the surface coating was deposited by voltage cycling and formed only when the anodic potential exceeded 1.24V, at which stage rhodamine B was deethylated and converted to rhodamine 110. This was then reversibly oxidized to form the surface modifying species. The prominent oxidation and reduction peaks were observed at 1.18 and 1.10V respectively in the cyclic voltammogram of rhodamine B at an unmodified SnO_2 glass electrode, which were suppressed by the surface modification. Rotating disk measurement gives a value of $3.2 \pm 0.2 \times 10^{-6}$ cm^2sec^{-1} for the diffusion co-efficient of 9.6×10^{-4}M rhodamine B in aqueous 0.05 M H_2SO_4. Cyclic voltammetric measurement gives a value of 1×10^{-2} cm sec^{-1} as the rate constant of quasi-reversible oxidation of rhodamine B which occurs around 1.18V at a SnO_2 glass electrode. Bauldrey and Archer [2] have reviewed the literature on the electrochemical and non electrochemical modification of the electrode surfaces and have proposed a mechanism for the electrochemical deposition of layers of thionine and related dyes using the information gained from cyclic voltammetric studies of these systems. Quickenden and Bassett [3] have studied the anodic deposition of the dye from aqueous rhodamine B solution to gold electrodes and found that substantial deethylation occurred during the deposition process and that the electrodes thus coated possessed enhanced photosensitivity. Bowen [4] has examined rhodamine B solution by cyclic voltammetry using Pt electrode and also determined the electron transfer rate constant for the Fe^{3+}/Fe^{2+} couple at rhodamine B coated Pt electrode by rotating disk method. However, the author did not determine the electrodic rate constants for electron transfer to and from rhodamine B at such electrodes.

The cyclic voltammetric behaviour of chloropromazine (CPZ) at a carbon paste electrode in aqueous 0.1M HCl showed two anodic waves with peak potentials

of +0.66 and +0.99V vs. SCE, corresponding to the oxidation of CPZ to its cation radical (CPZ^{+}) and subsequently to its dication (CPZ^{2+}) [5,6]. Upon the scan reversal only the cation radical is found to be sufficiently stable to yield a cathodic wave. The dication reacts very rapidly in this medium, so that the reduction of dication is not observable even at scan rates upto 50 V/s.

In general, chemical or electrochemical oxidation of N-substituted phenothiazine in aqueous solution has been shown to yield the corresponding sulphoxides through the formation of mono-cations which are prone to facile hydrolysis in neutral and less acidic medium as compared to that in more acidic media [7]. On the other hand, a linear dependence of voltammetric peak current on the square root of the scan rates suggests that the cyclic voltammetric behaviour of thionine, which is attributed to two electron reduction of thionine to leucothionine, is of the diffusion type [8,9]. Quickenden and Harrison [10] studied electrochemical properties of thionine by cyclic voltammetry at uncoated and thionine coated photoelectrodes. Examining the cyclic voltammograms obtained during the deposition of thionine on Au and SnO_2 electrodes, they observed that the height of the characteristic thionine oxidation and reduction peaks increased with the number of cycles to asymptotic limits after about 70 cycles in the case of a Au electrode and after 500 cycles in the case of SnO_2. The areas within the voltammograms similarly reach plateu values. Because the areas, $\left(\int Idt\right)$, I being the current and t the time, are also independent of cycle speed, it can be concluded that complete oxidation and reduction of the electroactive species occur during each cycle, thus validating the use of areas under peaks for determining layer thickness.

During the cyclic deposition process on Au, the thionine reduction and leucothionine oxidation peaks which are originally at 0.43 and 0.49V respectively, shift in turn to 0.49 and 0.54V, and a small shoulder appears at about 0.43V. However, during the deposition on SnO_2, the thionine reduction peak at 0.435V does not shift. But the oxidation peak moves from 0.535 to 0.550V, and the shoulder on the reduction peak appears only temporarily during the middle stage of the deposition. Albery et.al.[11] observed that the reduction of thionine on clean Pt-electrode was reversible whereas on the coated electrode it was nearly reversible. From the measurement of the kinetic parameters for different electrodes, they concluded that

the electrochemical rate constant was decreased for electrodes coated at higher voltages and for longer times. In particular, there was a significant reduction in rate constant for electrodes coated at 1.4V or above for periods longer than one hour.

The reduction of methylene blue was studied by Wopschall and Shain [12] to test the theory of cyclic voltammetry for the case in which the product of the electrode reaction was strongly adsorbed. A brief investigation of the mechanism of two electron electrode reduction using both aqueous ethanol and aprotic solvent systems, indicated that the reduction probably proceeded through successive one electron charge transfer, with a rapid reversible protonation interposed between the charge transfers. The intermediate appeared to be more easily reduced than methylene blue.

In a study on electrochemical aspects of reaction between leucodye and Fe^{+3} in dye based photogalvanic systems, the authors [13,14] examined the electrochemical reduction of thionine, methylene blue and other alkylated thionine in the presence of Fe^{+3} in terms of catalytic regeneration mechanism. The catalytic current due to the homogeneous chemical reaction between progressively alkylated leucothiazine dyes and Fe^{+3} have been used to estimate rate constants of the coupled chemical reactions.

Chemical modification of electrodes is a major area of current interest in electroanalytical chemistry and photoelectrochemistry. Techniques such as covalent attachment or casting of polymer films on electrodes are widely employed as a means of modification. In electrochemical and photoelectrochemical studies of dye incorporated clay modified electrode, Kamat [15] observed that clay modified electrode exhibits a quasi-reversible oxidation wave (E_{pa} = 0.280V, E_{pc} = 0.190V vs SCE) which is comparable to the reversible wave of thionine in aqueous solution (E_{pa} = 0.265V, E_{pc} = 0.205V vs SCE). This shows that the electrochemical identity of the dye has been retained in the clay film. The electrochemical behaviour was similar to one observed with Albery's [11] thionine coated electrode. Presence of polyvinyl alcohol and colloidal Pt in the clay film were found to be critical in attaining better electrochemical activity of clay modified electrodes. In agreement with the work reported earlier [16], only a fraction of the incorporated dye was found to be electroactive in the clay film.

The dependence of the peak current on the square root of the scane rates was linear, suggesting that the observed cyclic voltammogram of SnO_2/clay-thionine as diffusion type. Normally, one would have expected a surface wave for these modified electrodes. The diffusion type cyclic voltammetric behaviour observed in the above systems suggests that the charge transport within the film is limited either by the diffusion of the electroactive dye to the electrode surface or by an electron hopping process within the clay film [15]

In addition to the clay minerals another potential inorganic modifier is zeolite. Recent reviews on the material science aspects of the zeolites and the use of zeolites to coat electrodes [17,18] have included discussions on the use of and interest in zeolite layers on electrodes.

Asakawa et al. [19] also successfully applied CV to evaluate the micelle diffusion coefficients of fluorocarbon surfactants using (ferrocenyl methyl) trimethyl ammonium bromide (FcTAB). The growth behaviour of micelles of cetyltrimethyl ammonium bromide (CTAB) was examined by Hasan and Yakhmi [20] by using cyclic voltammetry. The changes in the geometry of aggregate were examined by monitoring the changes in the self-diffusion coefficient of micelles. Temperature dependence of the diffusion coefficient of 1,1'-ferrocenedimethylenol [$Fe(MeOH)_2$] and 2,2,6,6-teramethyl-1-piperidinyloxy (TEMPO) in aqueous solution and in poly(n-isopropyl acryl amide-co-acrylic acid) NIPA-AA gels in their sollen state was studied by using steady-state valtammetry and chronoamperometry [21].

Mahajan et al. [22] also studied the effect of monomeric and polymeric glycol additives on micellar properties of two non ionic surfactants, tween 20 and tween 80. They determine the cmc of the surfactants by plotting peak current (I_p) versus [surfactant].

An understanding on the mechanism of the charge transport, control of the pore dimensions to enhance transport properties, and complete elucidation of the role of the electrolyte in ion exchange reaction and charge conduction are absolutely required.

5.2 Electrochemistry of Dyes

Apart from their potential applications in harvesting solar energy via photochemical and photoelectrochemical means, both thiazine and oxazine dyes are

finding increasing applications in the field of electrocatalysis of electrochemical redox process. The electrochemical reactions of progressively alkylated thiazine dyes to corresponding leucodyes at the stationary electrode in the presence of Fe^{+3} ions may be described by what is called "catalytic regeneration mechanism", according to which an initial electroactive species is regenerated by the homogeneous chemical reaction [23,24]. The peak potentials (E_{pa} and E_{pc}) are not sensitive to scan rates and ΔE_p's do not vary up to a scan rate of 300 mVS^{-1} except for azure C. This suggests that the electrode processes are very fast and quasi-reversibility is apparent only in azure C. However, chemically modified electrodes by phenoxazine dyes have been shown to be useful in electrocatalytic oxidation of the co-enzyme NADH in the context of enzyme based biosensors. At least two kinetic parameters are of crucial importance, one of them relates to the electron transfer kinetics between the adsorbed or bound mediators (dye miolecules) and the substrate electrode and the other is the rate constant of the chemical redox reaction between NADH and the mediators. For efficient electrocatalysis to proceed both the kinetics must be fast. Some studies on phenoxazine dyes have been reported in the literature where slowest reaction with k around 10 lit. $mol^{-1}s^{-1}$ was found for adsorbed nile blue, having $E^{0'}$ = - 0.42V versus SCE, i.e., for the redox potential difference between $E^{0'}$ of mediator and NADH couples of 0.14V. The fastest reaction with k exceeding 10^4 lit. $mol^{-1}s^{-1}$ proceeded with adsorbed meldola blue, characterized by $E^{0'}$ = - 0.175V and thus with a redox potential difference of 0.39 V. Because of the large slope of log k versus E, exceeding 12 V^{-1} as can be deduced from the data presented in a previous report [25], it seems very desirable to tune the redox potential of the mediator to an appropriate extent towards the positive directive. For this aim, two approaches are known. Firstly, the redox potential of any mediator redox couple can be shifted by the chemical modification of the mediator structure. Another approach to shift in the redox potential is the inclusion of any mediator in some inorganic matrix. The introduction of a naphthoyl group into the structure of nile blue shifts the redox potential from - 0.43 to - 0.21 V versus SCE at pH 7 resulting in an increase of the rate constant with NADH from 10 to 10^4 or 10^5 $lit.mol^{-1}S^{-1}$. A simple conversion of an amino group to a naphthamide group in toluidine blue (TB) results in a shift of $E^{0'}$ from - 0.285 to - 0.135 V versus SCE. However, the above values of rate constants have been estimated following the method of extropolation of the peak separation to the zero value of

the peak current i.e., to zero coverage of the electrode [26]. This method always give higher values of the constants compared to the method usually applied in determining the heterogeneous rates of electrode processes [27] In this chapter results of cyclic votammetric experiments with progressively alkylated thiazine dyes (viz. thionine, azure A, azure B, azure C, methylene blue) in aqueous, aqueous-alcohol and nonionic micellar media are reported. The molecular structures of thiazine dyes are given in Figure 1.4 (chapter 1).

5.3 Experimental

Cyclic voltammetric experiments with the five thiazine dyes, viz. thionine, azure A (AzA), azure B (AzB), azure C (AzC) and methylene blue (MB) are carried out in water, water-ethanol mixture and in triton X-100, a non-ionic surfactant, at $25^0C \pm 1^0C$ to understand their electro-chemical behavior on glassy carbon electrode (GCE). All the dyes are supplied by Aldrich Chemical Co. (USA) and method of purification, used for thiazine dyes are presented in Chapter 4.

Cyclic voltammetric experiments are carried out employing BAS cyclic voltammograph (USA, Model CV-27), fitted with a three undivided electrode cell and a Houston X - Y recorder (Model-100). The experiments are performed taking 25 ml dye solution in the presence of 0.1M H_2SO_4 in the said media as a supporting electrolyte with one working GCE (MF - 2012), one Pt - auxiliary electrode and a saturated calomel (SCE) reference electrode at $25^0C \pm 1^0C$. All solutions are purged with pure nitrogen before the experiment at least for 20 minutes.

Cyclic voltammograms of the dye solutions (5×10^{-5} M) are recorded in water, water-ethanol mixture and triton X - 100 (0.001 M) as mentioned at various scan rates up to 300 mVs^{-1}. Cyclic voltammograms of the concentrated (1×10^{-4}M) dye solutions are also recorded at different scan rates using 0.01M KCl as supporting electrolyte at various pH. Surface area of the electrode is 0.0804 cm^2.

5.4 Results and Discussion

In solution the dyes form dimers and higher aggregates at high concentrations ($\sim 10^{-4}$ M). Ahmed [28] calculated the dimerization constant values of the dyes in water and water-ethanol mixtures at different temperatures from

spectroscopic data. In aqueous medium at 30°C the values are 1.76 x 10^{-3}, 2.35 x 10^{-3}, 3.38 x 10^{-3}, 6.25 x 10^{-3} and 3.68 x 10^{-3} lit.mol^{-1} whereas, in 5% alcohol, these values are 1.45 x 10^{-3}, 1.86 x 10^{-3}, 2.13 x 10^{-3}, 4.58 x 10^{-3} and 2.46 x 10^{-3} lit.mol^{-1} respectively. Aggregation of the dyes is an important factor for the interpretation of the cyclic voltammetric data.

All the dyes are reduced to the colourless leuco-dyes on forward scan (Figure 5.1 - 5.10) [8]. The systems undergo reversible electrode reaction on the GCE in 0.1M H_2SO_4 (supporting electrolyte), up to scan rate 100 mVS^{-1} in water, water-ethanol and triton X-100 media. Other criteria, namely separation of the peak potentials and the half peak potential values are also in conformity with the reversibility of the system up to the above scan rate. The values of cyclic voltammetric data are given in Table 5.1 - 5.5. The values of anodic peak current (i_{pa}) and cathodic peak current (i_{pc}) should be identical for a simple reversible (fast) couple; i.e. ideally $(i_{pa}/i_{pc}) = 1$. But this ratio (shown in Table 5.1 - 5.5) deviates from unity even at the slow scan rates in the present systems. However, the deviation becomes less if the calculation is done using the modified equation as suggested by Nicholson [29] and Gary [23]

$$\frac{i_{pa}}{i_{pc}} = \frac{(i_{pa})_0}{(i_{pc})_0} + \frac{0.485(i_\lambda)_0}{i_{pc}} + 0.086 \qquad (5.1)$$

where $(i_{pc})_0$ is the peak current for the forward process; $(i_\lambda)_0$ is the absolute current at the switching potential; $(i_{pa})_0$ is the uncorrected return peak current measured from the current axis. The values for $i_{pa}/i_{pc} < 1$, which decreases further with increasing, scan rates for the thiazine dyes suggest that the electrogenerated lucodyes are involved in the reactions which prevent their reoxidation upon scan reversal.

Cyclic voltammetric measurements of 5 x 10^{-5}M dye solution in the presence of 0.1M H_2SO_4 are consistent with two electron reversible redox couples of dye/leucodye pairs up to scan rate 100 mVs^{-1}. The formal potential values for the two electron dye/leucodye couples are found to be 0.205, 0.175, 0.207, 0.281 and 0.196V (average values for scan rate between 5-100 mVs^{-1}) for Th, AzC, AzA, AzB and MB respectively in aqueous medium. But the value of 0.058/ΔE is rather low for

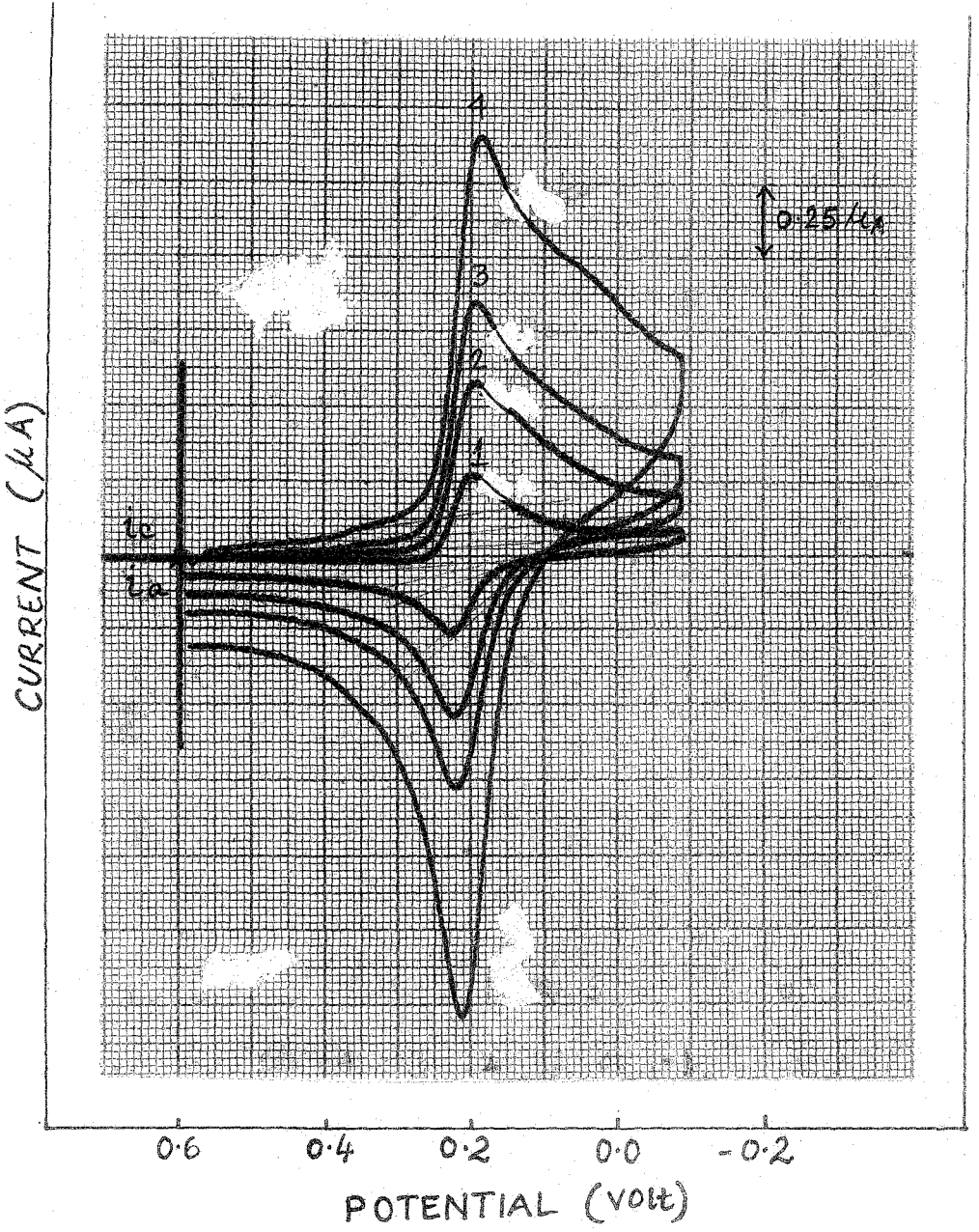

Figure 5.1 Cyclic Voltammograms of thionine (5×10^{-5}M) in water with scan rates [1 – 4],

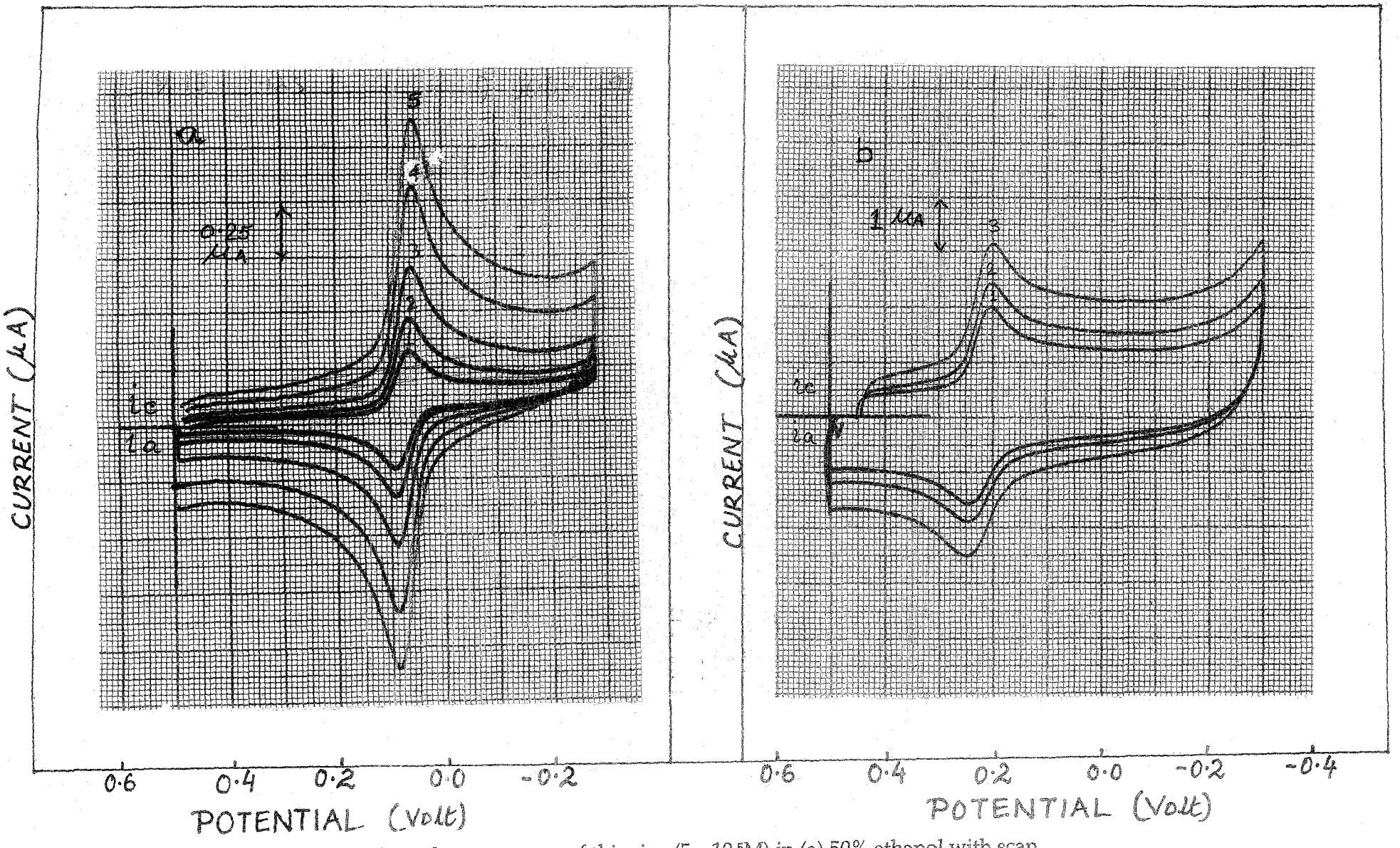

Figure 5.2 Cyclic Voltammograms of thionine (5×10^{-5}M) in (a) 50% ethanol with scan
5 1.5, 10, 20, 40 and 60 mVs^{-1} and (b) in 0.001M triton X-100 with scan

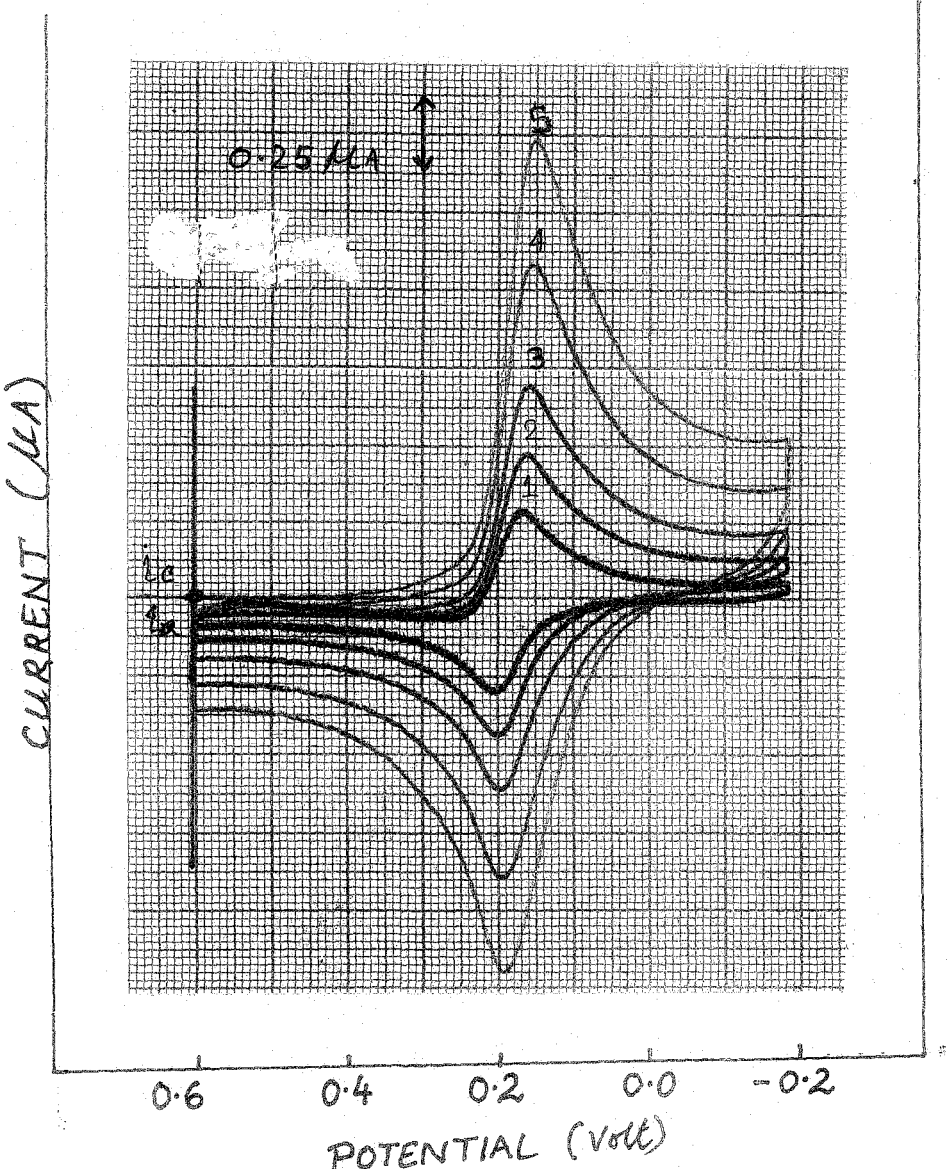

Figure 5.3 Cyclic Voltammograms of Azure C (5×10^{-5}M) in water with scan rates [1 – 5], 5, 10, 20, 40 and 60 mVs^{-1} in the presence of 0.1M H_2SO_4.

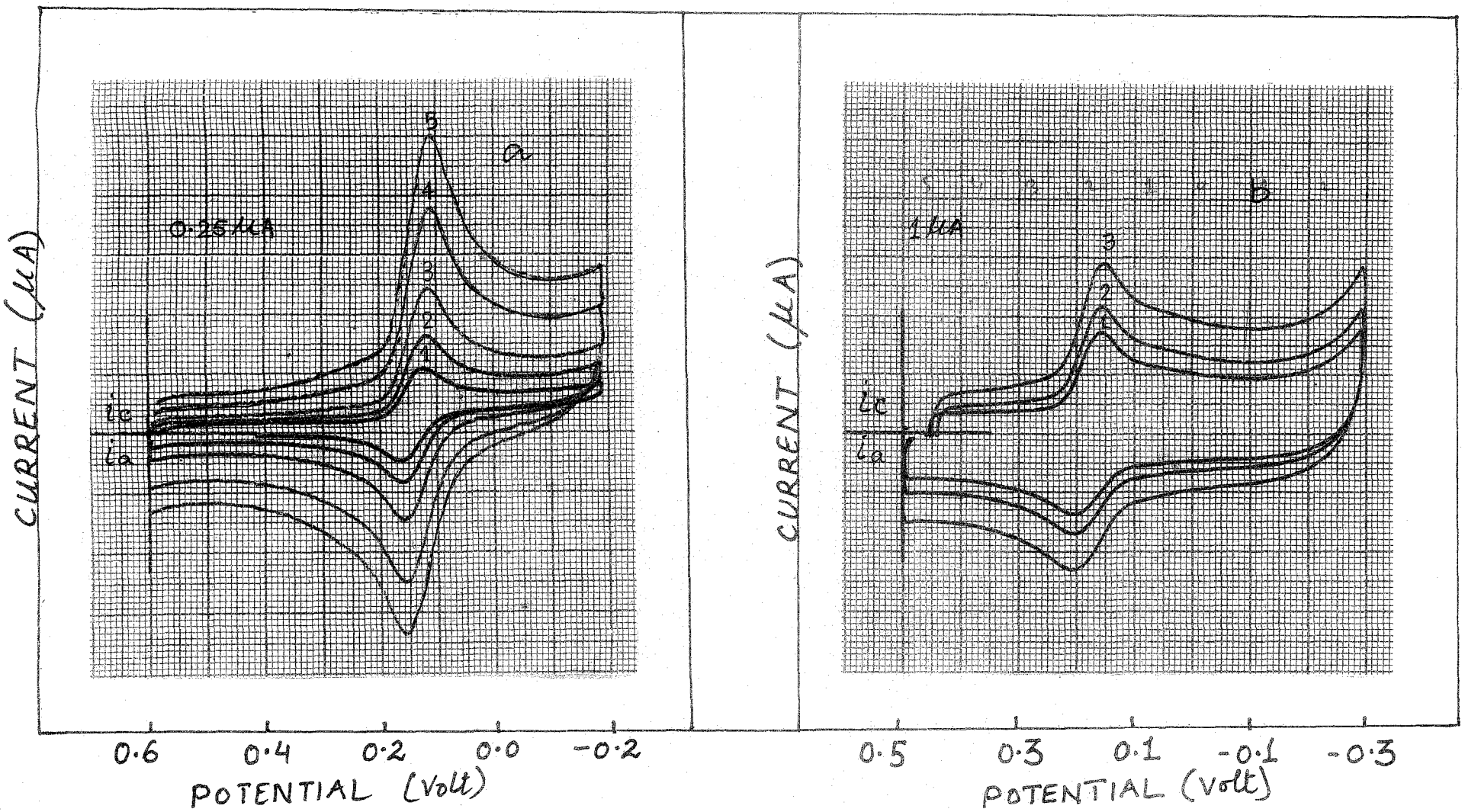

Figure 5.4 Cyclic Voltammograms of Azure C (5×10^{-5}M) in (a) 50% ethanol with scan rates [1 – 5] 5, 10, 20, 40 and 60 mVs^{-1} and (b) in 0.001M triton X-100 with scan rates [1 – 3] 150, 200 and 300 mVs^{-1} in the presence of 0.1M H_2SO_4.

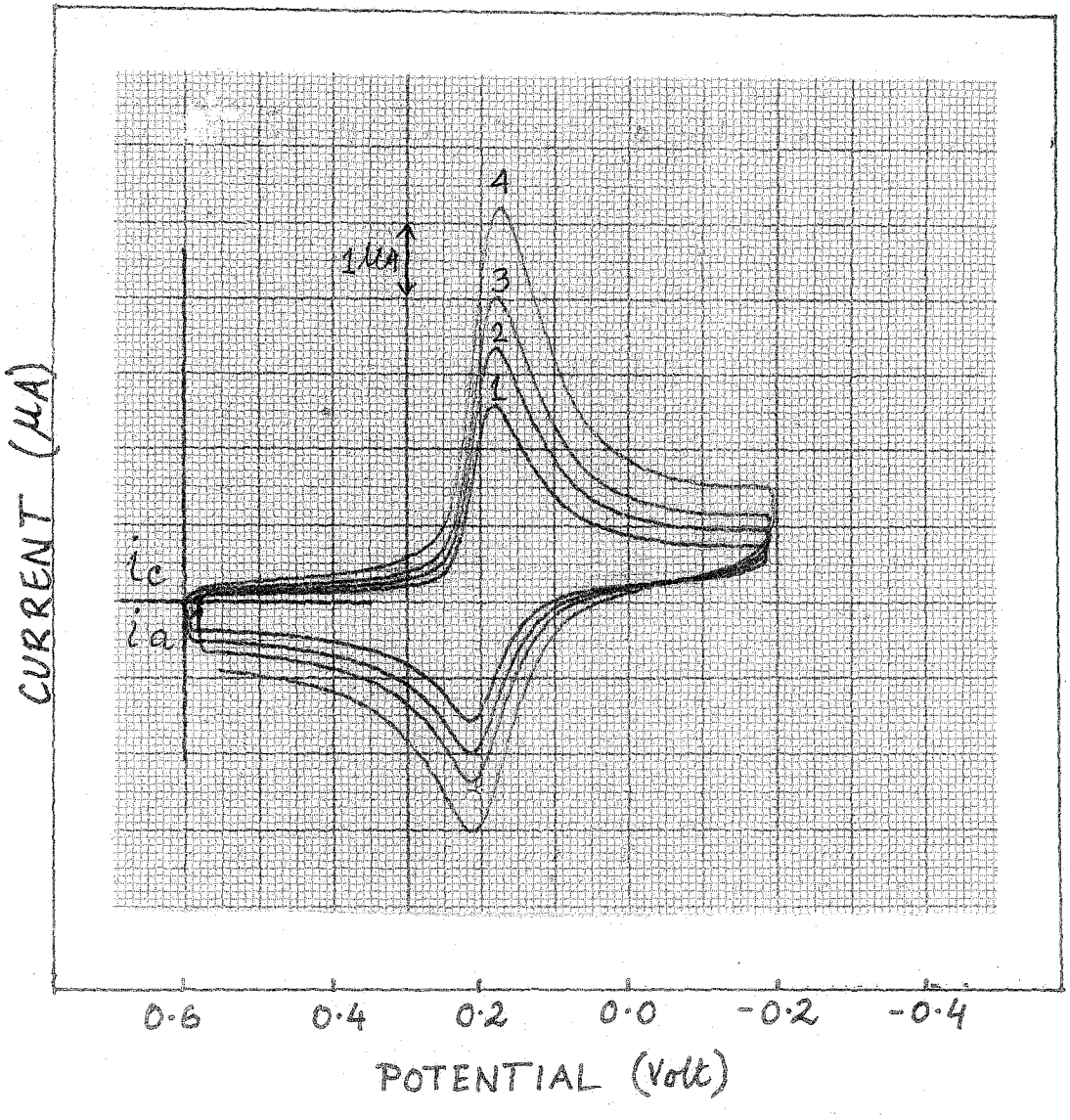

Figure 5.5 Cyclic Voltammograms of Azure A (5×10^{-5}M) in water with scan rates [1 – 4], 100, 150, 200 and 300 mVs^{-1} in the presence of 0.1M H_2SO_4

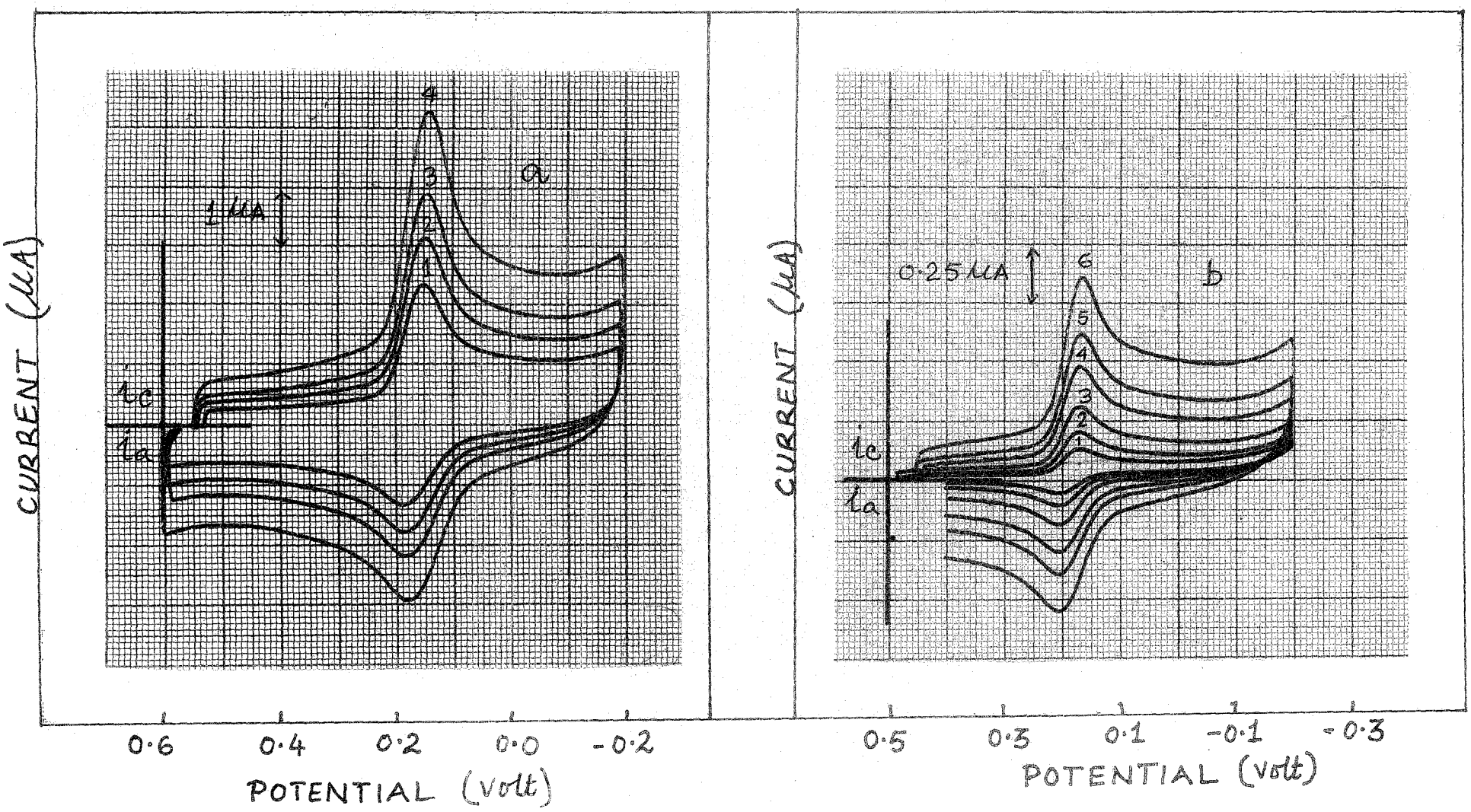

Figure 5.6 Cyclic Voltammograms of Azure A (5×10^{-5}M) in (a) 50% ethanol with scan rates [1 – 4 | 100, 150, 200 and 300 mVs^{-1} and (b) in 0.001M triton X-100 with

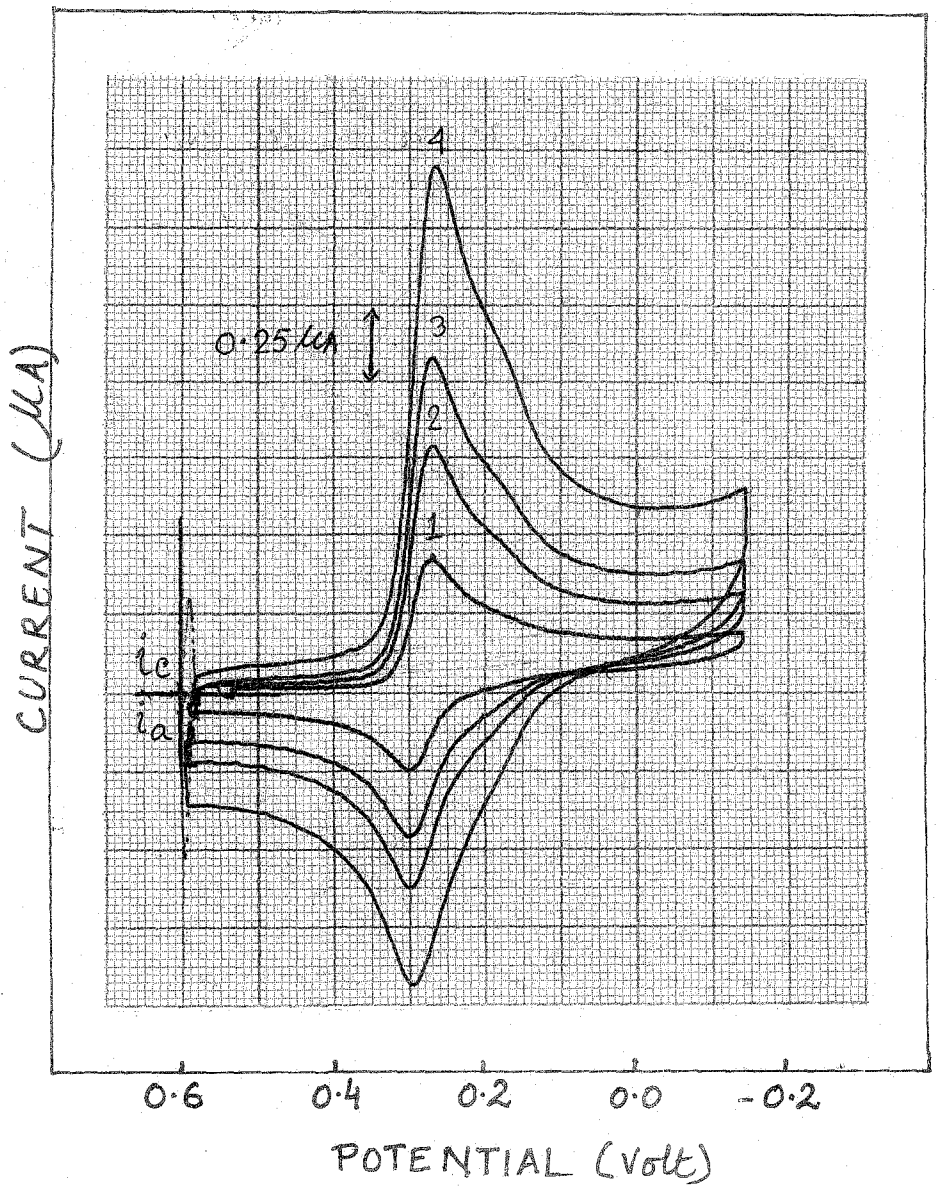

Figure 5.7 Cyclic Voltammograms of Azure B (5×10^{-5}M) in) in water with scan rates [1 –4],

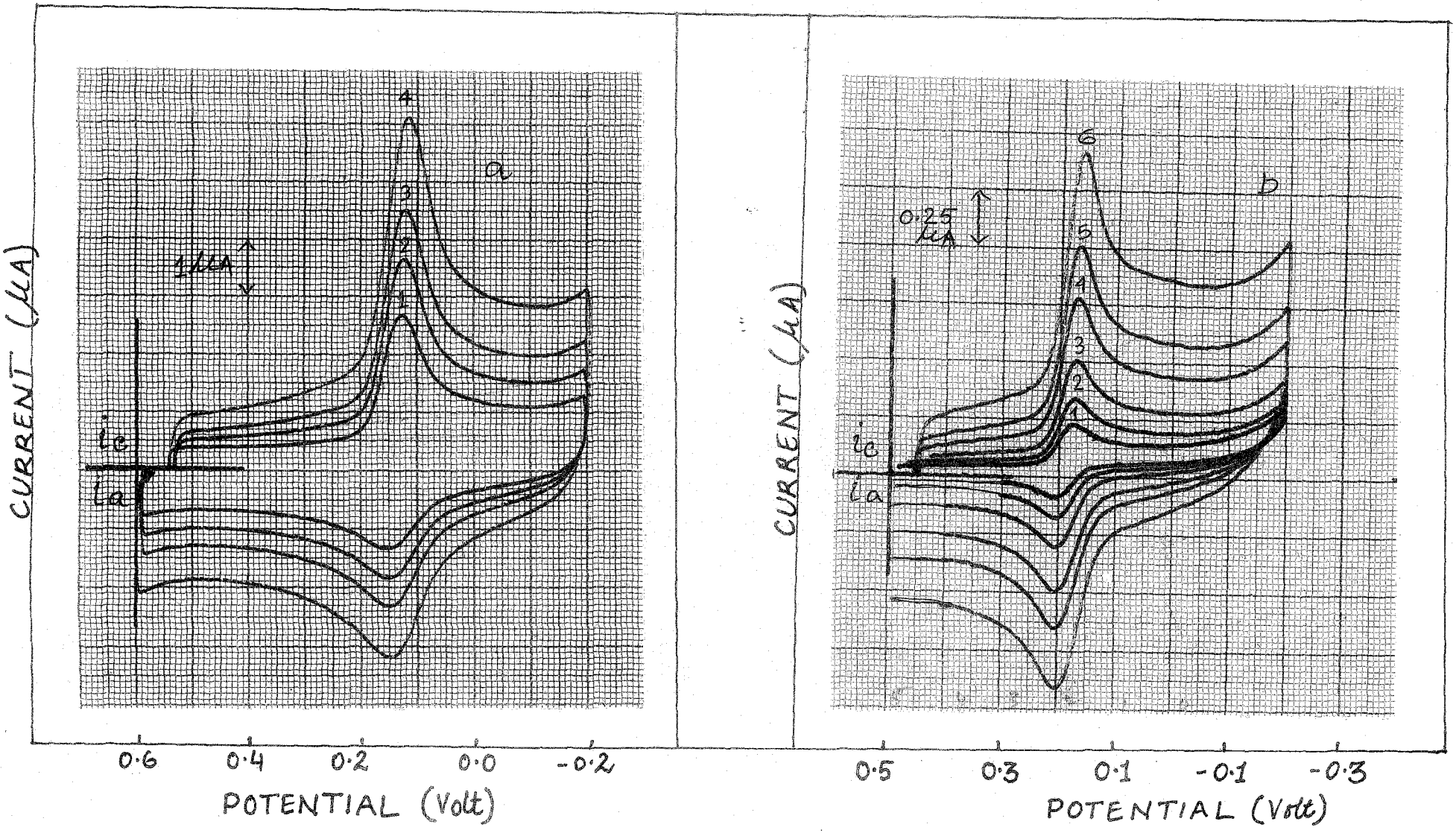

Figure 5.8 Cyclic Voltammograms of Azure B (5×10^{-5}M) in (a) 50% ethanol with scan rates [1 – 4] 100, 150, 200 and 300 mVs^{-1} and (b) in 0.001M triton X-100 with scan rates [1 – 6] 5, 10, 20, 40, 60 and 100 mVs^{-1} in the presence of 0.1M H_2SO_4

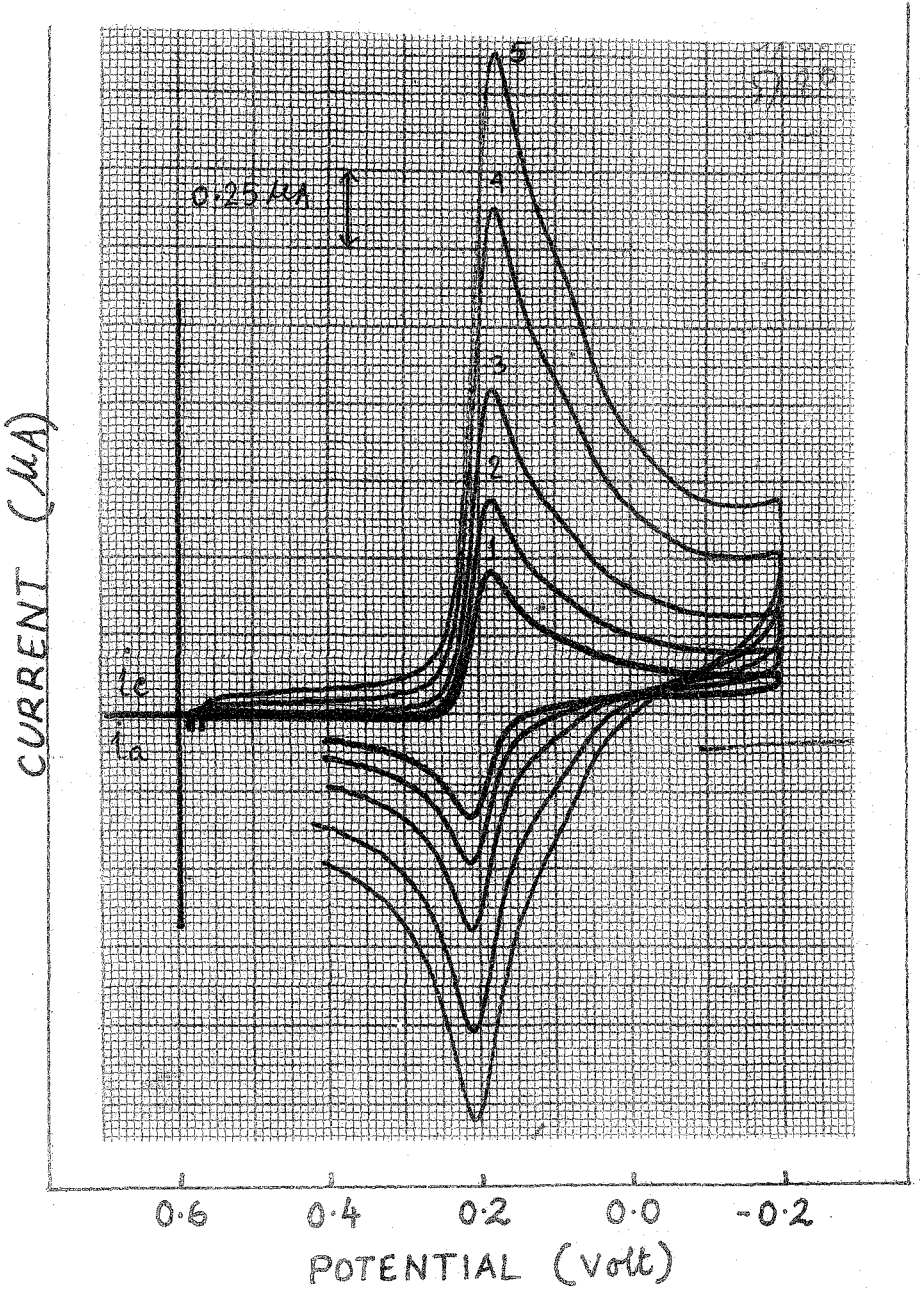

Figure 5.9 Cyclic Voltammograms of Methylene Blue (5×10^{-5}M) in) in water with scan rates [1 -5] 5, 10, 20, 40 and 60 mVs^{-1} in the presence of 0.1M H_2SO_4

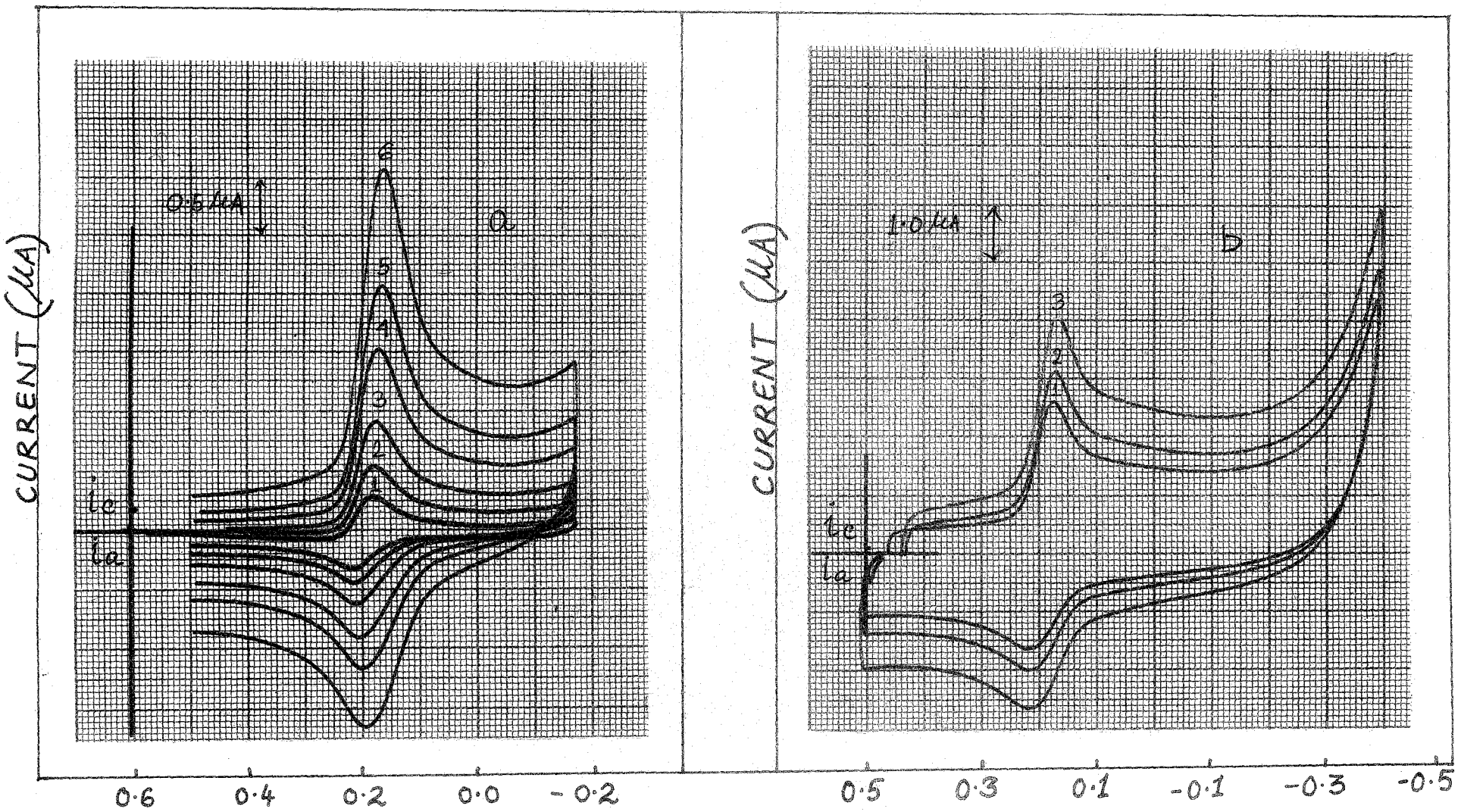

Figure 5.10 Cyclic Voltammograms of Methylene Blue (5×10^{-5}M) in (a) 50% ethanol with scan rates [1 – 6] 5, 10, 20, 40, 60 and 100 mVs^{-1} and (b) in 0.001M triton X-100

Table 5.1
Electrochemical data for cyclic voltammetry of 5 x 10^{-5}M Thionone in different media in the presence of 0.1M H_2SO_4

S.R.	E_{pa}	E_{pc}	ΔE_p	i_{pa}/i_{pc}	$E_{pc/2} - E_{pc}$	$I_{pc}v^{-1/2}$	$0.058/\Delta E_p$
			Water				
5	0.225	0.195	0.030	0.87	0.025	3.93	1.93
10	0.223	0.193	0.030	0.89	0.026	5.50	1.93
20	0.220	0.190	0.030	0.90	0.027	5.32	1.93
40	0.220	0.190	0.030	0.98	0.030	6.25	1.93
60	0.215	0.185	0.030	0.93	0.032	6.15	1.93
100	0.215	0.185	0.030	0.95	0.032	6.65	1.93
150	0.213	0.183	0.030	0.90	0.033	7.49	1.93
200	0.213	0.183	0.031	0.97	0.033	7.72	1.93
300	0.210	0.180	0.031	0.98	0.035	8.59	1.93
			EtOH – Water (50% v/v)				
5	0.190	0.160	0.030	0.87	0.027	3.93	1.93
10	0.190	0.160	0.030	0.90	0.027	3.88	1.93
20	0.190	0.158	0.032	0.91	0.028	4.07	1.81
40	0.192	0.155	0.037	0.91	0.032	4.32	1.57
60	0.192	0.155	0.037	0.81	0.036	4.61	1.57
100	0.193	0.152	0.041	0.80	0.038	4.75	1.41
150	0.193	0.150	0.043	0.79	0.042	4.90	1.35
200	0.194	0.150	0.044	0.74	0.042	5.15	1.32
300	0.195	0.148	0.047	0.72	0.045	5.57	1.23
			0.001M Triton X-100				
5	0.235	0.205	0.030	0.94	0.030	3.02	1.93
10	0.235	0.204	0.031	0.80	0.030	3.10	1.87
20	0.236	0.203	0.033	0.89	0.032	3.19	1.75
40	0.237	0.202	0.035	0.85	0.033	3.25	1.65
60	0.238	0.200	0.038	0.82	0.035	3.38	1.53
100	0.240	0.198	0.042	0.75	0.036	3.48	1.38
150	0.242	0.197	0.045	0.79	0.040	3.61	1.29
200	0.243	0.197	0.046	0.78	0.045	3.60	1.26
300	0.245	0.196	0.049	0.79	0.048	3.47	1.18

Table 5.2
Electrochemical data for cyclic voltammetry of 5 x 10^{-5}M Azure C in different media in the presence of 0.1M H_2SO_4

S.R.	E_{pa}	E_{pc}	ΔE_p	i_{pa}/i_{pc}	$E_{pc/2} - E_{pc}$	$I_{pc}v^{-1/2}$	$0.058/\Delta E_p$
				Water			
5	0.198	0.165	0.033	0.80	0.035	5.00	1.75
10	0.198	0.163	0.035	0.88	0.035	5.25	1.65
20	0.196	0.160	0.036	0.80	0.037	4.96	1.61
40	0.195	0.158	0.037	0.76	0.038	5.50	1.56
60	0.191	0.150	0.041	0.84	0.040	5.64	1.41
100	0.185	0.145	0.040	0.83	0.042	6.33	1.45
150	0.182	0.140	0.042	0.79	0.042	6.46	1.38
200	0.182	0.135	0.047	0.77	0.043	6.04	1.23
300	0.180	0.130	0.050	0.77	0.045	7.31	1.16
				EtOH – Water (50% v/v)			
5	0.162	0.118	0.044	0.89	0.040	3.21	1.32
10	0.158	0.116	0.042	0.83	0.041	3.25	1.38
20	0.156	0.113	0.043	0.87	0.043	3.28	1.35
40	0.153	0.110	0.043	0.83	0.044	3.50	1.35
60	0.152	0.108	0.044	0.72	0.045	3.99	1.32
100	0.151	0.107	0.044	0.69	0.045	4.11	1.32
150	0.150	0.105	0.045	0.65	0.047	4.39	1.29
200	0.150	0.103	0.047	0.61	0.049	4.70	1.23
300	0.150	0.100	0.050	0.57	0.050	5.12	1.16
				0.001M Triton X-100			
5	0.195	0.160	0.035	0.80	0.035	2.85	1.66
10	0.196	0.158	0.038	0.80	0.037	2.50	1.55
20	0.197	0.157	0.040	0.80	0.038	2.84	1.45
40	0.198	0.156	0.042	0.72	0.039	3.13	1.38
60	0.199	0.155	0.044	0.81	0.040	3.28	1.32
100	0.200	0.154	0.046	0.74	0.041	3.32	1.26
150	0.202	0.153	0.049	0.69	0.041	3.36	1.18
200	0.203	0.152	0.051	0.69	0.043	3.58	1.14
300	0.204	0.150	0.054	0.63	0.045	3.47	1.07

Table 5.3
Electrochemical data for cyclic voltammetry of 5 x 10^{-5}M Azure A in different media in the presence of 0.1M H_2SO_4

S.R.	E_{pa}	E_{pc}	ΔE_p	i_{pa}/i_{pc}	$E_{pc/2} - E_{pc}$	$I_{pc}v^{-1/2}$	$0.058/\Delta E_p$
				Water			
5	0.229	0.198	0.031	0.89	0.028	6.43	1.87
10	0.226	0.195	0.031	0.88	0.028	6.25	1.87
20	0.224	0.192	0.032	0.83	0.030	6.38	1.81
40	0.222	0.191	0.031	0.79	0.032	6.75	1.87
60	0.220	0.188	0.032	0.73	0.035	6.97	1.81
100	0.218	0.186	0.032	0.69	0.038	8.22	1.87
150	0.216	0.182	0.034	0.65	0.040	8.01	1.70
200	0.214	0.180	0.034	0.61	0.043	8.05	1.70
300	0.212	0.178	0.034	0.59	0.045	8.40	1.70
				EtOH – Water (50% v/v)			
5	0.205	0.175	0.030	0.90	0.030	3.92	1.93
10	0.206	0.172	0.034	0.84	0.030	4.15	1.70
20	0.207	0.170	0.037	0.77	0.032	4.60	1.57
40	0.208	0.168	0.040	0.66	0.035	5.12	1.45
60	0.210	0.167	0.043	0.62	0.038	5.32	1.35
100	0.212	0.165	0.047	0.58	0.038	6.01	1.23
150	0.213	0.160	0.053	0.51	0.040	6.59	1.09
200	0.214	0.155	0.059	0.48	0.042	6.93	0.98
300	0.215	0.150	0.065	0.44	0.043	7.49	0.89
				0.001M Triton X-100			
5	0.200	0.170	0.030	0.80	0.032	3.57	1.93
10	0.202	0.168	0.034	0.86	0.032	3.50	1.70
20	0.204	0.166	0.038	0.80	0.034	3.54	1.53
40	0.206	0.164	0.042	0.71	0.035	3.50	1.38
60	0.208	0.162	0.046	0.74	0.037	3.89	1.26
100	0.210	0.160	0.050	0.62	0.040	4.11	1.16
150	0.212	0.158	0.054	0.65	0.043	4.39	1.07
200	0.214	0.156	0.058	0.63	0.046	4.25	1.00
300	0.215	0.155	0.060	0.61	0.050	4.20	0.96

Table 5.4
Electrochemical data for cyclic voltammetry of 5 x 10^{-5}M Methylene Blue in different media in the presence of 0.1M H_2SO_4

S.R.	E_{pa}	E_{pc}	ΔE_p	i_{pa}/i_{pc}	$E_{pc/2} - E_{pc}$	$I_{pc}v^{-1/2}$	$0.058/\Delta E_p$
				Water			
5	0.215	0.183	0.032	0.84	0.028	6.78	1.81
10	0.215	0.182	0.033	0.81	0.030	6.75	1.76
20	0.214	0.181	0.033	0.75	0.032	7.27	1.76
40	0.212	0.180	0.032	0.61	0.032	7.75	1.81
60	0.210	0.180	0.030	0.61	0.035	8.20	1.93
100	0.205	0.175	0.030	0.63	0.036	9.01	1.93
150	0.200	0.170	0.030	0.65	0.037	9.56	1.93
200	0.197	0.165	0.032	0.66	0.038	10.06	1.81
300	0.195	0.160	0.035	0.65	0.040	10.97	1.66
				EtOH – Water (50% v/v)			
5	0.215	0.180	0.035	0.87	0.027	5.71	1.66
10	0.121	0.178	0.034	0.72	0028	5.50	1.70
20	0.210	0.174	0.036	0.60	0.030	5.85	1.61
40	0.205	0.170	0.035	0.53	0.032	6.75	1.66
60	0.200	0.160	0.040	0.52	0.032	6.55	1.45
100	0.195	0.155	0.044	0.52	0.034	7.59	1.45
150	0.180	0.140	0.040	0.44	0.035	8.27	1.45
200	0.178	0.135	0.043	0.43	0.036	8.95	1.35
300	0.175	0.130	0.045	0.41	0.038	9.32	1.29
				0.001M Triton X-100			
5	0.210	0.180	0.030	0.75	0.025	4.29	1.93
10	0.212	0.180	0.032	0.75	0.028	4.00	1.81
20	0.214	0.178	0.036	0.73	0.029	4.07	1.61
40	0.215	0.178	0.037	0.72	0.030	4.13	1.57
60	0.216	0.176	0.040	0.71	0.031	4.61	1.45
100	0.216	0.175	0.041	0.60	0.033	4.90	1.41
150	0.218	0.174	0.044	0.55	0.035	5.17	1.32
200	0.218	0.173	0.045	0.52	0.038	5.15	1.29
300	0.220	0.172	0.048	0.51	0.040	5.30	1.21

Table 5.5
Electrochemical data for cyclic voltammetry of 5 x 10^{-5}M Azure B in different media in the presence of 0.1M H_2SO_4

S.R.	E_{pa}	E_{pc}	ΔE_p	i_{pa}/i_{pc}	$E_{pc/2} - E_{pc}$	$I_{pc}v^{-1/2}$	$0.058/\Delta E_p$
				Water			
5	0.300	0.270	0.030	0.87	0.028	5.54	1.93
15	0.300	0.268	0.032	0.85	0.029	6.00	1.81
25	0.298	0.265	0.033	0.84	0.030	6.17	1.76
50	0.297	0.262	0.035	0.84	0.035	6.93	1.66
100	0.295	0.260	0.035	0.77	0.038	7.59	1.66
150	0.294	0.260	0.034	0.73	0.040	8.01	1.70
200	0.293	0.258	0.035	0.66	0.042	8.05	1.66
300	0.293	0.257	0.036	0.58	0.045	8.04	1.61
				EtOH – Water (50% v/v)			
5	0.165	0.135	0.030	0.80	0.030	3.57	1.93
10	0.165	0.132	0.033	0.82	0.032	4.25	1.76
20	0.165	0.130	0.035	0.81	0.034	4.78	1.66
40	0.160	0.127	0.033	0.78	0.034	5.50	1.76
60	0.160	0.125	0.035	0.76	0.038	6.04	1.66
100	0.150	0.120	0.030	0.61	0.042	6.96	1.93
150	0.148	0.116	0.032	0.59	0.043	7.24	1.81
200	0.146	0.112	0.034	0.53	0.044	7.49	1.70
300	0.145	0.110	0.035	0.52	0.045	7.31	1.66
				0.001M Triton X-100			
5	0.205	0.175	0.030	0.85	0.032	2.50	1.93
10	0.203	0.173	0.030	0.81	0.032	2.75	1.93
20	0.201	0.170	0.031	0.80	0.035	2.66	1.87
40	0.200	0.168	0.032	0.78	0.036	2.88	1.81
60	0.198	0.163	0.035	0.68	0.038	2.97	1.66
100	0.196	0.159	0.037	0.66	0.042	3.08	1.57
150	0.196	0.159	0.037	0.65	0.044	3.36	1.57
200	0.194	0.154	0.040	0.66	0.047	3.36	1.45
300	0.194	0.152	0.042	0.61	0.048	3.29	1.38

Table 5.6

Values of Diffusion Coefficient of the dyes in different medium
D.C. x 10^6 (cm^2s^{-1})

Dye	Water	50% EtOH	TX – 100
Thionine	3.05	1.80	1.10
Azure C	2.66	1.16	0.87
Azure A	4.40	2.29	1.36
Azure B	4.13	2.47	0.76
Methylene Blue	5.70	3.70	1.80

all dyes. This deviation is more prominent in water-alcohol and micellar media. Some early examination of Wopschall et al. [12] also found a low value (1.66) of this parameter contrarary to the coulometric value of 2 for methylene blue, and interpreted it as due to the result of two successive one electron reversible charge transfer, with fast protonation of the intermediate to form a species which is more easily reduced than methylene blue.

Separation between the peak potentials (ΔE_p) increases slowly with the increases in scan rate because the dye/leucodye couple deviates more and more from the reversibility. Quasi-reversibility of the electrode processes in the present system is also apparent from the difference between the peak potentials (ΔE_p) and the half peak potential ($\Delta E_{pc} - \Delta E_{p/2}$), where in an ideal reversible reaction these values should be 30 mV [31]. However, appreciable deviation of ΔE_p from ideal reversible value is apparent only at very high scan rates, which suggests that electrodic processes involved are very fast.

The plots of i_{pc} as a function of $V^{1/2}$ (i_{pc} measured for forward scan of the first cycle) indicate that the variation of the current is linear with $V^{1/2}$ upon a scan rate of ~100mVs^{-1} and the line drawn through the experimental points at slow scan rates passes through the origin (Figure 5.11 - 5.15). At higher scan rates the points deviate from the straight line in all cases studied. The foregoing observation also indicates that the electrode process is diffusion controlled at slow scan rates.

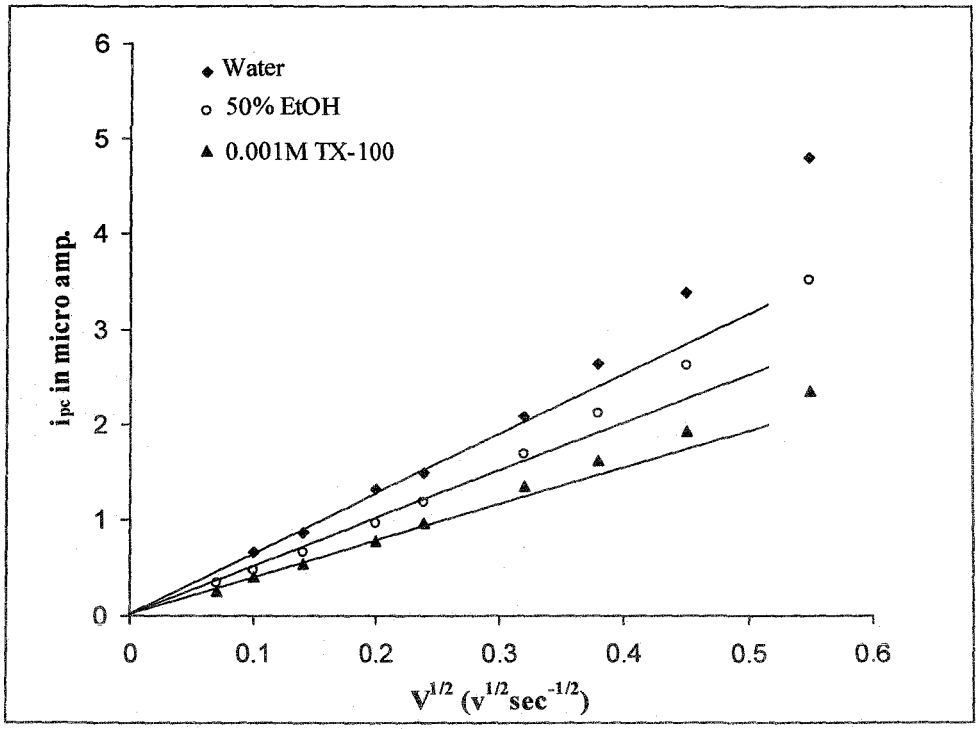

Figure 5.11 Plot of cathodic peak currents as a function of (scan rates)$^{1/2}$ for thionine (5 x 10^{-5} M) in different solvents at GCE.

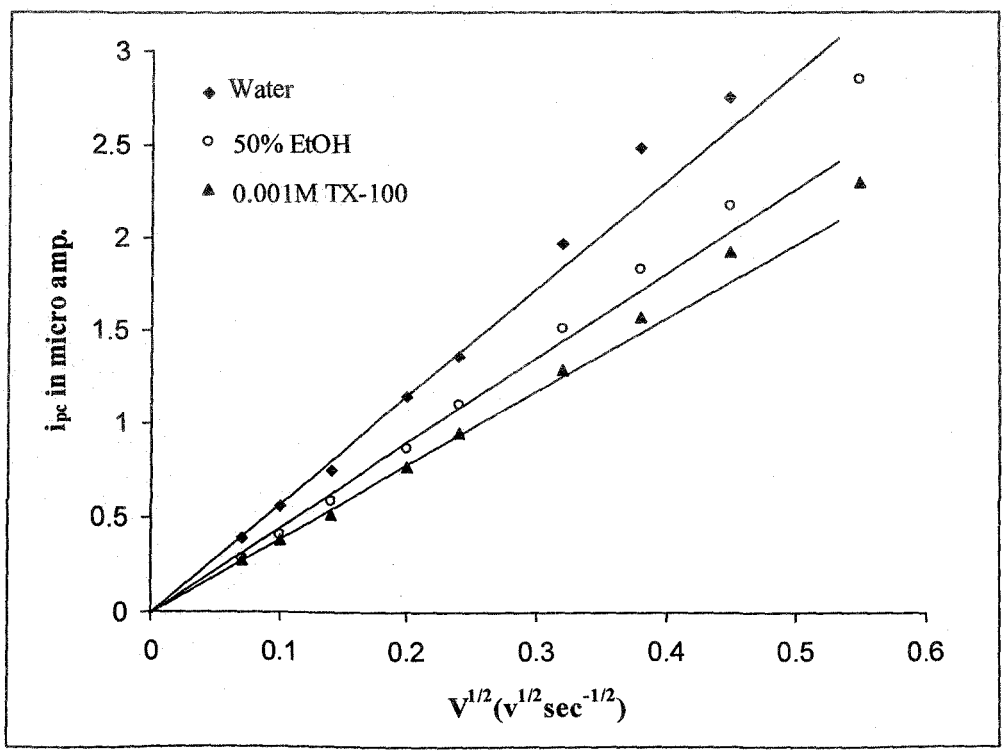

Figure 5.12 Plot of cathodic peak currents as a function of (scan rates)$^{1/2}$ for Azure C (5 x 10^{-5} M) in different solvents at GCE.

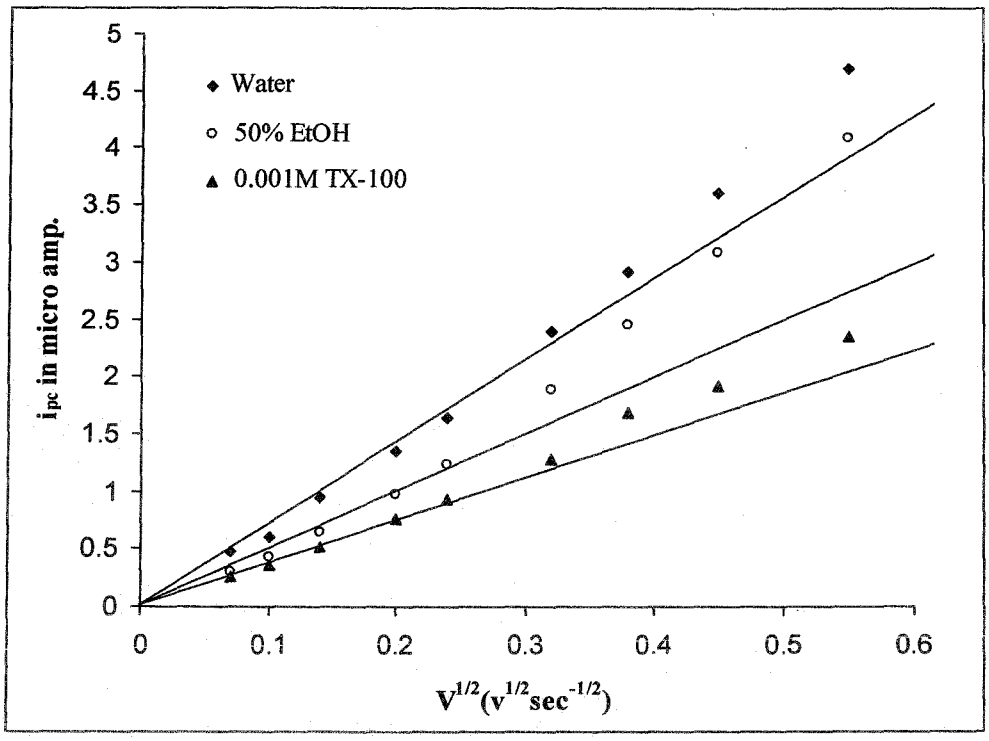

Figure 5.13 Plot of cathodic peak currents as a function of (scan rates)$^{1/2}$ for Azure A (5 x 10^{-5} M) in different solvents at GCE.

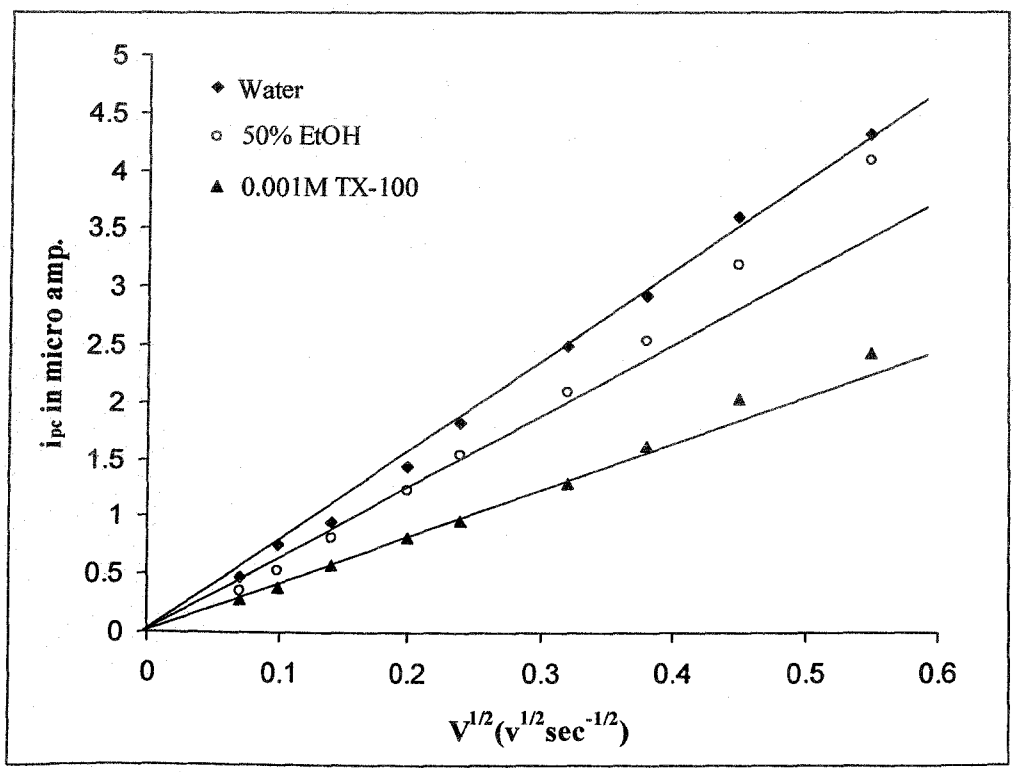

Figure 5.14 Plot of cathodic peak currents as a function of (scan rates)$^{1/2}$ for Azure B (5 x 10^{-5} M) in different solvents at GCE.

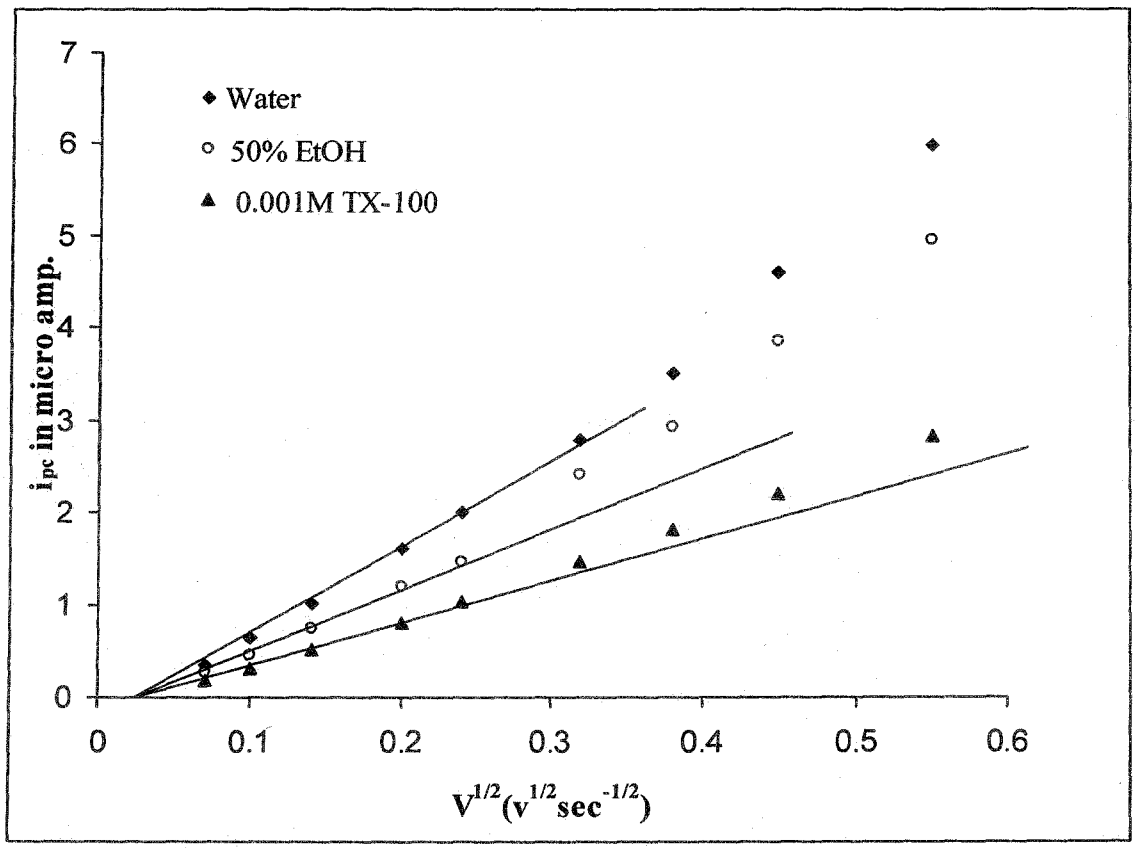

Figure 5.15 Plot of cathodic peak currents as a function of (scan rates)$^{1/2}$ for Methylene Blue (5×10^{-5} M) in different solvents at GCE.

The effective diffusion coefficient values of the dyes in water, water/alcohol and triton X-100 are summarized in Table 5.6. The values have been calculated using Randles Seveik equation [32] for one electron reversible process

$$i_p = (2.69 \times 10^{-5}) n^{3/2} A D^{1/2} V^{1/2} C_0 \qquad (5.2)$$

where i_p is the peak current (in amperes), A is the area of the electrode (in cm^2), D is the diffusion coefficient (in cm^2sec^{-1}), C_0 is the concentration (in vol/cm^3), V is the potential (in Volt/sec), n is the number of electrons transferred in the redox process. Finally the coefficients are derived from the slope of the curves plotting i_{pc} vs. $V^{1/2}$ (Figures 5.11 - 5.15) up to the scan rate $20mVs^{-1}$. The values for methylene blue and thionine are 5.70×10^{-6} cm^2s^{-1} and 3.05×10^{-6} cm^2s^{-1} respectively on GCE. A value of 7.60×10^{-6} cm^2s^{-1} for MB and 2.28×10^{-6} cm^2s^{-1} for thionine were reported by previous workers measured at Pt-wire type HMDE and indium doped SnO_2 electrode [13,12]. AzC has the lowest value (2.66×10^{-6} cm^2s^{-1} in water) in the present study. And there is no systematic change in the diffusion coefficient values with the progressive alkylation. However the preliminary study shows the diffusion coefficient values in water-alcohol and micellar media are interestingly much smaller.

Previous workers deposited dye layers on metal electrode by maintaining the electrode at some empirical selected potential while it was immersed in a solution of the dye [3,33,34]. Quickenden and Harrison [10] on the other hand, developed a method of deposition of dye layers by repetitive cycling of the potential scan. From the comparison of CV's obtained when the thionine coated electrodes are immersed in background and thionine containing electrolyte that the thionine and leucothionine peaks observed with the coated electrodes originates almost entirely from the dye coating, rather than for any thionine solution.

In Figure 5.16, 5.17 results the repetitive cycle of voltage scan on a GCE for the present dyes are shown. The behaviour of the thionine and four other dyes at 6.5×10^{-5} M (in 0.1M H_2SO_4) on GCE, is substantially different from the previous study of thionine on Au-electrode [2,10]. Instead of progressive increase of anodic and cathodic currents on cycling, the peak currents in the present systems decrease. The peak current attains a constant value in each case after 10–20 cycles. This behaviour is to some extent similar to that of rhodamine B on SnO_2 glass electrode [1]. Of course in the later case the currents were found to decrease continuously on every repetitive

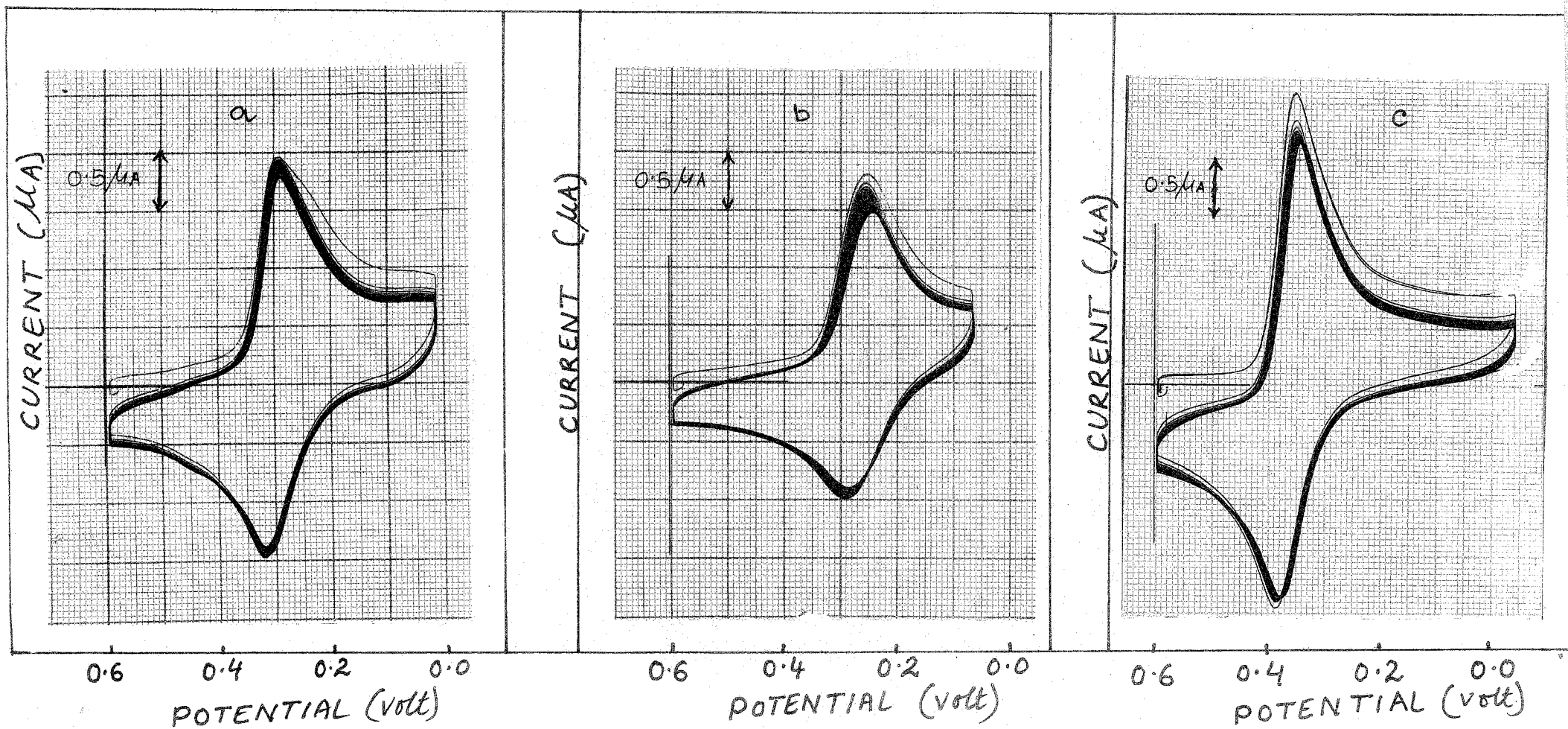

Figure 5.16 Cyclic Voltammograms of (a) Thionine (6.5×10^{-5}M), (b) Azure C (6.5×10^{-5}M), (c) Azure A (6.5×10^{-5}M) with repetitive cycling at scan rate 100 mVs^{-1} in the presence of 0.1M H_2SO_4.

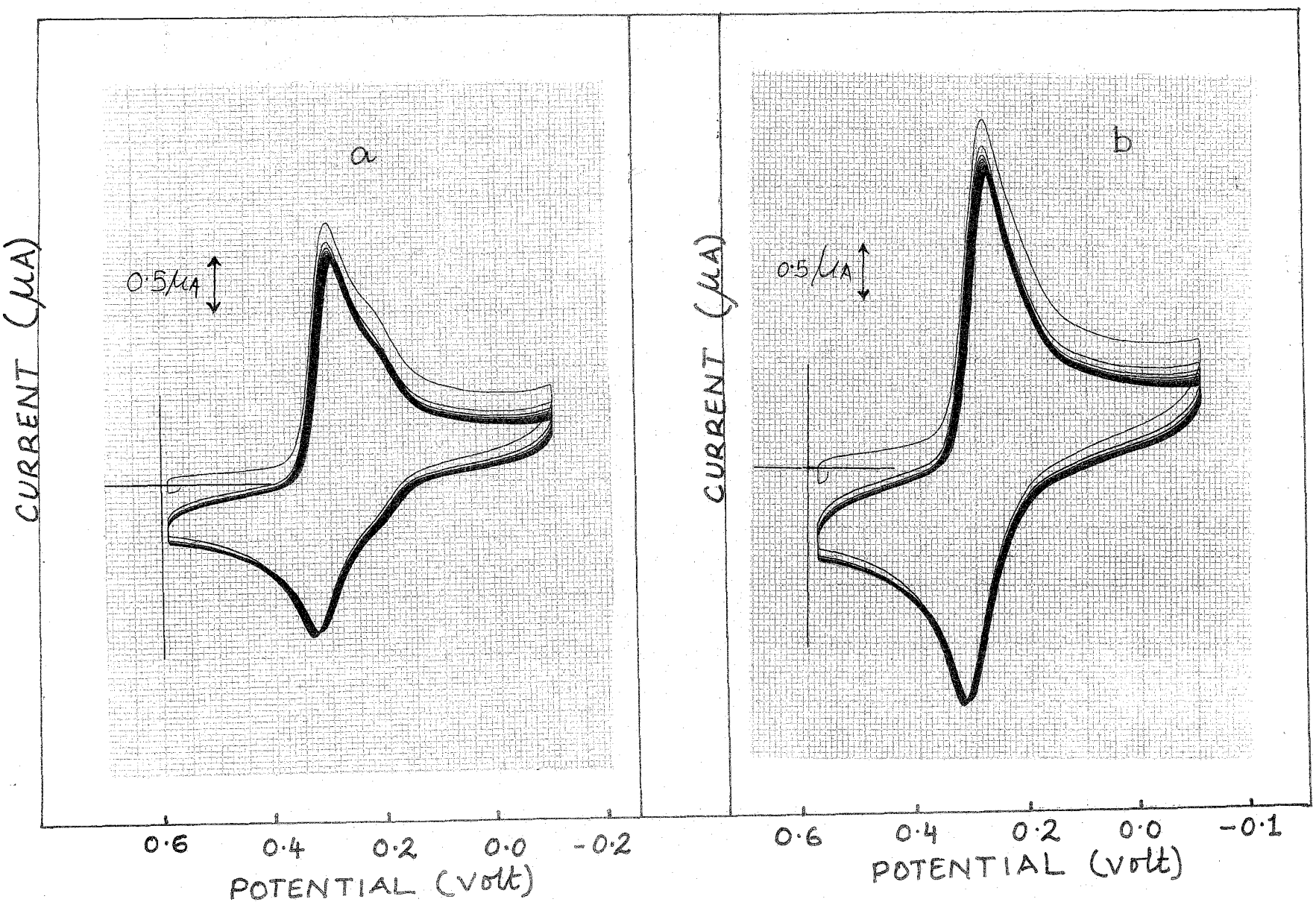

Figure 5.17 Cyclic Voltammograms of (a) Azure B (6.5×10^{-5}M) and (b) Methylene Bluew (6.5×10^{-5}M), with repetitive cycling at scan rate 100 mVs^{-1} in the presence of 0.1M H_2SO_4.

cycle and ultimately merged with the background currents. Present results suggest that under the experimental conditions, although previously assumed tendency of the thionine dye adsorption on a GCE surface is rather weak in the presence of 0.1M H_2SO_4, partial electrode poisoning towards the process of oxidation and reduction of the adsorbed dyes may be responsible for such observation. However, it is also reported by the previous workers that the cyclic voltammogram does not changes with repeated cycling unless a certain potential is exceeded during sweep [1]. It has been shown that for concentration below about 0.2 x 10^{-3}M the methylene blue system fits the simple theory of cyclic voltammetry in which the absorption of the reactant is ignored [12]. It was argued that above 0.2 x 10^{-3}M concentrations, the adsorption of methylene blue must be considered. In Figure 5.18–5.22 representative cyclic voltammograms of the dyes (1 x 10^{-4} – 2 x 10^{-4}M) in the presence of 0.1M KCl at various pH's are shown. It is evident from the figures that the presence of 0.1M KCl and at comparatively higher pH's, both anodic and cathodic peak potentials are shifted toward more negative potentials than those observed in the presence of 0.1M H_2SO_4. Moreover, the voltammograms display cathodic and anodic post/pre peaks which are the characteristics of strong adsorption of reactant and/or products. Observed nature of the voltammograms via-a-vis the adsorption characteristics of various dyes are summarized in Table 5.7. At a concentration of 1 x 10^{-4} M, thionine gives voltammogrames with small cathodic prepeaks as well as anodic postpeaks at pH 3.6 – 4.2 indicating that the products are strongly adsorbed. At pH 5.3 and above, cathodic postpeaks and anodic prepeaks are observed which indicate strong adsorption of the reactant dye. Similarly AzC exhibits cathodic prepeak and anodic postpeak at pH 4.1 indicating that the products are strongly adsorbed. At pH 5.1 cathodic postpeak and anodic prepeak appears which indicates that the reactant dye is also adsorbed strongly. However, at pH 6.0 and above cyclic voltammogramms are suggestive of strong adsorption of products only. While voltammograms of AzA show evidence of strong product adsorption within the pH range of 5.2 and 6.2, AzB exhibits evidence of reactant adsorption at low pH and product adsorption at high pH values. MB, on the other hand, gives cathodic postpeak and anodic prepeak up to pH of 4.8 indicating strong reactant adsorption, while at high pH both reactant and the product are adsorbed.

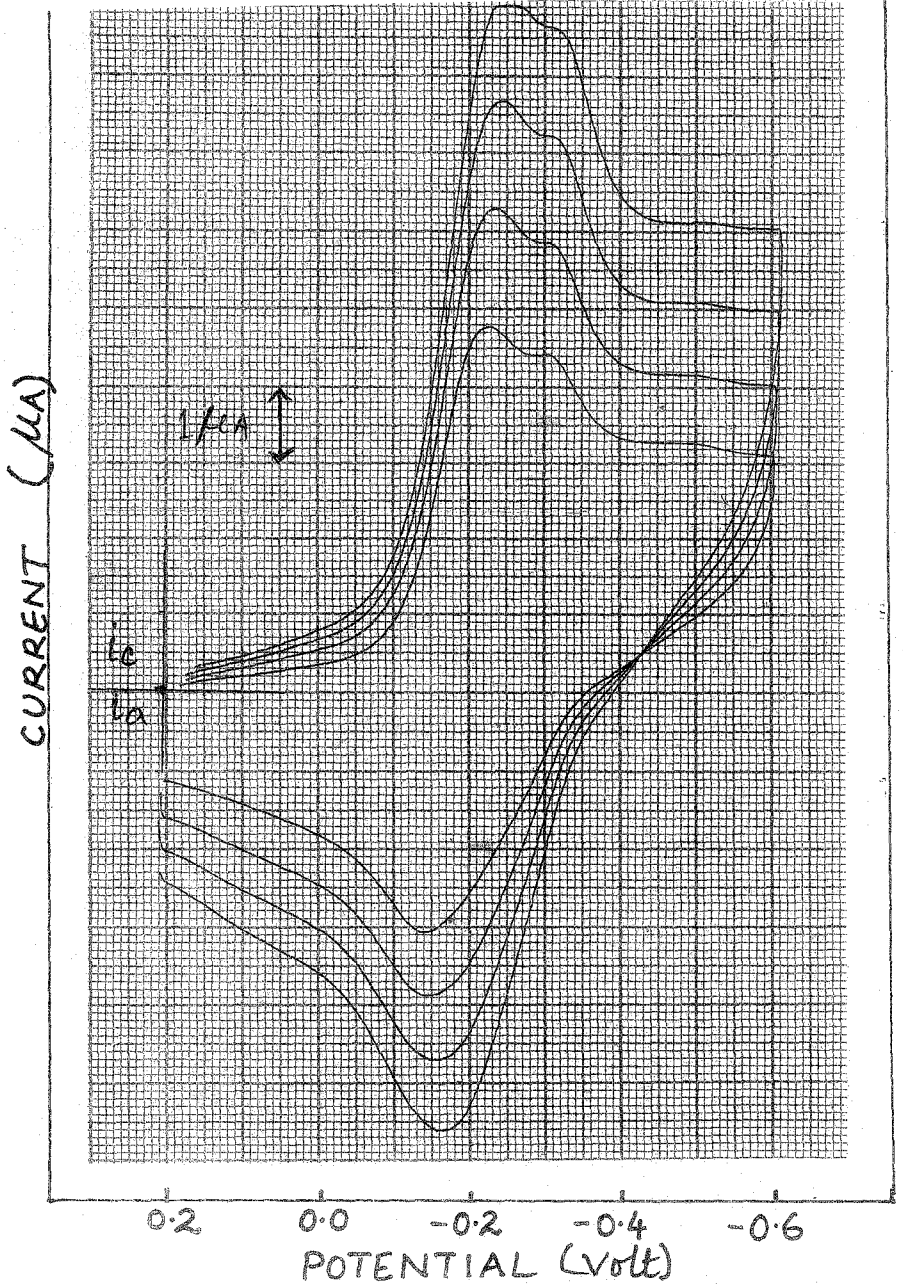

Figure 5.18 Cyclic Voltammograms of Thionine (1.0×10^{-4}M) at pH 5.8 in the presence of 0.1M KCl at different scan rates.

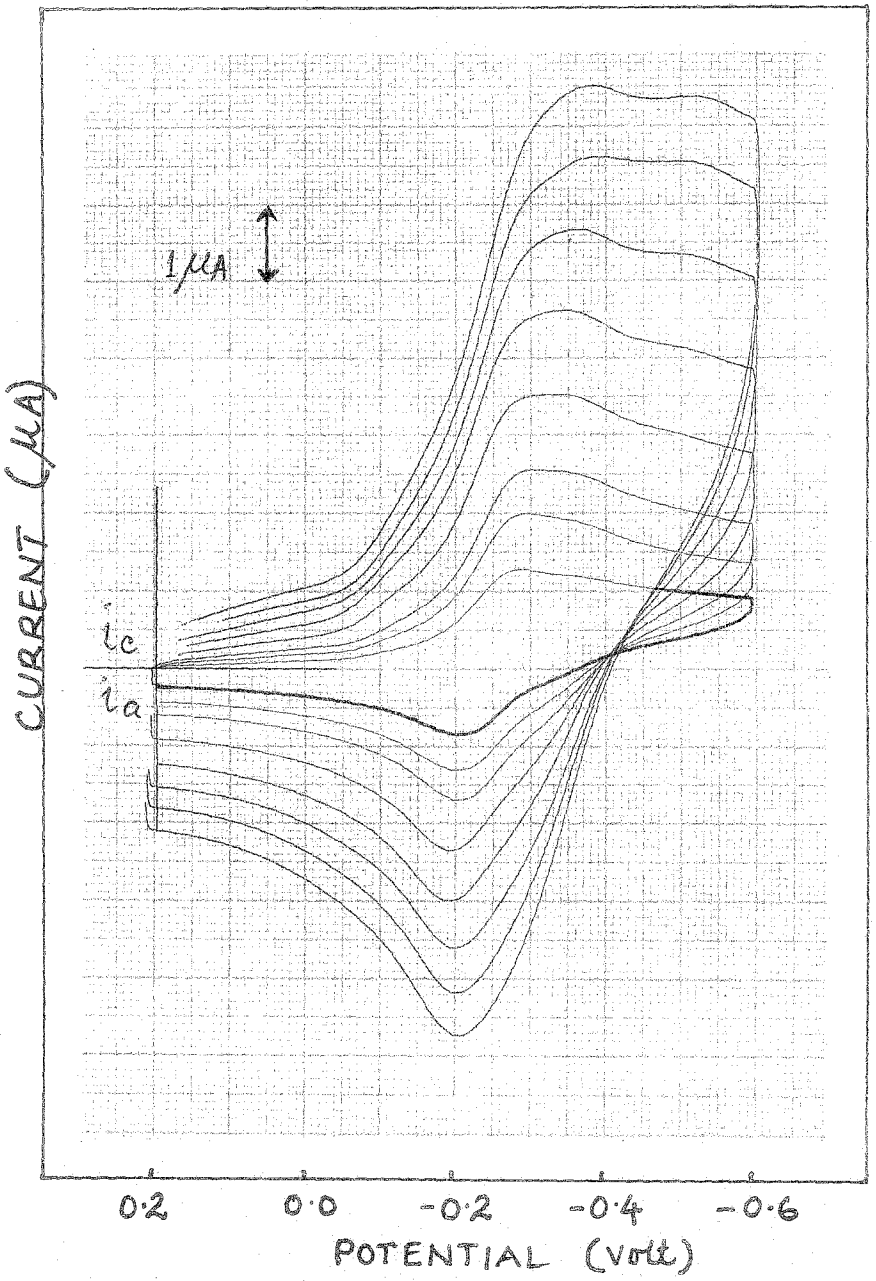

Figure 5.10 Cyclic Voltammograms of Azure C (2.0×10^{-4}M) at pH 5.1 in the presence of

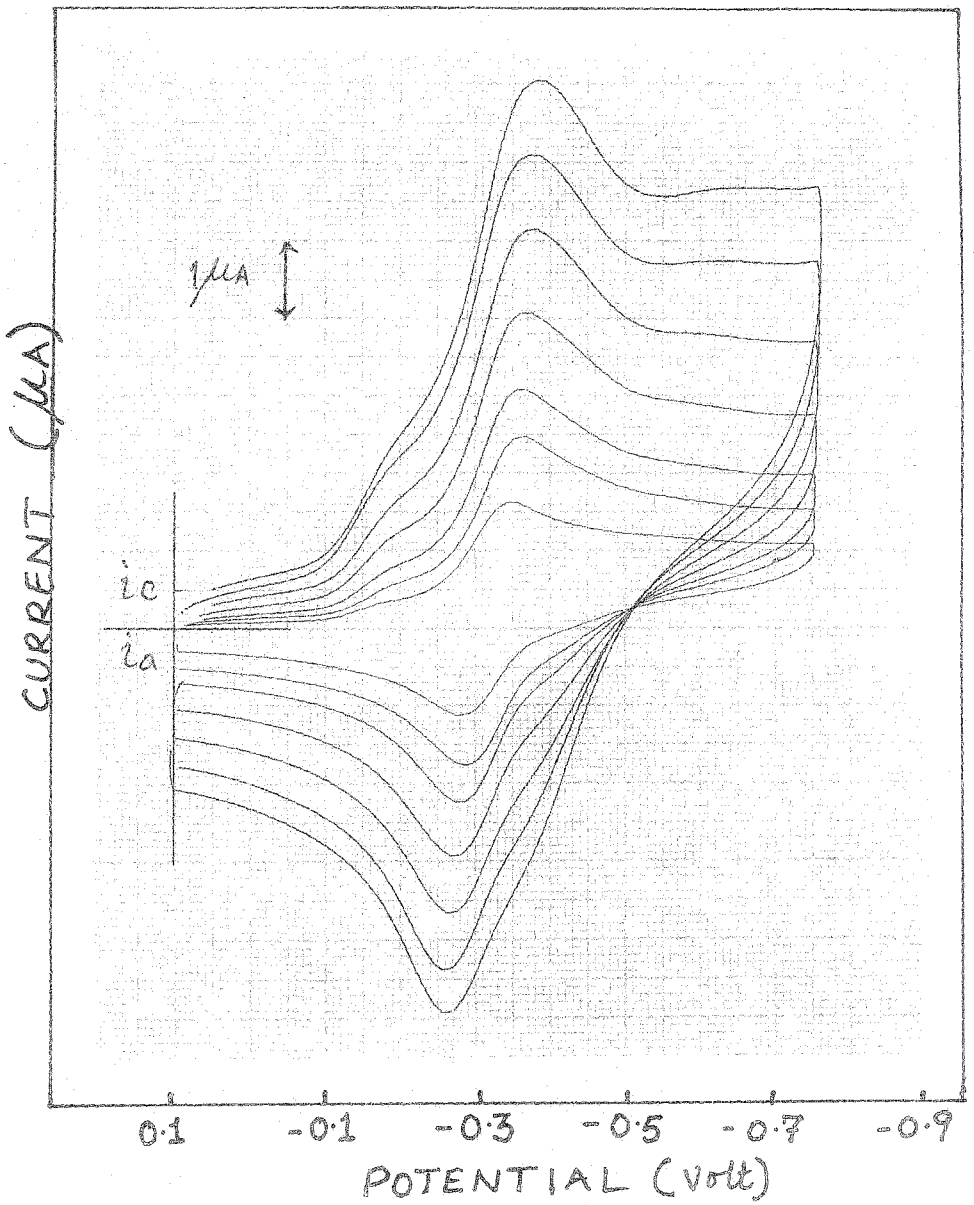

Figure 5.20 Cyclic Voltammograms of Azure A (2.0×10^{-4}M) at pH 5.2 in the presence of 0.1M KCl at different scan rates.

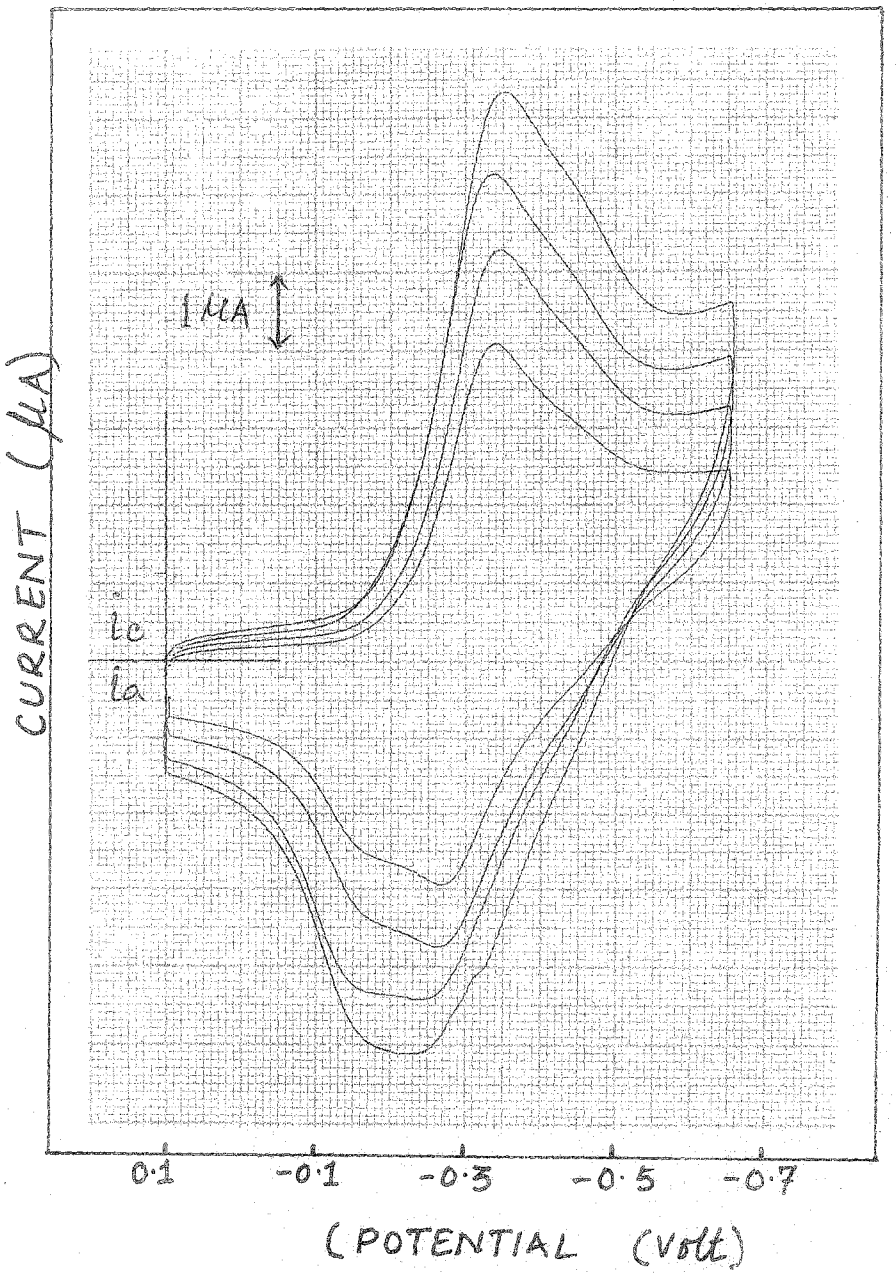
1 μA
CURRENT (μA)
ic
ia
0·1
-0·1
-0·3
-0·5
-0·7
(POTENTIAL (volt)

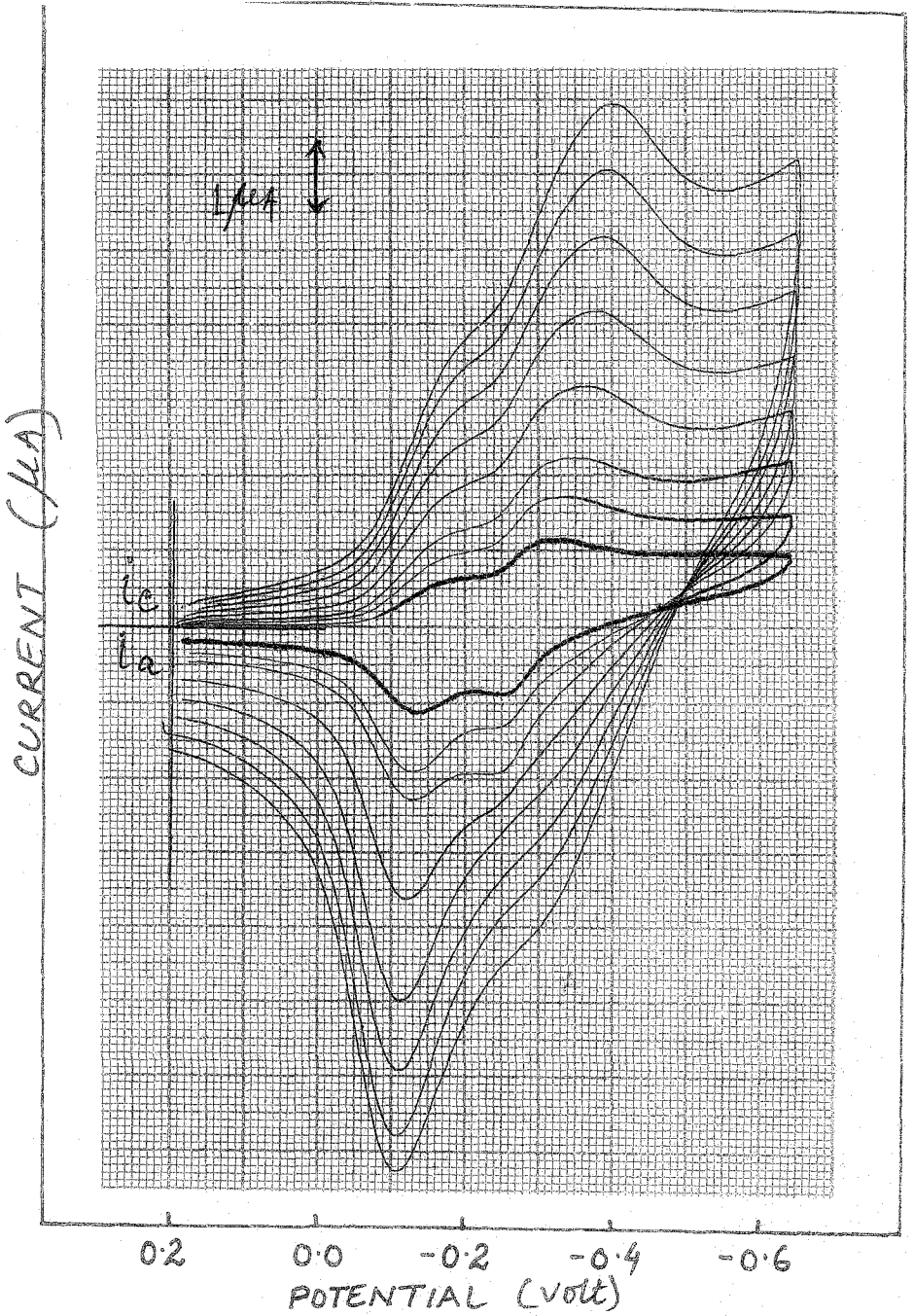
1μA
CURRENT (μA)
i_c
i_a
0·2
0·0
-0·2
-0·4
-0·6
POTENTIAL (volt)

Table 5.7

Effect of pH on the Cyclic Voltammograms of the dye solutions

Dye	pH	Changes/Observations	Adsorption
Thionine (1×10^{-4}M) in 0.1M KCl	3.6	Pre cathodic and post anodic peaks	Product strongly adsorbed
	4.2	-Do-	-Do-
	5.3	Post cathodic and pre anodic peaks	Reactant strongly adsorbed
	5.8	-Do-	-Do-
Azure C (2×10^{-4}M) in 0.1M KCl	4.1	Pre cathodic and post anodic peaks	Product strongly adsorbed
	5.1	Post cathodic and pre anodic peaks	Reactant strongly adsorbed
	6.0	Post anodic peaks	Product strongly adsorbed
	7.0	Pre cathodic and pre and post anodic peaks	Product strongly adsorbed
Azure A (2×10^{-4}M) in 0.1M KCl	5.2	Pre cathodic and post anodic peaks	Product strongly adsorbed
	5.4	-Do-	-Do-
	5.7	-Do-	-Do-
	6.2	Anodic peak current is greater than cathodic	Product weakly adsorbed
Azure B (2×10^{-4}M) in 0.1M KCl	4.8	Post cathodic and pre anodic peaks	Reactant strongly adsorbed
	5.3	-Do-	-Do-
	5.7	Post anodic peaks	Product strongly adsorbed
	6.2	Anodic peak currents high	Product weakly adsorbed
Methylene Blue (2×10^{-4}M) in 0.1M KCl	4.6	Post cathodic and pre anodic peaks	Reactant strongly adsorbed
	4.8	-Do-	-Do-
	6.0	Anodic peak currents increases sharply	Product weakly adsorbed
	8.4	Slight cathodic post peak and anodic peak currents increases sharply	Both reactant and product adsorbed

Sackett et al. [6] have also observed the pH dependence of the initial oxidation of promethiazine whereas similar processes for chloropromazine were completely independent of pH above the value of zero. Apparently, the proximity of the highly charged ring system in the oxidized form lowers the pK_a of the side chain amine to cause the deprotonation. The pH dependence of the oxidation potential of promethiazine has been noted even before and was attributed to electronic interaction between the ring system and the amine [35]. Results indicated that oxidation of the ring lowers the pK_a of the side chain amine by at least 5 units, resulting in deprotonation of the amine in the oxidatised form. Similarly in the case of thiazine dyes it can be argued that although amino nitrogen are very weakly basic, the same groups which could be protonated along the bridging nitrogen at low pH in leucodyes, are deprotonated at high pH. While the effects of pH on the voltammograms of the present dyes are similar, enhanced irreversibility of the redox processes is also accompanied by certain changes in the shapes of the voltammogram at high pH values.

It has been shown that for quasi-reversible electrode processes, the separation between corresponding oxidation and reduction peaks in the cyclic voltammogram is a function of the corresponding electrodic rate constants. Nicholson [27] had provided a table of the computed relationship between the peak separation and a kinetic factor ψ. The latter is related to the rate constant k for a quasi-reversible oxidation by

$$\psi = (D_0/D_r)^{\alpha/2} k\{D_0 \pi \nu (nF/RT)\}^{-1/2} \qquad (5.3)$$

where the subscripts 0 and r designate oxidation and reduction processes, respectively, and α is the transfer coefficient and all other symbols have their usual meanings. It is assumed that the diffusion coefficient of dyes and leucodyes are not very different, the quantity $(D_o/D_r)^{\alpha/2}$ is very close to unity regardless of α value and the rate constant for the electrodic oxidation of dyes dyes at a GCE can be obtained. Figure 5.23 shows the working curve of the variation of peak potential separation with ψ, drawn for the relevant region of peak potential separation of the

---

This ψ is different from the wave function ψ, as appeared in chapter 4.

present study, Computed ψ values of this figure are taken from the table given by Nicholson [27]. Table 5.8 gives the values of ψ at various scan rates for the electrodic process of the present cationic dyes. Kinetic factors at the various scan rates are measured from the curve. When ψ's are sufficiently large, the results become identical to one where the electron transfer is assumed to be Nerstian. On the other hand, for very small ψ, the back reaction for electron transfer is unimportant and the processes for oxidation and reduction can be treated separately as the totally irreversible case. At lower scan rates, all the thiazine dyes displayed reversible electrode reactions. Quasi-reversibilities are prominent above 300 mVs^{-1} scan rates. As such, kinetic measurements are made within the range 300 - 1000 mVs^{-1} scan rates. The heterogeneous rate constants of the electron transfer of the five thiazine dyes are given in Table 5.8. The table shows that the order of the kinetic parameter is same for all the dyes. However, the values of the parameter increase slightly with alkylation in dye molecule from thionine to AzB, while MB gives a little lower value than AzB.

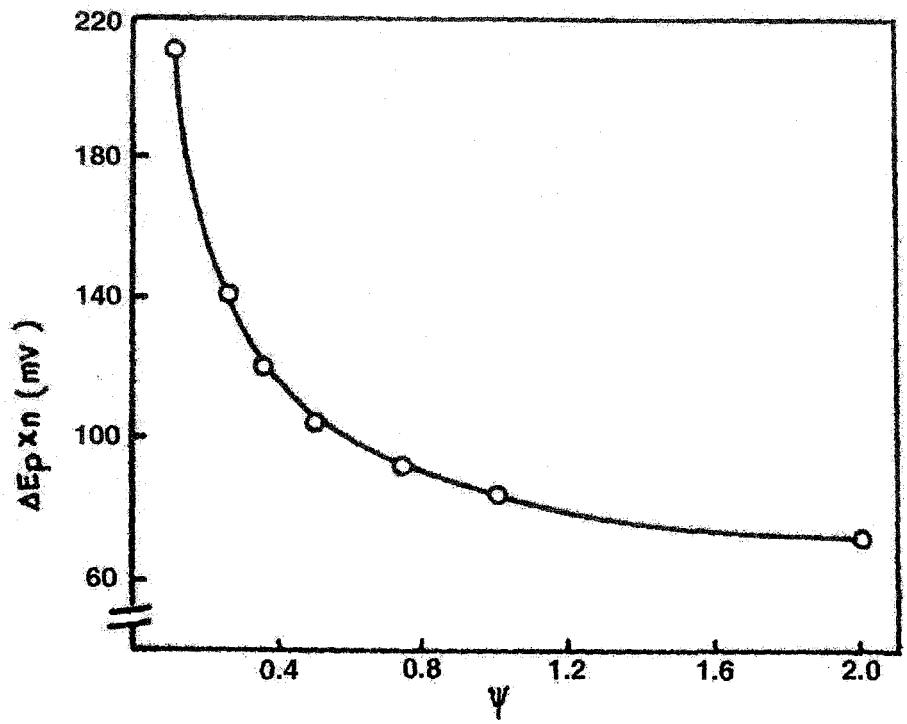

Figure 5.23 Working curve showing variation of peak potential separation with ψ.

Table 5.8

Dye	Scan rate ($Volt.s^{-1}$)	ΔE_p x n (Volt)	ψ	k x 10^3 ($cm.s^{-1}$)
Thionine	1.0	0.140	0.24	6.55
	0.8	0.130	0.29	7.08
	0.6	0.120	0.35	7.61
	0.5	0.110	0.46	8.88
	0.4	0.100	0.58	10.02
	0.3	0.80	1.14	17.05
Azure C	1.0	0.130	0.29	7.39
	0.8	0.120	0.35	7.98
	0.6	0.100	0.58	11.46
	0.5	0.900	0.78	14.07
	0.4	0.800	1.14	18.39
	0.3	0.700	–	–
Azure A	1.0	0.120	0.36	11.81
	0.8	0.110	0.46	13.49
	0.6	0.100	0.58	14.74
	0.5	0.900	0.78	18.09
	0.4	0.800	1.14	23.65
	0.3	–	–	–
Azure B	1.0	0.130	0.29	10.04
	0.8	0.120	0.36	11.14
	0.6	0.100	0.58	15.55
	0.5	0.900	0.78	19.09
	0.4	0.800	1.14	24.96
	0.3	–	–	–
Methylene Blue	1.0	0.140	0.24	8.96
	0.8	0.120	0.36	12.02
	0.6	0.110	0.46	13.30
	0.5	0.100	0.58	15.31
	0.4	0.900	0.78	18.42
	0.3	–	–	–

References

1. Austin, J. M.; Harrison, I.R.; Quichenden, T.I. *J. Phys. Chem.* **1986**, *90*, 1839.
2. Bauldruy, J.M.; Archer, M.D. *Electrochim. Acta* **1983**, *28*, 1515.
3. Quickenden, T. I.; Bassett, R.L. *J. Phys. Chem.* **1981**, *85*, 2232.
4. Bowen, W.R. *Acta. Chem. Scand. Ser.* **1980**, *A 34*, 437.
5. Cheng, H.Y.; Sackett, P.H.; Mc. Creery, R.L. *J. Am. Chem. Soc.* **1978**, *100*, 962.
6. Sackett, P.H.; Mayansky, J.S.; Smith, T.; Kalus, S.; Mc Creery, R.L. *J. Med. Chem.* **1981**, *24*, 1342.
7. Sharma, L.R.; Verma, R.S.; Sharma, A.; Singh, G. *Ind. J. Chem.* **1984**, *23A*, 642.
8. Kamat, P.V. *J. Chem. Soc. Faraday Trans. 1.* **1985**, *81*, 509.
9. Murthy, A.S.N.; Reddy, K.S. *J. Chem. Soc. Faraday Trans. 1***1984**, *80*, 2745.
10. Quickenden, T.I.; Harrison, I.R.; *J. Electrochem. Soc.* **1985**, *132*, 81.
11. Albery, W.J.; Foulds, A.W.; Hall, K.J.; Hillman, A.R. *J. Electrochem. Soc.* **1980**, *127*, 654.
12. Wopschall, R.H; Shain, I. *Anal. Chem.* **1967**, *39*, 1527.
13. Murthy, A.S.N.; Srivastava, T.; *J. Chem. Soc. Faraday Trans.* **1990**, *86*, 105.
14. Murthy, A.S.N.; Reddy, K.S. *J. Chem. Soc. Faraday Trans 1.* **1984**, *80*, 2745.
15. Kamat, P.V. *Electro. Anal. Chem.* **1984**, *163*, 389.
16. Ghosh, P.K.; Bard, A.J. *J. Am. Chem. Soc.* **1983**, *105*, 5691.
17. Rolison, D.R. *Chem. Rev.* **1990**, *90*, 867.
18. Rolison D.R. in fundamental aspects of Corrosion Protection by Surface Modification; Mc. Cafferty, E.C.; Ouder, C.R.; J. Eds, The Electrochemical Society; Vol. 48-3, Pennington N.J.,1984.
19. Asakawa, T.; Sunagawa, H.; Miyagishi, S. *Langmuir* **1998**, *14*, 7091.
20. Hasan, P.A.; Yakhmi, J.V. *Langmuir* **2000**, *16*, 7187.
21. Zhang, W.; Ma, C.S.; Cizkowska, M. *J. Phys. Chem. B* **2001**, *105*, 3435.
22. Mahajan, R.K.; Chawla, J.; Bakshi, M.S. *Colloid Surf. A* **2004**, *237*, 119.
23. Ahmed, S.; Saha, S.K. *Can. J. Chem.* **1996**, *74*, 1896.
24. Brad, A.J.; Faulkner, L.R. *Electrochemical Methods: Fundamentals and Applications*, Johm Willy and Sons, New York, 1980.
25. Gorton, L. J. *Chem. Soc. Faraday Trans. 1.* **1986**, *82*, 1245.

26. Huck, H. *Phys. Chem. Chem. Phys.* **1999**, *1*, 855.

27. Nicholson, R.S. *Anal. Chem.* **1965**, *37*, 1351.

28. Ahmed, S., Ph.D. Thesis, University of North Bengal, India, 1996.

29. Nicholson, R.S. *Anal. Chem.* **1966**, *38*, 1406.

30. Mabbott, G.A. *J. Chem. Edu.* **1983**, *60*, 700.

31. Basu, J.; Kundu, K.K.; Rohatgi-Mukherjee, K.K. *Ind. J. Chem.* **1984**, *23A*, 630.

32. Bard, A.J.; Faulkner, L.R., *Electrochemical Methods Fundamentals and Applications*, John Wiley & Sons, New York, p. 429, 1980.

33. Albery, W.J.; Boutelle, M.G.; Colby, P.J.; Hillman, A.R. *ibid*, **1982**, *133*, 135.

34. Quickenden, T.I., Herring, D.P., Yim, G.K. *Electrochem. Acta* **1980**, *25*, 1397.

35. Kabaskalian, P.; McGlotten, J. *J. Anal. Chem.* **1959**, *31*, 431.

Chapter 6

Summary and Conclusion

Summary and Conclusions

In chapter 1, a general introduction covering the description of different type of surfactants, their properties and their molecular assemblies, viz., micelle and microemulsion are presented. The term micelle and reverse-micelle execute similar surfactant assemblies; only difference is that micelle bears an exterior polar surface with a hydrophobic core, whereas reveres-micelle has a non-polar exterior part having a polar core. However, in microemulsion, considerable amount of water in the reverse-micellar core (termed as water-pool) shows differences in physico-chemical properties (viz., viscosity, dielectric constant, etc.) from that of the bulk water. The physico-chemical properties of the organized assemblies are generally studied by introducing a probe molecule (e.g., different dyes) and monitoring the change in the properties of the probe in the new environment. Progressively alkylated thiazine dyes viz., thionine (Th), azure A (AzA), azure B (AzB), azure C (AzC) and methylene blue (MB) are selected not only for their differences in solubilities and other physico-chemical characteristics pertaining to photogalvanic efficiencies but also because they provide an excellent opportunity for studying the effects of molecular size and shapes on various physico-chemical parameters studied in this work. The importance of phenothiazine and the electrochemical behaviour of the dyes are also discussed briefly in this portion.

(Page No. 1 - 14)

The scope and object of the present investigation has been incorporated in chapter 2. Recently the role of the counterion binding has been recognized in the evaluation of the energetics of micellization process. The study of the effect of counterions eliminates some of the complications by leaving the properties of the amphiphilic ion as a constant factor and thus simplifies some of the interpretation of the experimental results. But, it often leads to complications connected with limited stability and preparative difficulties of the surfactant containing different counterions.

Compounds with polar groups such as alcohols can be expected to solubilize in the hydrophilic regions. Addition of alcohol can strongly influence the behaviour

of the micelles and changes the micellar size depending on the hydrophilic/hydrophobic character of the alcohol.

Dye-micelle interaction is effective to determine the cmc of the surfactant. On the other hand self aggregation of the dyes is important to understand the self quenching phenomena occurring in the photogalvanic cells and also the phenomena of energy transfer in biological systems. It is well known that the ionic dyes tend to aggregate in dilute solutions, leading to the formation of dimer and sometimes even higher order aggregates. In such a case the molecular nature of the dye aggregate is strongly affected by the structure of the dye, ionic strength, nature of counterion, temperature and the nature of the solvents.

The structure of the interfacial water of microemulsion systems is somewhat different from bulk water. In the micro-encapsulated domain, the presence of amphiphilic head groups and the counterion may significantly affect the water mobility. Because of the peculiar chemical and physical properties of the polar interior of reverse micellar aggregates, substantial efforts have been focused on the investigation of the state of water in the pool by comparing the aggregation properties as well as the excitonic parameters of progressively alkylated thiazine dye molecules in aqueous and microemulsion media.

Energy problem has opened new avenues in physical chemistry research ever since electrochemistry has been proved to be the most promising of all modern energy technologies. This is due to its capability in dealing with highest energy densities of all possible alternatives. Two essential features of research activities in this direction are (i) modification of the conventional technologies via incorporating emerging ideas and knowledge in various electrode and electrolytic processes and (ii) development and upgradation of new energy conversion techniques, especially that of solar energy conversion by incorporating new perception of chemistry of electrodics and ionics (specially metal free) at the interfaces and in the bulk. In view of this plan of a preliminary study has also been drawn on the electrochemistry of dyes at the microelectrode surfaces.

(Page No. 15 - 20)

In chapter 3, the results of the investigations on the effect of counterions and alcohols on the micellization properties of anionic surfactants in aqueous media are

presented. Two important anionic surfactants, viz., dodecyl sulfate and bis-(2-ethyl-1-hexyl) sulfosuccinate having different counterions (viz., Li^+, Na^+, K^+, NH_4^+, $N^+(CH_3)_4$, $N^+(C_2H_5)_4$, $N^+(C_3H_7)_4$ and $N^+(C_4H_9)_4$) have been studied as a function of temperature. Surfactants having different counterions are prepared by ion exchange technique. At a particular temperature (below 303K), cmc depends upon the nature of the counterion following the order $NH_4^+ > Li^+ > Na^+$ in dodecyl sulfate, whereas for AOT (bis-(2-ethyl-1-hexyl) sulfosuccinate), cmc decreases in the order $NH_4^+ > Na^+ > Li^+ > K^+$. But at high temperature (above 323K) AOT micelles are rather insensitive to temperature variation. Above trend was explained by considering the binding of counterions to micelles. It is found that at a concentration of 10 times the cmc, potassium dodecyl sulfate and potassium salt of AOT is not completely soluble in water at room temperature. The solution contains hydrated crystals dispersed in a micellar phase. Below 313K, K-AOT with K^+ as counter ion forms clear solution. Thus the micellization of K-AOT has been investigated in the limited range within 283-308K. However, in the case of potassium dodecyl sulfate, which has a Kraft temperature of 307K at the cmc it was impossible to investigate the micellization process since the temperature leading to a clear solution was too high (323K).

It has been observed that in case of dodecyl sulfate and AOT having tetraalkylammonium counterions the cmc values follow the order $N^+(CH_3)_4 > N^+(C_2H_5)_4 > N^+(C_3H_7)_4 > N^+(C_4H_9)_4$ (at temperature range <298K). It seems that the hydrodynamic size of the counterion plays an important role along with the hydrophobicity of tetraalkylammonium ions. The cmc in aqueous solution for a particular surfactant reflects the degree of binding of the counterion to the micelle. Increased binding of the counterion, in the aqueous system causes a decrease in the cmc of the surfactant. The extent of binding of the counterion increases also with increase in the polarizability and charge of the counterion and decreases with increase in its hydrated radius.

The thermodynamic parameters support the view that in order to form micelle the gain in entropy is the major factor leading to negative change in Gibbs free energy. For all counterions in both DS and AOT systems ΔH^0_m and ΔS^0_m contribute differently to get similar ΔG^0_m. However, like a variety of processes such as oxidation-reduction, hydrolysis, protein unfolding, etc., micellization process also exhibit a linear relationship between the enthalpy and entropy change which is

known as enthalpy-entropy compensation. The calculated compensation temperature value of 303.2 K for DS and 295.6 K for AOT satisfactorily follows the characteristic range of other ionic surfactants.

The surface excess concentration at surface saturation Γ_{max}, is a useful measure of the effectiveness of adsorption of the surfactant at air-solution interface, since it is the maximum value that adsorption can attain. With increasing temperature Γ_{max} for dodecyl sulfate follow more or less general trend as expected, which presumably due to increased thermal motion with a consequent decrease in the effectiveness of adsorption. But in the case of AOT surfactant with six different counter ions, the change of Γ_{max} does not follow a regular trend.

(Page No. 21 - 52)

The effect of short-chain alcohols (viz., ethanol, 1-propanol and 2-propanol) on the micellization of SDS and AOT are studied with solutions containing different proportion of alcohols and surfactants within a temperature range of 298K to 313K have also presented in this chapter. At a fixed proportion of alcohol the cmc and other associated thermodynamic parameters except the ionization degree (α) progressively decreases with temperature. This variation may also be well explained by the dehydration of the hydrocarbon tail of the surfactant molecule followed by the greater adherence of the alcohol molecules to the micellar pseudophase. In this respect it may be said that the alcohol content works quite similar to temperature with respect to the effect on micelle formation at constant pressure. The situation is very similar for both the surfactants. However in the case of AOT, all the effects are less pronounced due to the presence of hydrophobic double strand structure where the alcohol molecules perform less effectively than SDS.

(Page No. 52 - 59)

In chapter 4, results of the investigations on the nature of dye-surfactant interaction, dye-dye aggregation, the effect of increase of molecular size on aggregation, the probable structure of dye aggregates in aqueous and microemulsion media are presented. Dye-micelle interaction is utilized to determine the cmc of the surfactant. Self aggregation of the dyes is important to understand the self quenching phenomena occurring in the photogalvanic cells and also the phenomena of energy

transfer in biological systems. Analysis of monomer spectra of the progressively alkylated thiazine dyes in terms of Vibronic Exciton Model have been done in aqueous and microemulsion media. The binding force between the monomer units in a dimer and the structural dependency (i.e., progressive alkylation on thionine molecule) of aggregate geometries in aqueous solution and in microemulsion media have been examined in terms of Molecular Exciton Theory and presented in this chapter. Section 4.1.1 and 4.1.2 contain a brief review of the previous studies on the dye-surfactant interaction in sub-micellar and super-micellar concentrations of surfactant respectively, whereas section 4.1.3 bears the review of the previous studies on the dye-surfactant interaction in microemulsion media. In section 4.1.4, a brief review of previous studies on the general monomer-dimer equilibrium of dyes in the light of classical model is presented. Section 4.1.5 depicts the theoretical aspects of molecular exciton model and section 4.1.6 contains a review on spectral properties of dimer in terms of exciton theory and also includes some more recent development of the exciton theory which can be used to relate the distance and relative orientation of monomeric dye molecules in the dimer. Possibility of higher aggregate formation is avoided by choosing appropriate range of dye in solution.

(Page No. 67 - 96)

The cmc of SDS and AOT at a fixed temperature (303K) is determined spectrophotometrically by using thiazine dye probe. The association constants for each pair of dye-surfactant system shows a general trend. It has been observed that thionine stacked most strongly with the surfactant followed by other dyes in the order AzC > AzA > AzB > MB. It suggests that the dye-surfactant electrostatic attraction between the charged part of the dye molecule and the ionic head of amphiphile plays the key role during interaction at the postmicellar concentration of surfactant. The large negative ΔG^0 values also support in favour of electrostatic attraction. Dimerization constants for the dyes are determined by using a nonlinear least-square fitting with Microsoft Excel Solver (section 4.3.3). At 303K in aqueous medium the K_d values are 1.761×10^3, 2.350×10^3, 3.381×10^3, 6.258×10^3 and 3.658×10^3 lit/mol for Th, AzC, AzA, AzB and MB respectively. This indicates that the increased hydrophobicity in the dye molecule upon methylation increases dimerization tendency due to increased hydrophobic interaction, which in turn

minimizes the contact area of the dyes with water. In microemulsion media the K_d values are 2.214 x 10^3, 1.760 x 10^3, 3.504 x 10^3 and 4.112 x 10^3, 1.501 x 10^3 lit/mol for Th, AzC, AzA, AzB and MB respectively, do not follow any regular trend. It is therefore, evident that besides the structure of the dye molecules, nature of the solvent also plays important role on the strength of aggregation. The ΔG^0 for dimerization process for five thiazine dyes are negative and do not differ very much upon progressive methyl substitution, there is, however, a general trend of increasing effect of methylation in aqueous and microemulsion medium.

(Page No. 98 - 110)

In section 4.3.4, the result of progressive alkylation of thionine on the spectra of monomers which are present in equilibrium with dimers in aqueous and microemulsion media have been analyzed in terms of Vibronic Exciton Model:

$$I(\bar{\nu}) = I_{00} \sum_m \frac{X^m}{m!} \left(1 + \frac{mV}{\bar{\nu}_{00}}\right) \exp\left\{\left(-\frac{4 \ln 2}{b_g^2}\right)(\bar{\nu} - \bar{\nu}_{00} - mV)^2\right\}$$

where , I_{00} is the intensity, $\bar{\nu}_{00}$ is the position of the (0,0) band, b_g is the Gaussion band width X is the ratio of (1,0) to (0,0) band intensities and ν, the separation between the bands. The spectra were fitted to the above 'five parameter Gaussion equation'. This has been done on a computer by means of a general non-linear curve-fitting program, KINFIT. Results of fitting indicate that the present physical model describing a vibronic progression of a displaced harmonic oscillator with Gaussian bands of constant band width is well applicable in the present systems under investigation. (Page No. 110 - 115)

In section 4.3.5, the dimer spectra of the progressively alkylated thiazine dyes (viz, Th, AzA, AzB, AzC, MB) are analyzed in terms of Molecular Exciton Theory of dipole-dipole coupling. There are three types of dye aggregates: H-type, J-type or intermediate type. According to this model the parallel aggregates (H-aggregates) absorb at shorter wave length and head to tail aggregates (J-aggregates) show absorption at longer wavelengths compared to the monomer. Intermediate geometries give rise to band splitting, where the monomer units are thought to be

arranged parallely (Model I) or obliquely (Model II) (both models are discussed with a twist angle θ). The splitting of dimer spectra for the intermediate geometries leads to compute the angle θ between monomer units and intermolecular separation of the monomer molecules in the dimer. The dimer spectra are decomposed into two bands, which show that the monomer visible spectrum corresponds to an electronic transition with two vibronic bands. A systematic variation of oscillator strengths for both symmetric and anti-symmetric delocalized exciton states is observed. This may be due to the variation of geometrical disposition of the dimer in solution as a function of progressive alkylation of thionine molecule. The oscillator strength values of monomer are 0.603, 0.451, 0.552, 0.641 and 0.610 for Th, AzA, AzB, AzC and MB respectively in aqueous medium, whereas in microemulsion much smaller values of the oscillator strengths (0.382, 0.101, 0.202, 0.280 and 0.191) are observed.

Exciton theory allows determining the twist angle, θ which in case of thionine is found to be 34.8^0 in aqueous medium, whereas in microemulsion the value is 35.7^0. For other dyes, the angle changes from 28.4^0 to 28.1^0 in case of AzC, from 28.5^0 to 30.9^0 in case of AzA, from 30.2^0 to 25.3^0 in case of AzB and from 31.7^0 to 28.2^0 in case of MB. As discussed earlier the variation of physico-chemical characteristics of the water in the water-pool of the bulk water also plays important role in determining the structure of the dimer. While the twist angles displayed by all the five dyes are close to each other, no systematic variation is observed on progressive alkylation of the dye molecule. It seems apparent that apart from the steric effect due to the addition of successive methyl groups in the dye molecule, hydrophobic as well as electron donating nature of methyl groups play important role in dimer formation.

(Page No. 115 - 121)

The electrochemical behaviour of the dyes on clean glassy carbon electrodes have been discussed in chapter 5. A brief review of the previous work on the redox properties of various dyes on clean and modified electrodes using cyclic voltammetric technique is presented in section 5.1. (Page No. 131 - 134)

A brief review on the electrochemistry of the dyes is presented in section 5.2. The criteria related to the reversibility and the results thereof on a clean glassy carbon electrode (GCE) in different solvents are discussed in section 5.3. The formal

potential values (average) for the five dyes are found to be 0.205, 0.175, 0.207, 0.281 and 0.196V for Th, AzC, AzA, AzB and MB respectively in aqueous medium. Voltammetric measurements are consistent with two electron reversible redox couples of dye/leucodye pairs. The value of $0.058/\Delta E$ is rather low (<2) even at slow scan rates, possibly due to the result of two successive one electron reversible charge transfer, with a fast protonation of the intermediate to form a species which is more easily reduced than the dye molecule. The current ratio values, $i_{pa}/i_{pc} < 1$, suggest that the electrogenerated leucodyes are involved in reactions which prevent their reoxidation upon scan reversal. Assuming reversibility of electrode reaction, the effective diffusion coefficients of the dyes in different solvents have been calculated at scan rate of $20mVs^{-1}$. The values for thionine are 3.05×10^{-6}, 1.80×10^{-6} and 1.10×10^{-6} cm^2s^{-1} in water, ethanol (50% v/v) and triton X-100 (0.001M) respectively. No systematic change in the diffusion coefficient values with the progressive alkylation of dye molecule is observed. But the effect of solvent is found to be prominent. The nature of the cyclic voltammograms obtained from concentrated dye solution ($1 - 2 \times 10^{-4}$M) in the presence of 0.1M KCl and the effect of pH have also been discussed specially in view of reactant and/or product adsorption on the electrode surface. The heterogeneous rate constant, k for the quasi-reversible processes of the dyes is determined. The kinetic measurements are carried out within the range 300 - 1000 mVs^{-1} scan rates. All the values are found to be of the order of 10^{-3} $cm.s^{-1}$.

(Page No. 134 - 149)

List of Publications

1. Temperature Dependant Micellization of AOT in Aqueous Medium: Effect of the Nature of Counterions.

   Amitabha Chakraborty, Subrata Chakraborty, Swapan K. Saha

   Journal of Dispersion Science and Technology **2007**, *28*, 984 – 994.

2. Effect of Size of Tetraalkylammonium Counterions on the Temperature Dependent Micellization of AOT in Aqueous Medium.

   Amitabha Chakraborty, Swapan K. Saha, Subrata Chakraborty

   Colloid and Polymer Science **2008**, *286*, 927 – 934.